

**Analysis of Nitrogen Starvation Induced Filamentous
Growth and Characterization of Putative Essential Genes
in the Human Fungal Pathogen, *Candida albicans***

Dissertation zur Erlangung des naturwissenschaftlichen Doktorgrades der
Bayerischen Julius-Maximilians Universität Würzburg

vorgelegt von

Kajal Biswas
aus
(Nadia, India)

Würzburg
2005

Eingereicht am:.....

Mitglieder der Promotionskommission:

Vorsitzender:.....

Gutachter: Prof. Dr. J. Morschhäuser

Gutachter: Prof. Dr. J. Kreft

Tag des Promotionskolloquiums:.....

Doktorurkunde ausgehändigt am:.....

ERKLÄRUNGEN

Hiermit erkläre ich, dass ich die vorliegende Arbeit selbständig und nur unter Verwendung der angegebenen Quellen und Hilfsmittel angefertigt habe.

Diese Dissertation wurde weder in gleicher noch in ähnlicher Form in einem anderen Prüfungsverfahren vorgelegt.

Des weiteren erkläre ich, dass ich früher weder akademische Grade erworben noch zu erwerben versucht habe.

Datum: 03 Januar, 2005

Ort: Würzburg

Kajal Biswas

DECLARATION

I hereby declare that the submitted dissertation was completed by myself and no other, and I have not used any sources or materials other than those enclosed.

Moreover, I declare that the following dissertation has not been submitted further in this form and has not been used for obtaining any other equivalent qualification in any other organization. Additionally, other than this degree I have not applied or will not attempt to apply for any other degree, title or qualification in relation to this work.

Date: 03 January, 2005

Place: Wuerzburg

Kajal Biswas

*Dedicated to The Memory of My
Maa...*

ACKNOWLEDGEMENTS

I am associated with the *Candida* workgroup of the Institute for Molecular Infectionsbiology since July 2001. I express my deep sense of gratitude to my supervisor Prof. Dr. Joachim Morschhaeuser for his meticulous guidance and unwavering help and encouragement during the course of this study. I am grateful to him for providing the maximum facilities to work, nothing being unavailable and complete freedom to implement my ideas in research.

I acknowledge Prof. Dr. Dr. h. c. J. Hacker for providing the facilities during the course of the present study. I am especially thankful to my co-supervisor Prof. Dr. J. Kreft for his help.

I am grateful to Dr. Malcolm Whiteway, Dr. Klaus Schröppel, Dr. S. Rupp, Dr J. Köhler, Dr. J. Perez-Martin and Dr. David Shore for providing the strains and plasmids.

I take this opportunity to thank all the members of this institute for their help and cooperation. I owe my thanks to Dr. Christoph Hawk and Prof. Dr. J. Reidl for extending their lab facilities. Ms. Hilde Merkert deserves special thanks for helping me regarding the computers and microscopy.

I am lucky to have excellent lab mates, who have made the lab an enjoyable place to work. I appreciate the efforts made by Sonja for making me familiar with the work during my initial days in the institute. I thank Nim and Peter for the valuable discussions and constructive criticisms of my work among numerous other things. Thanks to Teresa, Oliver, Davina, Ulrich, Neelam, Julia, Steffiene and Anja for their help.

I would like to thank all my friends, who helped me in innumerable ways, both in my 'academic' and 'non-academic' ventures. Thanks to Subha Aka, Naresh and Manickyam for giving me good company. I owe my thanks to Sunit, Chandan, Gireesh, Ananda, Prabhat, Aditya, Arnab, Subhrajit, Kallal and Parthada-Banidi for standing by me through thick and thin.

I am deeply indebted to my Boromashi, Chhotomashi and all my in-laws for being affectionate, understanding and appreciative of everything I do. I thank my late parents, whose blessings and inspirations are always with me. Last but not least, I thank my wife, Manjistha, for her unrelenting love, support and encouragement in every step of my life.

CONTENTS

1. Summary.....	1
1. Zusammenfassung.....	3
2. Introduction.....	6
2.1. <i>Candida albicans</i>: an opportunistic human fungal pathogen.....	6
2.2. Virulence determinants of <i>C.albicans</i>.....	7
2.3. Nitrogen regulation: Role in virulence and dimorphism.....	13
2.3.1. Ammonium permeases and nitrogen starvation induced dimorphism of yeast.....	15
2.4. An approach towards anti-candida drug development.....	16
2.5. Aim of the study.....	18
3. Materials and Methods.....	19
3.1. Bacteria strain used.....	19
3.2. Plasmids used in this study.....	19
3.3. <i>C.albicans</i> strains used in this study.....	22
3.4. Primers used in this study.....	30
3.5. Sources of chemicals, enzymes and equipments used in this study.....	33
3.6. Commonly used molecular microbiological techniques.....	34
3.6.1. Growth and maintainance of strains.....	34
3.6.2. <i>In vitro</i> DNA manipulation.....	35
3.6.2.1. DNA digestion with restriction enzymes.....	35
3.6.2.2. Polymerase Chain Reaction (PCR).....	35
3.6.3. Gel electrophoresis and gel elution of DNA fragments.....	36
3.6.3.1. Agarose gel electrophoresis.....	36
3.6.3.2. Gel elution of inserts from agarose gel.....	36
3.6.4. Cloning of gene of interest in vectors.....	37
3.6.4.1. Ligation.....	37
3.6.4.2. Transformation of <i>E. coli</i>	37

3.6.4.3. Screening and analysis of recombinants.....	38
3.6.5. Transformation of <i>C.albicans</i>	40
3.6.6. Genomic DNA isolation from <i>C.albicans</i>	40
3.6.7. Southern hybridization technique.....	41
3.6.8. RNA isolation from <i>C.albicans</i>	43
3.6.9. Northern hybridization.....	43
3.7. Phenotypic assays.....	45
3.8. Microscopy.....	46
3.9. Ammonium uptake assays.....	47
3.10. X-Gal agarose overlay assay.....	47
4. Results.....	49
4.1. Nitrogen starvation induced filamentous growth and ammonium transporters of <i>C.albicans</i>.....	49
4.1.1. Nitrogen starvation induced filament formation in <i>C.albicans</i> is controlled by the availability of ammonium	49
4.1.2. Identification of <i>C.albicans</i> ammonium permeases.....	51
4.1.3. Construction of <i>C.albicans</i> strains with different <i>MEP</i> gene deletions.....	52
4.1.4. CaMep1p and CaMep2p are functional ammonium permeases.....	58
4.1.5. The CaMep2 ammonium permease is required for nitrogen starvation induced filamentous growth.....	60
4.1.6. Regulation of <i>CaMEP1</i> and <i>CaMEP2</i> expression.....	63
4.1.7. Nitrogen starvation induced filamentous growth depends on high <i>CaMEP2</i> expression levels.....	66
4.1.8. The C-terminal tail of CaMep2p contains a region important for filamentation.....	71
4.1.9. Regulation of filamentation by <i>CaMEP2</i> is dependent on both the MAP kinase cascade and the cAMP pathway.....	74
4.1.10. Ammonium suppresses CaMep2p signaling.....	76
4.2. Evaluation of putative essential genes as potential targets for antifungal drug development.....	78
4.2.1. Repressor/activator protein 1.....	78
4.2.1.1. Identification of the <i>C.albicans RAPI</i> gene.....	79
4.2.1.2. Expression of <i>CaRAPI</i> in temperature-sensitive <i>S.cerevisiae rap1</i> mutants	82
4.2.1.3. Construction of <i>C.albicans rap1</i> deletion mutants.....	82
4.2.1.4. Growth analysis of the <i>rap1</i> deletion mutants.....	84
4.2.1.5. Phenotypic analysis of $\Delta rap1$ mutants in hyphal growth induction medium.....	87
4.2.2. Centromere Binding Factor 1.....	88

4.2.2.1. Construction of <i>C.albicans cbf1</i> deletion mutants.....	89
4.2.2.2. Growth and phenotypic analysis of $\Delta cbf1$ mutants	91
4.2.2.3. <i>C.albicans</i> $\Delta cbf1$ mutants are methionine and cysteine auxotrophic.....	92
4.2.2.4. Chromosome stability in <i>C.albicans</i> $\Delta cbf1$ mutants.....	93
4.2.2.5. Phenotype of $\Delta cbf1$ mutants at the non-permissive temperature.....	99
4.2.3. <i>YIL19</i>.....	102
4.2.3.1. <i>In silico</i> characterization of Yil19 protein.....	103
4.2.3.2. <i>YIL19</i> is an essential gene in <i>C.albicans</i>	105
4.2.3.3. Construction of conditional <i>yil19</i> deletion mutant	106
4.2.3.4. <i>YIL19</i> deletion is lethal in <i>C.albicans</i>	109
4.2.3.5. <i>YIL19</i> depleted cells are impaired in the maturation of 18S rRNA.....	111
5. Discussion.....	115
5.1. Nitrogen starvation induced filamentous growth and ammonium transporters.....	115
5.2. Analysis of some putative essential genes in <i>C.albicans</i>.....	122
5.2.1. Repressor/Activator Protein 1.....	123
5.2.2. Centromere Binding Factor 1.....	124
5.2.3. <i>YIL19</i> : An essential gene in <i>Candida albicans</i>	127
Appendix.....	129
A.1. Construction of plasmids.....	129
A.2. Lee´s medium.....	141
A.3. Abbreviations.....	142
References.....	144
Curriculum vitae	
Lebenslauf	
Publications	

1. Summary

Candida albicans is an opportunistic human fungal pathogen that causes a variety of infections, ranging from superficial mucosal to deep-seated systemic infections, especially in immunocompromised patients. Although the ability of *C.albicans* to cause disease largely depends on the immune status of the host, the fungus also exhibits specific characteristics that facilitate colonization, dissemination, and adaptation to different host niches and thereby turn *C.albicans* from a harmless commensal to an aggressive pathogen. In response to various environmental stimuli *C.albicans* switches from growth as a budding yeast to invasive filamentous growth, and this morphogenetic switch plays an important role in *C.albicans* pathogenesis. Nitrogen limitation is one of the signals that induce filamentous growth in *C.albicans*, and the control of the morphogenetic transition by nitrogen availability was studied in detail in the present work.

Ammonium is a preferred nitrogen source for yeasts that is taken up into the cells by specific transporters. It was found in this study that *C.albicans* possesses two major ammonium transporters, encoded by the *CaMEP1* and *CaMEP2* genes, expression of which is induced by nitrogen starvation. Whereas $\Delta mep1$ or $\Delta mep2$ single mutants grew as well as the wild-type strain on limiting concentrations of ammonium, deletion of both transporters rendered *C.albicans* unable to grow at ammonium concentrations below 5 mM. In contrast to $\Delta mep1$ mutants, $\Delta mep2$ mutants failed to filament and grew only in the yeast form under nitrogen starvation conditions, indicating that in addition to its role as an ammonium transporter CaMep2p also has a signaling function in the induction of filamentous growth. CaMep2p was found to be a less efficient ammonium transporter than CaMep1p and to be expressed at much higher levels, a distinguishing feature important for its signaling function. By the construction and analysis of serially truncated versions of CaMep2p, the C-terminal cytoplasmic tail of the protein was shown to be essential for signaling but dispensable for ammonium transport, demonstrating that these two functions of CaMep2p are separable.

In *C.albicans* at least two signal transduction pathways, a MAP kinase cascade and a cAMP-dependent pathway ending in the transcriptional regulators Cph1p and Efg1p, respectively, control filamentous growth, and mutants defective in either one of these pathways are defective for filamentation under nitrogen starvation conditions. A hyperactive *CaMEP2* allele rescued the filamentation defect of a $\Delta cph1$ or a $\Delta efg1$ mutant, but not of a $\Delta cph1 \Delta efg1$ double mutant or a mutant deleted for *RAS1*, which acts upstream of and

activates both signaling pathways. Conversely, a dominant active *RAS1* allele or addition of exogenous cAMP rescued the filamentation defect of $\Delta mep2$ mutants. These results suggest that CaMep2p activates both the MAP kinase and the cAMP pathway in a Ras1p dependent manner to promote filamentous growth under nitrogen starvation conditions. At sufficiently high concentrations, ammonium repressed filamentous growth even when the signaling pathways were artificially activated. Therefore, *C.albicans* has established a regulatory circuit in which a preferred nitrogen source, ammonium, serves as an inhibitor of morphogenesis that is taken up into the cell by the same transporter that induces filamentous growth in response to nitrogen starvation.

Although a detailed understanding of virulence mechanisms of *C.albicans* may ultimately lead to novel approaches to combat infections caused by this pathogen, the identification and characterization of essential genes as potential targets for the development of antifungal drugs is a strategy favoured by most pharmaceutical companies. Therefore, *C.albicans* homologs of three genes that are essential in other fungi were selected in collaboration with an industrial partner and functionally characterized in this work. *RAP1* encodes the repressor/activator protein 1, a transcription factor and telomere binding protein that is essential for viability in the budding yeast *Saccharomyces cerevisiae*. However, deletion of the *C.albicans* *RAP1* homolog did not affect viability or growth of the mutants, suggesting that it is not a promising target. *CBF1* (centromere binding factor 1) is necessary for proper chromosome segregation and transcriptional activation of methionine biosynthesis genes in *S.cerevisiae* and is essential for viability in the related yeasts *Kluyveromyces lactis* and *Candida glabrata*. Deletion of *CBF1* in *C.albicans* did not result in an increased frequency of chromosome loss, indicating that it has no role in chromosome segregation in this organism. However, the *C.albicans* $\Delta cbf1$ mutants exhibited severe growth impairment, temperature sensitivity at 42°C, and auxotrophy for sulphur amino acids, suggesting that Cbf1p is a transcription factor that is important for normal growth of *C.albicans*. *YIL19* is an essential gene in *S.cerevisiae* that is involved in 18S rRNA maturation. *YIL19* was found to be an essential gene also in *C.albicans*. Conditional mutants in which the *YIL19* gene could be excised from the genome by inducible, FLP-mediated recombination were non-viable and accumulated rRNA precursors, demonstrating that *YIL19* is essential for this important cellular process and for viability of *C.albicans* and could serve as a target for the development of antifungal drugs.

1. Zusammenfassung

Candida albicans ist ein opportunistisch pathogener Hefepilz, der sowohl oberflächliche Infektionen der Schleimhaut als auch lebensbedrohliche systemische Infektionen hervorrufen kann. Obwohl die Fähigkeit von *C.albicans* Infektionen auszulösen weitgehend vom Immunstatus des Wirts abhängt, besitzt der Pilz doch auch spezifische Eigenschaften, die eine Kolonisierung, Disseminierung und Anpassung an unterschiedliche Wirtsnischen ermöglichen und ihn vom harmlosen Kommensalen zum gefährlichen Krankheitserreger werden lassen. Unter bestimmten Umweltbedingungen geht *C.albicans* vom Wachstum als sprossende Hefe zum invasiven, filamentösen Wachstum über, das eine wichtige Rolle in der Pathogenität des Pilzes spielt. Stickstoffmangel ist eines der Signale, die das filamentöse Wachstum in *C.albicans* induzieren, und die Kontrolle der Morphogenese durch die Verfügbarkeit von Stickstoff wurde in dieser Arbeit detailliert untersucht.

Ammonium ist für Hefepilze eine bevorzugte Stickstoffquelle, die über spezifische Transporter in die Zelle aufgenommen wird. In der vorliegenden Arbeit konnte gezeigt werden, dass *C.albicans* zwei Ammoniumpermeasen besitzt, deren Expression durch Stickstoffmangel induziert wird. Während die Deletion von *CaMEP1* oder *CaMEP2* keinen Einfluss auf das Wachstum bei limitierenden Ammoniumkonzentrationen hatte, konnten $\Delta mep1 \Delta mep2$ Doppelmutanten bei Ammoniumkonzentrationen unter 5 mM nicht mehr wachsen. Im Gegensatz zu $\Delta mep1$ Mutanten bildeten $\Delta mep2$ Mutanten unter Stickstoffmangel keine Hyphen mehr und wuchsen ausschließlich in der Hefeform. CaMep2p hat also nicht nur eine Funktion als Ammoniumtransporter, sondern spielt auch eine Rolle bei der Induktion des filamentösen Wachstums. Weitere Experimente zeigten, dass CaMep2p ein weniger effizienter Ammoniumtransporter als CaMep1p ist, dafür aber stärker exprimiert wird, und dass dieser Unterschied wichtig für die Signalfunktion von CaMep2p ist. Durch Deletionsanalysen konnte bewiesen werden, dass die C-terminale, cytoplasmatische Domäne von CaMep2p essentiell für die Induktion des Hyphenwachstums ist, für den Ammoniumtransport jedoch nicht benötigt wird, und diese beiden Funktionen von CaMep2p daher voneinander getrennt werden können.

In *C.albicans* gibt es mindestens zwei Signalwege die das filamentöse Wachstum steuern, eine MAP-Kinase-Kaskade und einen cAMP-abhängigen Signalweg, die in den Transkriptionsfaktoren Cph1p bzw. Efg1p enden. Bei Inaktivierung des einen oder des anderen Signalwegs induziert Stickstoffmangel kein filamentöses Wachstum mehr. Ein

hyperaktives *CaMEP2* Allel konnte den filamentösen Wachstumsdefekt sowohl von $\Delta cph1$ als auch $\Delta efg1$ Mutanten aufheben, nicht jedoch den einer $\Delta cph1 \Delta efg1$ Doppelmutante oder einer Mutante, der das G-Protein Ras1p fehlte, das beide Signalwege aktiviert. Umgekehrt wurde der filamentöse Wachstumsdefekt von $\Delta mep2$ Mutanten durch ein dominant-aktives *RAS1* Allel bzw. durch die Zugabe von cAMP aufgehoben. Diese Ergebnisse deuten darauf hin, dass CaMep2p bei Stickstoffmangel sowohl den MAP-Kinase- als auch den cAMP-abhängigen Signalweg aktiviert, um filamentöses Wachstum zu induzieren. In genügend hohen Konzentrationen reprimierte Ammonium das filamentöse Wachstum selbst wenn die Signalwege artifiziiell aktiviert waren. Die bevorzugte Stickstoffquelle Ammonium ist deshalb ein Inhibitor der Morphogenese, der durch denselben Transporter in die Zelle aufgenommen wird, der bei Stickstoffmangel das filamentöse Wachstum von *C.albicans* induziert.

Obwohl ein genaues Verständnis der Virulenzmechanismen von *C.albicans* auch neue Ansätze zur Bekämpfung von Infektionen durch diesen Pilz liefern kann, ist doch die Identifizierung und Charakterisierung von essentiellen Genen als potentielle Ziele für die Entwicklung neuer Antimykotika eine Strategie, die von der pharmazeutischen Industrie favorisiert wird. Aus diesem Grund wurden in Zusammenarbeit mit einem Industriepartner drei Gene von *C.albicans* ausgewählt, die in anderen Pilzen als essentiell beschrieben wurden, und im Rahmen dieser Arbeit funktionell charakterisiert. *RAP1* codiert für das Repressor/Aktivator Protein 1, ein Transkriptionsfaktor und Telomerbindeprotein, das in der Bäckerhefe *Saccharomyces cerevisiae* essentiell ist. Die Deletion des *RAP1* Gens in *C.albicans* beeinträchtigte jedoch nicht die Lebensfähigkeit der Mutanten, so dass *RAP1* kein vielversprechendes Ziel darstellt. *CBF1* (centromere binding factor 1) ist in *S.cerevisiae* wichtig für die korrekte Chromosomenverteilung während der Mitose und außerdem auch für die transkriptionelle Aktivierung der Methioninbiosynthesegene; in den verwandten Hefen *Kluyveromyces lactis* und *Candida glabrata* ist *CBF1* sogar essentiell. *C.albicans* $\Delta cbf1$ Mutanten wiesen jedoch keinen erhöhten Chromosomenverlust auf, so dass *CBF1* hier offensichtlich keine Rolle bei der Chromosomensegregation spielt. Allerdings waren die Mutanten auxotroph für schwefelhaltige Aminosäuren und generell stark im Wachstum beeinträchtigt, was zeigte, dass Cbf1p für das normale Wachstum von *C.albicans* wichtig ist. *YIL19* ist in *S.cerevisiae* ein essentielles Gen und hat eine Funktion bei der Reifung der 18S rRNA. *YIL19* stellte sich auch in *C.albicans* als essentiell heraus. Konditionale Mutanten, in denen *YIL19* durch induzierbare, FLP-vermittelte Rekombination aus dem Genom deletiert wurde, waren nicht lebensfähig und akkumulierten rRNA Vorstufen. Durch diese Untersuchungen konnte gezeigt werden, dass *YIL19* essentiell für diesen wichtigen zellulären

Prozess und für die Lebensfähigkeit von *C.albicans* ist und sich möglicherweise als Ziel für die Entwicklung antifungaler Substanzen eignet.

2. Introduction

2.1. *Candida albicans*: an opportunistic human fungal pathogen

The latter half of the twentieth century has seen enormous advancement in the field of medicine and surgery. This has led to the emergence of various forms of organ transplantation and cancer chemotherapy as essential medical treatment, automatically involving immunosuppression as part of the procedure. Although many health problems have been adequately addressed in this manner, the ceaseless development in modern medicine has led to the creation of “at risk individuals”, who are extremely susceptible to infections. The increasing number of immunodeficient individuals due to rapid increase in the incidence of AIDS has resulted in an epidemic of diseases caused by opportunistic fungal pathogens. Of particular interest is candidiasis, a disease caused by members of the *Candida* genus. The prevalent cause of candidiasis is *Candida albicans*, often regarded as the most common opportunistic fungal pathogen.

There are several predisposing factors for *C.albicans* to alter from a state of a relatively quiescent commensalism to an aggressive pathogenic lifecycle. When immune systems are weak (for example, as a result of cancer chemotherapy, HIV infection or in neonates) or when the competing flora is eliminated (for example, after antibiotic treatment), *C.albicans* colonizes and invades host tissues. Although HIV patients frequently suffer from recurring oral candidiasis and sometimes die from advanced oesophageal colonization, infections of mucosal tissues such as thrush and vaginitis are usually not life threatening. However, if the organism gains access to the bloodstream (a condition known as candidaemia), by invasion of host tissues or by contamination of indwelling catheters, the infection can progress to the growth of fungal masses in the kidney, heart or brain.

Current treatments for systemic fungal infections have toxic side effects and exhibit poor efficacy. Most commonly used antifungals inhibit the ergosterol biosynthetic pathway and chiefly include azoles, allylamines and morpholines. Others, such as polyenes and 5-FC, impair membrane barrier function and macromolecule synthesis respectively (Vanden Bossche, 1997). The incidence of *C.albicans* cells acquiring resistance to antifungals like azoles has increased considerably in recent years which has posed serious problems towards its successful chemotherapy (Cowen *et al.*, 2000; Kakeya *et al.*, 2000; White *et al.*, 1998; Rex *et al.*, 1995; Sternberg, 1994), probably due to rampant use of azole drugs on cancer and AIDS patients suffering from secondary fungal infections. Drug pressure leads to the generation of resistant cells with random mutations, or transient expression of genes which

can alter the phenotype of the cells (White *et al.*, 1998). New antifungal agents targeting *C.albicans* and other opportunistic pathogens are therefore urgently needed. To develop such new therapies and treatments for candidiasis, it is essential to dissect the infectious process of *C.albicans*.

Experimental work on *C.albicans* has long been hampered by its asexuality, its diploidy and its non-canonical codon usage (CUG encodes serine instead of leucine) (Scherer and Magee, 1990; Santos *et al.*, 1996). Molecular genetic techniques have overcome these difficulties and today a number of host strains and transformation vectors are available and efficient gene-disruption protocols have been developed (Fonzi and Irwin, 1993; Morschhäuser *et al.*, 1999; Wilson *et al.*, 1999). New molecular methods to study gene functions in *C.albicans* have been designed (Theiss *et al.*, 2002; Michel *et al.*, 2002; Gerami-Nejad *et al.*, 2001; De Backer *et al.*, 2001). Antibody based strategy has been employed to identify genes expressed during infection (Cheng *et al.*, 2003). Reporter genes encoding β -galactosidase, luciferase, and green fluorescent protein (GFP) are available (Srikantha *et al.*, 1996; Cormack *et al.*, 1997; Morschhäuser *et al.*, 1998; Uhl and Johnson, 2001). The *C.albicans* genome sequence is currently completed at Stanford University (<http://www-sequence.stanford.edu/group/candida/>), heralding new challenges in proteomic research and functional analysis of the gene products.

Rapid advances of many basic biological processes in *C.albicans* have been made as a result of their similarity to well studied processes in *Saccharomyces cerevisiae*, which diverged from *C.albicans* many years ago. There is hope that recently developed techniques of manipulating *C.albicans* and the sequencing of its genome will lead to a thorough understanding of the virulence and biology of this fungal pathogen, thus offering the possibility of a knowledge-based approach to developing novel antifungal agents.

2.2. Virulence determinants of *C.albicans*

C.albicans needs to use several attributes which are potential pathogenicity factors to establish pathogenesis in the host. These include cell surface composition and phenotypic switching which is accompanied by changes in antigen expression, enzyme production, dimorphism, colony morphology, and tissue affinities (Calderone and Fonzi, 2001). *C.albicans* virulence is a function of multiple factors working jointly to overcome the host defence systems. A lack or debility in any of these factors will negatively affect its infectivity

and make it difficult for *Candida* to establish itself, particularly in a healthy individual (Ghannoum and Abu-Elteen, 1990).

Lytic enzymes

Like many other pathogenic organisms, *C.albicans* secretes extracellular enzymes such as hydrolases with relative broad specificities, including proteinases, phospholipases, lipases, and an acid phosphomonoesterase. These are involved in fungal invasion and destruction of host tissue.

Phospholipases play a significant role in damaging cell membranes and invading host cells. High phospholipase production is correlated with an increased adherence and a higher mortality rate in animal models (Mayser *et al.*, 1996). The secreted aspartyl proteinases are thought to contribute to virulence through their effects on adherence, invasion, and pathogenicity. So far, ten distinct *SAP* genes (*SAP1* to *SAP10*) have been identified and recent studies by Hube, Sanglard and colleagues implicated the involvement of Sap proteins in virulence (Hube *et al.*, 1997; Sanglard *et al.*, 1997).

Adherence

The *C.albicans* cell surface possesses several ligands, such as receptors for C3d, iC3b, fibrinogen, laminin, fibronectin, or fucose, that bind specifically and selectively to host components. The surface adhesins of *C.albicans* can either bind to the host Arg-Gly-Asp (RGD) sequences or to the sugar moiety of host membrane glycoproteins. Important adhesins reported from *C.albicans* are Als1p, Ala1p/Als5p and Hwp1p which are members of a class of proteins termed as glycosylphosphatidylinositol-dependent cell wall proteins (GPI-CWP). Another protein, Int1p, not belonging to this class is also involved in adhesion (Sundstrom, 2002).

Dimorphism in *Candida albicans*

One of the most remarkable aspects of *C.albicans* biology is its ability to assume a variety of cell morphologies. It is almost universally described as ‘dimorphic’, yet its cell morphology actually lies on a pleomorphic continuum from ovoid yeast cells to filamentous hyphae. Thus, the various cell morphologies exhibited in the organism range from yeast-like cells to a plethora of elongated growth forms, including a thread-like hyphal growth form, germ tubes and pseudohyphae, which vary in shape from attached strings of yeast-like cells to long filaments (Fig. 1) (Corner and Magee, 1997). The elongation of buds in pseudohyphae

can be so extreme that these filaments can superficially resemble hyphae. Because of this, it is often useful to refer pseudohyphae and hyphae collectively and the term ‘filamentous form’ has been used further here for this purpose. Another morphological form is the chlamyospore, which is thick-walled, relatively large round structure with condensed cytoplasm. It is considered a resistance form and is believed to be produced generally under unfavorable environmental conditions for the fungus (Odds, 1988).

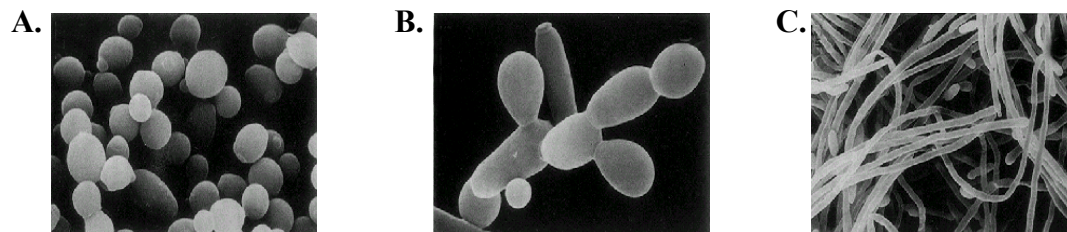


Fig. 1. Scanning electron micrographs of different morphologies of *Candida albicans*. **A.** Yeast **B.** Pseudohyphae. **C.** Hyphae (adapted from Odds, 1988).

Under *in vitro* conditions, the yeast or blastospore form is readily obtained following growth on most solid or liquid media. The transition into the hyphal (including pseudohyphal) form can occur under the influence of a variety of environmental factors such as changes in media composition, addition of serum, N-acetyl glucosamine (GlcNAc), or proline, growth under CO₂ or semi-anaerobic conditions, or even a shift from acidic to neutral pH. With regard to morphogenesis, there is a long history of attempts to prove a relationship between the filamentous form of *C. albicans* and virulence (Odds, 1988). The ability to switch to filamentous growth has been shown to be important for virulence of *C. albicans* (Lo *et al.*, 1997; Saville *et al.*, 2003; Zheng and Wang, 2004). As emphasized by numerous investigators, most lesions are populated by both morphological forms, suggesting that both have a role in the development and progression of the disease. The filamentous form may be required to evade the cells of the immune system, whereas the yeast form may be the mode of dissemination in the bloodstream. The filamentous forms might also be important for the colonization of organs, such as the kidney. The characterization of a filamentous state in the baker's yeast *S. cerevisiae* has made it possible to use this as a model to compare regulation of filamentation in *C. albicans* and *S. cerevisiae* (Gimeno *et al.*, 1992).

Signaling pathways and regulators involved in dimorphism of *C.albicans*

Recent studies indicate that *C.albicans* uses a common set of conserved pathways to regulate dimorphism, mating and phenotypic switching. Major pathways known to regulate dimorphism include a MAP Kinase pathway via Cph1p and the cAMP-dependent protein kinase pathway through Efg1p (Fig. 2). Dimorphism of *C.albicans* is also under the control of Tup1p-mediated repression through Rfg1p and Nrg1p (Braun and Johnson, 1997; Braun *et al.*, 2001; Murad *et al.*, 2001a and b; Khalaf and Zitomer, 2001; Kadosh and Johnson, 2001). In addition, a pH response is mediated by a pathway that activates the Rim101p transcription factor (Porta *et al.*, 1999; Ramon *et al.*, 1999; Davis *et al.*, 2000; El Barkani *et al.*, 2000) and a response to embedding in a solid matrix is mediated by a pathway that activates the Czf1p transcription factor (Brown *et al.*, 1999). A high proportion of the genes controlled by these signaling pathways contribute directly or indirectly to pathogenesis and virulence of *C.albicans*, therefore, virulence genes are co-regulated with cell morphogenesis (Liu, 2002).

a) MAP Kinase Pathway

A mitogen-activated protein kinase (MAPK) pathway is involved in filamentation in *C.albicans*. The cascade consists of the kinases Cst20p (homologous to the p21-activated kinase [PAK] kinase Ste20p), CaSte7p/Hst7p (homologous to the MAP kinase kinase Ste7p), and Cek1p (homologous to the Fus3p and Kss1p MAP kinases) (Clark *et al.*, 1995; Köhler and Fink, 1996; Leberer *et al.*, 1996; Singh *et al.*, 1997; Whiteway *et al.*, 1992). A transcription factor, Cph1p, which is homologous to Ste12p that regulates mating and pseudohyphal growth in *S.cerevisiae*, has been identified (Liu *et al.*, 1994). Null mutations in any of the genes in the MAP kinase cascade (Cst20p, Hst7p, or Cek1p) or the transcription factor Cph1p confer a hyphal defect on solid medium in response to many inducing conditions; however, all of these mutants filament normally in response to serum (Csank *et al.*, 1998; Köhler and Fink, 1996; Leberer *et al.*, 1996).

In addition to these components, a MAP kinase phosphatase, Cpp1p, has been identified which regulates filamentous growth in *C.albicans* (Csank *et al.*, 1997). Disruption of both alleles of the *CPPI* gene derepresses hyphal production and results in a hyperfilamentous phenotype. This hyperfilamentation is suppressed by deletion of the MAP kinase *CEK1* (Csank *et al.*, 1997). The *cpp1* mutant strains are also reduced for virulence in both systemic and localized models of candidiasis (Csank *et al.*, 1997; Guhad *et al.*, 1998a).

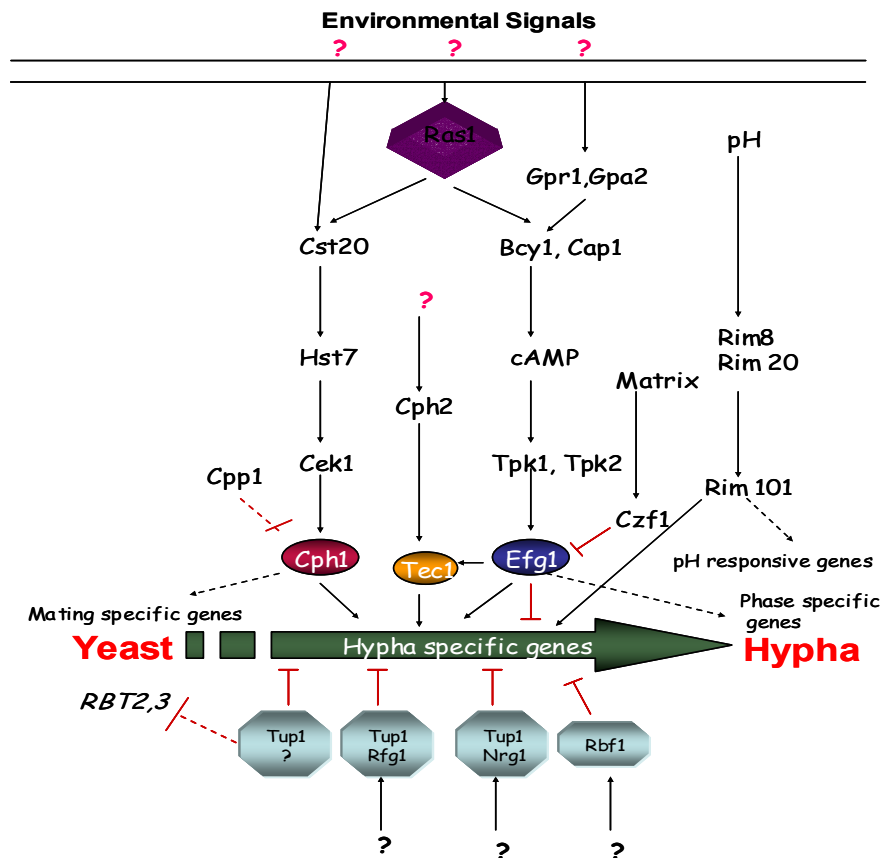


Fig. 2. Regulation of dimorphism in *C.albicans* by multiple signaling pathways (adapted from Liu, 2001).

b) cAMP-PKA Pathway

The cAMP-dependent protein kinase A (PKA) pathway plays a very important role in filamentation in *S.cerevisiae*, *C.albicans* and other fungi (Sonneborn *et al.*, 2000). In *C.albicans*, an increase in cAMP level accompanies the yeast to hyphal transition, and inhibition of the cAMP phosphodiesterase induces this transition (Sabie and Gadd, 1992).

Genes similar to *GPA2*, encoding a small G-protein, and *GPR1*, coding for a G-protein coupled receptor have been reported to regulate morphogenesis and hypha formation in *C.albicans* and they act upstream of the cAMP signaling pathway (Miwa *et al.*, 2004), but *GPA2* also has been shown to act upstream of the MAP kinase pathway (Sanchez-Martinez and Perez-Martin, 2002). *C.albicans* has a single gene homologous to the *S.cerevisiae* adenylate cyclase gene (*CDC35/CYR1*). The cyclase is not essential for growth in *C.albicans*, but is required for hyphal development (Rocha *et al.*, 2001). Recently, the adenylate cyclase associated protein (*CAP1*) has been identified and disrupted (Bahn and Sundstrom, 2001). An

increase in cytoplasmic cAMP is seen to precede germ tube emergence in wild-type strains, but not in *cap1* mutants. The *cap1* mutant is defective in germ tube formation and hyphal development, the defects being suppressible by exogenous cAMP or dibutyryl cAMP. The *cap1* strains are avirulent in a mouse model for systemic candidosis.

A single Ras (small G-protein) homolog, Ras1p, has been identified in *C.albicans*, which is not essential for survival (Feng *et al.*, 1999). The *ras1* mutant strains have a severe defect in hyphal growth in response to serum and other conditions (Feng *et al.*, 1999). In addition, while a dominant negative Ras1 mutation (Ras1^{G16A}) caused a defect in filamentation, a dominant active Ras1 mutation (Ras1^{G13V}) enhanced the formation of hyphae (Feng *et al.*, 1999). The *in vitro* defects in morphological transition were reversed by either supplementing the growth media with cAMP or over expressing components of the filament inducing MAP Kinase cascade, demonstrating that it functions upstream of both the cyclic AMP as well as the MAP Kinase pathway (Leberer *et al.*, 2001). The Ras1 protein is likely to activate the two protein kinase A (PKA) isoforms, Tpk1p and Tpk2p of the cAMP pathway through activation of the adenylate cyclase (Bockmühl *et al.*, 2001; Cloutier *et al.*, 2003). Efg1p, a basic helix-loop-helix (bHLH) protein functions at downstream of the PKAs. Under standard induction conditions, using serum or GlcNAc as inducers in liquid or on solid media, there is a complete block of hyphal formation in *efg1* null mutants (Lo *et al.*, 1997; Stoldt *et al.*, 1997). Contrastingly, under microaerophilic or embedded conditions hyphal formation is not defective at all in homozygous *efg1* mutants, but rather appears stimulated (Giusani *et al.*, 2002). These results indicate that depending on environmental cues (and depending on the genetic background) Efg1p has a dual role as a transcriptional activator and repressor, whose balanced activity is essential for yeast, pseudohyphal and hyphal morphogenesis of *C.albicans*. Strains with mutations in both Cph1p and Efg1p are defective in filament formation in most of the filament inducing mediums and are avirulent in mouse model of infection (Lo *et al.*, 1997). Recent studies have shown the involvement of *EFG1* in normal biofilm formation (Ramage *et al.*, 2002). Studies by Sohn *et al.* (2003) revealed that this transcription factor is a major regulator of cell wall dynamics in *C.albicans*.

Apart from these two major signal transduction pathways, other genes like *TEC1* or *CPH2* have also been found to regulate hyphal development in *C.albicans* (Schweizer *et al.*, 2000, Lane *et al.*, 2001b). The *tec1* mutants exhibit suppressed filamentation in liquid serum-containing media and the *EFG1* overexpression does not suppress the morphological defect of the *tec1* mutant, whereas *TEC1* overexpression has a partial phenotype in the *efg1* mutant (Schweizer *et al.*, 2000). These results, coupled with the fact that the *efg1* strains have a more

severe defect in hyphal development than do *tec1* strains, suggest that *TEC1* is one of the downstream effectors of Efg1p. The function of Cph2p in hyphal transcription is mediated, in part, through Tec1p (Lane *et al.*, 2001b).

A picture of the complex regulatory network that controls morphogenetic switch of *C.albicans* is emerging but a major challenge is to determine how this organism senses the environmental factors that induce yeast cells to form hyphae and pseudohyphae.

Other factors involved in virulence

Several other factors are known to influence the virulence of *C.albicans* though the mechanisms involved are still not clear. *C.albicans* is capable of undergoing a different type of morphological change that has been termed as “phenotypic switching”. A simpler, biphasic ‘white-opaque’ switching system, found in *C.albicans* strain WO-1, involves a switch between white, domed colonies that contain typical yeast cells and opaque, flat colonies that contain characteristically oblong cells. White and opaque cultures have different virulence properties (Soll, 1992). Stage specific gene expression of *C.albicans* in human blood showed that differentially expressed genes included those that are involved in the general stress response, antioxidative response, glyoxalate cycle as well as putative virulence attributes (Fradin *et al.*, 2003).

Among the different virulence properties of this fungus, the morphological conversion from yeast to filamentous growth forms are of particular interest because these morphological spectra are thought to be required for adaptation in warm-blooded hosts, rapid colonization of tissues and spread of infection. Numerous conditions promote yeast-hypha morphogenesis *in vitro*. However, the exact nature of many morphogenetic signals is poorly understood, particularly how the fungus senses nutrient starvation, e.g. nitrogen starvation.

2.3. Nitrogen regulation: Role in virulence and dimorphism

It is essential that microorganisms sense the nutrients available in the surroundings and respond rapidly to changes of the nutritional status. Therefore, the cells must be able to perceive how much of each required nutrient is available in its immediate surroundings (sensing), transmit this information to the nucleus (signaling) and switch specific sets of genes on or off (transcription) to initiate cellular programs to respond to the specific conditions. Nitrogen (N) plays a critical role in microorganism biochemistry, being needed for the synthesis of many compounds, including amino acids, purines, pyrimidines, some

carbohydrates and lipids, enzyme co-factors and proteins, all of which are essential for growth processes. Many microorganisms have the ability to use a variety of nitrogen-containing compounds as the sole source of all cellular nitrogen. Certain nitrogenous compounds (e.g. ammonia, glutamine and glutamate) are preferentially used by the fungi and are considered as a good nitrogen sources. However, when these nitrogen sources are not available or are present at concentrations low enough to limit growth, many different nitrogen sources can be used, e.g., nitrate, nitrite, purines, amides, most amino acids and proteins. This ability of an organism to use any compound as nitrogen source requires permeases for the transport of these compounds into the cell and enzymes for the generation of ammonia by their metabolism. Once inside the cell, ammonia in the presence of the NADP-linked enzyme glutamate dehydrogenase, can react with α -ketoglutarate, provided by the metabolism of the carbon source of the growth medium, to produce glutamate. Glutamine synthetase catalyzes the incorporation of ammonium into glutamate to form glutamine. Glutamate and glutamine serve as the source of cellular nitrogen (Magasanik, 1992). Utilization of any of the secondary nitrogen sources is highly regulated and nearly always requires the synthesis of a set of pathway specific catabolic enzymes and permeases which are otherwise repressed in the presence of good nitrogen sources (nitrogen catabolite repression). Nitrogen regulation is controlled by global positive and negative transcription factors, as well as pathway specific transcription factors (Coffman *et al.*, 1997; Marzluf, 1997). The global factors are members of the GATA family of transcription factors, the name reflecting the core DNA sequence recognized by the defining zinc-finger domain (Teakle and Gilmartin, 1998). The principal transcriptional activator is highly conserved amongst fungi and typified by the AREA protein of *Aspergillus* spp., NIT-2 of *Neurospora crassa* and, the dual factors encoded by *GLN3* and *GAT1* of *S.cerevisiae* (Marzluf, 1997). In the absence of, or limitation of, a primary nitrogen sources like ammonium, these factors activate expression of genes involved in secondary nitrogen metabolism either alone or in conjunction with pathway specific factors (Marzluf, 1997). Evidence of nitrogen catabolite repression in the opportunistic fungal pathogen *Candida albicans* includes the observations that ammonium inhibits expression of peptide transporters (Payne *et al.*, 1991; Basrai *et al.*, 1992), induction of proline uptake (Holmes and Shepherd, 1987) and expression of secreted aspartyl proteinase (Ross *et al.*, 1990; Banerjee *et al.*, 1991; Hube *et al.*, 1994; White and Agabian, 1995).

Nutritional limitation of various types, particularly nitrogen deprivation appears to have a link to pathogenesis and other morphological switches. For instance, haploid MAT α cells of *Cryptococcus neoformans*, which typically grow as yeast, will develop fruiting bodies

and hyphae in response to nitrogen deficiency and the fruiting bodies form haploid basidiospores, which are suspected to be the infectious propagule (Wickes *et al.*, 1996). Virulence of *Aspergillus fumigatus* is dependent upon its ability to respond to nitrogen limitation *in vivo* (Hensel *et al.*, 1998). Nitrogen starvation signals the development of rice blast disease symptoms by *Magnaporthe grisea* (Talbot *et al.*, 1997). Recently Limjindaporn *et al.* (2003) have shown that mutation in the zinc-finger containing transcriptional activator *GAT1*, which control nitrogen catabolite repression of several genes, causes the attenuation of virulence in a murine model of disseminated candidiasis. This indicates a significant role of nitrogen regulation in the infectious process of *C.albicans*. Thus, it seems possible that loss of a major nitrogen regulatory factor will significantly reduce the virulence of plant or animal pathogenic fungi.

2.3.1. Ammonium permeases and nitrogen starvation induced dimorphism of yeast

Severe nitrogen starvation induces diploid *S.cerevisiae* yeast cells to differentiate into a filamentous, pseudohyphal growth form, which may enable these non-motile organisms to seek a preferable environment (Gimeno *et al.*, 1992). Moreover, the yeast to pseudohyphal transition of *S.cerevisiae* is under nitrogen catabolite repression (Gimeno *et al.*, 1992; Lorenz and Heitman, 1998a, b) and for the nitrogen repression a good nitrogen source like ammonium has to be transported inside the cell. Multiple transport systems with different kinetic properties and regulation are often present to transport molecules into the cells and enable the cells to grow in different environmental conditions. The first evidence that specific ammonium transport system acts in fungi came from the work of Hackette *et al.* (1970) in *Penicillium chrysogenum*. The genes involved in ammonium transport were cloned from yeast (Marini *et al.*, 1994), *Arabidopsis* (Ninnemann *et al.*, 1994), bacteria (Thomas *et al.*, 2000), fungi (Monahan *et al.*, 2002a, b; Montanini *et al.*, 2002; Javelle *et al.*, 2003a, b; Smith *et al.*, 2003) and homologues have been found in humans (Marini *et al.*, 2000a). All members in the MEP/AMT family are membrane proteins with an extracytosolic amino terminus and a central hydrophobic core of 10-12 transmembrane helices (Thomas *et al.*, 2000; Javelle *et al.*, 2003b). In *S.cerevisiae* ammonium uptake is well characterized and possibly involves at least 3 ammonium permeases named as Mep1p, Mep2p and Mep3p. Mep2p displays highest affinity for ammonium (K_m 1-2 μ M), followed closely by Mep1p (K_m 5-10 μ M), and finally Mep3p, whose affinity is much lower (K_m ~1.4-2.1 mM) (Marini *et al.*, 1997). The *MEP* genes are subject to nitrogen control and on poor nitrogen sources *MEP2* expression is much higher than *MEP1* or *MEP3* expression (Marini *et al.*, 1997). A mutant strain lacking all three

Mep proteins can not grow on media containing less than 5 mM ammonium as the sole nitrogen source, while the presence of individual ammonium transporters enables growth on these media. Growth on media containing higher than 20 mM ammonium does not require any of these permeases (Marini *et al.*, 1997). The Mep transporters are also required to retain ammonium inside the cells during growth on some nitrogen sources other than ammonium (Marini *et al.*, 1997). Among the three Mep proteins, the Mep2p, but not Mep1p or Mep3p, has been proposed to act as an ammonium sensor that generates a signal to induce filamentous growth of *S.cerevisiae* in low ammonium conditions (Lorenz and Heitman, 1998a). However, how ammonium is sensed by Mep2p and how this signal is transduced to activate pseudohyphal growth has not been resolved. The pseudohyphal growth defect of $\Delta mep2$ mutants of *S.cerevisiae* was not suppressed when the MAP kinase cascade was activated by the dominant *STE11-4* allele, but it was suppressed by activated alleles of *GPA2* or *RAS2* or by exogenous cAMP, indicating that Mep2p signals through the cAMP pathway to induce pseudohyphal growth under low ammonium conditions (Lorenz and Heitman, 1998a). Recently it has also been shown that one of the *MEP* homologs from the plant pathogenic fungus *Ustilago maydis* is required for triggering filamentous growth on low nitrogen medium (Smith *et al.*, 2003). Moreover, this gene can complement the pseudohyphal growth defect of the *mep2* mutant in *S.cerevisiae* (Smith *et al.*, 2003).

Nitrogen starvation induces filamentous growth also in the yeast *Candida albicans* (Csank *et al.*, 1998) and recent work has implicated *GCN4*, which regulates the general amino acid starvation response, and *CSH3* which is specifically required for proper uptake and sensing extracellular amino acids, in the regulation of dimorphism (Tripathi *et al.*, 2002; Martinez and Ljungdahl, 2003) of this pathogen. The potential importance of nitrogen regulation and ammonium transporters, in dimorphism of *C.albicans* is of particular interest to understand the molecular basis of one of the virulence determinants of this pathogenic fungus.

2.4. An approach towards anti-candida drug development

C.albicans is eukaryote and therefore shares many biological processes with humans. Most of the antifungal drugs used to control *Candida* infections have deleterious side effects and at the doses used, are fungistatic rather than fungicidal. Moreover, the use of these drugs has resulted in resistant *C.albicans* strains and limits the use of these agents. So, it is an

important goal of *C.albicans* research to identify appropriate targets for antifungal technologies. Understanding virulence properties of this opportunist may lead to the development of therapies that will prevent or treat candidiasis in susceptible patients. On the other hand, completion of the genome sequencing of this pathogen allows the identification of all the potential antifungal targets in a genome, that is, all the gene products whose inactivation would lead to growth arrest, and optimally, fungal death. On this basis, rational approaches can be developed to search for new antifungal compounds that inhibit the function of these gene products and have a fungistatic or fungicidal effect. Target prioritization is nevertheless needed for optimal drug development and can rely on several criteria including conservation among other pathogenic fungi and significant divergence in higher eukaryotes, fungicidal and availability of a gene expression or proteomic signature upon target depletion as well as biochemical criteria (Black and Hare, 2000).

A category of targets that has attracted interest is virulence factors, as their inactivation is likely to block the progression of disease before the return to normal immunological status. But the studies, aimed at characterizing the virulence proteins suggest that virulence does not depend upon a single molecular determinant. It has therefore become evident that the search for new antifungal targets must take into account those genes that are essential both *in vitro* and *in vivo*. The term 'essential genes' refers most frequently to those genes necessary for microbial growth on rich medium. Various technologies to study essential genes in *C.albicans* have been developed in recent years which include post transcriptional gene silencing by antisense RNA (De Backer *et al.*, 2001), conditional gene expression by deleting one allele of the target gene and placing the second copy under the control of a regulatable promoter (Care *et al.*, 1999; Backen *et al.*, 2000; Nakayama *et al.*, 2000) and an approach of making conditional lethal null mutants based on inducible deletion of essential genes by FLP-mediated excision from the genome (Michel *et al.*, 2002). These approaches should enable researchers to identify and characterize essential genes of this opportunistic pathogen, which is the subject of intense research efforts in both academia and industry. Moreover, conditional expression of an essential gene allows the design of high-throughput screens for candidate drug identification and target validation. From a more academic viewpoint, several essential genes identified are of unknown function and their characterization will represent an interesting source of knowledge on the biology of fungi.

2.5. Aim of the study

The yeast *Candida albicans*, the most important human pathogenic fungus, serves as a model organism for studying fungal virulence. The virulence of this pathogen is associated with the ability to switch between the yeast and hyphal morphologies and nutrient starvation acts as an inducer for this switch. To understand the virulence properties of *C.albicans*, the nitrogen starvation induced filament formation and the role of ammonium and ammonium permeases in this transition were analyzed. Moreover, in an attempt to identify a candidate gene for antifungal drug development some genes were also characterized to analyze the essentiality of those genes in this pathogen. To select the putative essential genes knowledge of functional genomics of *S.cerevisiae* was used and *RAP1* (Repressor/Activator protein1), *CBF1* (Centromere Binding Factor1) and *YLL19* were chosen based on their essential function in *S.cerevisiae* or in other yeasts, conservation among other pathogenic fungi and absence of their highly similar homologs in higher eukaryotes. Those genes were functionally characterized in *C.albicans* to select an essential gene for antifungal drug design.

3. Materials and Methods

3.1. Bacteria strain used

Escherichia coli K12 : *E.coli* strain DH5 α (F⁻, *endA1*, *hsdR17* [*r_k*⁻, *m_k*⁻], *supE44*, *thi-1*, *recA1*, *gyrA96*, *relA1*, Δ [*argF-lac*]U169, λ ⁻, ϕ 80*dlacZ* Δ M15) was used for cloning experiments.

3.2. Plasmids used in this study

Cloning vector used in this study was pBluescript KS II (Stratagene, Heidelberg, Germany).

Table 1.

Plasmid	Relevant insert	Reference
For <i>CaMEP1</i> and <i>CaMEP2</i> deletion		
pMEP1M1	[5' <i>YMR211-FRT-SAP2P-caFLP-ACT1T-URA3-FRT-3' MEP1</i>]-Fragment	This study
pMEP1M2	[5' <i>MEP1-FRT-SAP2P-caFLP-ACT1T-URA3-FRT-3' MEP1</i>]-Fragment	This study
pMEP1M3	[5' <i>MEP1-ACT1T-URA3-3' ACT1</i>]-Fragment	This study
pMEP1M4	[5' <i>MEP1-ACT1T-URA3-3' MEP1</i>]-Fragment	This study
pMEP2M1	[5' <i>MEP2-FRT-SAP2P-caFLP-ACT1T-URA3-FRT-3' CBF1</i>]-Fragment	This study
pMEP2M2	[5' <i>MEP2-FRT-SAP2P-caFLP-ACT1T-URA3-FRT-3' MEP2</i>]-Fragment	This study
pMEP2M3	[5' <i>CBF1-ACT1T-URA3-3' MEP2</i>]-Fragment	This study
pMEP2M4	[5' <i>MEP2-ACT1T-URA3-3' MEP2</i>]-Fragment	This study
Plasmids containing <i>lacZ</i> reporter gene fusions		
pAU36	<i>Streptococcus thermophilus lacZ</i>	(Uhl and Johnson, 2001)
pLACZ2	[<i>lacZ</i>]-Fragment	This study
pLACZ3	[<i>lacZ-ACT1T</i>]-Fragment	This study
pLACZ4	[<i>ACT1P-lacZ-ACT1T</i>]-Fragment	This study

Plasmid	Relevant insert	Reference
pMEP1LACZ2	[MEP2P-lacZ-ACT1T-URA3-3'MEP1]-Fragment	This study
pMEP1LACZ3	[MEP1P-lacZ-ACT1T-URA3-3'MEP1]-Fragment	This study
pMEP2LACZ1	[MEP2P-lacZ]-Fragment	This study
pMEP2LACZ2	[MEP2P-lacZ-ACT1T-URA3-3'MEP2]-Fragment	This study
CaMEP1 and CaMEP2 under different promoters		
pMEP1K1	[MEP1P-MEP1-ACT1T-URA3-3'MEP1]-Fragment	This study
pMEP1K2	[MEP2P-MEP1-ACT1T-URA3-3'MEP2]-Fragment	This study
pMEP1E2	[ADH1P-MEP1-ACT1T-URA3-3'ADH1]-Fragment	This study
pMEP2K1	[MEP2P-MEP2-ACT1T-URA3-3'MEP2]-Fragment	This study
pMEP2K2	[MEP1P-MEP2-ACT1T-URA3-3'MEP1]-Fragment	This study
pMEP2E2	[ADH1P-MEP2-ACT1T-URA3-3'ADH1]-Fragment	This study
pYPR127E2	[ADH1P-YPR127-ACT1T-URA3-3'ADH1]-Fragment	(Kusch <i>et al.</i> , 2004)
GFP-tagged CaMEP1 and CaMEP2 genes		
pADH1G2	[ADH1P-GFP-ACT1T-URA3-3'ADH1]-Fragment	(Kusch <i>et al.</i> , 2004)
pOP4G1	[OP4P-OP4-GFP-ACT1T-URA3-3'OP4]-Fragment	(Park YN, unpublished)
pMEP1G1	[MEP1P-MEP1-GFP-ACT1T-URA3-3'MEP1]-Fragment	This study
pMEP1G2	[MEP2P-MEP1-GFP-ACT1T-URA3-3'MEP2]-Fragment	This study
pMEP1G3	[ADH1P-MEP1-GFP-ACT1T-URA3-3'ADH1]-Fragment	This study
pMEP2G1	[MEP2P-MEP2-GFP-ACT1T-URA3-3'OP4]-Fragment	This study
pMEP2G2	[MEP2P-MEP2-GFP-ACT1T-URA3-3'MEP2]-Fragment	This study
pMEP2G4	[ADH1P-MEP2-GFP-ACT1T-URA3-3'ADH1]-Fragment	This study
pMEP2G5	[MEP1P-MEP2-GFP-ACT1T-URA3-3'MEP1]-Fragment	This study
Truncation of CaMEP1 and CaMEP2 genes		
pMEP1ΔC1	[MEP1P-MEP1ΔC ⁴⁰⁴ -ACT1T-URA3-3'MEP1]-Fragment	This study
pMEP1ΔC2	[MEP1P-MEP1ΔC ⁴³⁸ -ACT1T-URA3-3'MEP1]-Fragment	This study
pMEP2ΔC1	[MEP2P-MEP2ΔC ⁴⁰⁶ -ACT1T-URA3-3'MEP2]-Fragment	This study
pMEP2ΔC2	[MEP2P-MEP2ΔC ⁴⁴⁰ -ACT1T-URA3-3'MEP2]-Fragment	This study
pMEP2ΔC3	[MEP2P-MEP2ΔC ⁴²³ -ACT1T-URA3-3'MEP2]-Fragment	This study
pMEP2ΔC4	[MEP2P-MEP2ΔC ⁴¹³ -ACT1T-URA3-3'MEP2]-Fragment	This study

Plasmid	Relevant insert	Reference
MEP Hybrids		
pMEP12H2	[MEP1P-MEP1 ¹⁻⁴¹⁶ -MEP2 ⁴¹⁹⁻⁴⁸⁰ -ACTIT-URA3-3'MEP1]-Fragment	This study
pMEP12H3	[MEP2P-MEP1 ¹⁻⁴¹⁶ -MEP2 ⁴¹⁹⁻⁴⁸⁰ -ACTIT-URA3-3'MEP2]-Fragment	This study
pMEP12H4	[MEP2P-MEP1 ¹⁻⁴¹⁶ -MEP2 ⁴¹⁹⁻⁴⁴⁰ -ACTIT-URA3-3'MEP2]-Fragment	This study
pMEP21H2	[MEP2P-MEP2 ¹⁻⁴¹⁸ -MEP1 ⁴¹⁷⁻⁵³⁴ -ACTIT-URA3-3'MEP2]-Fragment	This study
Dominant active RAS1^{G13V} and GPA2^{Q354L} alleles		
pGFP31	[ACT1P-GFP-ACTIT-URA3-3'ACTI]-Fragment	(Morschhäuser <i>et al.</i> , 1998)
pGPA2	[5'CBF1-GPA2 ^{Q354L} -URA3-FRT-3'ACTI]-Fragment	This study
pRAS1E1	[ACT1P-RAS1 ^{G13V} -ACTIT-URA3-3'ACTI]-Fragment	This study
pGPA2E1	[ACT1P-GPA2 ^{Q354L} -ACTIT-URA3-3'ACTI]-Fragment	This study
For CaRAP1 deletion and complementation		
pRAP1M1	[5'YMR211-FRT-SAP2P-caFLP-ACTIT-URA3-FRT-3'RAP1]-Fragment	This study
pRAP1M2	[5'RAP1-FRT-SAP2P-caFLP-ACTIT-URA3-FRT-3'RAP1]-Fragment	This study
pRAP1M3	[5'CBF1-ACTIT-URA3-3'RAP1]-Fragment	This study
pRAP1M4	[5'RAP1-ACTIT-URA3-3'RAP1]-Fragment	This study
pRAP1K1	[RAP1P-RAP1-ACTIT-URA3-3'RAP1]-Fragment	This study
pRSRAP1 ^a	[RAP1P-RAP1-ACTIT]-Fragment	This study
For the analysis of CaCBF1		
pCBF1M1	[5'YMR211-FRT-SAP2P-caFLP-ACTIT-URA3-FRT-3'CBF1]-Fragment	This study
pCBF1M2	[5'CBF1-FRT-SAP2P-caFLP-ACTIT-URA3-FRT-3'CBF1]-Fragment	This study
pCBF1M3	[5'CBF1-ACTIT-URA3-3'ACTI]-Fragment	This study
pCBF1M4	[5'CBF1-ACTIT-URA3-3'CBF1]-Fragment	This study
pCBF1K1	[CBF1P-CBF1-ACTIT-URA3-3'CBF1]-Fragment	This study
pADE2M1	[5'ADE2-ACTIT-URA3-3'CBF1]-Fragment	This study
pADE2M2	[5'ADE2-ACTIT-URA3-3'ADE2]- Fragment	This study
For the deletion of YIL19		
pYIL19M1	[5'YIL19-FRT-SAP2P-caFLP-ACTIT-URA3-FRT-3'MEP1]-Fragment	This study
pYIL19M2	[5'YIL19-FRT-SAP2P-caFLP-ACTIT-URA3-FRT-3'YIL19]-Fragment	This study
pYIL19	[YIL19P-YIL19-3'YIL19]-Fragment	This study

Plasmid	Relevant insert	Reference
pAFI3	[<i>ACT1P-FRT-MPA^R-FRT-3'ACT1</i>]-Fragment	(Staib <i>et al.</i> , 1999)
pYIL19D1	[<i>ACT1P-FRT-YIL19P-YIL19-3'YIL19-MPA^R-FRT-3'ACT1</i>]-Fragment	This study
pSFL213	[<i>SAP2-1P-ecaFLP-ACT1T-URA3-3'SAP2</i>]-Fragment	(Staib <i>et al.</i> , 2000).
pSFL28	[5' <i>SAP2-URA3-3'SAP2</i>]-Fragment	(Staib <i>et al.</i> , 1999).

Details of plasmid constructions are described in section A.1.

^a Vector backbone in this plasmid is *S.cerevisiae* 2 μ plasmid pRS426.

3.3. *C.albicans* strains used in this study

Table 2.

Strain	Parent	Genotype ^a	Reference
SC5314		Wild type strain	(Gillum <i>et al.</i> , 1984)
CAI4	SC5314	Δ <i>ura3::imm434</i> / Δ <i>ura3::imm434</i>	(Fonzi and Irwin., 1993)
Δmep1 mutants and reintegrants			
MEP1M1A	CAI4	Δ <i>mep1-1::URA3-FLIP^b</i> / <i>MEP1-2</i>	This study
MEP1M1B	CAI4	<i>MEP1-1</i> / Δ <i>mep1-2::URA3-FLIP</i>	This study
MEP1M2A	MEP1M1A	Δ <i>mep1-1::FRT</i> / <i>MEP1-2</i>	This study
MEP1M2B	MEP1M1B	<i>MEP1-1</i> / Δ <i>mep1-2::FRT</i>	This study
MEP1M3A	MEP1M2A	Δ <i>mep1-1::FRT</i> / Δ <i>mep1-2::URA3-FLIP</i>	This study
MEP1M3B	MEP1M2B	Δ <i>mep1-1::URA3-FLIP</i> / Δ <i>mep1-2::FRT</i>	This study
MEP1M4A	MEP1M3A	Δ <i>mep1-1::FRT</i> / Δ <i>mep1-2::FRT</i>	This study
MEP1M4B	MEP1M3B	Δ <i>mep1-1::FRT</i> / Δ <i>mep1-2::FRT</i>	This study
MEP1M5A	MEP1M4A	Δ <i>mep1-1::FRT</i> / Δ <i>mep1-2::URA3</i>	This study
MEP1M5B	MEP1M4B	Δ <i>mep1-1::URA3</i> / Δ <i>mep1-2::FRT</i>	This study
MEP1MK1A	MEP1M4A	Δ <i>mep1-1::FRT</i> / Δ <i>mep1-2::MEP1-URA3</i>	This study
MEP1MK1B	MEP1M4B	Δ <i>mep1-1::MEP1-URA3</i> / Δ <i>mep1-2::FRT</i>	This study
Δmep2 mutants and reintegrants			
MEP2M1A	CAI4	Δ <i>mep2-1::URA3-FLIP</i> / <i>MEP2-2</i>	This study

Strain	Parent	Genotype^a	Reference
MEP2M1B	CAI4	<i>MEP2-1/Δmep2-2::URA3-FLIP</i>	This study
MEP2M2A	MEP2M1A	<i>Δmep2-1::FRT/MEP2-2</i>	This study
MEP2M2B	MEP2M1B	<i>MEP2-1/Δmep2-2::FRT</i>	This study
MEP2M3A	MEP2M2A	<i>Δmep2-1::FRT/Δmep2-2::URA3-FLIP</i>	This study
MEP2M3B	MEP2M2B	<i>Δmep2-1::URA3-FLIP/Δmep2-2::FRT</i>	This study
MEP2M4A	MEP2M3A	<i>Δmep2-1::FRT/Δmep2-2::FRT</i>	This study
MEP2M4B	MEP2M3B	<i>Δmep2-1::FRT/Δmep2-2::FRT</i>	This study
MEP2M5A	MEP2M4A	<i>Δmep2-1::FRT/Δmep2-2::URA3</i>	This study
MEP2M5B	MEP2M4B	<i>Δmep2-1::URA3/Δmep2-2::FRT</i>	This study
MEP2MK1A	MEP2M4A	<i>Δmep2-1::FRT/Δmep2-2::MEP1-URA3</i>	This study
MEP2MK1B	MEP2M4B	<i>Δmep2-1::MEP1-URA3/Δmep2-2::FRT</i>	This study
Δmep1 Δmep2 mutants and reintegrants			
MEP12M1A	MEP2M4A	<i>Δmep1-1::URA3-FLIP/MEP1-2 Δmep2-1::FRT/Δmep2-2::FRT</i>	This study
MEP12M1B	MEP2M4B	<i>MEP1-1/Δmep1-2::URA3-FLIP Δmep2-1::FRT/Δmep2-2::FRT</i>	This study
MEP12M2A	MEP12M1A	<i>Δmep1-1::FRT/MEP1-2 Δmep2-1::FRT/Δmep2-2::FRT</i>	This study
MEP12M2B	MEP12M1B	<i>MEP1-1/Δmep1-2::FRT Δmep2-1::FRT/Δmep2-2::FRT</i>	This study
MEP12M3A	MEP12M2A	<i>Δmep1-1::FRT/Δmep1-2::URA3-FLIP Δmep2-1::FRT/Δmep2-2::FRT</i>	This study
MEP12M3B	MEP12M2B	<i>Δmep1-1::URA3-FLIP/Δmep1-2::FRT Δmep2-1::FRT/Δmep2-2::FRT</i>	This study
MEP12M4A	MEP12M3A	<i>Δmep1-1::FRT/Δmep1-2::FRT Δmep2-1::FRT/Δmep2-2::FRT</i>	This study
MEP12M4B	MEP12M3B	<i>Δmep1-1::FRT/Δmep1-2::FRT Δmep2-1::FRT/Δmep2-2::FRT</i>	This study
MEP12M5A	MEP12M4A	<i>Δmep1-1::FRT/Δmep1-2::URA3 Δmep2-1::FRT/Δmep2-2::FRT</i>	This study
MEP12M5B	MEP12M4B	<i>Δmep1-1::URA3/Δmep1-2::FRT Δmep2-1::FRT/Δmep2-2::FRT</i>	This study
MEP12M6A	MEP12M4A	<i>Δmep1-1::FRT/Δmep1-2::FRT Δmep2-1::FRT/Δmep2-2::URA3</i>	This study

Strain	Parent	Genotype^a	Reference
MEP12M6B	MEP12M4B	$\Delta mep1-1::FRT/\Delta mep1-2::FRT$ $\Delta mep2-1::URA3/\Delta mep2-2::FRT$	This study
MEP12MK1A	MEP12M4A	$\Delta mep1-1::FRT/\Delta mep1-2::MEP1-URA3$ $\Delta mep2-1::FRT/\Delta mep2-2::FRT$	This study
MEP12MK1B	MEP12M4B	$\Delta mep1-1::MEP1-URA3/\Delta mep1-2::FRT$ $\Delta mep2-1::FRT/\Delta mep2-2::FRT$	This study
MEP12MK2A	MEP12M4A	$\Delta mep1-1::FRT/\Delta mep1-2::FRT$ $\Delta mep2-1::FRT/\Delta mep2-2::MEP2-URA3$	This study
MEP12MK2B	MEP12M4B	$\Delta mep1-1::FRT/\Delta mep1-2::FRT$ $\Delta mep2-1::MEP2-URA3/\Delta mep2-2::FRT$	This study
Reporter strains expressing <i>lacZ</i> from <i>ACT1</i>, <i>CaMEP1</i>, or <i>CaMEP2</i> promoter			
CALACZ1	CAI4	<i>ACT1/lac1::ACT1P-lacZ-URA3</i>	This study
CLACZ1A	CAI4	$\Delta mep1-1::MEP1P-lacZ-URA3/MEP1-2$	This study
CLACZ1B	CAI4	<i>MEP1-1/$\Delta mep1-2::MEP1P-lacZ-URA3$</i>	This study
CLACZ2A	CAI4	$\Delta mep2-1::MEP2P-lacZ-URA3/MEP2-2$	This study
CLACZ2B	CAI4	<i>MEP2-2/$\Delta mep2-2::MEP2P-lacZ-URA3$</i>	This study
Strains expressing <i>CaMEP1</i> or <i>CaMEP2</i> from the <i>ADH1</i>, <i>CaMEP1</i>, or <i>CaMEP2</i> promoter			
MEP12ME1A	MEP12M4A	<i>ADH1/adh1::ADH1P-MEP1</i>	This study
MEP12ME1B	MEP12M4B	<i>ADH1/adh1::ADH1P-MEP1</i>	This study
MEP12ME2A	MEP12M4A	<i>ADH1/adh1::ADH1P-MEP2</i>	This study
MEP12ME2B	MEP12M4B	<i>ADH1/adh1::ADH1P-MEP2</i>	This study
MEP12MK3A	MEP12M4A	$\Delta mep1-1::FRT/\Delta mep1-2::FRT$ $\Delta mep2-1::FRT/\Delta mep2-2::MEP2P-MEP1-URA3$	This study
MEP12MK3B	MEP12M4B	$\Delta mep1-1::FRT/\Delta mep1-2::FRT$ $\Delta mep2-1::MEP2P-MEP1-URA/\Delta mep2-2::FRT$	This study
MEP12MK4A	MEP12M4A	$\Delta mep1-1::MEP1P-MEP2-URA3/\Delta mep1-2::FRT$ $\Delta mep2-1::FRT/\Delta mep2-2::FRT$	This study
MEP12MK4B	MEP12M4B	$\Delta mep1-1::FRT/\Delta mep1-2::MEP1P-MEP2-URA3$ $\Delta mep2-1::FRT/\Delta mep2-2::FRT$	This study
Strains expressing <i>GFP</i>-tagged <i>MEP</i> genes from the <i>ADH1</i>, <i>CaMEP1</i>, or <i>CaMEP2</i> promoter in a wild-type or $\Delta mep1 \Delta mep2$ mutant background			
CMEP1EGA	CAI4	<i>ADH1/adh1::ADH1P-MEP1-GFP-URA3</i>	This study
CMEP1EGB	CAI4	<i>ADH1/adh1::ADH1P-MEP1-GFP-URA3</i>	This study
CMEP2EGA	CAI4	<i>ADH1/adh1::ADH1P-MEP2-GFP-URA3</i>	This study
CMEP2EGB	CAI4	<i>ADH1/adh1::ADH1P-MEP2-GFP-URA3</i>	This study

Strain	Parent	Genotype^a	Reference
CMEP1GA	CAI4	<i>Δmep1-1::MEP1-GFP-URA3/MEP1-2</i>	This study
CMEP1GB	CAI4	<i>MEP1-1/Δmep1-2::MEP1-GFP-URA3</i>	This study
CMEP2GA	CAI4	<i>Δmep2-1::MEP2-GFP-URA3/MEP2-2</i>	This study
CMEP2GB	CAI4	<i>MEP2-2/Δmep2-2::MEP2-GFP-URA3</i>	This study
CMEP2G1A	CAI4	<i>Δmep1-1::MEP1P-MEP2-GFP-URA3/MEP1-2</i>	This study
CMEP2G1B	CAI4	<i>MEP1-1/Δmep1-2::MEP1P-MEP2-GFP-URA3</i>	This study
CMEP1G2A	CAI4	<i>Δmep2-1::MEP2P-MEP1-GFP-URA3/MEP2-2</i>	This study
CMEP1G2B	CAI4	<i>MEP2-2/Δmep2-2::MEP2P-MEP1-GFP-URA3</i>	This study
MEP12MEG1A	MEP12M4A	<i>ADH1/adh1::ADH1P-MEP1-GFP-URA3</i>	This study
MEP12MEG1B	MEP12M4B	<i>ADH1/adh1::ADH1P-MEP1-GFP-URA3</i>	This study
MEP12MEG2A	MEP12M4A	<i>ADH1/adh1::ADH1P-MEP2-GFP-URA3</i>	This study
MEP12MEG2B	MEP12M4B	<i>ADH1/adh1::ADH1P-MEP2-GFP-URA3</i>	This study
MEP12MG1A	MEP12M4A	<i>Δmep1-1::FRT/Δmep1-2::MEP1-GFP-URA3 Δmep2-1::URA3/Δmep2-2::FRT</i>	This study
MEP12MG1B	MEP12M4B	<i>Δmep1-1::MEP1-GFP-URA3/Δmep1-2::FRT Δmep2-1::URA3/Δmep2-2::FRT</i>	This study
MEP12MG2A	MEP12M4A	<i>Δmep1-1::FRT/Δmep1-2::FRT Δmep2-1::MEP2-GFP-URA3/Δmep2-2::FRT</i>	This study
MEP12MG2B	MEP12M4B	<i>Δmep1-1::FRT/Δmep1-2::FRT Δmep2-1::FRT/Δmep2-2::MEP2-GFP-URA3</i>	This study
MEP12MG3A	MEP12M4A	<i>Δmep1-1::FRT/Δmep1-2::FRT Δmep2-1::MEP2P-MEP1-GFP-URA3/Δmep2-2::FRT</i>	This study
MEP12MG3B	MEP12M4B	<i>Δmep1-1::FRT/Δmep1-2::FRT Δmep2-1::FRT/Δmep2-2::MEP2P-MEP1-GFP-URA3</i>	This study
MEP12MG5A	MEP12M4B	<i>Δmep1-1::FRT/Δmep1-2::MEP1P-MEP2-GFP-URA3 Δmep2-1::FRT/Δmep2-2::FRT</i>	This study
MEP12MG5B	MEP12M4A	<i>Δmep1-1::MEP1P-MEP2-GFP-URA3/Δmep1-2::FRT Δmep2-1::FRT/Δmep2-2::FRT</i>	This study
Strains expressing truncated or hybrid MEP genes in <i>Δmep1 Δmep2</i> mutant			
MEP12MK1AΔC1	MEP12M4A	<i>Δmep1-1::MEP1ΔC⁴⁰⁴-URA3/Δmep1-2::FRT Δmep2-1::URA3/Δmep2-2::FRT</i>	This study
MEP12MK1BΔC1	MEP12M4B	<i>Δmep1-1::FRT/Δmep1-2::MEP1ΔC⁴⁰⁴-URA3 Δmep2-1::URA3/Δmep2-2::FRT</i>	This study
MEP12MK1AΔC2	MEP12M4A	<i>Δmep1-1::MEP1ΔC⁴³⁸-URA3/Δmep1-2::FRT Δmep2-1::FRT/Δmep2-2::FRT</i>	This study

Strain	Parent	Genotype ^a	Reference
MEP12MK1BΔC2	MEP12M4B	$\Delta mep1-1::FRT/\Delta mep1-2::MEP1\Delta C^{438}-URA3$ $\Delta mep2-1::FRT/\Delta mep2-2::FRT$	This study
MEP12MK2AΔC1	MEP12M4A	$\Delta mep1-1::FRT/\Delta mep1-2::FRT$ $\Delta mep2-1::MEP2\Delta C^{406}-URA3/\Delta mep2-2::FRT$	This study
MEP12MK2BΔC1	MEP12M4B	$\Delta mep1-1::FRT/\Delta mep1-2::FRT$ $\Delta mep2-1::FRT/\Delta mep2-2::MEP2\Delta C^{406}-URA3$	This study
MEP12MK2AΔC2	MEP12M4A	$\Delta mep1-1::FRT/\Delta mep1-2::FRT$ $\Delta mep2-1::MEP2\Delta C^{440}-URA3/\Delta mep2-2::FRT$	This study
MEP12MK2BΔC2	MEP12M4B	$\Delta mep1-1::FRT/\Delta mep1-2::FRT$ $\Delta mep2-1::FRT/\Delta mep2-2::MEP2\Delta C^{440}-URA3$	This study
MEP12MK2AΔC3	MEP12M4A	$\Delta mep1-1::FRT/\Delta mep1-2::FRT$ $\Delta mep2-1::MEP2\Delta C^{423}-URA3/\Delta mep2-2::FRT$	This study
MEP12MK2BΔC3	MEP12M4B	$\Delta mep1-1::FRT/\Delta mep1-2::FRT$ $\Delta mep2-1::FRT/\Delta mep2-2::MEP2\Delta C^{423}-URA3$	This study
MEP12MK2AΔC4	MEP12M4A	$\Delta mep1-1::FRT/\Delta mep1-2::FRT$ $\Delta mep2-1::MEP2\Delta C^{413}-URA3/\Delta mep2-2::FRT$	This study
MEP12MK2BΔC4	MEP12M4B	$\Delta mep1-1::FRT/\Delta mep1-2::FRT$ $\Delta mep2-1::FRT/\Delta mep2-2::MEP2\Delta C^{413}-URA3$	This study
MEP12MK21H2A	MEP12M4B	$\Delta mep1-1::FRT/\Delta mep1-2::FRT$ $\Delta mep2-1::MEP2^{1-418}-MEP1^{417-534}-URA3/\Delta mep2-2::FRT$	This study
MEP12MK21H2B	MEP12M4A	$\Delta mep1-1::FRT/\Delta mep1-2::FRT$ $\Delta mep2-1::FRT/\Delta mep2-2::MEP2^{1-418}-MEP1^{417-534}-URA3$	This study
MEP12MK12H2A	MEP12M4A	$\Delta mep1-1::MEP1^{1-416}-MEP2^{419-480}-URA3/\Delta mep1-2::FRT$ $\Delta mep2-1::FRT/\Delta mep2-2::FRT$	This study
MEP12MK12H2B	MEP12M4B	$\Delta mep1-1::FRT/\Delta mep1-2::MEP1^{1-416}-MEP2^{419-480}-URA3$ $\Delta mep2-1::FRT/\Delta mep2-2::FRT$	This study
MEP12MK12H3A	MEP12M4A	$\Delta mep1-1::FRT/\Delta mep1-2::FRT$ $\Delta mep2-1::MEP2P-MEP1^{1-416}-MEP2^{419-480}-URA3/\Delta mep2-2::FRT$	This study
MEP12MK12H3B	MEP12M4B	$\Delta mep1-1::FRT/\Delta mep1-2::FRT$ $\Delta mep2-1::FRT/\Delta mep2-2::MEP2P-MEP1^{1-416}-MEP2^{419-480}-URA3$	This study
MEP12MK12H4A	MEP12M4B	$\Delta mep1-1::FRT/\Delta mep1-2::FRT$ $\Delta mep2-1::MEP2P-MEP1^{1-416}-MEP2^{419-440}-URA3/\Delta mep2-2::FRT$	This study
MEP12MK12H4B	MEP12M4A	$\Delta mep1-1::FRT/\Delta mep1-2::FRT$ $\Delta mep2-1::FRT/\Delta mep2-2::MEP2P-MEP1^{1-416}-MEP2^{419-440}-URA3$	This study
Signaling mutants expressing wild type or hyperactive <i>CaMEP2</i> alleles			
JKC18	CAI4	$\Delta cph1::hisG/\Delta cph1::hisG$	(Liu <i>et al.</i> , 1994)
$\Delta cph1$ MEP2K2A	JKC18	$\Delta mep2-1::MEP2-URA3/MEP2-2$	This study
$\Delta cph1$ MEP2K2B	JKC18	$MEP2-2/\Delta mep2-2::MEP2-URA3$	This study

Strain	Parent	Genotype ^a	Reference
<i>Δcph1</i> MEP2K2AΔC2	JKC18	<i>Δmep2-1::MEP2ΔC⁴⁴⁰-URA3/MEP2-2</i>	This study
<i>Δcph1</i> MEP2K2BΔC2	JKC18	<i>MEP2-2/Δmep2-2::MEP2ΔC⁴⁴⁰-URA3</i>	This study
HLC67	CAI4	<i>Δefg1::hisG/Δefg1::hisG</i>	(Lo <i>et al.</i> , 1997)
<i>Δefg1</i> MEP2K2A	HLC67	<i>Δmep2-1::MEP2-URA3/MEP2-2</i>	This study
<i>Δefg1</i> MEP2K2B	HLC67	<i>MEP2-2/Δmep2-2::MEP2-URA3</i>	This study
<i>Δefg1</i> MEP2K2AΔC2	HLC67	<i>Δmep2-1::MEP2ΔC⁴⁴⁰-URA3/MEP2-2</i>	This study
<i>Δefg1</i> MEP2K2BΔC2	HLC67	<i>MEP2-2/Δmep2-2::MEP2ΔC⁴⁴⁰-URA3</i>	This study
HLC69	CAI4	<i>Δcph1::hisG/Δcph1::hisG</i> <i>Δefg1::hisG/Δefg1::hisG</i>	(Lo <i>et al.</i> , 1997)
<i>Δcph1 Δefg1</i> MEP2K2A	HLC69	<i>Δmep2-1::MEP2-URA3/MEP2-2</i>	This study
<i>Δcph1 Δefg1</i> MEP2K2B	HLC69	<i>MEP2-2/Δmep2-2::MEP2-URA3</i>	This study
<i>Δcph1 Δefg1</i> MEP2K2AΔC2	HLC69	<i>Δmep2-1::MEP2ΔC⁴⁴⁰-URA3/MEP2-2</i>	This study
<i>Δcph1 Δefg1</i> MEP2K2BΔC2	HLC69	<i>MEP2-2/Δmep2-2::MEP2ΔC⁴⁴⁰-URA3</i>	This study
CaAS15	CAI4	<i>Δtec1::hisG/Δtec1::hisG</i>	(Schweizer <i>et al.</i> , 2000)
<i>Δtec1</i> MEP2K2A	CaAS15	<i>Δmep2-1::MEP2-URA3/MEP2-2</i>	This study
<i>Δtec1</i> MEP2K2B	CaAS15	<i>MEP2-2/Δmep2-2::MEP2-URA3</i>	This study
<i>Δtec1</i> MEP2K2AΔC2	CaAS15	<i>Δmep2-1::MEP2ΔC⁴⁴⁰-URA3/MEP2-2</i>	This study
<i>Δtec1</i> MEP2K2BΔC2	CaAS15	<i>MEP2-2/Δmep2-2::MEP2ΔC⁴⁴⁰-URA3</i>	This study
CDH108	CAI4	<i>Δras1::hisG/Δras1::hisG</i>	(Leberer <i>et al.</i> , 2001)
<i>Δras1</i> MEP2K2A	CDH108	<i>Δmep2-1::MEP2-URA3/MEP2-2</i>	This study
<i>Δras1</i> MEP2K2B	CDH108	<i>MEP2-2/Δmep2-2::MEP2-URA3</i>	This study
<i>Δras1</i> MEP2K2AΔC2	CDH108	<i>Δmep2-1::MEP2ΔC⁴⁴⁰-URA3/MEP2-2</i>	This study
<i>Δras1</i> MEP2K2BΔC2	CDH108	<i>MEP2-2/Δmep2-2::MEP2ΔC⁴⁴⁰-URA3</i>	This study
CCS14	CAI4	<i>Δgpa2::hisG/Δgpa2::hisG</i>	(Sanchez-Martinez and Perez-Martin, 2002b)
<i>Δgpa2</i> MEP2K2A	CCS14	<i>Δmep2-1::MEP2-URA3/MEP2-2</i>	This study
<i>Δgpa2</i> MEP2K2B	CCS14	<i>MEP2-2/Δmep2-2::MEP2-URA3</i>	This study

Strain	Parent	Genotype ^a	Reference
$\Delta gpa2$ MEP2K2A Δ C2	CCS14	$\Delta mep2-1::MEP2\Delta C^{440}-URA3/MEP2-2$	This study
$\Delta gpa2$ MEP2K2B Δ C2	CCS14	$MEP2-2/\Delta mep2-2::MEP2\Delta C^{440}-URA3$	This study
CR276	CAI4	$\Delta cdc35::hisG/\Delta cdc35::hisG$	(Rocha <i>et al.</i> , 2001)
$\Delta cdc35$ MEP2K2A	CR276	$\Delta mep2-1::MEP2-URA3/MEP2-2$	This study
$\Delta cdc35$ MEP2K2B	CR276	$MEP2-2/\Delta mep2-2::MEP2-URA3$	This study
$\Delta cdc35$ MEP2K2A Δ C2	CR276	$\Delta mep2-1::MEP2\Delta C^{440}-URA3/MEP2-2$	This study
$\Delta cdc35$ MEP2K2B Δ C2	CR276	$MEP2-2/\Delta mep2-2::MEP2\Delta C^{440}-URA3$	This study

Strains expressing dominant active *GPA2* or *RAS1* alleles or *GFP* in wild-type and $\Delta mep2$ backgrounds

CAG31	CAI4	$ACT1/act1::ACT1P-GFP-URA3$	(Morschhäuser <i>et al.</i> , 1998)
MEP2MAG1A	MEP2M4A	$ACT1/act1::ACT1P-GFP-URA3$	This study
MEP2MAG1B	MEP2M4B	$ACT1/act1::ACT1P-GFP-URA3$	This study
GPA2E1A	CAI4	$ACT1/act1::ACT1P-GPA2^{Q354L}-URA3$	This study
GPA2E1B	CAI4	$ACT1/act1::ACT1P-GPA2^{Q354L}-URA3$	This study
MEP2M GPA2E1A	MEP2M4A	$ACT1/act1::ACT1P-GPA2^{Q354L}-URA3$	This study
MEP2MGPA2E1B	MEP2M4B	$ACT1/act1::ACT1P-GPA2^{Q354L}-URA3$	This study
RAS1E1A	CAI4	$ACT1/act1::ACT1P-RAS1^{G13V}-URA3$	This study
RAS1E1B	CAI4	$ACT1/act1::ACT1P-RAS1^{G13V}-URA3$	This study
MEP2MRAS1E1A	MEP2M4A	$ACT1/act1::ACT1P-RAS1^{G13V}-URA3$	This study
MEP2MRAS1E1B	MEP2M4B	$ACT1/act1::ACT1P-RAS1^{G13V}-URA3$	This study

$\Delta rap1$ mutants and reintegrants

RAP1M1A	CAI4	$RAP1/\Delta rap1::URA3-FLIP$	This study
RAP1M1B	CAI4	$RAP1/\Delta rap1::URA3-FLIP$	This study
RAP1M2A	RAP1M1A	$RAP1/\Delta rap1::FRT$	This study
RAP1M2B	RAP1M1B	$RAP1/\Delta rap1::FRT$	This study
RAP1M3A	RAP1M2A	$\Delta rap1::URA3-FLIP/\Delta rap1::FRT$	This study
RAP1M3B	RAP1M2B	$\Delta rap1::URA3-FLIP/\Delta rap1::FRT$	This study
RAP1M4A	RAP1M3A	$\Delta rap1::FRT/\Delta rap1::FRT$	This study

Strain	Parent	Genotype^a	Reference
RAP1M4B	RAP1M3B	<i>Δrap1::FRT/Δrap1::FRT</i>	This study
RAP1M5A	RAP1M4A	<i>Δrap1::FRT/Δrap1::URA3</i>	This study
RAP1M5B	RAP1M4B	<i>Δrap1::FRT/Δrap1::URA3</i>	This study
RAP1MK1A	RAP1M4A	<i>Δrap1::FRT/RAP1-URA3</i>	This study
RAP1MK1B	RAP1M4B	<i>Δrap1::FRT/RAP1-URA3</i>	This study
Strains used for the analysis of <i>CaCBF1</i>			
CBF1M1A	CAI4	<i>CBF1/Δcbf1::URA3-FLIP</i>	This study
CBF1M1B	CAI4	<i>CBF1/Δcbf1::URA3-FLIP</i>	This study
CBF1M2A	CBF1M1A	<i>CBF1/Δcbf1::FRT</i>	This study
CBF1M2B	CBF1M1B	<i>CBF1/Δcbf1::FRT</i>	This study
CBF1M3A	CBF1M2A	<i>Δcbf1::URA3-FLIP/Δcbf1::FRT</i>	This study
CBF1M3B	CBF1M2B	<i>Δcbf1::URA3-FLIP/Δcbf1::FRT</i>	This study
CBF1M4A	CBF1M3A	<i>Δcbf1::FRT/Δcbf1::FRT</i>	This study
CBF1M4B	CBF1M3B	<i>Δcbf1::FRT/Δcbf1::FRT</i>	This study
CBF1M5A	CBF1M4A	<i>Δcbf1::FRT/Δcbf1::URA3</i>	This study
CBF1M5B	CBF1M4B	<i>Δcbf1::FRT/Δcbf1::URA3</i>	This study
CBF1MK1A	CBF1M4A	<i>Δcbf1::FRT/CBF1-URA3</i>	This study
CBF1MK1B	CBF1M4B	<i>Δcbf1::FRT/CBF1-URA3</i>	This study
ADE2M1A	CAI4	<i>ADE2/ade2::URA3</i>	This study
ADE2M1B	CAI4	<i>ADE2/ade2::URA3</i>	This study
ADE2ΔcbfM1A1	CBF1M4A	<i>ADE2/ade2::URA3</i>	This study
ADE2ΔcbfM1A2	CBF1M4A	<i>ADE2/ade2::URA3</i>	This study
ADE2ΔcbfM1B1	CBF1M4B	<i>ADE2/ade2::URA3</i>	This study
ADE2ΔcbfM1B2	CBF1M4B	<i>ADE2/ade2::URA3</i>	This study
Strains used for the analysis of <i>YIL19</i>			
YIL19M1A	CAI4	<i>Δyil19-1::URA3-FLIP/YIL19-2</i>	This study
YIL19M1B	CAI4	<i>YIL19-1/Δyil19-2::URA3-FLIP</i>	This study
YIL19M2A	YIL19M1A	<i>Δyil19-1::FRT/YIL19-2</i>	This study
YIL19M2B	YIL19M1B	<i>YIL19-1/Δyil19-2::FRT</i>	This study

Strain	Parent	Genotype ^a	Reference
YIL19M3A	YIL19M2A	<i>Δyil19-1::FRT/YIL19-2</i> <i>ACT1/act1::FRT-YIL19-MPA^R-FRT</i>	This study
YIL19M3B	YIL19M2B	<i>YIL19-1/Δyil19-2::FRT</i> <i>ACT1/act1::FRT-YIL19-MPA^R-FRT</i>	This study
YIL19M4A	YIL19M3A	<i>Δyil19-1::FRT/Δyil19-2::URA3-FLIP</i> <i>ACT1/act1::FRT-YIL19-MPA^R-FRT</i>	This study
YIL19M4B	YIL19M3B	<i>Δyil19-1::URA3-FLIP/Δyil19-2::FRT</i> <i>ACT1/act1::FRT-YIL19-MPA^R-FRT</i>	This study
YIL19M5A	YIL19M4A	<i>Δyil19-1::FRT/Δyil19-2::FRT</i> <i>ACT1/act1::FRT-YIL19-MPA^R-FRT</i>	This study
YIL19M5B	YIL19M4B	<i>Δyil19-1::FRT/Δyil19-2::FRT</i> <i>ACT1/act1::FRT-YIL19-MPA^R-FRT</i>	This study
YIL19M6A	YIL19M5A	<i>Δyil19-1::FRT/Δyil19-2::FRT</i> <i>ACT1/act1::FRT-YIL19-MPA^R-FRT</i> <i>sap2-1::SAP2-1P-ecaFLP/SAP2-2</i>	This study
YIL19M6B	YIL19M5B	<i>Δyil19-1::FRT/Δyil19-2::FRT</i> <i>ACT1/act1::FRT-YIL19-MPA^R-FRT</i> <i>sap2-1::SAP2-1P-ecaFLP/SAP2-2</i>	This study
YIL19M7A	YIL19M3A	<i>Δyil19-1::FRT/YIL19-2</i> <i>ACT1/act1::FRT-YIL19-MPA^R-FRT</i> <i>sap2-1::SAP2-1P-ecaFLP/SAP2-2</i>	This study
YIL19M7B	YIL19M3B	<i>YIL19-1/Δyil19-2::FRT</i> <i>ACT1/act1::FRT-YIL19-MPA^R-FRT</i> <i>sap2-1::SAP2-1P-ecaFLP/SAP2-2</i>	This study
YIL19M8A	YIL19M5A	<i>Δyil19-1::FRT/Δyil19-2::FRT</i> <i>ACT1/act1::FRT-YIL19-MPA^R-FRT</i> <i>sap2-1::URA3/SAP2-2</i>	This study
YIL19M8B	YIL19M5B	<i>Δyil19-1::FRT/Δyil19-2::FRT</i> <i>ACT1/act1::FRT-YIL19-MPA^R-FRT</i> <i>sap2-1::URA3/SAP2-2</i>	This study

a. Apart from the indicated features, all strains constructed in this study are identical to their parent strain.

b. *URA3-FLIP* denotes the *URA3* flipper cassette.

3.4. Primers used in this study

Primers were obtained either from MWG (Ebersberg, Germany) or ARK-Sigma (Darmstadt, Germany). Introduced restriction sites are underlined and the bases which were changed from the original sequence either to incorporate the restriction site or to change amino acids are in lower-case letters. Start or stop codons in the primer sequences are shown in bold letters.

Table 3.

Name	No of nucleotides	T _m (°C)	Sequence
MEP3	34	62.1	5'-TAAATACggTACCCAAACGATTGGCTTGAATGTC-3'
MEP4	29	63.9	5'-TTGAACACATCTCgAgCTGTGCCTGTTCC-3'
MEP5	28	58.2	5'-GAACCTATCaGaTCTACTACTATAAGCC-3'
MEP6	29	59.6	5'-TTCTACTATGAGGctCCTTCTATGGTAACC-3'
MEP7	29	74.7	5'-TTGAACACATCTCCAgaTcTGCCTGTTCC-3'
MEP8	28	70.4	5'-GAACCTATCCGTTCTgCagCTATAAGCC-3'
MEP9	29	68.2	5'-CCATGAGTTGAGatctCAGTATCATTGTG-3'
MEP11	27	75.4	5'-TTGCGATGGGTaccAAAGCTTGAAACG-3'
MEP12	26	65.2	5'-CTTCTGCTGACtcGAgGTGTATAGAC-3'
MEP13	30	72.1	5'-AGAGAAGCAgatcTgCAGTGGAATATCGTC-3'
MEP14	26	62.5	5'-ATGAGTAAATGAGctcTTAGTATGCG-3'
MEP15	26	70.1	5'-GTTTCACCTcgagGTTGTTGTTGTTG-3'
MEP16	26	54.1	5'-AAAAATATAgATctACCTGACTAATC-3'
MEP17	27	62.1	5'-TGTATTACTagaTCTGCTGACATGATG-3'
MEP18	27	76.7	5'-GCGATGGGTTctcgAGCTTGAAACGAG-3'
MEP19	34	74.7	5'-AATGGGAgatctTaCATGGCAAGCAAAATAATGG-3'
MEP20	33	67.4	5'-AGGGAagaTcTTaAAATGACAAAACATAATATGG-3'
MEP21	33	72.0	5'-GTTAAAtctCgAgaATGTCTGGAAATTTCACTGG-3'
MEP22	34	73.3	5'-TGGGTTGagaTCtaATCGTCATCAGCATAATAGG-3'
MEP23	35	68.6	5'-AGAAATCagaTCTaCACTTCAACGTAATCATAAGC-3'
MEP24	30	64.9	5'-CCAGACAActcgaGTTATTA ACTATT CAGAG-3'
MEP25	31	78.7	5'-TTGGGCCAgaTCtGTTCaCAACATTTCTCG-3'
MEP26	32	73.7	5'-TCGTGGAGAtcttaTCTGAGAATGGGATTCTG-3'
MEP27	30	68.4	5'-AGTCTATctcgAgaATGTCAGCAGAAGAAG-3'
MEP32	29	68.4	5'-AAAGAACTGgATccATTTTTAGCTTCTCC-3'
MEP33p	21	66.5	5'-TTCGTGGAGACGGATTCTGAG-3'
MEP34p	22	64.3	5'-AATGGAGAAGAAGCTGGTGTG-3'

Name	No of nucleotides	T _m (°C)	Sequence
MEP35	38	78.9	5'-CCTTAGA <u>ATCGATT</u> ATGACGAGGAAATGTTG-GGAACCG-3'
MEP37	29	77.0	5'-ACCTGAC <u>ggATCc</u> ACTGGGACGATATTCC-3'
ACT16	28	59.3	5'-TTCTA <u>AGAtct</u> AAATTCTGGAAATCTG-3'
ACT19	35	62.0	5'-ATATA <u>CCGCGG</u> ACATTTTATGATGGAATGAATGGG-3'
ACT20	38	56.5	5'-TTT <u>Gtcgac</u> TTATATTTTTTTAATATTAATATCGAG-3'
ACT31	27	58.9	5'-CAGCGTCAAA <u>tCTAGAGA</u> AATAATAAAG-3'
LACZ1	34	62.1	5'-CAGCC <u>ctcgaga</u> ATGAACATGACTGAAAAAATTC-3'
LACZ2	22	57.7	5'-CCATGTACCGTGTGTTTCAAGG-3'
RAS1	59	82.9	5'-CATAT <u>gtcgACCATG</u> TTGAGAGAATATAAAATTAGTT-GTTGTTG GAGGTGtTGGTGTGG-3'
RAS2	31	66.4	5'-TTTAG <u>gagatCTC</u> AAACAATAACACAACATCC-3'
GPA1	30	77.6	5'-AACTT <u>gtcgACCATG</u> GGTTCCTTGTGCTTCG-3'
GPA2	30	63.4	5'-ACCAACATCAAATAAATTCATATTTAATCC-3'
GPA3	30	67.6	5'-GGTtAAGGTCAGAAAGAAAAAATGGATC-3'
GPA4	35	63.5	5'-TGCAT <u>tagatCT</u> ATAAAATACCACTATCTTTAAGAG-3'
RAP3	27	56.6	5'-AGTAGGTAT <u>GGaTC</u> CTAGATGTTTAAC-3'
RAP5	28	59.6	5'-ATATTCACAAC <u>ggTACC</u> ATTTGGAGCAG-3'
RAP6	28	59.6	5'-GTCCATCATCTT <u>CtcgAG</u> ATGAATAAGG-3'
RAP7	30	63.7	5'-AAACAC <u>cgcGGT</u> AGTTGTGTCCACTTATCC-3'
RAP8	30	65.1	5'-GATGAATAAGGAT <u>ccTTC</u> ATACTTTATTGG-3'
RAP9	34	66.2	5'-CATACTTTACAATCT <u>gcaGAG</u> AGATAGATTTAGG-3'
RAP10	29	73.0	5'-CAAACACAAAC <u>gagCTc</u> GTAGTTGTGTCC-3'
RAP11	27	67.5	5'-CATAATTTCA <u>ggaTCC</u> CTGATTAACCC-3'
CBF1	26	67.5	5'-GTCACGAGGT <u>AccAAG</u> GGGGCAGGAG-3'
CBF2	28	58.2	5'-CCATATCATCT <u>CcgAG</u> AAATCTTATTGGC-3'
CBF3	26	61.2	5'-GAGAGGGA <u>AGAtcTA</u> AGGGGGATAAG-3'
CBF4	32	64.8	5'-CCTGTATTGTCA <u>gagCTC</u> TTCTTTTCACGGG-3'
CBF5	28	64.0	5'-GAGAGGGAAG <u>ActgcAG</u> GGGGATAAG-3'
CBF6	28	56.7	5'-CCATATCATCTTT <u>AGAtcT</u> CTTATTGGC-3'

Name	No of nucleotides	T _m (°C)	Sequence
CBF7	29	56.8	5'-CTCCAAACTTAT _{Tagat} CTTATTTCTTCCC-3'
ADE3	25	69.7	5'-ACTGTTGGT _{Acc} TTAGGAGGTGGCC-3'
ADE4	29	67.6	5'-CAACAAAGTT _{Aga} TCTACCATCATACGCC-3'
ADE5	28	66.0	5'-TAGAATGTCT _{Gc} AGTATGCTATTGAAGC-3'
ADE6	22	53.9	5'-CAGTTAAAT _{Gagc} TCATATCC-3'
YIL 1	24	67.5	5'-ATTACGTGT _{GgTa} CCCCTTGATCC-3'
YIL2	23	66.0	5'-CATCTTCACT _{Cgag} ATAGCCCAG-3'
YIL3	23	52.9	5'-AAAGAAGAT _{Tct} AACGTACAATAG-3'
YIL4	26	64.2	5'-CTGAAACTCAG _{Agetc} TATGGGTAAG-3'
YIL5	28	71.8	5'-GAGGTCAA _{ACTCga} GGTGGTAGAACACC-3'
YIL6	27	66.7	5'-TTCATCA _{AAGCTt} AATGTGAAGATTTTCG-3'
ITS1.3	22	71.4	5'-GACCTCTGGC _{GGC} CAGGCTGGGC-3'
ITS 2.1	26	68.0	5'-CAACACCAA _{ACCC} CAGCGGTTTGAGGG-3'

3.5. Sources of chemicals, enzymes and equipments used in this study

Chemicals used were of analytical grade from Applichem (Darmstadt, Germany), Merck (Darmstadt, Germany), Roth (Karlsruhe, Germany) or molecular biology grade mostly from Sigma (Taufkirchen, Germany). Restriction enzymes and DNA modifying enzymes were obtained from NEB (Schwalbach/Taunus, Germany), Invitrogen (Karlsruhe, Germany), or Amersham (Freiburg, Germany). Buffers provided with the enzymes or one-for-all buffer were used. Media used were from Oxoid (Wesel, Germany), Invitrogen (Karlsruhe, Germany) or Roth (Karlsruhe, Germany).

Table 4.

Name of the equipments used	Source
Incubators For <i>E.coli</i> (37°C) (Type B6200) For <i>C.albicans</i> (30°C) (Model 400)	Heraus Memmert

Name of the equipments used	Source
Shaking incubators For <i>E.coli</i> (37°C) Innova 4300 For <i>C.albicans</i> (30°C) Innova 4230	New Brunswick Scientific
Electrophoresis apparatus Agarose gel (DNA Sub Cell/GNA 100) Agarose-Formaldehyde-Gel	Bio-Rad/Pharmacia Fröbel
Electroporation apparatus (Easyject prima)	Equibio
Geldocumentation system	Bio-Rad
Hybridization oven	MWG
Spectrophotometer	Pharmacia
Thermocycler	Techne
UV-crosslinker (GS Gene linker)	Bio-Rad
Tabletop centrifuge	Heraeus Sepatech

3.6. Commonly used molecular microbiological techniques

All solutions and media were made in double distilled and distilled water respectively. All solutions and media were sterilized by autoclaving at 15 lb/sq inch for 15 minutes or filter sterilized by passing through a 0.22 micron Millipore filter. All % shown are on a w/v basis unless mentioned otherwise.

3.6.1. Growth and maintainance of strains

Recombinant *E.coli* strains were routinely grown in LB liquid medium (1% Tryptone, 0.5% NaCl, 0.5% Yeast Extract) containing 100 µg/ml ampicillin and were maintained on LB agar plates (1.5% agar) containing 100 µg/ml ampicillin. The *C.albicans* strains were routinely grown in YPD liquid medium (1% Yeast extract, 2% Peptone, 2% Dextrose) and were maintained on SD agar plates (0.67% Yeast nitrogen base without amino acids [BIO 101 Vista Calif.], 2% dextrose, 1X CSM-URA [BIO 101 Vista Calif.] and 1.5% agar). To support growth of uridine-auxotrophic strains, 100 µg/ml uridine was added to the media. The *ura3*-negative derivatives of strains containing the *URA3* flipper were isolated after inducing *FLP* expression by overnight growth in YCB-BSA (23.4 g Yeast Carbon Base [Difco], 2 g Yeast extract, 0.4% BSA [Bovine serum albumin, Fraction V, Gerbu], pH 4.0) containing 100 µg/ml uridine and screening for smaller colonies after growing the cells on SD agar plates

containing 10 µg/ml uridine. Selection of the transformants for mycophenolic acid (MPA) resistance was done in SD agar plates containing 10 µg/ml MPA (Sigma, Deisenhofen, Germany). To screen for MPA-resistant and MPA-sensitive clones, 100-200 cfu was plated on SD agar containing 1.8 µg/ml MPA which resulted in the generation of large MPA^R and small MPA^S colonies, respectively (Staib *et al.*, 1999). *E.coli* and *C.albicans* strains were routinely grown at 37°C and 30°C respectively.

To study *CaMEP1* and *CaMEP2* expression in response to nitrogen availability, strains were grown to log phase in liquid SD-CSM medium (0.67% Yeast nitrogen base without amino acids [BIO 101 Vista Calif.], 2% dextrose), washed twice in YNB medium (0.17% YNB without amino acids and [NH₄]₂SO₄ [BIO 101 Vista Calif.], 2% Dextrose, pH 4.0), and grown for six hours in fresh YNB medium in which the standard ammonium concentration of 76 mM (38 mM [NH₄]₂SO₄) was altered or replaced by other nitrogen sources as indicated. Growth at different ammonium concentrations was assayed by incubating the strains for 4 days at 30°C on YNB agar plates (2% agar [washed 4 times]) containing the indicated ammonium concentrations.

3.6.2. *In vitro* DNA manipulation

3.6.2.1. DNA digestion with restriction enzymes

Digestions of DNA was done in 1X 'one-for all buffer' (33 mM Tris-acetate pH 7.9, 66 mM K-acetate, 10 mM Mg-acetate, 0.5 mM DTT, 0.1 mg/ml BSA) and the manufacturer's instructions were followed with respect to the amount of enzyme per µg of DNA, incubation temperature and reaction time. The digests were then mixed with 10X DNA stop buffer (0.2% Bromophenol blue, 0.2M EDTA, 50% Glycerol) to a final concentration of 1X, and loaded on a 1% agarose gel along with 1 kb DNA ladder (Invitrogen).

3.6.2.2. Polymerase Chain Reaction (PCR)

PCR was carried out using either Elongase-Enzyme-Mix (Invitrogen) or Pfu-DNA-Polymerase (Promega, Mannheim, Germany). Typically the amplification reactions were carried out for 30 cycles.

The program was as follows

Denaturation at 94°C for 2 minutes only in the first cycle

Denaturation at 94°C for 1 minute for all cycles

Optimum annealing temperature ($T_{a\text{OPT}}$) for 30 seconds, for all cycles

Extension at 68°C (72°C for Pfu-DNA-Polymerase) for 1 minute for 1 kb product (2 minutes extension time for 1 kb product in case of Pfu-DNA-Polymerase) for all cycles.

Finally to fill the incomplete extension products, the reaction mix was incubated at 68°C (72°C for Pfu-DNA-Polymerase) for 10 minutes.

The annealing temperature was adjusted on the basis of the T_m of the primers used to amplify the product. Using the above parameters, the template amount and number of cycles were varied and an ideal combination was arrived at to maximize the yield. Usually the reaction was carried out in a 50 µl reaction mix containing 1-2 ng plasmid DNA or 0.1-1.0 µg genomic DNA as template, 0.2 mM of each dNTPs, 1 unit of enzyme and the provided buffer in 1X concentration.

Successful amplification was confirmed by agarose gel electrophoresis and the PCR product then extracted once with phenol: chloroform: IAA (25:24:1) and once with chloroform: IAA (24:1). It was then precipitated with 1/10th volume of 3M sodium acetate pH 5.2 and 2.5 volumes of 100% ethanol. After precipitation excess salts were removed by washing in 70% ethanol and the DNA was dissolved in an appropriate volume of sterile double distilled water for further process (e.g. restriction digestion).

3.6.3. Gel electrophoresis and gel elution of DNA fragments

3.6.3.1. Agarose gel electrophoresis

Agarose gel electrophoresis of DNA was routinely carried out in 1X TAE (50X TAE stock solution: 242 g Tris base, 57.1 ml Glacial acetic acid and 100 ml 0.5 M EDTA pH 8.0 for 1 litre). For most purposes a 1% gel was used. After electrophoresis, the gels were stained in ethidium bromide (10 mg/ml in water) and photographed using a gel documentation system. The sizes of the fragments were estimated by measuring the relative mobility of the bands in comparison to markers of known molecular size (1 kb DNA ladder, Invitrogen), run in a lane alongside.

Before performing any Southern blot, the integrity of the nucleic acid was also verified by such methods. All procedures were performed according to Sambrook *et al.*, 1989, or Ausubel *et al.*, 1994.

3.6.3.2. Gel elution of inserts from agarose gel

Large scale digestion of the plasmid containing the DNA of interest was done with appropriate enzymes to release the insert. The digested DNA was loaded on the agarose gel

and run at low voltage till the band of interest was well separated from the vector backbone. The band of interest was cut out with a scalpel. The DNA was prepared from the gel slice using the 'Gene Clean Kit' (QBiogene, Heidelberg, Germany). 400 µl NaI was added to the gel slice and incubated at 50°C till the agarose melted (5-10 minutes). After thorough mixing with 7 µl glass-milk, it was then incubated on ice for 5 minutes and washed 3 times with 200 µl 'New Wash' solution. 11 µl distilled water was added to the pellet, mixed well, and incubated at 50°C for 5 minutes. After centrifugation at 13,000 rpm for 2 minutes in a tabletop centrifuge, the supernatant was taken which contains the fragment of interest. PCR products were purified from the gel similarly. For transformation of *C.albicans* linear DNA fragments were eluted in 6 µl distilled water, instead of 11 µl.

3.6.4. Cloning of gene of interest in vectors

3.6.4.1. Ligation

The vector most commonly used in these studies was pBluescript KS II (Stratagene, Heidelberg, Germany). All the preparative digestions for the preparation of inserts were generally set up in a 50 µl reaction volume containing 10-15 µg of plasmid DNA. For the preparation of vectors 1-2 µg of plasmid DNA was digested in a 50 µl reaction volume. Digests were resolved on a 1% agarose gel and appropriate DNA fragments were eluted from the gel piece using 'Gene Clean Kit' (see section 3.6.3.2). DNA amounts were empirically estimated and ligation reactions were set up at 1:4 ratio of vector and insert (in general) in a 15 µl reaction volume containing 1X ligase buffer and 1 unit of T4 DNA ligase (Invitrogen). A vector-only control ligation reaction was also set up during each ligation experiment. Ligation reactions were carried out at room temperature (RT) for 3 hours.

3.6.4.2. Transformation of *E. coli*

Preparation of *E. coli* DH5α competent cells

DH5α cells were streaked on a fresh LB agar plate from a glycerol stock. A single colony was inoculated from the freshly streaked plate in 10 ml LB medium and grown at 37°C with shaking at 200 rpm for 16-18 hours.

The overnight grown culture was diluted 1:100 in fresh LB medium and incubated at 37°C with shaking at 200 rpm till A₆₀₀ reached 0.7-0.9 (3-4 hours). The culture was then

transferred to chilled 50 ml tubes and centrifuged at 3,000 rpm for 10 min at 4°C in a chilled rotor. The supernatant was discarded and the cell pellet was suspended in 100 mM calcium chloride in 4/5th volume of the starting culture. The cell mix was incubated on ice for 30-45 minutes and centrifuged at 3,000 rpm for 10 minutes at 4°C. Competent cells were then suspended in 100 mM calcium chloride in 1/20th volume of the starting culture volume and 86% glycerol was added to a final concentration of 15% (v/v). Cells were aliquoted in the microfuge tubes and stored at -70°C until further use.

Transformation of competent cells

For each transformation, an aliquot of 200 µl competent cells was used. The ligation mixture was added to the competent cells and incubated for 45 minutes on ice with gentle mixing at regular intervals. The cells were subjected to heat shock in a 42°C water-bath for 90 seconds and then chilled on ice for 5 minutes. After adding 1 ml LB medium the cells were allowed to grow for 90 minutes at 37°C.

Plating of transformation mix

An aliquot of 200 µl from the 1 ml transformation mix was spread on a selection plate (e.g. LB plate containing 100 µg/ml ampicillin). The rest of the transformation mix was concentrated and plated on another selection plate. The plates were dried in laminar flow air and incubated at 37°C until the colonies appeared (~16 hours).

3.6.4.3. Screening and analysis of recombinants

Plasmid isolation

The recombinant colonies were picked and streaked on a fresh LB agar plate containing ampicillin and simultaneously inoculated into 3 ml LB medium containing 100 µg/ml ampicillin. The cells in liquid culture were grown at 37°C in a shaking incubator for 18-20 hours and the plate was incubated at 37°C until the colonies appeared (~16 hours).

The cultures were processed to isolate plasmid DNA by the miniprep protocol and analyzed by restriction digestion.

Small scale plasmid DNA isolation was carried out by modified alkaline lysis method (Sambrook *et al.*, 1989). Cells were centrifuged at 12,000 rpm for 30 seconds at room temperature. The supernatant was removed by aspiration, leaving the bacterial pellet as dry as

possible. The pellets were suspended completely in 100 μ l TEG (25 mM Tris-HCl pH 8.0, 10 mM EDTA pH 8.0, 50 mM Dextrose). 200 μ l freshly prepared Solution II (1% SDS, 0.2N NaOH) was added and the tubes were inverted a few times to mix well. The tubes were incubated on ice for 5 minutes till a visible cell lysis occurred and the liquids became transparent. 150 μ l Solution III (3M sodium acetate pH 5.2) was added to the cell lysates and mixed well. These were then incubated at RT for 10 minutes and centrifuged at 12,000 rpm for 7 minutes at RT. The supernatant was transferred to another tube, extracted once with phenol: chloroform: IAA (25:24:1) and 1 ml 100% ethanol was added to the each supernatant. These were then mixed by inversion and incubated at RT for 5-10 minutes to precipitate the plasmid DNA. The plasmid pellets were recovered by centrifugation at 12,000 rpm for 5 minutes at RT. The supernatants were removed by gentle aspiration, pellets were washed once with 70% ethanol and dried. The pellets were dissolved in 50 μ l double distilled water and 1 μ l RNase A (50 mg/ml) was added to each sample.

From each sample 3 μ l (100-200 ng) DNA was digested with suitable restriction enzymes at the appropriate temperature (mostly at 37°C) in a 20 μ l reaction mix for 1-2 h and separated on a 1% agarose gel along with the marker. After staining in ethidium bromide the gel was observed in geldocumentation system and correct recombinants were selected based on their expected band pattern on gel.

DNA-Sequencing

Sequencing of DNA was done according to the chain termination method (Sanger *et al.*, 1977). For sequencing of the cloned fragments, plasmid DNA was isolated as described above and after RNase treatment 150 μ l distilled water was added to it. After extracting once with phenol: chloroform: IAA (25:24:1) and once with chloroform: IAA (24:1), the DNA was precipitated by addition of 1/10th volume 3M sodium acetate pH 5.2 and 2.5 volumes 100% ethanol and incubation at -70°C for 1 h. After washing with 70% ethanol the DNA pellet was dissolved in 26 μ l distilled water. Sequencing was done using the 'Thermo-Sequenase fluorescent labelled primer cycle sequencing kit with 7-deaza-dGTP' [RPN 2438] (Amersham) with 1 pmol fluorescence labelled (IRD 800) sequencing primer (MWG) and 6 μ l plasmid (~500 ng) in a thermocycler. The programme was: denaturation at 95°C for 2 minutes and then for 30 cycles 95°C for 30 seconds (denaturation), primer annealing for 30 seconds, 70°C for 30 seconds (polymerization). The product was then run on a polyacrylamide gel and analysed using a 'LI-COR' model 4000 automated sequencer (MWG).

3.6.5. Transformation of *C.albicans*

Transformation was done by electroporation as described by Köhler *et al.*, (1997) with the gel-purified linear DNA fragments. A single colony of the uridine-auxotrophic *C.albicans* strain to be transformed was inoculated in 10 ml of YPD supplemented with uridine and grown at 30°C at 200 rpm shaking for 16-18 hours. 5 µl of the preculture was added to 50 ml YPD and grown till the culture reached mid log phase (O.D₆₀₀= 1.8 to 2.0). The cells were then centrifuged at 4,000 rpm at RT for 5 minutes. The pellet was suspended in 8 ml sterile distilled water and, 1 ml 1M lithium acetate and 1 ml 10X TE buffer pH 7.5 (100 mM Tris-Cl pH 7.5, 10 mM EDTA) were added. The cell mix was then incubated at 30°C in a water-bath with gentle shaking. After 45-60 minutes incubation 250 µl 1M DTT was added to the cell mix and incubated at 30°C water bath for another 30 minutes with gentle shaking. 40 ml sterile distilled water was added and the cell mix was centrifuged at 4,000 rpm for 5 minutes at 4°C. The cell pellet was then washed once with 25 ml sterile distilled water and once with 5 ml 1M sorbitol. The supernatant was discarded and the cell pellet was suspended in the residual liquid. 5 µl DNA was then mixed with 40 µl of competent cells in a 0.2 cm electroporation cuvette (Peq lab, Erlangen, Germany). For control, 5 µl sterile distilled water was used instead of DNA. These mixtures were then electroporated at 1.8 Kv using an electroporation apparatus. After electroporation 1 ml 1M sorbitol was added to the cells and 100 µl was plated on selection plates. The remaining cells were concentrated and plated on another plate. The plates were then dried and incubated at 30°C until the colony appeared (2 days).

3.6.6. Genomic DNA isolation from *C.albicans*

Glass-bead method

The *C.albicans* strains were inoculated in 10 ml YPD and grown at 30°C with shaking at 200 rpm for 18-20 hours. The cells were collected by centrifugation at 5,000 rpm for 5 minutes, suspended in 0.5 ml distilled water and transferred to micro centrifuge tubes. The cells were washed by centrifugation at 5,000 rpm for 2 minutes and the supernatants were decanted. The cell pellets were then suspended in the residual liquid. 0.2 ml of freshly prepared breaking buffer (10 mM Tris-Cl pH 8.0, 1% SDS, 1 mM EDTA, 2% Triton-X-100 and 100 mM NaCl) was added to each tube. After adding 0.2 ml phenol: chloroform: isoamylalcohol (25:24:1) and 0.3 g glass beads (0.2-0.4 micron, Roth), the cells were

vortexed at full speed for 4 minutes and centrifuged at 10,000 rpm for 5 minutes in a microcentrifuge. The aqueous layer was transferred to a new tube and 1 ml chilled 100% ethanol was added to precipitate DNA. The tubes were centrifuged at 10,000 rpm for 5 minutes. After discarding the supernatant, the pellets were air-dried, and suspended in 0.4 ml distilled water. 30 µg RNaseA was added to each sample and after incubation at 37°C for 15 minutes 10 µl 4M ammonium acetate and 1 ml 100% ethanol was added to each sample and mixed gently by inverting the tubes, to precipitate DNA. The tubes were centrifuged at 10,000 rpm for 5 minutes. The DNA pellets were then washed with 70% ethanol, air-dried, and dissolved in 50 µl distilled water.

Enzymatic method

After overnight growth in 10 ml YPD at 30°C the cells were collected by centrifugation at 5,000 rpm for 5 minutes, suspended in 1 ml 1M sorbitol and transferred to the 2 ml micro centrifuge tubes. The cells were washed by centrifugation at 5,000 rpm for 5 minutes and the supernatant was discarded. The cell pellet was then suspended in 1 ml lyse buffer (1M sorbitol, 100 mM sodium citrate pH 5.8, 50 mM EDTA, 2% β-mercaptoethanol, 500 u/ml lyticase [Sigma]) and incubated at 37°C for 45 minutes. The cells were then centrifuged (13,000 rpm, 5 minutes), suspended in 800 µl proteinase-buffer (100 mM Tris-Cl pH 7.5, 50 mM EDTA pH 7.5, 0.5% SDS, 1 mg/ml proteinase K [Sigma]) and incubated at 60°C for 30 minutes. After 2 times extraction with phenol: chloroform: IAA (25:24:1), the nucleic acids were precipitated by adding 600 µl isopropyl alcohol to the each sample. After centrifugation at 13,000 rpm for 5 minutes the pellet was washed with 70% ethanol, air-dried and dissolved in 200 µl distilled water containing 2 µl RNaseA (10 mg/ml). After 30 minutes incubation at 37°C, the DNA was extracted once with phenol: chloroform: IAA (25:24:1) and once with chloroform: IAA (24:1) and precipitated with 200 µl isopropanol. It was then centrifuged at 13,000 rpm for 5 minutes, washed in 70% ethanol, air-dried and dissolved in 100 µl distilled water. The concentration of DNA was estimated by measuring the absorbance at 260 nm ($OD_{260} 1.0 = 50 \mu\text{g/ml DNA}$).

3.6.7. Southern hybridization technique

This technique was developed by Southern (1975), for the detection of specific DNA fragments among a population of digested DNA separated by gel electrophoresis.

Restriction digestion of genomic DNA

10 µg of genomic DNA from *C.albicans* transformants was digested with appropriate restriction enzymes in a 30 µl reaction volume at 37°C. After overnight incubation reactions were stopped by adding DNA stop buffer to 1X final concentration.

Agarose gel electrophoresis

The digestions, along with 1 kb DNA ladder (Invitrogen) as marker, were loaded on a 1% agarose gel. The gel was run as usual with 1X TAE buffer at constant low voltage overnight. After electrophoresis, the gel was stained with ethidium bromide, and photographed.

DNA transfer

A Nylon membrane was pre-wet for few seconds in distilled water and equilibrated in 20X SSC (3M sodium acetate and 0.3M tri-sodium citrate) for 15 minutes. The gel was rinsed with distilled water and aligned on top of the membrane in a vacuum blot. Depurination of the DNA was done under vacuum for 15 minutes with 0.25N HCl. The solution was discarded and the gel was treated with denaturing solution (0.6M NaCl and 0.4N NaOH) for 15 minutes and with neutralizing solution (1.5M NaCl, 0.5M Tris-Cl pH 7.5) for 15 minutes, under similar conditions. Transfer was done with 20X SSC for 90 minutes. After transfer, the membrane was soaked in 0.4N NaOH for 1 minute to denature the DNA. The membrane was then neutralized in 0.2M Tris-HCl (pH 7.5)/1X SSC for 1 minute. UV-cross linking of nucleic acids to the membrane was done in Stratalinker.

Hybridization

The membrane was pre-wet in 2X SSC for 1 minute and then placed in a hybridization bottle and prehybridized for 1-2 h, using the prehybridization buffer of the 'ECL labelling and detection kit' (Amersham) at 42°C in a hybridization oven. The probe was prepared according to the manufacturer's instruction using 100 ng gel eluted DNA and 2 ng 1 kb DNA ladder (Invitrogen) and added to the prehybridization buffer. Hybridization was carried out in hybridization bottles at 42°C for 16 hours. After hybridization, the membrane was washed at 42°C, 1X with 5X SSC for 10 minutes, 2X with Wash Buffer I (6M Urea, 0.4% SDS, 0.5X SSC) for 10 minutes and finally in 2X SSC at RT for 10 minutes. Signal detection was done according to the manufacturer's instructions. The membrane was then wrapped securely in saran wrap, and exposed to Amersham hyperfilm ECL in a film cassette for 5-90 minutes. To

rehybridize the membrane, it was incubated in detection solution overnight, washed in 2X SSC for 1 minute and rehybridized with another probe.

3.6.8. RNA isolation from *C.albicans*

Total RNA from *C.albicans* cells was isolated by the hot phenol method (Ausubel *et al.*, 1994). All the solutions used for RNA isolation were made either in DEPC treated water or treated with DEPC after preparing the solutions. For DEPC treatment 0.1% DEPC (v/v) was added and the solutions were incubated at 37°C overnight and autoclaved.

The cell pellets from various conditions to be tested were collected by centrifugation and suspended in 600 µl TES buffer (10 mM Tris-Cl pH 7.5, 10 mM EDTA, 0.5% SDS). 600 µl water saturated phenol was added and mixed thoroughly. The mixture was incubated at 65°C for 1 h with intermittent mixing. The hot mixture was then chilled in an ethanol-dry ice bath for 5 seconds and then centrifuged at 12,000 rpm for 10 minutes at RT. The aqueous phase was carefully transferred to another tube, without disturbing the interphase, even if it meant leaving some of the aqueous phase behind. The aqueous phase was then extracted once again with water saturated phenol and twice with TE saturated phenol: chloroform: IAA (25:24:1). The RNA was precipitated by adding 1/10th volume 3M sodium acetate pH 5.2 and twice the volume chilled 100% ethanol. The RNA was recovered by centrifugation at 12,000 rpm for 10 minutes at RT in a microfuge. The RNA pellet was washed with 70% ethanol (prepared in DEPC water), dried and dissolved in DEPC treated water.

3.6.9. Northern hybridization

Agarose gel electrophoresis of RNA and Northern blotting

Formaldehyde denatured RNA gel was prepared as described by Sambrook *et al.* (1989). Formaldehyde (Applichem) of pH 3-3.5, was used. Formamide was deionised and stored at 4°C. To prepare the RNA sample, 30 µg RNA in 11.25 µl DEPC water was mixed with 5 µl 10X MOPS buffer (0.2M MOPS pH 7.0, 20 mM sodium acetate, 10 mM EDTA), 25 µl formamide and 8.75 µl formaldehyde. After incubation at 55°C for 15 minutes, 10 µl loading buffer (50% glycerol, 1 mM EDTA, 0.002% bromophenol blue and 0.002% xylene cyanol) was added to the mix.

1.2% agarose gel containing 1X MOPS buffer and 2.2M formaldehyde was prepared. The denatured RNA was loaded in the wells and the electrophoresis was done in 1X MOPS buffer at constant voltage (150V) till the bromophenol blue had migrated 2/3 length of the gel (2-3 hours).

After electrophoresis, the gel was rinsed in DEPC treated water for 1 h, followed by soaking in 10X SSC for 45 minutes. The RNA was transferred to a Nylon membrane by capillary transfer using 20X SSC as transfer buffer. The amount of RNA loaded was verified by methylene blue staining (0.02% methylene blue in 0.3M sodium acetate) of the blot. The RNA was cross linked to the membrane by UV-cross linking.

Probe labelling and hybridization

The membrane was pre-wet in 6X SSC for 1 minute and then placed in 15 ml prehybridization solution (50% deionized formamide, 5X SSC, 0.1% SDS, 1 mM EDTA pH 7.5, 5X Denhardt's solution [50X Denhardt's solution: 1 g polyvinyl pyrrolidone, 1 g Ficoll 400 and 1 g BSA in 100 ml distilled water], 50 mM Tris-Cl pH 7.5, 100 µg/ml denatured Salmon sperm [10 mg/ml in 1X TE pH 8.0, sonicated and extracted with phenol: chloroform: IAA twice and once with chloroform: IAA, precipitated with ethanol, washed and resuspended and boiled at 100°C for 10 minutes and then chilled (Sambrook *et al.*, 1989)]) in a hybridization bottle and prehybridized for 4 hours at 42°C. Labelling of probe was done using the random labelling kit (Invitrogen). 100 ng template DNA fragment (gel eluted) was taken in 23 µl distilled water. The DNA was denatured by incubating in a boiling water bath for 10 minutes and then chilled by quickly placing on ice for 5 minutes, and centrifuged briefly at 4°C. The DNA was then mixed with 15 µl 10X Labelling Buffer which includes Random Octadeoxyribonucleotides, 6 µl dNTP mixture (2 µl each of dCTP, dTTP, and dGTP), 5 µl α ³²P-dATP (50 µCi from 3,000 Ci/mmol specific activity) and 1 µl DNA Polymerase I-Klenow fragment (5 units). The reaction mix was incubated at 37°C for 1 h and terminated by adding 5 µl stop buffer (provided with kit).

For labelling oligonucleotides to use as probe, a kinase reaction was carried out using γ ³²P-ATP in a reaction mixture containing 30 pmol oligo, 30 pmol γ ³²P-ATP (the molar ratio of oligo and γ ³²P-ATP should be 1:1), 5 µl 10X T4 PNK (polynucleotide kinase) buffer and 2 µl T4 PNK (5 units) (NEB). The reaction mixture was incubated at 37°C for 40 minutes.

Before adding to the prehybridization solution the labelled probe was denatured by incubation at 100°C for 10 minutes and quickly placed on ice for 5 minutes.

Hybridization was carried out in hybridization bottles, at 42°C for 16 hours in a hybridization oven. The membrane was washed with Wash solution I (2X SSC, 0.1% SDS) for 10 minutes at 42°C and 2X for 10 minutes in Wash solution II (0.1X SSC and 0.1% SDS) at 56°C. Washing time was varied according the radioactivity present in the blot. After each wash the background count was monitored with a Hand Monitor to avoid washing off the specifically bound signal. The membrane was then wrapped securely in a polythene packet and was exposed to Kodak X-Omat™ film in a film cassette, and incubated at -80°C for 6 hours to 2 days, depending on the signal strength. The film was developed and aligned with the blot to mark the positions of the bands.

3.7. Phenotypic assays

To study nitrogen starvation induced filamentation, the strains were grown for 6 days at 37°C on YNB agar plates (see section 3.6.1) containing ammonium or other nitrogen sources at the concentrations described in the text. Where indicated, 10 mM dibutyryl cAMP (Sigma, Deisenhofen, Germany) was added. Filamentous growth was also induced by growing the cells for 6 days at 37°C on agar plates containing 10% fetal calf serum (FCS) or by embedding the cells in YPS agar (2% peptone, 1% yeast extract, 2% sucrose, 1.5% agar) and incubating the plates at 25°C for 6 days. Filamentation in liquid medium was studied by inoculating cell grown overnight in YPD into the RPM I 1640 medium with 10% fetal calf serum or in 2.5 mM N-acetyl glucosamine (GlcNAc) in salt base (0.45% NaCl and 0.335% YNB without amino acids [BIO 101 Vista Calif.], adopted from Delbruck and Ernst, 1993), 10 mM MES-Tris buffer pH 6.4 supplemented with 1 mM proline (Holmes and Shepherd, 1987), Lee'S medium (see section A.2), or Spider medium (1% Nutrient Broth, 1% Mannitol, 0.2% K₂HPO₄ pH 7.2 adopted from Liu *et al.*, 1994) and incubating at 37°C for 6-8 hours.

Growth and temperature sensitivity of the strains were tested by incubating them on YPD agar plates at 30°C, 37°C, and 42°C. To measure survival of the cells at 42°C the strains were grown overnight in YPD medium at 30°C, diluted 10⁻² in fresh YPD medium and grown to log phase (OD₆₀₀ =1.5 to 2.0). The culture was then transferred to 42°C and incubated for 24 hours. Alternatively, 1 ml of the culture was washed in PBS (0.8% NaCl, 0.02% KCl, 0.144% Na₂HPO₄, 0.024% KH₂PO₄, pH 7.0), suspended in 1 ml PBS, and incubated for

24 hours at 42°C. In both cases samples were taken at 0 h and 24 hours after transfer to 42°C. Appropriate dilutions were spread on YPD plates and incubated at 30°C to determine the number of viable cells. The % survival was calculated by dividing the number of colonies obtained after 24 hours at 42°C by the number of colonies obtained at 0 h. For auxotrophy tests, strains were grown on SD agar plates without CSM, supplemented with methionine, or cysteine, or no amino acids. Thiabendazole sensitivity was tested by spotting serial 10-fold dilutions of stationary phase cells of the strains on YPD agar plates with or without 100 µg/ml thiabendazole and monitoring growth at 30°C.

3.8. Microscopy

Microscopic analysis of *C.albicans* cells was performed with a Zeiss Axiolab microscope equipped for epifluorescence microscopy with a 50-W mercury high-pressure bulb using a 40x objective. To determine the percentage of yeast and pseudohyphal cells, cells were grown to mid log phase in YPD medium at 30°C, fixed with PBS containing 4% formaldehyde and counted in a Neubauer hemocytometer. For chitin staining the cells were fixed with PBS containing 4% formaldehyde and then washed in PBS. One hundred microlitres of the cell suspensions were mixed with 10 µl of 1 mg/ml calcofluor solution, incubated in the dark at RT for 1 h, and washed five times in PBS. For visualizing nuclei cells were fixed in 70% ethanol and resuspended in PBS. One hundred and fifty microlitres of the cell suspensions were mixed with 20 µl of 1:1500 diluted Hoechst dye 33258 and incubated in the dark at room temperature for 30 minutes. For visualizing live cells, log phase cells were suspended in 0.1M MOPS-50 mM citric acid pH 3.0 and CFDA (Molecular Probes, Karlsruhe, Germany) was added from a 5 mg/ml stock in 100% dimethyl sulfoxide to a final concentration of 50 µg/ml. The cells were then incubated in the dark at 37°C for 45 minutes with gentle agitation and stored on ice until analysis (Bowmann *et al.*, 2002). To visualize dead cells, log phase cells were washed, suspended in 0.1M MOPS pH 7.0 and DiBAC (Molecular Probes, Karlsruhe, Germany) was added from 1 mg/ml stock in 100% ethanol to a final concentration of 2 µg/ml. After 1 h incubation in the dark at RT with gentle agitation, cells were washed twice with 0.1M MOPS pH 7.0 and stored on ice until analysis (Bowmann *et al.*, 2002). The stained cells were observed by phase contrast and epifluorescence microscopy.

Fluorescence of cells expressing GFP fusions was detected using a Zeiss LSM 510 inverted confocal laser scanning microscope equipped with a ZEISS Axiovert 100

microscope. Imaging scans were acquired with an Argon laser of 488 nm wavelength and corresponding filter settings for GFP and parallel transmission images. Observation was performed with 63× immersion oil objective.

3.9. Ammonium uptake assays

Ammonium uptake was assayed as described previously (Lorenz and Heitman, 1998a; Marini et al., 1994). Briefly, strains were grown to late log phase in minimal proline medium (0.17% YNB without amino acids and $[\text{NH}_4]_2\text{SO}_4$ [BIO 101 Vista Calif.], 0.1% proline, 2% glucose) and the cultures were diluted to an OD_{600} of 1.0 in the same medium plus 500 μM ammonium sulfate. At the indicated times a portion of the culture (1 ml) was taken, the cells removed by centrifugation, and the ammonium concentration in the culture supernatant determined using a glutamate dehydrogenase-linked assay in a reaction mixture containing 50 mM imidazole pH 7.3, 20 mM α -ketoglutarate, 0.1 mg/ml NADH, 0.01 mg/ml EDTA and 10 units of glutamate dehydrogenase from bovine liver (Sigma). In this reaction $\text{NH}_4^+ + \text{NADH} + \text{H}^+ + \alpha$ -ketoglutarate is converted to glutamate + $\text{NAD}^+ + \text{H}_2\text{O}$ and an increase in the NADH concentration (measured by determining the absorbance at 340 nm) indicates ammonium removal by the cells.

3.10. X-Gal agarose overlay assay

β -galactosidase activity was determined using an X-Gal agarose overlay assay as described by the Herskowitz lab (<http://biochemistry.ucsf.edu/%7Eherskowitz/xgalagar.html>). Strains were grown as single colonies on YNB agar plates containing the indicated ammonium concentrations at 37°C for 6 days. To perform the assay, 5 mg/ml low melting agarose was boiled in 10 ml stock solution containing 9.3 ml 0.5M potassium phosphate buffer pH 7.0 (61 ml of 1M K_2HPO_4 and 39 ml of 1M KH_2PO_4 was mixed to make 200 ml of buffer, and filter sterilized). Then 0.5 mg/ml X-Gal and 1 drop of β -mercaptoethanol (i.e., about 50 μl / 100 ml) was added to the warm solution (50-60°C) and using a Pasteur pipette, the surface of each plate was covered with this warm solution. After the agarose solidifies (~5-10 minutes), plates were incubated for 2 hours at 30°C until the blue color developed.

4. Results

4.1. Nitrogen starvation induced filamentous growth and ammonium transporters of *C.albicans*

4.1.1. Nitrogen starvation induced filament formation in *C.albicans* is controlled by the availability of ammonium

Candida albicans grows in different morphological forms: yeast, pseudohyphae and hyphae. These morphological transitions are induced by various factors like, pH, temperature, presence of serum, or nutritional starvation. On agar plates containing low ammonium concentrations (100 μ M) *C.albicans* switches from yeast to filamentous growth, with hyphae and pseudohyphae emanating from the borders of the colonies after several days of incubation at 37°C (Csank *et al.*, 1998). To study nitrogen starvation induced filamentous growth in more detail, the *C.albicans* wild-type strain SC5314 was grown on agar plates containing various concentrations of ammonium and other nitrogen sources. The strain formed filaments at low ammonium concentration but grew in the yeast form at 10 mM or higher concentrations of ammonium (Fig. 3A). Filamentous growth was also observed when ammonium was replaced by urea or different amino acids as sole source of nitrogen, and was inhibited by the addition of 10 mM or higher concentrations of ammonium (Fig. 3B). In contrast, when the concentration of amino acids in the agar plates were increased from 100 μ M to 10 mM, the colonies still exhibited various degrees of filamentation, but filamentous growth was suppressed when sufficient amounts of ammonium were provided in addition (Fig. 3C). Although some amino acids have been reported to be inducers of filament formation in *C.albicans* (Land *et al.*, 1975), these results demonstrate that the filamentous growth seen under these conditions is a response of *C.albicans* to nitrogen starvation or to an imbalance in nitrogen metabolites which is suppressed by the presence of sufficient amounts of a preferred nitrogen source, ammonium. In contrast, ammonium even at very high concentration could not repress the filamentation induced by other environmental signals, like the presence of serum (Fig. 3D).

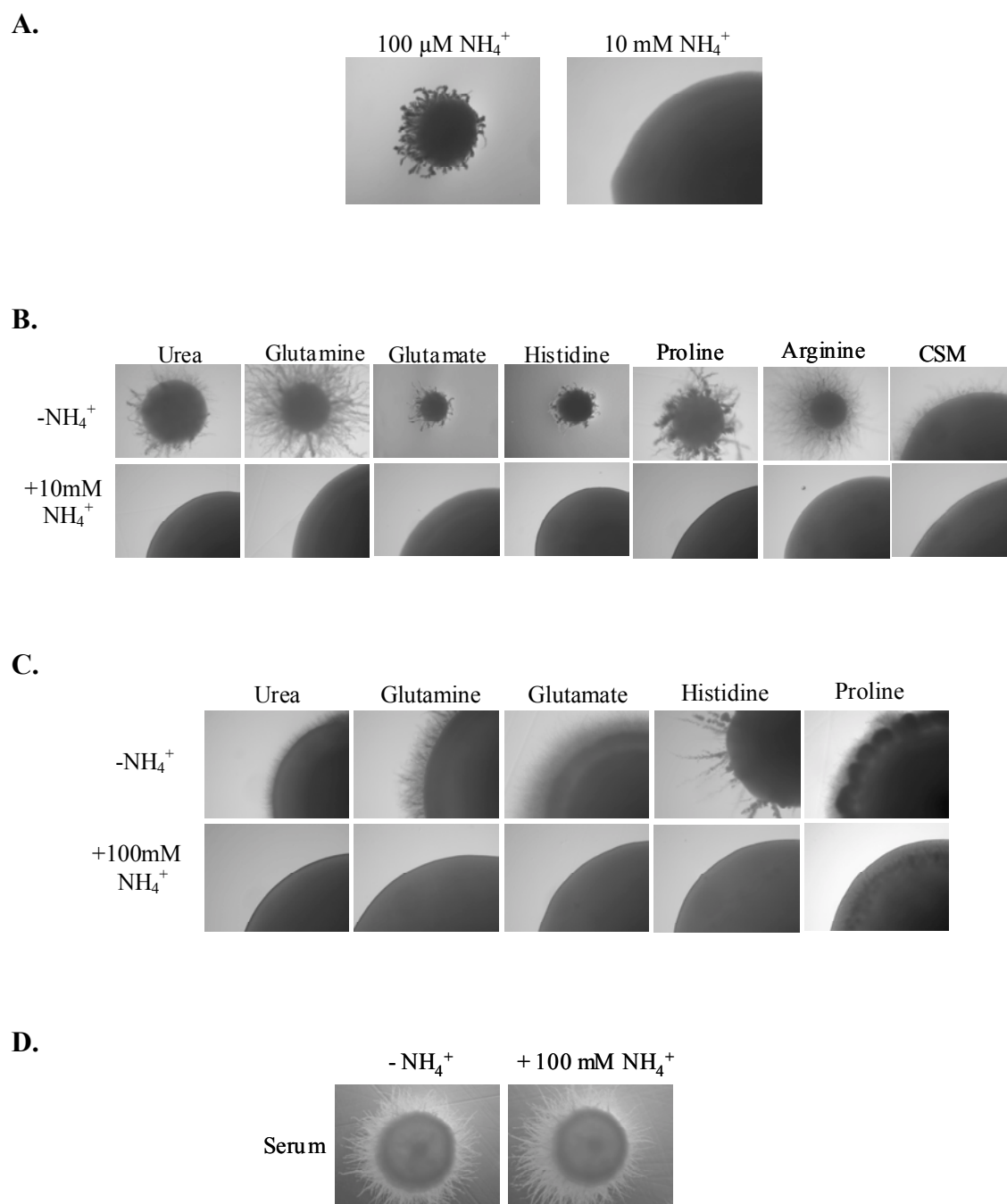


Fig. 3. Nitrogen starvation induced filamentous growth of *C. albicans* is controlled by ammonium availability. The wild-type strain SC5314 was grown on the indicated agar plates for 6 days at 37°C and individual representative colonies were photographed. **(A)** Growth on YNB plates containing 100 μM (SLAD) or 10 mM ammonium as the sole nitrogen source. **(B)** Growth on YNB plates containing urea, glutamine, glutamate, histidine, proline, arginine, or complete supplement medium (CSM) at 100 μM concentration as the sole nitrogen source (upper row) or together with 10 mM ammonium (lower row). **(C)** Growth on YNB plates containing urea, glutamine, glutamate, histidine or proline at 10 mM concentration as the sole nitrogen source (upper row) or together with 100 mM ammonium (lower row). **(D)** Serum induced filamentous growth in the absence (left) or presence of 100 mM ammonium (right).

4.1.2. Identification of *C. albicans* ammonium permeases

Since ammonium controls the filamentation of *C. albicans* in the presence of limiting nitrogen concentrations, it was interesting to study the role of ammonium permeases in *C. albicans* morphogenesis. A BLAST search of the *C. albicans* genome sequence (<http://www-sequence.stanford.edu/group/candida/>) identified two putative ammonium permeases Mep1p and Mep2p on the basis of high homology to *S. cerevisiae* Mep1, Mep2 and Mep3 proteins. ORF 6.6912 encodes a putative 51.9 kD protein of 480 amino acids that exhibits highest similarity to ScMep2p (72% similarity, 64% identity). This ORF shows lower level of homologies to ScMep1p (51%/41%) and ScMep3p (52%/42%) and so the corresponding gene was termed *CaMEP2*. ORF 6.1090 encodes a putative 59.4 kD protein of 534 amino acids that exhibits high similarity to both ScMep1p (63%/54%) and ScMep3p (65%/57%), and lower similarity to ScMep2p (52%/41%) and the corresponding gene was termed as *CaMEP1*. A third open reading frame, ORF 6.7259, encodes a protein that has much lower homology than CaMep1p and CaMep2p to all three ScMep proteins (43 to 45% similarity, 32 to 36% identity) and the results of this study (see below) suggest that this ORF may not encode a functional ammonium permease. CaMep1p and CaMep2p have 52% similarity and 43% identity to each other. All these three proteins have 11 transmembrane domains, with an extracytosolic N-terminus and a C-terminal cytoplasmic tail, as predicted by the TMpred programme (Fig. 4).

	OUT	IN	
CaMep1p	MSAEVEIQYISRRLKFTENNE-YNES	YLLLFTHIASSMIWIMIPGLAFLYSGLARRKSALS	59
ORF 6.7259	-----MSTDVEPMTSLDVTGLNS	LYMLYCTAPLPLVVIQIAFFYSGLTQRRSALT	51
CaMep2p	MSGNFTGTGTGGDVFKVDLNEQFDRAD	MVWIGTASVLVWIMIPGVGLLYSGISRKKHALS	60
	.	:	*:::****::: **:
	OUT		
CaMep1p	MIWIVIMSSFVGIQWYFWGYSLAFSDTSKNS	FIGDLHFFGFKNLLGASDDKTT-----Y	114
ORF 6.7259	MFAVPFLLAPMIIDWFIWGYSLCYSASS-NHF	FIGNLNVVLRQFRNALTAFTNTRGHV	110
CaMep2p	LMWAALMAACVAAFQWFWWGYSLVFAHNG-SV	FLGTLQNFCLKDVLGAPSIKVT-----V	114
	::	::	*:::****::: .. *:* * . : : . * *
	IN	OUT	
CaMep1p	PDIAYSLFQLQFLLVTLAI IAGGCI	AERGRFLPALVFMFCWATVVYCPVYWI	WGG-GWA 173
ORF 6.7259	LAGAHVLFNMFKLI	CVSLTFPGCIAERGRVLPMLF	AFIWSVIIYNPVTYWFWNSNGWL 170
CaMep2p	PDILFCLYQGMFAAVT	AILMAG-AGCERARLGPMMVFLFIWLT	VVYCPYAYWTWGGNGWL 173
	. *::	* :	. **.* * ::* * * ::* * :.* * . **
	IN		
CaMep1p	SSYR--SGALDYAGGGPVEILSGMSAFVYSA	FLGRRNETLMIN---YRPHNISTIFLGT	227
ORF 6.7259	SVDLGRLPVLDFA	GGNCVHIVSGFTCLAYSII	LGRNPKLLYN---YRNSNTGHIIFGT 226
CaMep2p	VS----LGALDFAGGGPVHENS	GFAALAYSLLWLGKRHDPVAKGKVPKYKPHSVSSIVMGT	229
	.**:***. *	**:::..** ** *:	: . * : . . * : **
	OUT	IN	
CaMep1p	SLLYVWGLFFNGFSCGNPSLKVAYSMM	NTHLCGAFGAISWCLLD-FRLEN-----	276
ORF 6.7259	FLVFMGWIGYIAGCDFKFSFNS	IYIILNTLIAACASGIVWTAIDFFFSSVPLEGESVGLK	286
CaMep2p	IFLWFGWYGFNGGSTGNS	SMRSWYACVNTNLAATGGLTWMLVDWFR	TGG----- 279
	:::.* :	. * :	** :.. . : * : * *

```

CaMep1p      -----KWSMVAVCSGCISGLV 292
ORF 6.7259   HGDSKLSNSSGDNHSPMLQAIIVSRTGVSINQRLHESKSNFVEKRKFSMISFSSGIMTGLV 346
CaMep2p      -----KWSTVGLCMGAIAGLV 295
                                     *: * : . . . * : : * * *

                OUT                                IN
CaMep1p      AATPSSGMIP---LWASVILGITAGIVCNLSTKIKYLLHVDDSLDVWAEHGMAGVVGLI 348
ORF 6.7259   VFTPGGGYVSSNAEFWKGIIIFGVVGAISGNLATRLKYFFNIDDALDLFAVHGIPIGVGSM 406
CaMep2p      GITPAAGYVP---VYTSVIFGIVPAIICNFVAVDLKDLLQIDGMDVWALHGVGGFVGNF 351
                * * . * * : . : : * * : . * * : . : * * : : : * * : * * : * * * :

                                OUT                                IN
CaMep1p      FNALFGSATVIGYDGVTDHQGGWIDHNWKQLYIQIVYILATMAYSGVVTAILCFVINNKIP 408
ORF 6.7259   LTGIFAN-----DLYDSKGGWVKGHWKQFGYQLLGLLVVTSAYVFIMSMVFLYLIDLIP 459
CaMep2p      MTGLFAADYVAMIDG-TEIDGGWMNHHWKQLGYQLAGSCAVAAWSFTVTSIILLAMDRIPI 410
                : : : * * . : : : * * : . : * * : : : * * : : : * * : * *
                                               ΔC404
                                               ΔC406
                                OUT                                IN
CaMep1p      GLHLRIDYNGEEAGVDEDQIGEFAYDYVEVRRDFLDWGIPTVNPYQNSINDQQQQQPE 468
ORF 6.7259   GFHLRIDKDFNRREKRTLKAKQLDQELSESQTS-----PQQVPHMSNSTEQMSFWEQVE 514
CaMep2p      FLRIRLHEDEMLGTDLAQIGEYAY-YADDD-----PETNPYVLEPIRSTTISQP-- 459
                : : * * : : : : : : : : : : : : * * : : . . : : :
                ΔC413      ΔC423      ΔC440
                                OUT                                IN
CaMep1p      VPEITSQQKRGGGLSGIEEAEKQVQGIPIKRQTQIIDGTTTQNSDTSNTS IQEKHDP 528
ORF 6.7259   LQGTGDGYEFNGEFMLDFMEFIRAIRPQDYEDDDLKDI IQAPNQYEGYIQDFELHQEGVH 574
CaMep2p      LPHIDG-----VADGSSNNDGSEAKN----- 480
                : : : : : : : : : : : : : : : : : : : : : : : : : : : : : : : :
                : : : : : : : : : : : : : : : : : : : : : : : : : : : : : : : :

CaMep1p      VEYRPS 534
ORF 6.7259   NLTKRE 580
CaMep2p      -----

```

Fig. 4. Sequence alignment of CaMep1p, ORF 6.7259 and CaMep2p using the ClustalW program (<http://www.ebi.ac.uk/clustalw/#>). Amino acid positions are shown on the right. Identical, conserved, and semi-conserved residues are indicated by stars, colons, and dots, respectively, below the sequence. The 11 transmembrane domains predicted by the TMpred program (http://www.ch.embnet.org/software/TMPRED_form.html) are highlighted in red. The extracytosolic and intracellular domains of the permeases are labeled as OUT and IN, respectively. The positions of the generated C-terminal truncations in CaMep1p and CaMep2p are marked by open triangles.

4.1.3. Construction of *C.albicans* strains with different *MEP* gene deletions

In order to study the role of *CaMEP1* and *CaMEP2* in ammonium uptake and filamentous growth of *C.albicans*, a series of mutants was constructed in which these genes were specifically deleted from the genome. To construct the mutant strains in the diploid *C.albicans* the *URA3*-flipping strategy (Morschhäuser *et al.*, 1999) was used. The *URA3* flipper cassette contains the *C.albicans* *URA3* gene as a selectable marker and *C.albicans* adapted recombinase *caFLP* gene under control of the inducible *SAP2* promoter, flanked by *FLP* recognition sites (*FRT*).

When such a construct is cloned between the upstream and downstream regions of a gene and integrated into the yeast genome by homologous recombination, one of the two alleles of the target gene is inactivated. Upon induction of the *SAP2* promoter the *FLP*

recombinase is expressed and recombines its target sites, resulting in the excision of the *URA3* flipper cassette from the genome. The *ura3* derivatives can easily be identified on SD agar plates containing 10 $\mu\text{g/ml}$ uridine where these strains grow as smaller colonies than *URA3* strains. A second round of insertion/excision of the *URA3* flipper generates homozygous mutant. To construct complemented strains and appropriate controls, these *ura3* homozygous mutants serve as a host for the integration of *URA3* marker alone or along with a complete copy of the gene of interest into one of the inactivated alleles. This process is schematically explained in Fig. 5.

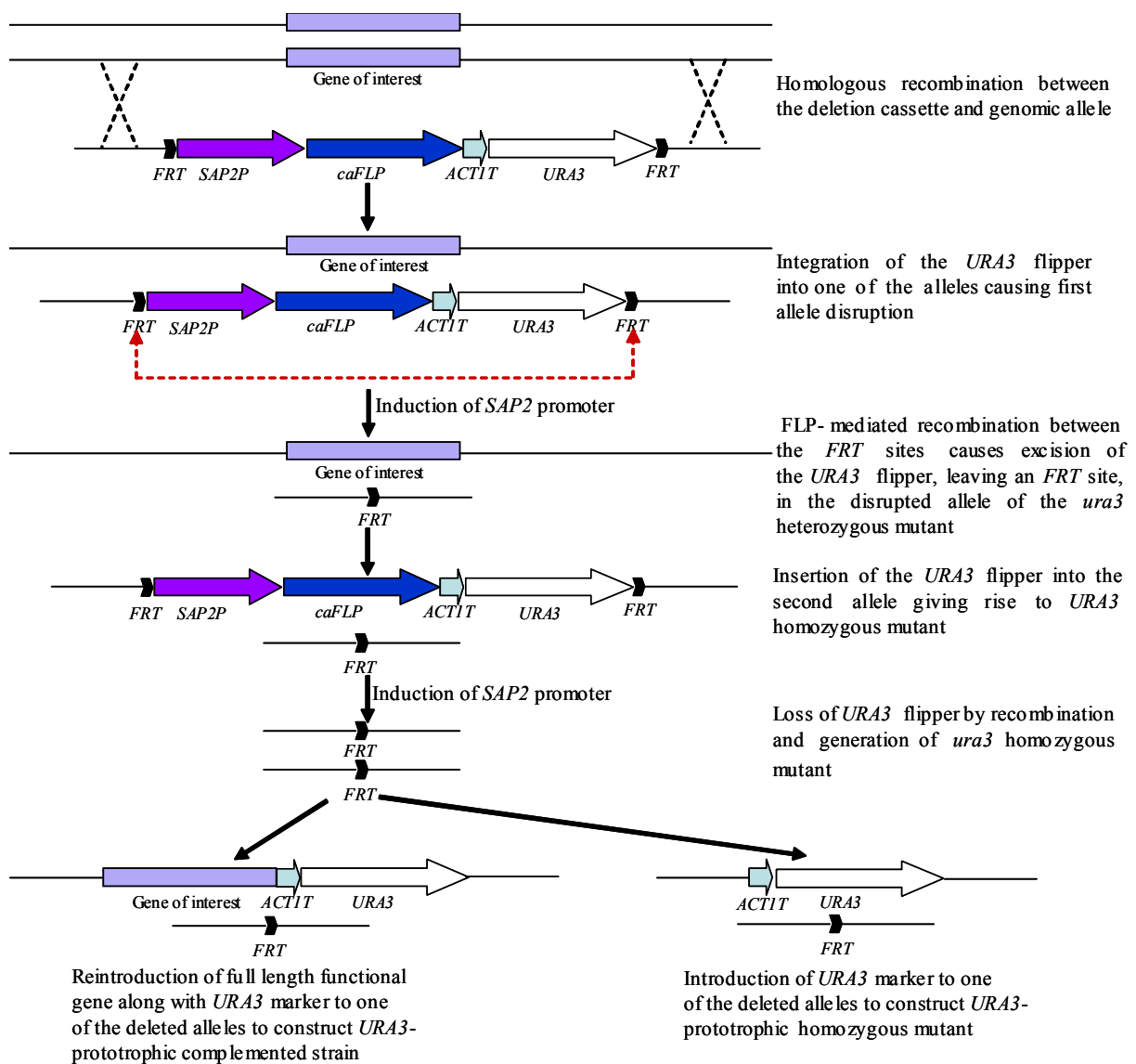


Fig. 5. Schematic representation of disruption of a gene of interest in *C. albicans* and reintroduction of a functional allele.

To obtain a $\Delta mep2$ mutant, the *ura3*-negative strain CAI4 was transformed with a deletion cassette in which the whole *CaMEP2* coding sequence had been replaced by the *URA3* flipper (see section 3.2 and Fig. 6A). The two *CaMEP2* alleles of strain CAI4 could be distinguished by *EcoRI* restriction site polymorphism. In each case, the two alleles were arbitrarily assigned a suffix (e.g., *MEP2-1* and *MEP2-2*), and two transformants carrying the integration of the *URA3* flipper in either of the two possible *CaMEP2* alleles were selected. The *URA3* flipper was then excised by FLP-mediated recombination from two transformants in which the deletion cassettes had been correctly integrated into either the *CaMEP2-1* allele (strains MEP2M1A) or into the *CaMEP2-2* allele (MEP2M1B, Fig. 7, lanes 2 and 3), resulting in the uridine-auxotrophic strains MEP2M2A and MEP2M2B (Fig. 7, lanes 4 and 5). When these strains were transformed again with the same deletion cassette, integrations were successfully targeted to the remaining wild-type *MEP2* alleles in several transformants of both parent strains and generated the strains MEP2M3A and MEP2M3B (Fig. 7, lanes 6 and 7). The *URA3* flipper was excised again from MEP2M3A and MEP2M3B to generate the uridine-auxotrophic derivatives MEP2M4A and MEP2M4B (Fig. 7, lanes 8 and 9).

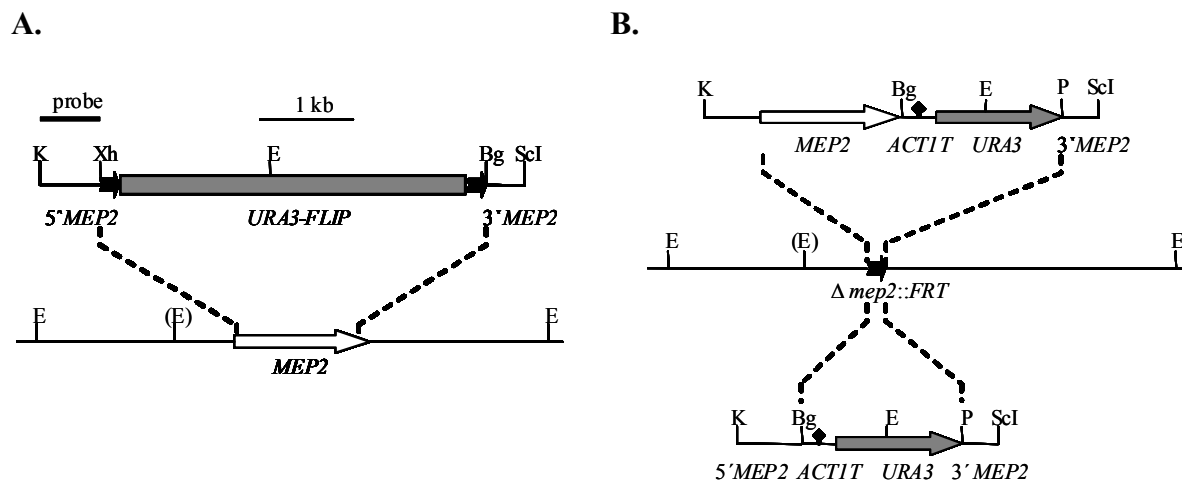


Fig. 6. (A) Structure of the deletion cassette from plasmid pMEP2M2 (top) and genomic structure of the *CaMEP2* locus in the parent strain CAI4 (bottom). The *CaMEP2* coding region is represented by the white arrow, and the upstream and downstream sequences by the solid lines. Details of the *URA3* flipper (grey rectangle bordered by *FRT* sites [black arrows]) are presented in Fig. 5. The 34 bp *FRT* sites are not drawn to scale. The probe used for Southern hybridization analysis of the mutants is indicated by the black bar. (B) Structure of the DNA fragments from pMEP2K1 (top) and pMEP2M4 (bottom), which were used for reintegration of an intact *CaMEP2* copy (white arrow) or only the *URA3* marker (grey arrow), respectively, into one of the inactivated $\Delta mep2$ alleles (middle). The *ACT1* transcription termination sequence (*ACT1T*) is indicated by the black diamond. Only relevant restriction sites are given. Bg, *Bgl*II; E, *Eco*RI; K, *Kpn*I; P, *Pst*I; ScI, *Sac*I; Xh, *Xho*I. The *Eco*RI site shown in parentheses is present only in the *CaMEP2-1* allele.

The strains MEP2M4A and MEP2M4B served as hosts for the generation of two independent, prototrophic, homozygous $\Delta mep2$ mutant MEP2M5A and MEP2M5B (Fig. 6B, bottom and Fig. 7, lanes 10 and 11) and the corresponding complemented strains MEP2MK2A and MEP2MK2B (Fig. 6B, top and Fig. 7, lanes 12 and 13) by reintroduction of the *URA3* selection marker alone or a complete copy of the *CaMEP2* gene into one of the inactivated $\Delta mep2$ alleles.

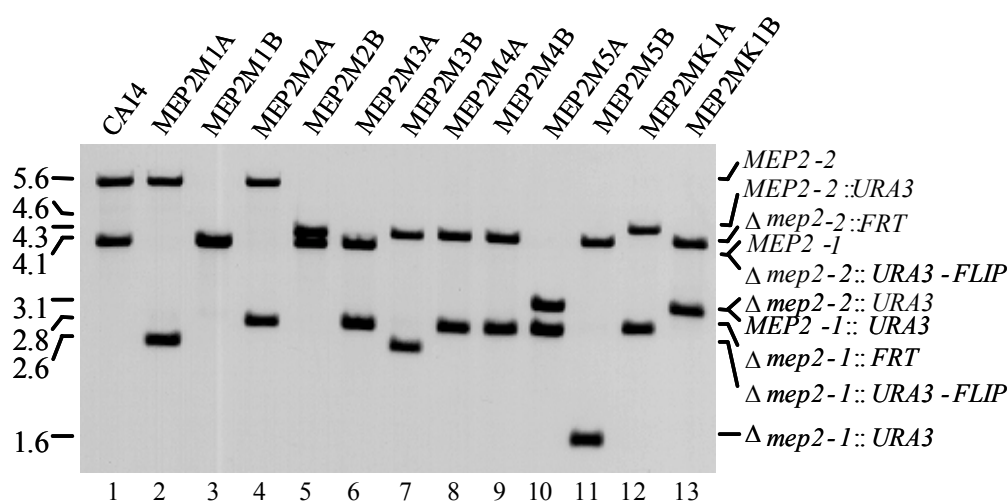


Fig. 7. Southern hybridization of *EcoRI*-digested genomic DNA of the parent strain CAI4 and mutant derivatives with a *CaMEP2*-specific probe shown in Fig. 6A. The sizes of the hybridizing fragments (in kb) are given on the left side of the blot and their identities are indicated on the right.

CaMEP1 gene was deleted using a similar procedure to generate $\Delta mep1$ single as well as $\Delta mep1 \Delta mep2$ double mutants. A deletion cassette in which the whole *CaMEP1* coding sequence had been replaced by the *URA3* flipper (see section 3.2 and Fig. 8A) was constructed. The construction of $\Delta mep1$ single mutants has been documented in Fig. 8 and Fig. 9. The parental strain CAI4 was used to generate $\Delta mep1$ single mutants. The two *CaMEP1* alleles of CAI4 and its derivatives could be distinguished by *ClaI* restriction site polymorphism and were arbitrarily assigned a suffix (e.g., *MEP1-1* and *MEP1-2*). Two transformants in which the *URA3* flipper was integrated into either the *CaMEP1-1* allele (MEP1M1A, Fig. 9, lanes 2) or into the *CaMEP1-2* allele (MEP1M1B, Fig. 9, lanes 3) were selected and the *URA3* flipper was excised by FLP-mediated recombination to generate the uridine-auxotrophic strains MEP1M2A and MEP1M2B (Fig. 9, lanes 4 and 5). These strains were then again transformed with the same deletion cassette and the integrations were

successfully targeted to the remaining wild-type *CaMEP1* allele in several transformants of both parent strains. The *URA3* flipper was excised again from the two independent homozygous $\Delta mep1$ mutants MEP1M3A and MEP1M3B (Fig. 9, lanes 6 and 7), generating the uridine-auxotrophic derivatives MEP1M4A and MEP1M4B (Fig. 9, lanes 8 and 9).

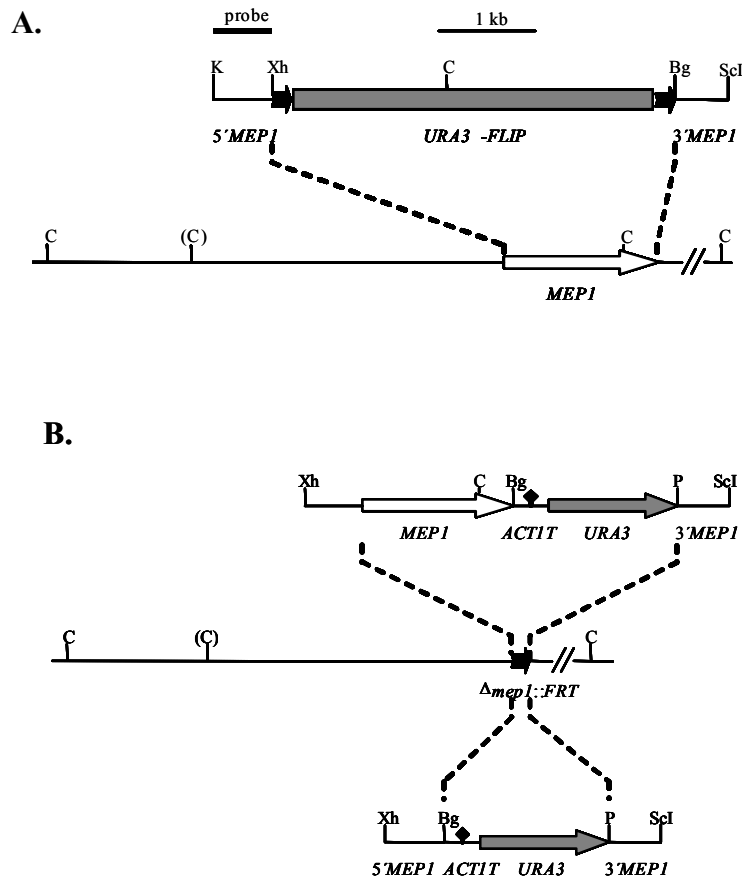


Fig. 8. (A) Structure of the deletion cassette from plasmid pMEP1M2 (top) and genomic structure of the *CaMEP1* locus in the parent strain CA14 (bottom). The *CaMEP1* coding region is represented by the white arrow, and the upstream and downstream sequences by the solid lines. The 34 bp *FRT* sites are not drawn to scale. The probe used for Southern hybridization analysis of the mutants is indicated by the black bar. (B) Structure of the DNA fragments from pMEP1K1 (top) and pMEP1M4 (bottom), which were used for reintegration of an intact *CaMEP1* copy (white arrow) or only the *URA3* marker (grey arrow), respectively, into one of the inactivated $\Delta mep1$ alleles (middle). The *ACT1* transcription termination sequence (*ACT1T*) is indicated by the black diamond. Only relevant restriction sites are given. Bg, *Bgl*II; C, *Cl*aI; K, *Kpn*I; P, *Pst*I; Scl, *Sac*I; Xh, *Xho*I. The *Cl*aI site shown in parentheses is present only in the *CaMEP2-1* allele.

To generate the prototrophic $\Delta mep1$ mutants the *URA3* selection marker alone was integrated into either of the two inactivated $\Delta mep1$ alleles (see section 3.2 and Fig. 8B, bottom) of the homozygous $\Delta mep1$ mutants MEP1M4A and MEP1M4B, resulting to the generation of the strains MEP1M5A and MEP1M5B (Fig. 9, lanes 10 and 11). For the reintroduction of the complete copy of the *CaMEP1* gene (see section 3.2 and Fig. 8B) along with the *URA3* marker, an intact *CaMEP1* copy was integrated into either of the inactivated $\Delta mep1$ alleles in strains MEP1M4A and MEP1M4B to generate the complemented strains MEP1MK1A and MEP1MK1B (Fig. 9, lanes 12 and 13).

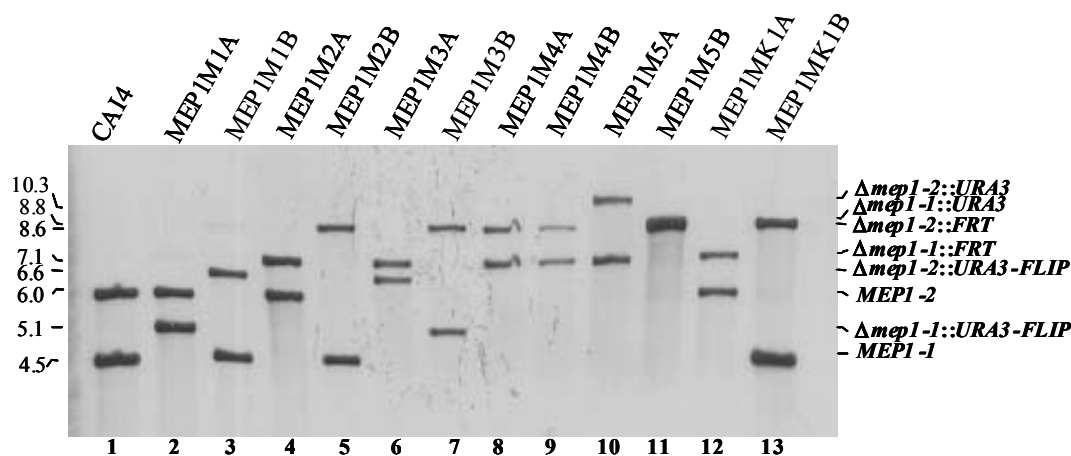


Fig. 9. Southern hybridization of *Cla*I-digested genomic DNA of the parent strain CAI4 and mutant derivatives with a *CaMEP1*-specific probe shown in Fig. 8A. The sizes of the hybridizing fragments (in kb) are given on the left side of the blot and their identities are indicated on the right.

To construct $\Delta mep1 \Delta mep2$ double mutants the $\Delta mep2$ mutants, MEP2M4A and MEP2M4B (see section 3.3) were transformed with the *CaMEP1* deletion cassette. From each parent strains, one transformant in which the *URA3* flipper was integrated into either the *CaMEP1-1* allele of strain MEP2M4A (MEP12M1A, Fig. 10, lanes 4) or into the *CaMEP1-2* allele of strain MEP2M4B (MEP12M1B, Fig. 10, lanes 5) was selected. The *URA3* flipper was excised from these strains by FLP-mediated recombination, resulting in the uridine-auxotrophic strains MEP12M2A and MEP12M2B (Fig. 10, lanes 6 and 7). Deletion of the remaining *CaMEP1* wild-type alleles in a second round of insertion/excision of the *URA3* flipper generated strains MEP12M3A and B (Fig. 10, lanes 8 and 9) and their *ura3*-negative derivatives MEP12M4A and B (Fig. 10, lanes 10 and 11). The homozygous $\Delta mep1 \Delta mep2$ double mutants (MEP12M4A and B) then served as host strains for reintroduction of an intact *CaMEP1* copy with the help of the *URA3* marker (Fig. 8B, top) into either of the two inactivated $\Delta mep1$ alleles, resulting in strains MEP12MK1A and B (Fig. 10A, lanes 16 and 17), or of an intact *CaMEP2* copy into either of the two inactivated $\Delta mep2$ alleles, resulting in strains MEP12MK2A and B (Fig. 10B, lanes 18 and 19). To obtain appropriate control strains, the *URA3* marker alone was inserted in the identical way (see Fig. 8B, bottom and Fig. 6B, bottom) into either of the four possible alleles, thereby generating the prototrophic, homozygous $\Delta mep1 \Delta mep2$ double mutants MEP12M5A and B and MEP12M6A and B (Fig. 10A and B, lanes 12 to 15).

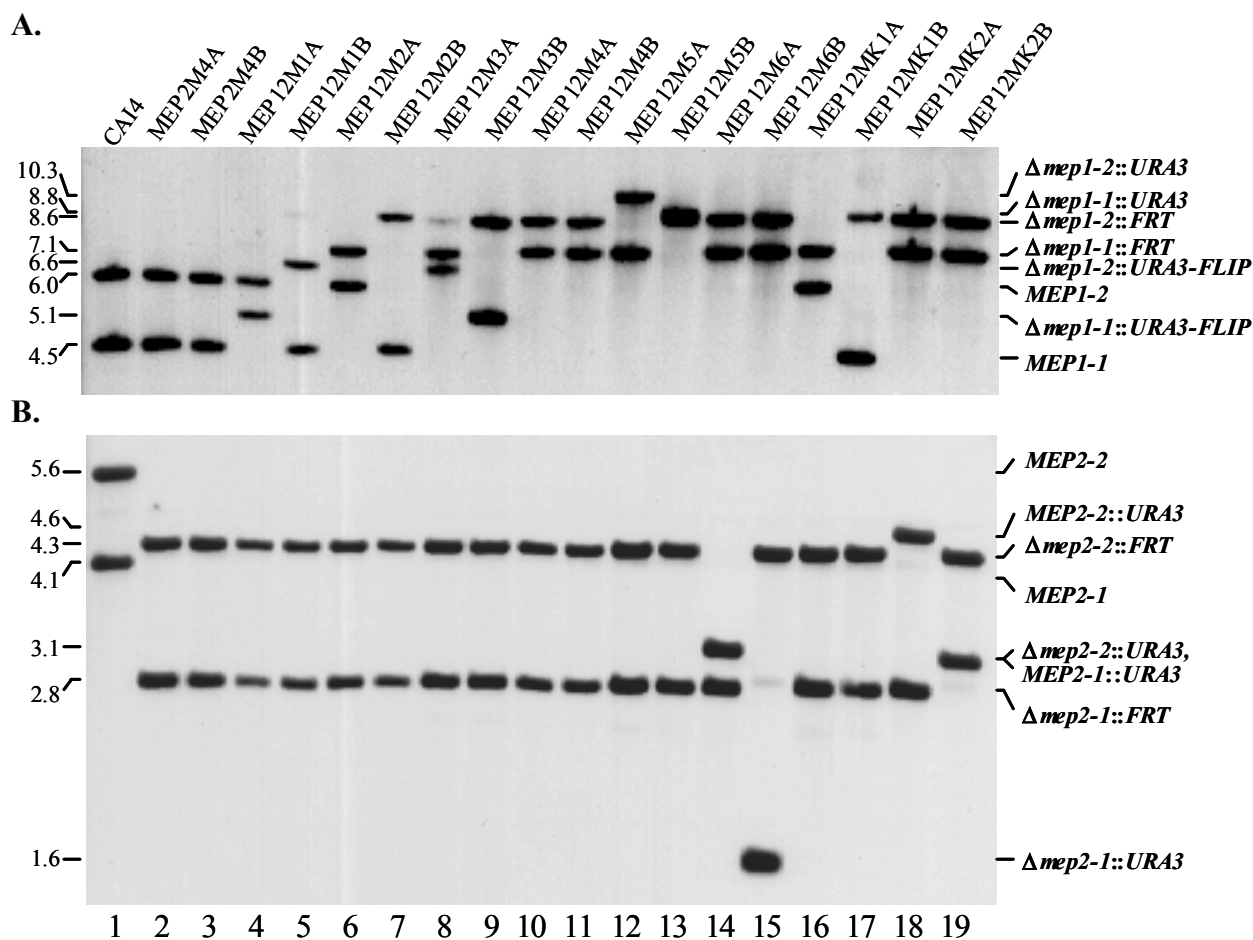


Fig. 10. Construction of *C. albicans* $\Delta mep1 \Delta mep2$ double mutants and complemented strains. (A) Southern hybridization of *Cla*I-digested genomic DNA of the wild-type strain CA14, the $\Delta mep2$ parental strains MEP2M4A and B, and *mep1* mutant derivatives with a *CaMEP1*-specific probe shown in Fig. 8A. The sizes of the hybridizing fragments (in kb) are given on the left side of the blot and their identities are indicated on the right. (B) Southern hybridization of *Eco*RI-digested genomic DNA of the same strains with the *CaMEP2*-specific probe shown in Fig. 6A.

4.1.4. CaMep1p and CaMep2p are functional ammonium permeases

The ability of all *mep* mutants to grow on media containing various ammonium concentrations as the sole nitrogen source (Fig. 11) was tested. Strains lacking both the Mep proteins showed a severe growth defect on media containing less than 5 mM ammonium. At high ammonium concentrations (76 mM) the $\Delta mep1 \Delta mep2$ double mutants grew well, presumably because under these conditions sufficient ammonium can diffuse across the cytoplasmic membrane in an unmediated manner fast enough to allow optimal growth (Marini *et al.*, 1997; Soupene *et al.*, 2001). Compared to the wild-type strain, cells with a single *MEP* gene deletion were not affected for growth on all ammonium concentrations tested (data not shown). In contrast to the double mutants, cells expressing a single Mep protein were able to

complement the growth defect at low ammonium concentrations. Uridine-auxotrophic strains behaved like their prototrophic counterparts (data not shown).

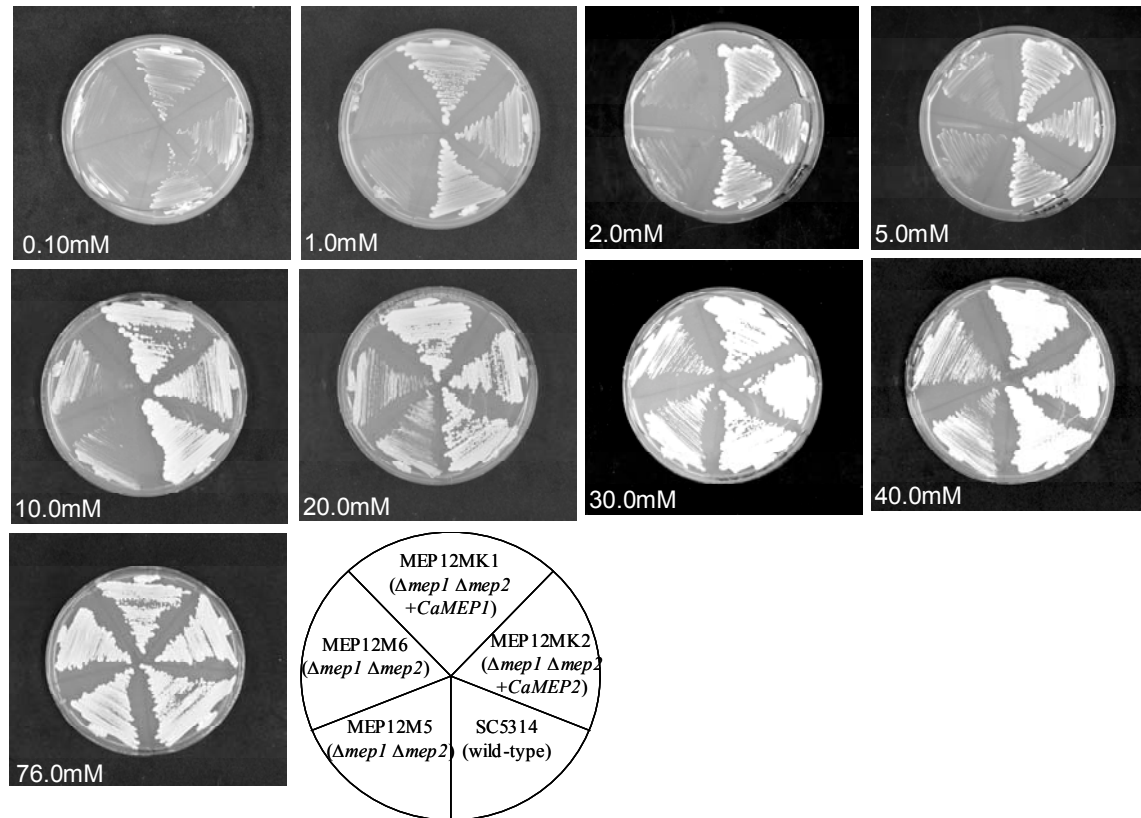


Fig. 11. Growth of the wild-type strain SC5314, the $\Delta mep1 \Delta mep2$ double mutants MEP12M5 and MEP12M6, and the complemented strains MEP12MK1 and MEP12MK2 in which an intact copy of *CaMEP1* or *CaMEP2*, respectively, was reintroduced, on YNB agar plates containing the indicated ammonium concentrations. The plates were incubated at 30°C for 4 days. The strain pairs A and B behaved identically and only one of them is shown in each case. The $\Delta mep1$ and $\Delta mep2$ single mutants grew as well as the wild-type strain and are not included in the figure.

The ability of Δmep mutants to extract the ammonium from minimal proline medium containing 1mM ammonium (see section 3.9) was then examined. In comparison to the wild-type strain and strains expressing either of the Mep proteins, $\Delta mep1 \Delta mep2$ double mutants exhibited no ammonium uptake capacity (Fig. 12). Cells expressing either of the Mep proteins did not exhibit any difference in the ammonium uptake capacity compared to the wild-type. These findings are consistent with the growth of these strains on ammonium limiting medium. These results provide experimental evidence that both these proteins are functional ammonium permeases and the expression of either of the two permeases is sufficient to allow growth of *C.albicans* under low ammonium conditions.

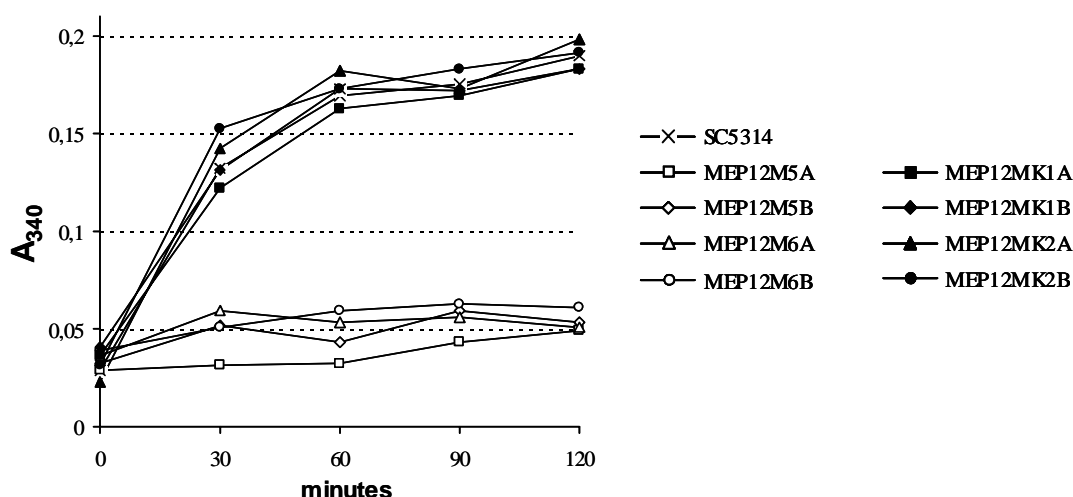


Fig. 12. Ammonium uptake from the medium by the wild-type strain SC5314, the $\Delta mep1 \Delta mep2$ double mutants MEP12M5A/B and MEP12M6A/B, and the complemented strains MEP12MK1A/B ($\Delta mep1 \Delta mep2 + CaMEP1$) and MEP12MK2A/B ($\Delta mep1 \Delta mep2 + CaMEP2$). For experimental details see section 3.9.

4.1.5. The CaMep2 ammonium permease is required for nitrogen starvation induced filamentous growth

To test whether these two ammonium permeases affect filamentous growth in low nitrogen medium, the morphology of a series of *mep* mutants was tested after growth for 6 days at 37°C on plates containing 100 μ M ammonium (Fig. 13). Strains lacking Mep2 showed a severe defect in filamentation in low nitrogen medium, however, these strains had no apparent growth defect. In contrast, deletion of *CaMEP1* had no effect on hyphal growth as noted above. Strains lacking both ammonium permeases showed severe growth defect on low nitrogen medium, but when these strains were complemented either with *CaMEP1* or *CaMEP2*, the growth defect was complemented. However, the filamentation defect was complemented only when *CaMEP2* was reintroduced (Fig. 13, first row).

In *S.cerevisiae*, *ScMEP2* is essential for pseudohyphal growth at low ammonium concentrations, but *ScMEP2* deletion does not affect pseudohyphae formation when limiting concentrations of other nitrogen sources, like amino acids are present instead of ammonium, which led to the current model that ScMep2p is an ammonium sensor regulating pseudohyphal differentiation (Lorenz and Heitman, 1998a). Therefore, whether *CaMEP2* is involved in the induction of filamentous growth of *C.albicans* by other environmental signals was tested. The $\Delta mep1 \Delta mep2$ strains did not show any growth defect when the media contain limiting concentrations of urea or amino acids like glutamine, proline, glutamate, histidine, or

arginine as the sole nitrogen source. However, except when arginine was used, in all other conditions the capacity to switch from yeast to filamentous growth depended on the presence of a functional *CaMEP2* gene (Fig. 13). All those phenotypes were seen in both *URA3* and *ura3* mutants when the mutants were compared with their respective control strains (data not shown).

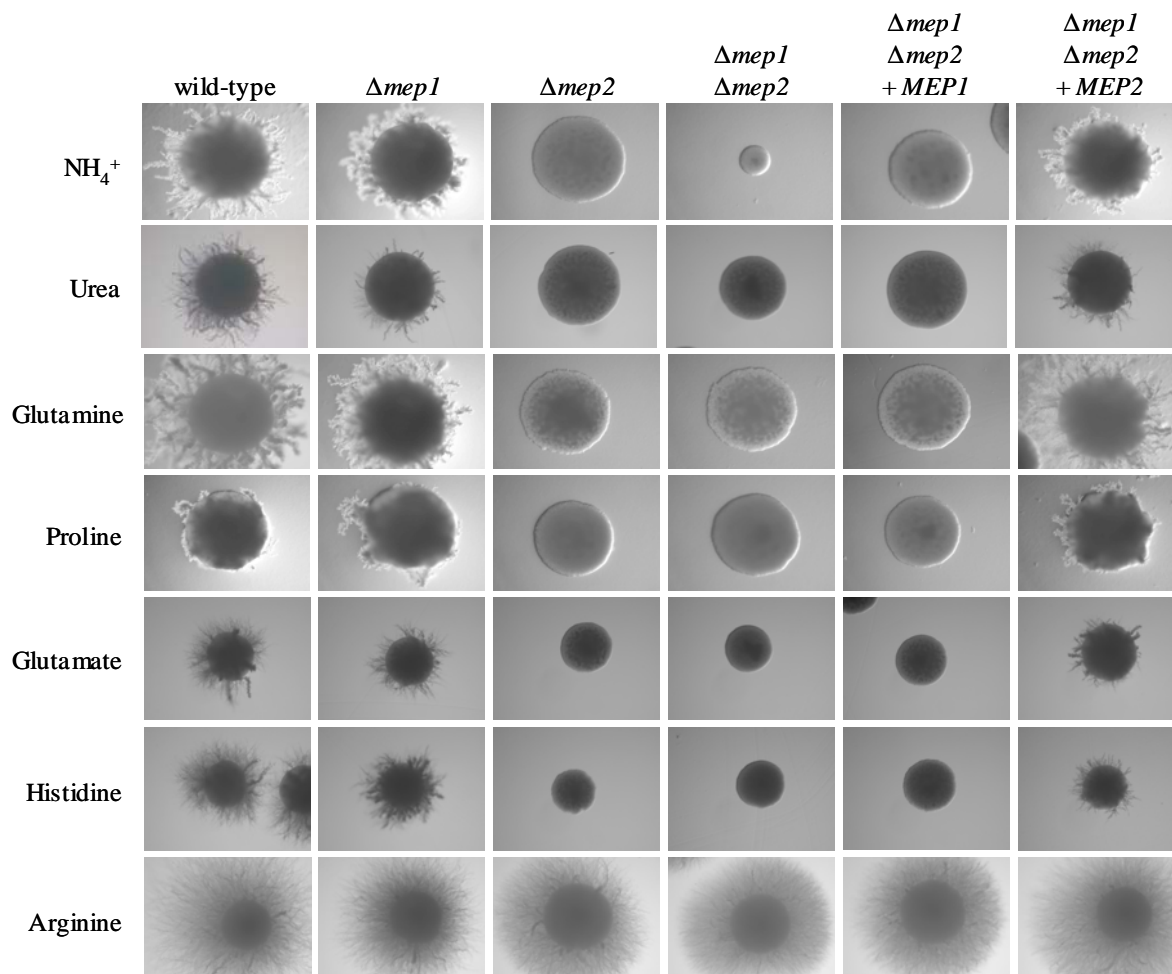


Fig. 13. *CaMEP2* is required for nitrogen starvation induced filamentous growth of *C.albicans*. (A) YPD precultures of the strains were appropriately diluted and spread on YNB plates containing the indicated nitrogen sources at a concentration of 100 μM . Individual colonies were photographed after incubation for 6 days at 37°C. The small colonies produced by the $\Delta mep1 \Delta mep2$ double mutants on plates containing 100 μM ammonium (SLAD) are due to residual growth after transfer from rich medium and no growth was observed when these strains were restreaked on the same plates. The following strains were used: wild-type, SC5314; $\Delta mep1$, MEP1M5A and B, $\Delta mep2$, MEP2M5A and B, $\Delta mep1 \Delta mep2$, MEP12M5A and B and MEP12M6A and B; $\Delta mep1 \Delta mep2 + MEP1$, MEP12MK1A and B; $\Delta mep1 \Delta mep2 + MEP2$, MEP12MK2A and B. Independently constructed mutants and complemented strains behaved identically and only one of them is shown in each case.

Apart from nitrogen starvation, filamentous growth of *C.albicans* can be induced by many other environmental factors, like the presence of serum, a shift from acidic to neutral pH, or embedding in agar. When the mutant strains were incubated in other hyphal inducing media, like on serum containing plates or after embedding in agar, they showed no defect in hyphal formation (Fig. 14). Moreover, $\Delta mep2$ mutants had no defect in hyphal induction in any of the liquid hyphal inducing media tested, which indicates that *CaMEP2* has no role in hyphal induction under those conditions (Fig. 15).

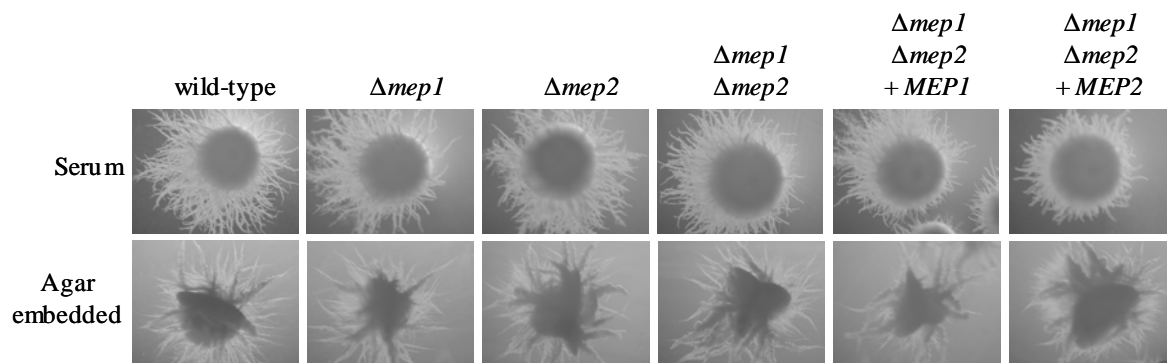


Fig. 14. Hyphal growth was induced in plates containing 10% serum (top row) or by embedding the cells in YPS agar (bottom row). Photographs were taken after 6 days of growth at 37°C (serum) or at 25°C (YPS). Deletion of *CaMEP2* did not affect hyphal growth under these conditions. The following strains were used: wild-type, SC5314; $\Delta mep1$, MEP1M5A and B, $\Delta mep2$, MEP2M5A and B, $\Delta mep1 \Delta mep2$, MEP12M5A and B and MEP12M6A and B; $\Delta mep1 \Delta mep2 + MEP1$, MEP12MK1A and B; $\Delta mep1 \Delta mep2 + MEP2$, MEP12MK2A and B. Independently constructed mutants and complemented strains behaved identically and only one of them is shown in each case.

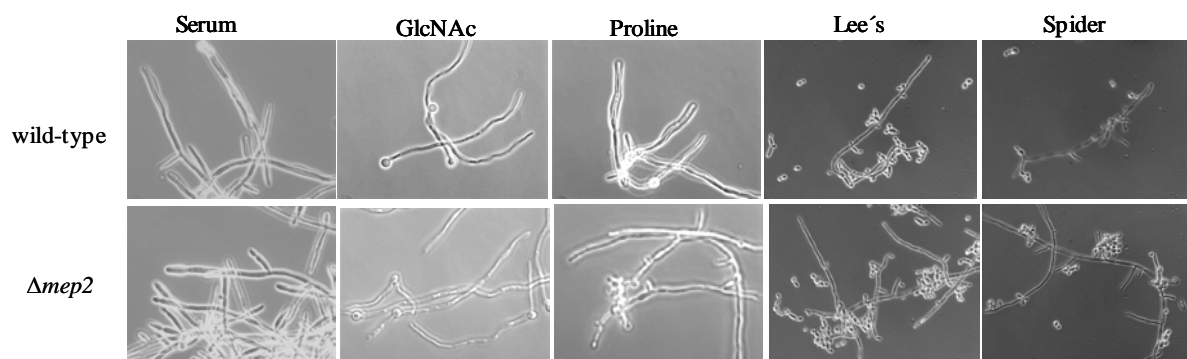


Fig. 15. Filamentous growth of cells in liquid culture. YPD grown cells were diluted 1:100 in the hyphal inducing media and photographs were taken after 6 hours incubation at 37°C. Deletion of *CaMEP2* had no effect in hyphal induction in these media. The following strains were used: wild-type, SC5314; $\Delta mep2$, MEP2M5A. Independently constructed mutants and complemented strains behaved identically.

4.1.6. Regulation of *CaMEP1* and *CaMEP2* expression

The physiological role of ammonium permeases is to scavenge external ammonium for use as a nitrogen source. The results above demonstrated that *CaMEP1* and *CaMEP2* are functional ammonium permeases, but *CaMEP2* has an additional function in the switch from yeast to filamentous growth under nitrogen starvation conditions. In order to understand these functional differences, the regulation of *CaMEP1* and *CaMEP2* expression by nitrogen availability was investigated.

Northern hybridization using RNA from the wild-type strain SC5314, grown at different concentrations of ammonium or other nitrogen sources, showed a single band hybridizing with the probe used to detect *CaMEP2* transcript. The intensity of the signal varied according to the nitrogen sources available in the medium. No or very low amounts of *CaMEP2* RNA were detected when cells were grown at 20 mM or higher concentrations of ammonium, but *CaMEP2* expression was strongly induced when the ammonium concentration was decreased to 10 mM and below (Fig. 16, lanes 1-4). Comparable levels of *CaMEP2* mRNA were detected when 100 μ M of urea or different amino acids were used as the sole source of nitrogen (Fig. 16, lanes 5-10), indicating that the presence of ammonium is not required to induce *CaMEP2* expression under nitrogen limiting conditions. In several repeat experiments no *CaMEP1* transcript could be detected in any of the conditions tested, even in a $\Delta mep2$ background (data not shown). However, the phenotype of $\Delta mep1 \Delta mep2$ double mutants demonstrates that at least under low ammonium conditions sufficient expression of *CaMEP1* must occur to support growth.

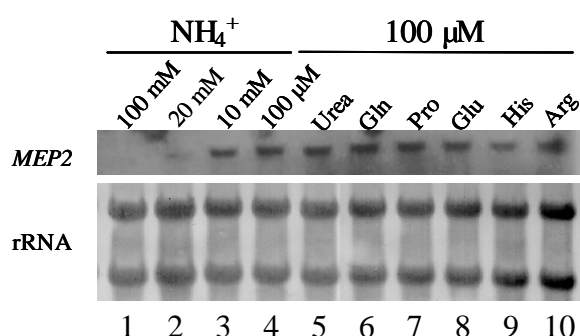


Fig. 16. Detection of *CaMEP2* mRNA by Northern hybridization analysis of the wild-type strain SC5314 grown at 30°C to log phase in liquid YNB medium containing the indicated concentrations of ammonium, urea, or amino acids (see section 3.6.1 for growth conditions).

Since no good quality RNA could be isolated from cells growing as agar invading filaments on plates, *lacZ* reporter fusions were used to analyze expression of the *CaMEP1* and *CaMEP2* promoters on solid media containing different ammonium concentrations. At 10 mM or lower concentrations of ammonium the *CaMEP2* promoter was strongly induced, producing intense blue stained colonies in X-Gal agarose overlay assay (see section 3.10), whereas on plates containing 20 mM or higher concentrations of ammonium the *CaMEP2P-lacZ* fusion produced β -galactosidase activity that was only slightly above the background (Fig. 17, last row). This result indicates that the regulation of *CaMEP2* expression by ammonium levels on the solid media is similar to that seen in liquid media. At high ammonium concentrations, colonies of strains carrying a *CaMEP1P-lacZ* fusion showed a somewhat stronger color production than those expressing *lacZ* from the *CaMEP2* promoter, but the *CaMEP1* promoter was also clearly induced when ammonium levels decreased to 10 mM or below (Fig. 17, third row). These results indicate that both *CaMEP1* and *CaMEP2* are induced when ammonium levels become limiting and require transporter mediated uptake.

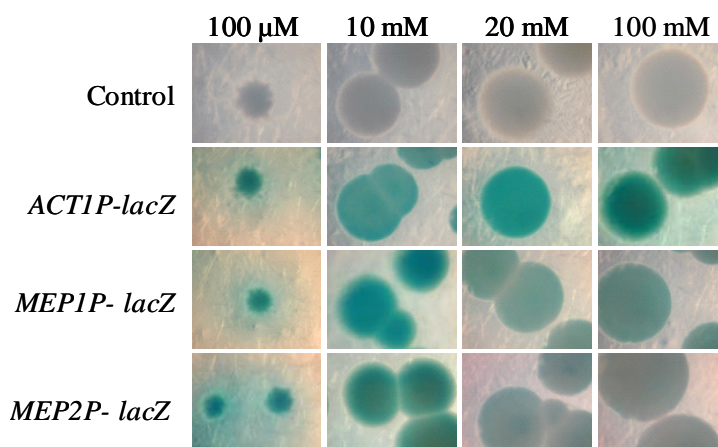
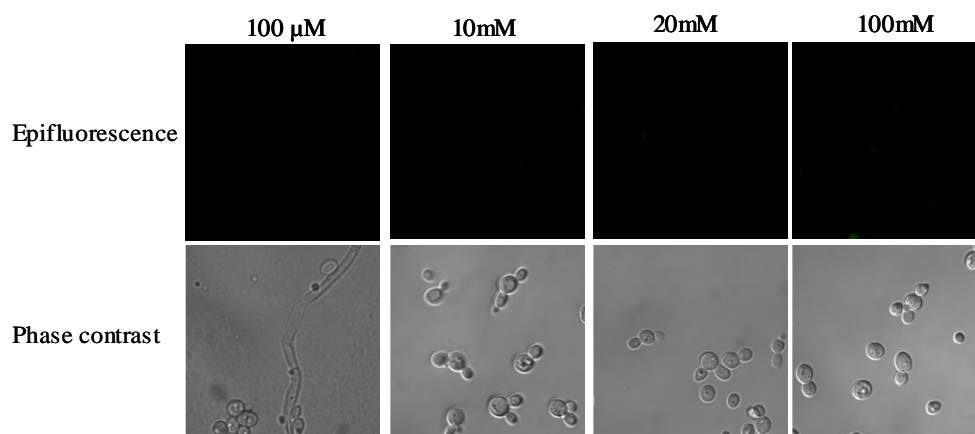


Fig. 17. Induction of the *CaMEP1* and *CaMEP2* promoters on solid media with varying ammonium concentrations. Strains carrying *MEP1P-lacZ* or *MEP2P-lacZ* reporter fusions were grown on YNB agar plates containing the indicated concentrations of ammonium and β -galactosidase activity was measured using an X-Gal agarose overlay assay (see section 3.10). Individual colonies were photographed. The strain pairs CLACZ1A/B (*MEP1P-lacZ*) and CLACZ2A/B (*MEP2P-lacZ*) behaved identically and only one of them is shown in each case. Strain CALACZ1, which carries a *ACT1P-lacZ* fusion (Uhl and Johnson, 2001), served as a positive control, and the wild-type strain SC5314 was used as a negative control.

Since the *lacZ* reporter fusion experiment did not detect differences in the expression levels of the two permeases at low ammonium concentrations, which was in contrast to the results of the Northern analysis, strains expressing GFP-tagged CaMep1p or CaMep2p (see

section 3.3) were used to compare the expression of *CaMEP1* and *CaMEP2* in different growth conditions. When expressed in a $\Delta mep1 \Delta mep2$ double mutant background, the *GFP*-tagged *CaMEP1* and *CaMEP2* genes restored ammonium uptake and growth on SLAD plates (see section 4.1.7), demonstrating that they encode functional ammonium permeases.

A.



B.

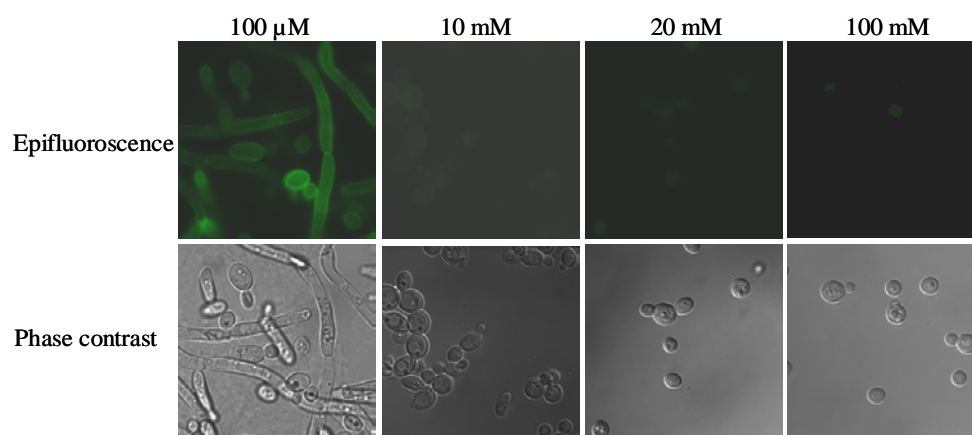


Fig. 18. Expression of GFP-tagged CaMep1p (**A**) or CaMep2p (**B**) after 6 days of growth at 37°C on YNB agar plates containing the indicated concentrations of ammonium. Fluorescence of the cells was observed by confocal microscopy. The strain pairs CMEP1GA/B (*MEP1-GFP*) and CMEP2GA/B (*MEP2-GFP*) behaved identically and only one of them is shown in each case.

Expression of the GFP-tagged CaMep2p could be detected by fluorescence of the cells at their peripheries when the reporter strains were grown at low ammonium concentrations, whereas no fluorescence was detected at higher ammonium concentrations (Fig. 18B). In accordance with the results of Northern hybridization experiments (Fig. 16) no significant

difference in expression of the CaMep2p-GFP fusion was detected during logarithmic growth in liquid medium containing 100 μM or 10 mM ammonium (Fig. 19). On solid medium, cells grown at 100 μM ammonium exhibited stronger fluorescence than cells grown at 10 mM ammonium, suggesting *CaMEP2* is expressed at higher levels when *C.albicans* switches from yeast to filamentous growth (Fig. 18B). No fluorescence of cells carrying the *CaMEP1-GFP* fusion was detectable at any ammonium concentration (Fig. 18A), which is in line with the results of the Northern hybridization experiments. Altogether these results showed that at low ammonium concentrations the promoters of both *CaMEP1* and *CaMEP2* are induced (as seen from the *lacZ* reporter fusions) but *CaMEP2* is expressed much more strongly than *CaMEP1* (as judged the amounts of mRNA and GFP-tagged proteins).

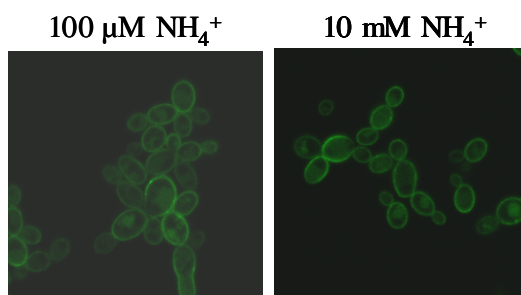


Fig. 19. Expression of CaMep2-GFP fusion protein in cells grown at 30°C to log phase in liquid YNB medium containing 100 μM or 10 mM ammonium. Fluorescence of the cells was observed by confocal microscopy. The two independently constructed reporter strains MEP12MG2A and B behaved identically and only one of them is shown.

4.1.7. Nitrogen starvation induced filamentous growth depends on high *CaMEP2* expression levels

To investigate whether the differences in the expression level of the two ammonium permeases determine their different role in filament induction, both genes were expressed under the control of the strong *ADH1* promoter. In addition, promoter swapping experiments were also performed, where *CaMEP1* was expressed from the *CaMEP2* promoter and vice versa (Fig. 20A and B).

Expression of *CaMEP1* from the *ADH1* promoter rescued the growth defect of Δmep1 Δmep2 double mutants on SLAD plates and restored ammonium uptake to wild-type levels, but did not result in filamentous growth. When *CaMEP1* was expressed under the control of

CaMEP2 promoter, ammonium uptake and growth on SLAD plates were also restored, and a minor percentage of the colonies even showed a weak filamentation. In contrast, the defects in ammonium uptake and growth on SLAD plates of $\Delta mep1 \Delta mep2$ double mutants were only partially rescued when *CaMEP2* was expressed from the *ADH1* or the *CaMEP1* promoter. Importantly, these strains were also unable to filament on SLAD plates (Fig. 20A and B).

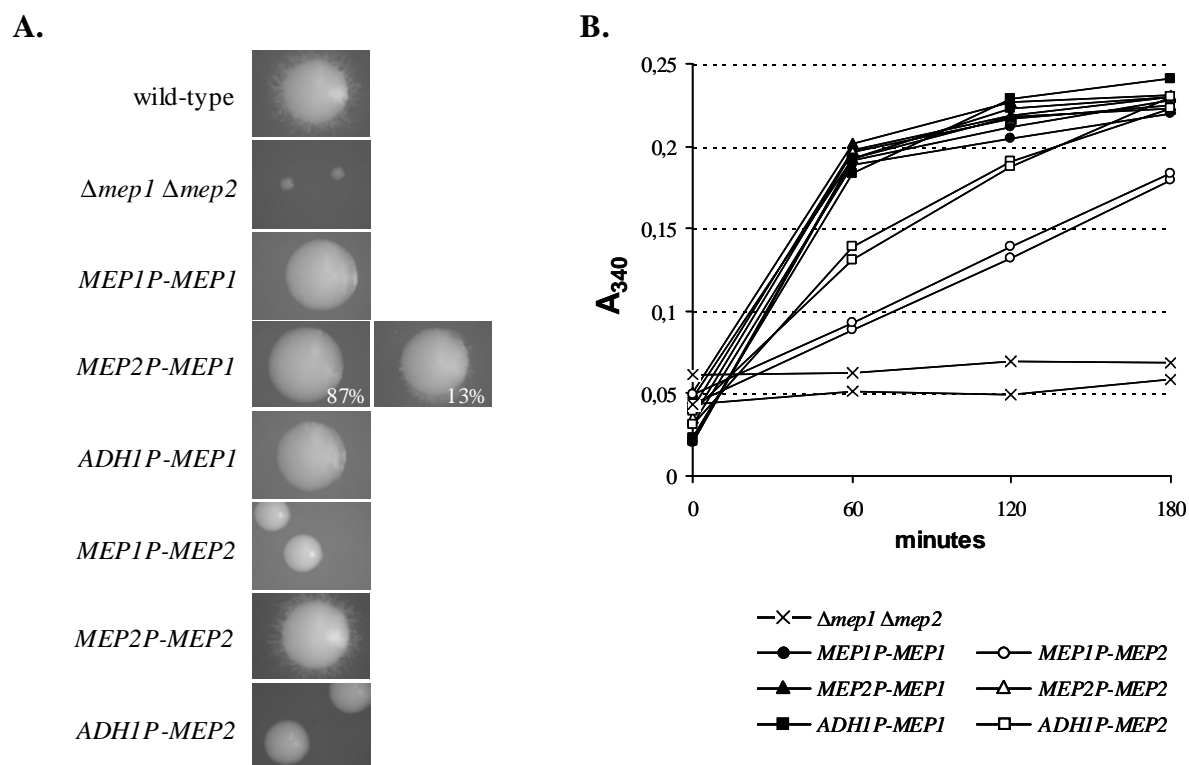


Fig. 20. Growth and ammonium uptake of strains expressing a single copy of *CaMEP1* or *CaMEP2* under control of the *CaMEP1*, *CaMEP2*, or *ADH1* promoter. (A) $\Delta mep1 \Delta mep2$ double mutants carrying the indicated fusions were grown for 6 days at 37°C on SLAD plates. All colonies are shown at the same magnification. Transformants of the independently generated $\Delta mep1 \Delta mep2$ mutants MEP12M4A and B behaved identically and only one of them is shown in each case. The wild-type strain SC5314 and a $\Delta mep1 \Delta mep2$ double mutant were included for comparison. (B) Ammonium uptake of the same strains was measured as described in Materials and methods. The following strains were used: $\Delta mep1 \Delta mep2$, MEP12M5A and MEP12M6A; *MEP1P-MEP1*, MEP12MK1A and B; *MEP2P-MEP1*, MEP12MK3A and B; *ADH1P-MEP1*, MEP12ME1A and B; *MEP1P-MEP2*, MEP12MK4A and B; *MEP2P-MEP2*, MEP12MK2A and B; *ADH1P-MEP2*, MEP12ME2A and B.

In order to relate the phenotypes of strains to the expression levels of the ammonium permeases, expressions of *CaMEP1* and *CaMEP2* from the *CaMEP1*, *CaMEP2*, or *ADH1* promoters were monitored using the *GFP* fusions. The amounts of mRNA levels were compared using *GFP* as a probe in Northern hybridizations of cells grown in SLAD medium. No *CaMEP1-GFP* mRNA was detected when it was expressed from the native *CaMEP1*

promoter, but the *CaMEP1-GFP* transcript was readily observed when expressed under control of the *CaMEP2* promoter, and mRNA levels increased further when it was expressed from the *ADH1* promoter (Fig. 21, lanes 1-3). The same hierarchy of promoter strength was observed for *CaMEP2-GFP* expression (Fig. 21, lanes 4-6). Of note, the levels of *CaMEP2-GFP* mRNA were always higher than those of the *CaMEP1-GFP* transcript expressed from the same promoter. These results demonstrate that under nitrogen starvation conditions the *CaMEP2* promoter is more strongly induced than the *CaMEP1* promoter and also suggest that the *CaMEP2* transcript is more stable than the *CaMEP1* mRNA.

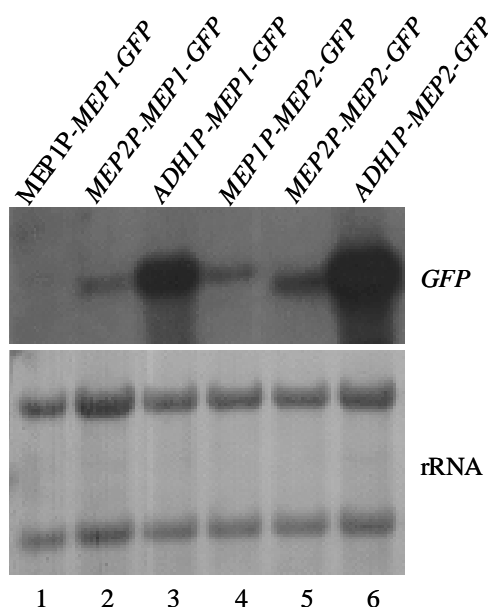


Fig. 21. Expression of *CaMEP1-GFP* or *CaMEP2-GFP* fusions under control of the *CaMEP1*, *CaMEP2*, or *ADH1* promoter in a wild-type background. The strains were grown to log phase in liquid SLAD medium at 30°C and then used for RNA isolation and Northern hybridization analysis with a *GFP*-specific probe. The following strains were used: *MEP1P-MEP1-GFP*, CMEP1GA and B; *MEP2P-MEP1-GFP*, CMEP1G2A and B; *ADH1P-MEP1-GFP*, CMEP1EGA and B; *MEP1P-MEP2-GFP*, CMEP2G1A and B; *MEP2P-MEP2-GFP*, CMEP2GA and B; *ADH1P-MEP2-GFP*, CMEP2EGA and B. Independent transformants gave identical results and only one of them is shown in each case.

Analysis of the strains by fluorescence microscopy confirmed that the GFP-tagged ammonium permeases were more strongly expressed from the *CaMEP2* promoter than from the *CaMEP1* promoter and the fluorescence of cells expressing *CaMEP2-GFP* was much stronger than that of cells expressing *CaMEP1-GFP* from the same promoter (Fig. 22). In contrast, the high transcript levels produced from the *ADH1* promoter did not result in high amounts of protein (Fig. 21 and Fig. 22). Expression of the *CaMEP1-GFP* either from the

ADH1 or *CaMEP2* promoter resulted in comparable fluorescence, and fluorescence of cells expressing *GFP*-tagged *CaMep2p* from *ADH1* promoter was even weaker than when it was expressed from the *CaMEP2* promoter, suggesting that the translation of the *CaMEP1-GFP* and *CaMEP2-GFP* transcripts carrying the *ADH1* upstream region was relatively inefficient.

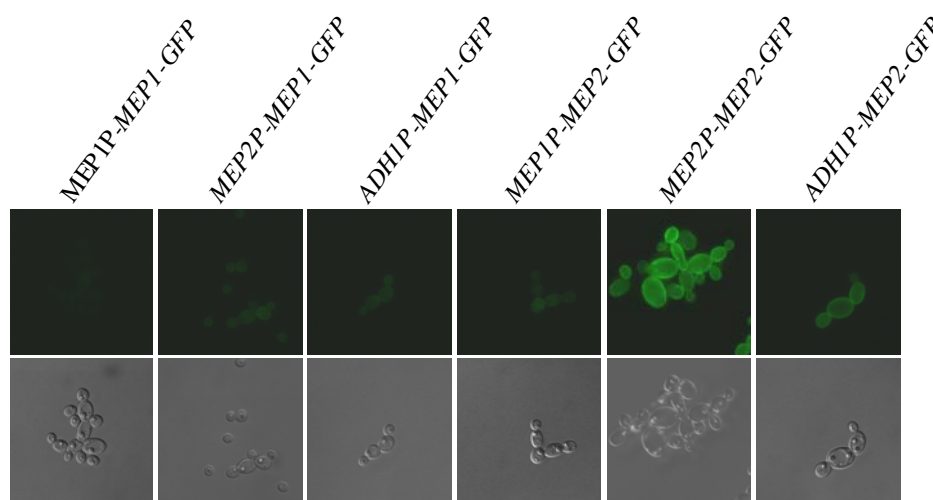


Fig. 22. Expression of *CaMEP1-GFP* or *CaMEP2-GFP* fusions under control of the *CaMEP1*, *CaMEP2*, or *CaADH1* promoter in a wild-type background. The strains were grown to log phase in liquid SLAD medium at 30°C and then fluorescence of the cells was examined by confocal microscopy. The following strains were used: *MEP1P-MEP1-GFP*, CMEP1GA and B; *MEP2P-MEP1-GFP*, CMEP1G2A and B; *ADH1P-MEP1-GFP*, CMEP1EGA and B; *MEP1P-MEP2-GFP*, CMEP2G1A and B; *MEP2P-MEP2-GFP*, CMEP2GA and B; *ADH1P-MEP2-GFP*, CMEP2EGA and B. Independent transformants gave identical results and only one of them is shown in each case.

The phenotypes of cells expressing the *GFP*-tagged *CaMEP* genes from the different promoters were comparable to those expressing the untagged genes from the same promoters (compare Fig. 20A and B with Fig. 23A and B). Expression of *CaMEP1-GFP* from either of the promoters in a $\Delta mep1\Delta mep2$ double mutant resulted in wild type levels ammonium uptake and growth on SLAD plates, including the weak filamentation of some colonies of strains carrying the fusion under control of the *CaMEP2* promoter (Fig. 23A and B). The reduced expression of *CaMep2p-GFP* from the *ADH1* and *CaMEP1* promoters as compared with the *CaMEP2* promoter correlated with inefficient ammonium uptake, reduced growth on SLAD plates, and defective filamentation under nitrogen limiting conditions. These data showed that *CaMEP2* needs to be expressed at high levels (as from its own promoter) to mediate efficient ammonium uptake and to support optimal growth and strong filamentation

under low ammonium conditions. In contrast, the low levels of *CaMEP1* expression seem to be sufficient to support ammonium uptake and optimal growth at limiting ammonium concentrations, indicating that *CaMep1p* is more efficient permease than *CaMep2p*. When artificially expressed at higher levels, *CaMEP1* could even partially rescue the filamentation defect of $\Delta mep2$ mutants. Therefore, it can be concluded that the specific role of *CaMEP2* in nitrogen starvation induced filamentous growth results at least in part from its high expression as compared with *CaMEP1*.

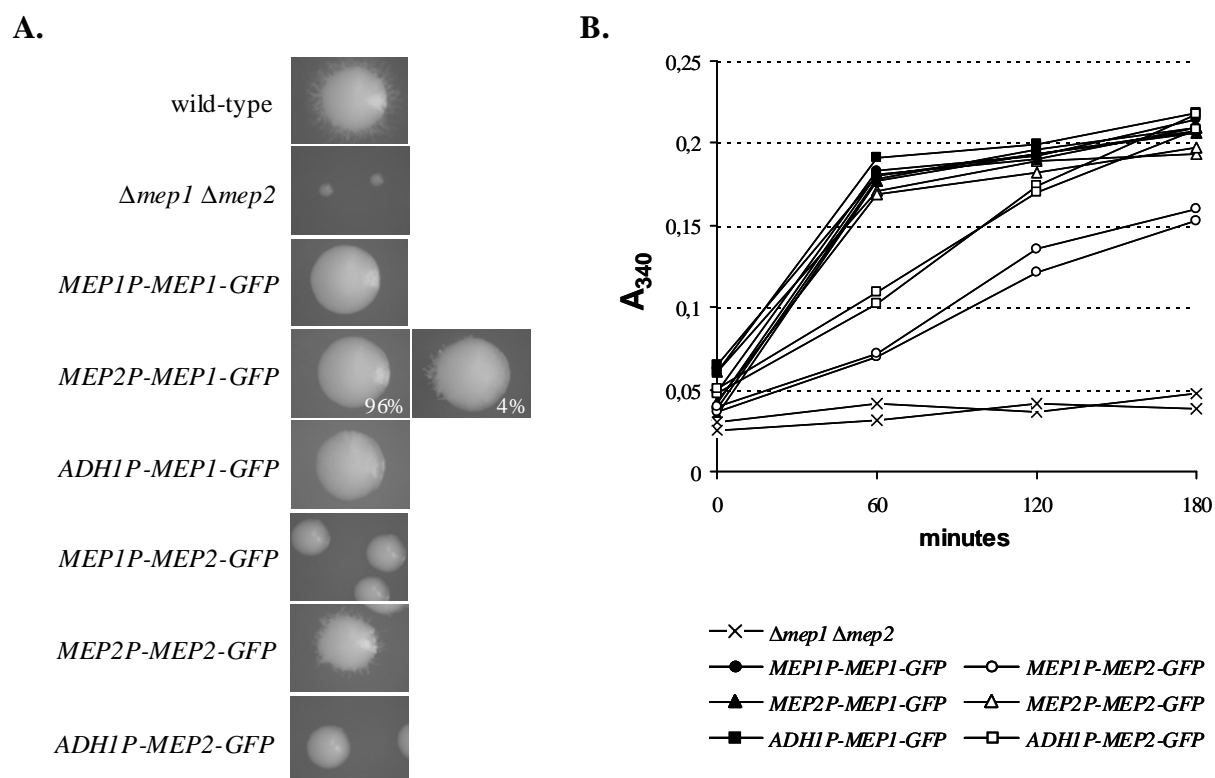


Fig. 23. Growth and ammonium uptake of strains expressing a single copy of *CaMEP1-GFP* or *CaMEP2-GFP* fusion under control of the *CaMEP1*, *CaMEP2*, or *CaADH1* promoter. **(A)** $\Delta mep1 \Delta mep2$ double mutants carrying the indicated fusions were grown for 6 days at 37°C on SLAD plates. All colonies are shown at the same magnification. Transformants of the independently generated $\Delta mep1 \Delta mep2$ mutants MEP12M4A and B behaved identically and only one of them is shown in each case. The wild-type strain SC5314 and a $\Delta mep1 \Delta mep2$ double mutant are shown for comparison. **(B)** Ammonium uptake of the same strains was measured as described in section 3.9. The following strains were used: $\Delta mep1 \Delta mep2$, MEP12M5A and MEP12M6A; *MEP1P-MEP1-GFP*, MEP12MG1A and B; *MEP2P-MEP1-GFP*, MEP12MG3A and B; *ADH1P-MEP1-GFP*, MEP12MEG1A and B; *MEP1P-MEP2-GFP*, MEP12MG5A and B; *MEP2P-MEP2-GFP*, MEP12MG2A and B; *ADH1P-MEP1-GFP*, MEP12MEG2A and B.

4.1.8. The C-terminal tail of CaMep2p contains a region important for filamentation

As CaMep2p is a transmembrane protein and was predicted to have a cytoplasmic tail of about 74 amino acids, it was hypothesized that the C-terminal cytoplasmic tail of CaMep2p might have a signaling function. This hypothesis was tested by expressing C-terminally truncated versions of CaMep2p in a $\Delta mep1 \Delta mep2$ double mutant background. It was found that deletion of the last 57 amino acids of CaMep2p abolished filamentation without affecting the transport function of the protein, because cells expressing $CaMEP2\Delta C^{423}$ showed wild-type ammonium uptake rates (Fig. 25) and grew on SLAD plates as well as cells expressing wild-type $CaMEP2$, but only in the yeast form (Fig. 24, No.3). Therefore the functions of CaMep2p in ammonium transport and filamentous growth are separable. Deletion of 74 amino acids from the C-terminus of CaMep2p resulted in a non-functional protein, since the cells expressing $CaMEP2\Delta C^{406}$ were unable to grow on SLAD plates and behaved like $\Delta mep1 \Delta mep2$ double mutants (Fig. 24, No.5). An analogous truncation of CaMep1p ($\Delta C404$) also rendered the cells unable to grow in limiting ammonium conditions (Fig. 24, No. 8). Depending on the algorithm used, the last amino acids in these truncated proteins are predicted to be located either directly behind (Marini *et al.*, 2000b) (see also Fig. 4) or within their last transmembrane domains (Marini and Andre, 2000). When 67 amino acids from the C-terminus of CaMep2p were deleted, resulting a slightly longer CaMep2p than the non-functional truncated version of CaMep2p, the growth defects of $\Delta mep1 \Delta mep2$ double mutant were partially rescued, but the colonies had an irregular shape (Fig. 24, No.4), probably because ammonium uptake capacity of the truncated permease was still impaired (Fig. 25).

An interesting phenotype was observed in cells expressing a truncated CaMep2p from which only the last 40 amino acids were removed ($\Delta C440$). These cells exhibited a hyperfilamentous phenotype on SLAD plates (Fig. 24, No.2). Northern analysis showed that $CaMEP2\Delta C^{440}$ transcript levels were strongly increased as compared with wild-type $CaMEP2$ mRNA (Fig. 26, lane 3), indicating that the hyperfilamentous phenotype was not caused by the removal of the C-terminal 40 amino acids but resulted from overexpression of the truncated $CaMEP2$ due to increased mRNA stability. A similar truncated version of CaMep1p ($\Delta C438$) retained its transporter function but did not induce filamentous growth (Fig. 24, No.7) and expression of $CaMEP1\Delta C^{438}$ remained below the detection limit by Northern hybridization (not shown). Importantly, the truncated $CaMEP2\Delta C^{423}$ allele, which did not restore filamentation, was overexpressed to the same extent as the $CaMEP2\Delta C^{440}$ allele that produced the hyperfilamentous phenotype (Fig. 26, lane 4). These results demonstrate that at

least some residues in the region between amino acids 423 and 440 of CaMep2p are essential for inducing hyphal growth in response to nitrogen starvation.

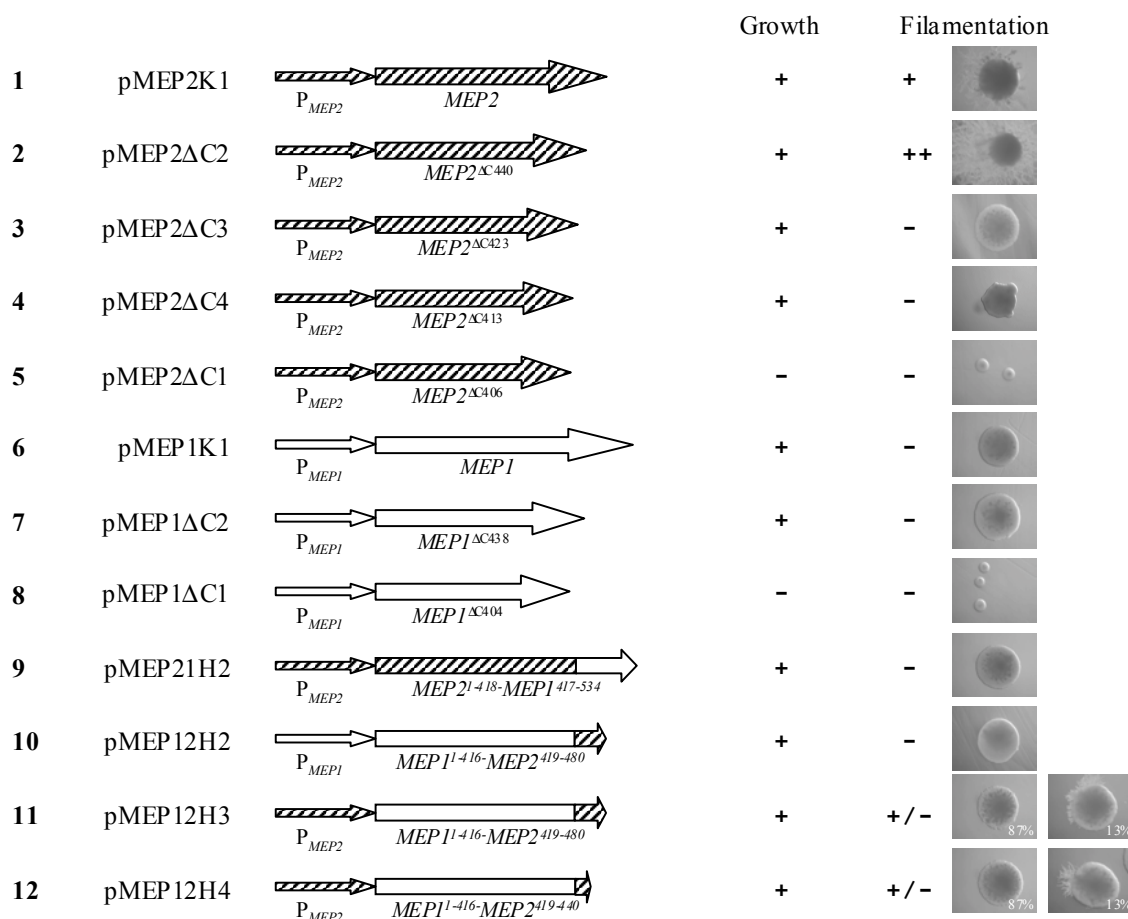


Fig. 24. Ability of C-terminally truncated versions and hybrid proteins of CaMep1p and CaMep2p to mediate growth and filamentation under ammonium starvation conditions. The names of the plasmids containing the various constructs are given on the left. Promoters and coding regions are symbolized by the thin and thick arrows, respectively. Regions derived from *CaMEP1* and *CaMEP2* are represented by white and hatched staining, respectively. + and - indicate growth/filamentation and no growth/filamentation, respectively, on SLAD plates. ++: hyperfilamentous growth; +/-: only some colonies showed a weak filamentation (the percentage of smooth and filamentous colonies is given). The appearance of the colonies after 6 days of growth on SLAD plates at 37°C is shown on the right. All constructs were expressed in $\Delta mep1 \Delta mep2$ double mutant backgrounds. The following strains were used: *MEP2P-MEP2*, MEP12MK2A and B; *MEP2P-MEP2*^{ΔC440}, MEP12MK2AΔC2 and MEP12MK2BΔC2; *MEP2P-MEP2*^{ΔC423}, MEP12MK2AΔC3 and MEP12MK2BΔC3; *MEP2P-MEP2*^{ΔC413}, MEP12MK2AΔC4 and MEP12MK2BΔC4; *MEP2P-MEP2*^{ΔC406}, MEP12MK2AΔC1 and MEP12MK2BΔC1; *MEP1P-MEP1*, MEP12MK1A and B; *MEP1P-MEP1*^{ΔC438}, MEP12MK1AΔC2 and MEP12MK1BΔC2; *MEP1P-MEP1*^{ΔC404}, MEP12MK1AΔC1 and MEP12MK1BΔC1; *MEP2P-MEP2*^{1-418-MEP1}⁴¹⁷⁻⁵³⁴, MEP12MK21H2A and B; *MEP1P-MEP1*^{1-416-MEP2}⁴¹⁹⁻⁴⁸⁰, MEP12MK12H2A and B; *MEP2P-MEP1*^{1-416-MEP2}⁴¹⁹⁻⁴⁸⁰, MEP12MK12H3A and B; *MEP2P-MEP1*^{1-416-MEP2}⁴¹⁹⁻⁴⁴⁰, MEP12MK12H4A and B. Transformants of the independently generated $\Delta mep1 \Delta mep2$ mutants MEP12M4A and B behaved identically and only one of them is shown in each case.

To test whether the C-terminal cytoplasmic domain of CaMep2p is sufficient to confer signaling activity upon an ammonium permease, a fusion protein was generated in which the last 62 amino acids of CaMep2p were substituted for the corresponding part of CaMep1p (see section 3.2 and Fig. 24, No.10). This hybrid protein complemented the growth defect of $\Delta mep1 \Delta mep2$ double mutants on low ammonium medium (100 μM), consistent with the restoration of ammonium transport (Fig. 24, No.10), but failed to restore the filamentation defect of the double mutants. Expression of this fusion protein from the *CaMEP2* promoter resulted the same phenotype as overexpression of the wild-type *CaMEP1* gene from the *CaMEP2* promoter, i.e., a weak filamentation of the minority of the colonies (Fig. 24, No.11). Removal of the last 40 amino acids from the CaMep2p part did not increase filamentation of the cells expressing the hybrid protein (Fig. 24, No.12). Therefore, although the C-terminal cytoplasmic domain of CaMep2p is essential for signaling, its substitution for the corresponding domain in CaMep1p did not increase the signaling efficiency of the CaMep1p. Conversely, substitution of the C-terminal cytoplasmic domain of CaMep1p for the corresponding region of CaMep2p abolished hyphae formation on SLAD plates (Fig. 24, No.9), although the amount of the hybrid *CaMEP2*¹⁻⁴¹⁸-*CaMEP1*⁴¹⁷⁻⁵³⁴ mRNA was comparable to the wild-type *CaMEP2* mRNA (Fig. 26, lanes 1 and 2). These results suggested that specific interactions between the signaling and transporter domains of CaMep2p are required to efficiently induce filamentous growth under nitrogen starvation conditions.

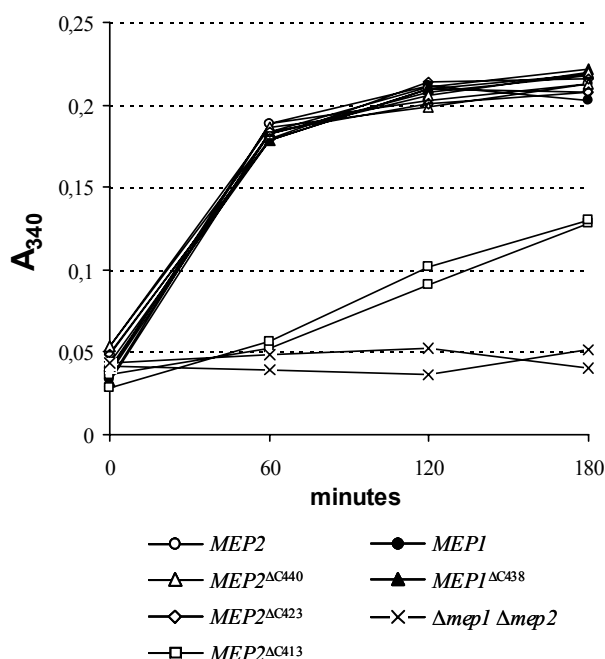


Fig. 25. Ammonium uptake of strains expressing full-length and C-terminally truncated *CaMEP1* and *CaMEP2* ORFs from their native promoters in a $\Delta mep1 \Delta mep2$ double mutant background. For experimental details see section 3.9. The following strains were used: *MEP2*, *MEP12MK2A* and *B*; *MEP2*^{ΔC440}, *MEP12MK2A*ΔC2 and *MEP12MK2B*ΔC2; *MEP2*^{ΔC423}, *MEP12MK2A*ΔC3 and *MEP12MK2B*ΔC3; *MEP2*^{ΔC413}, *MEP12MK2A*ΔC4 and *MEP12MK2B*ΔC4; *MEP2*^{ΔC406}, *MEP12MK2A*ΔC1 and *MEP12MK2B*ΔC1; *MEP1*, *MEP12MK1A* and *B*; *MEP1*^{ΔC438}, *MEP12MK1A*ΔC2 and *MEP12MK1B*ΔC2; *MEP1*^{ΔC404}, *MEP12MK1A*ΔC1 and *MEP12MK1B*ΔC1.

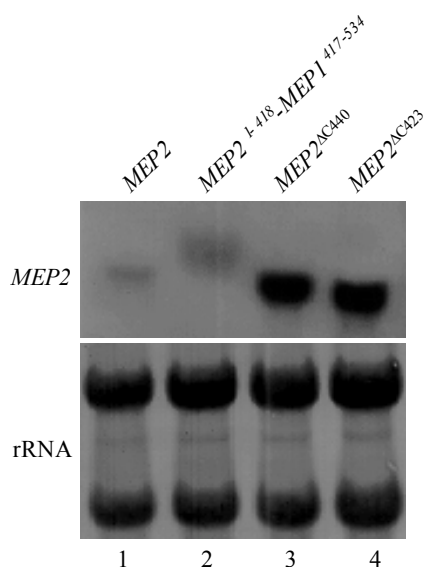


Fig. 26. Expression of full length, truncated, and hybrid *CaMEP2* ORFs. $\Delta mep1 \Delta mep2$ double mutants carrying the indicated *CaMEP2* versions were grown to log phase in liquid SLAD medium at 30°C and *CaMEP2* mRNA was detected by Northern hybridization with a *CaMEP2*-specific probe. The following strains were used: *MEP2*, MEP12MK2A and B; *MEP2*⁻⁴¹⁸-*MEP1*⁴¹⁷⁻⁵³⁴, MEP12MK21H2A and B; *MEP2*^{ΔC440}, MEP12MK2AΔC2 and MEP12MK2BΔC2; *MEP2*^{ΔC423}, MEP12MK2AΔC3 and MEP12MK2BΔC3. Transformants of the independently generated $\Delta mep1 \Delta mep2$ mutants MEP12M4A and B behaved identically and only one of them is shown in each case.

4.1.9. Regulation of filamentation by *CaMEP2* is dependent on both the MAP kinase cascade and the cAMP pathway

The results shown above demonstrated that nitrogen starvation induces *CaMEP2* expression, which in turn induces the cells to switch from yeast to filamentous growth. In *C. albicans* two pathways regulate the filament formation: A MAP kinase cascade that ends in the transcription factor Cph1p and a cAMP-dependent signaling pathway that ends in the transcription factor Efg1p. Several components of these two pathways have been shown to be required for filamentous growth of *C. albicans* in response to low ammonium concentrations (Bahn and Sundstrom, 2001; Csank *et al.*, 1998; Rocha *et al.*, 2001; Sanchez-Martinez and Perez-Martin, 2002). To test whether *CaMep2p* induces filamentous growth by activating one of these pathways, the hyperactive *CaMEP2*^{ΔC⁴⁴⁰} allele was substituted for one of the resident *CaMEP2* alleles in the wild-type strain CAI4 and in mutants deleted for the transcription factor *CPH1*, which is activated by the MAP kinase cascade, or the *EFG1* and *TEC1* transcription factors, which are involved in the cAMP-dependent pathway (Lane *et al.*, 2001a). A control construct with the full length *CaMEP2* ORF was integrated in an identical manner. As compared with the wild-type, the $\Delta cph1$, $\Delta efg1$, and $\Delta tec1$ mutants displayed a filamentation defect on SLAD plates (Fig. 27). Expression of the hyperactive *CaMEP2*^{ΔC⁴⁴⁰} allele restored filamentous growth in all three mutants, although the hyperfilamentation caused by the *CaMEP2*^{ΔC⁴⁴⁰} allele was stronger in a wild-type background. In contrast, the filamentous growth defect of a $\Delta cph1 \Delta efg1$ double mutant could not be rescued by

expression of the *CaMEP2* ΔC^{440} allele (Fig. 27). These results suggested that CaMep2p activates both the Cph1p- and the Efg1p-dependent signaling pathways and that hyperactivation of one of these pathways by the *CaMEP2* ΔC^{440} allele is sufficient to induce filamentous growth in response to nitrogen starvation. In contrast, in a wild-type background both pathways are required for filamentation under these conditions.

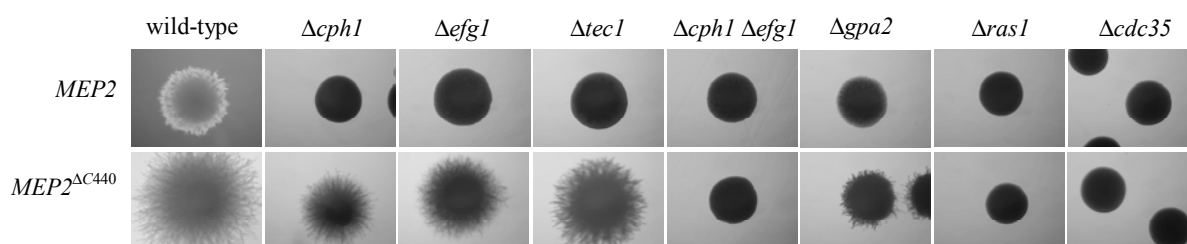


Fig. 27. The hyperactive *CaMEP2* ΔC^{440} allele rescues the filamentation defect of some signal transduction mutants. The *CaMEP2* ΔC^{440} allele or a control construct with the wild-type *CaMEP2* ORF was substituted for one of the resident *CaMEP2* alleles in the indicated mutants. Shown are representative colonies of the various strains after six days of growth at 37°C on SLAD plates. Independent transformants gave identical results and only one of them is shown in each case.

The G-proteins Ras1p and Gpa2p have been reported to induce filamentous growth in *C.albicans* by activating both the MAP kinase and the cAMP signaling pathways (Feng *et al.*, 1999; Leberer *et al.*, 2001; Miwa *et al.*, 2004; Sanchez-Martinez and Perez-Martin, 2002). To investigate if these proteins are required for signaling by CaMep2p, the hyperactive *CaMEP2* ΔC^{440} allele was expressed in $\Delta ras1$ and $\Delta gpa2$ mutants and also in a $\Delta cdc35$ mutant lacking adenylyl cyclase, which has been shown to be required for filamentous growth of *C.albicans* under all conditions tested (Rocha *et al.*, 2001). Expression of hyperactive *CaMEP2* ΔC^{440} allele partially suppressed the filamentation defect of the $\Delta gpa2$ mutant, whereas $\Delta ras1$ and $\Delta cdc35$ were still unable to filament on SLAD plates (Fig. 27). These results suggested that upon nitrogen starvation CaMep2p may activate the MAP kinase and the cAMP signaling pathways through Ras1p, but Gpa2p is also required for full induction of filamentous growth under these conditions. The fact that the hyperactive *CaMEP2* ΔC^{440} allele could rescue the filamentation defect of a $\Delta efg1$ mutant but not of a $\Delta cdc35$ mutant supported

the previous suggestion that both Efg1p and components of the MAP kinase cascade depend on adenylyl cyclase activity to induce the switch from yeast to filamentous growth (Rocha *et al.*, 2001).

4.1.10. Ammonium suppresses CaMep2p signaling

The results obtained with the hyperactive *CaMEP2* ΔC^{440} allele suggested that CaMep2p induces filamentous growth by activating the MAP kinase and the cAMP signaling pathways in response to nitrogen limitation. Therefore, artificial activation of downstream components of these pathways should bypass the requirement of *CaMEP2* for filamentation. Indeed, the expression of dominant active alleles of *GPA2* or *RAS1* in $\Delta mep2$ mutants restored their ability to switch to filamentous growth at low ammonium concentrations (Fig. 28, upper panels). Similarly, the addition of exogenous cAMP rescued the filamentous growth defect of $\Delta mep2$ mutants on SLAD plates, but did not increase filamentation of the wild-type strain SC5314 under these conditions (Fig. 29A).

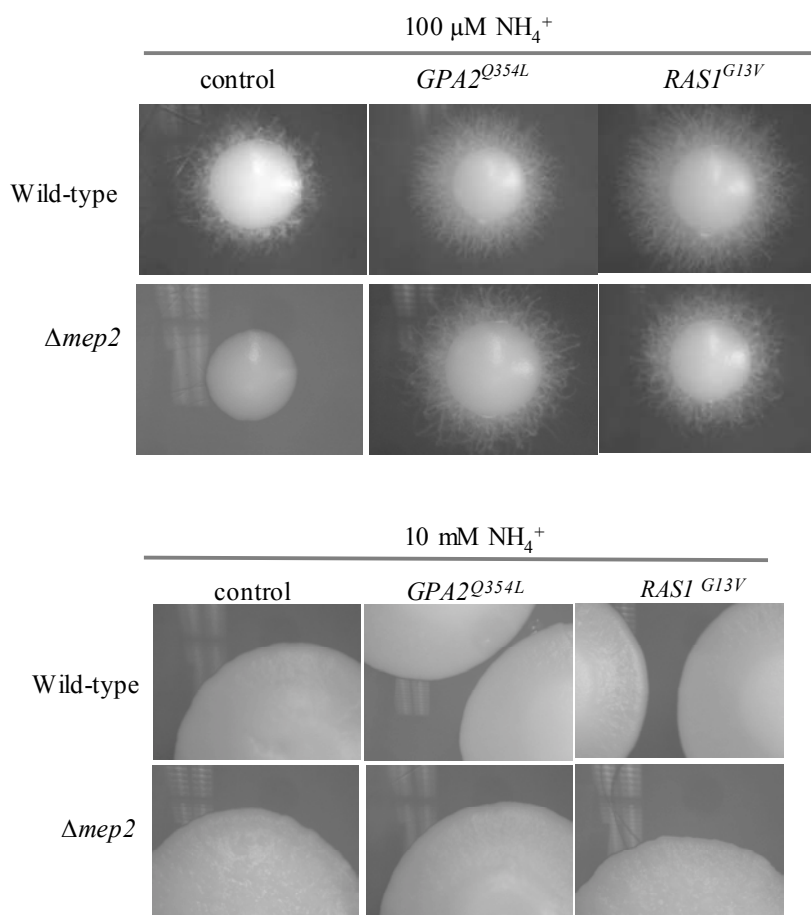
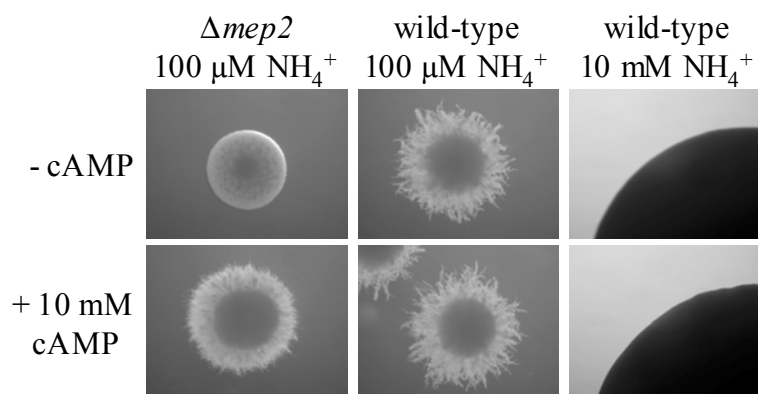


Fig. 28. Dominant active *GPA2*^{Q354L} or *RAS1*^{G13V} alleles suppress the filamentation defect of $\Delta mep2$ mutants on SLAD plates (100 μM NH₄⁺, top panels) but do not induce filamentous growth under ammonium-replete conditions (10 mM NH₄⁺, bottom panels). The plates were incubated at 37°C for 6 days.

Interestingly, however, increasing the ammonium concentration in the plates to 10 mM suppressed filamentous growth even in cells expressing the dominant active *GPA2*^{Q354L} or *RASI*^{G13V} alleles (Fig. 28, lower panel), or in cells expressing the hyperactive *CaMEP2* Δ C⁴⁴⁰ allele (Fig. 29B). In addition, exogenous cAMP did not induce filamentous growth in ammonium-replete conditions (Fig. 29A). These results demonstrated that ammonium suppresses the CaMep2p-dependent filamentous growth of *C.albicans* even when components of the signaling pathways are artificially activated.

A.



B.

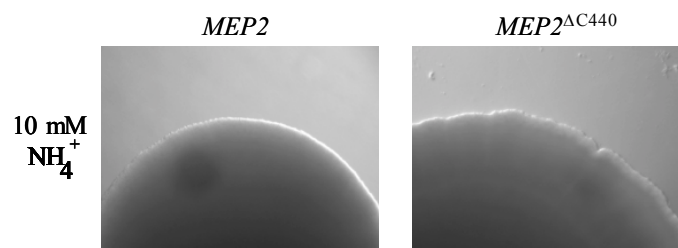


Fig. 29. (A) Exogenous cAMP rescues the filamentation defect of $\Delta mep2$ mutants on SLAD plates (left) but does neither increase filamentation in the wild-type (middle) nor induce filamentous growth under ammonium-replete conditions (right). (B) The hyperactive *CaMEP2* Δ C⁴⁴⁰ allele does not induce filamentation at 10 mM ammonium concentration. All plates were incubated at 37°C for 6 days. The following strains were used: wild-type, SC5314; $\Delta mep2$, MEP2M5A or B; *MEP2*, MEP12MK2A or B; *MEP2* Δ C⁴⁴⁰, MEP12MK2A Δ C2 or MEP12MK2B Δ C2. Independent transformants gave identical results and only one of them is shown.

4.2. Evaluation of putative essential genes as potential targets for antifungal drug development

C. albicans infections in immunocompromised patients have become a major medical problem because of the limited availability of clinically useful antifungal drugs. There are four classes of licensed drugs for the therapy of the *Candida* infections. These include polyenes (e.g. the various formulations of amphotericin B), nucleoside analogs (flucytosine), azoles (fluconazole, itraconazole, and voriconazole), and echinocandins (caspofungin). But, with the increasing resistance of *Candida* to these drugs, the demand to increase the arsenal of the anti-fungal drugs is great. For the past several decades, drug discovery has focused primarily on a limited number of families of ‘druggable’ genes against which medicinal chemists could readily develop compounds with a desired biochemical effect. However, nowadays the genomics approach has undoubtedly increased the opportunities to developing new therapies and the characterization of genes essential for fungal growth will be an important step in the identification and development of novel antifungal drugs. But the targets should be prioritized based on their conservation among most pathogenic fungi and significant divergence in higher eukaryotes. Using those criteria *RAP1*, a repressor-activator protein; *CBF1*, a centromere binding factor and *YIL19*, a previously uncharacterized gene were selected and characterized to test their potential as putative targets in this study.

4.2.1. Repressor/activator protein 1

The repressor/activator protein 1 (Rap1p), an essential transcription factor in *S. cerevisiae* is a multifunctional protein involved in transcriptional activation, transcriptional silencing, and telomere function (Shore and Nasmyth, 1987; Conrad *et al.*, 1990; Lustig *et al.*, 1990; Kurtz and Shore, 1991; Shore, 1994). Rap1p consists of 827 amino acids and can be divided into three regions, a central DNA binding domain, a N-terminal domain that is associated with DNA bending and a C-terminal domain which contains both a transcriptional activation domain and domains involved in telomere function and silencing. Among these three domains only the DNA binding domain is essential for cell viability (Graham *et al.*, 1999). The N-terminus of the protein is dispensable for cell viability, although it may be involved in regulating the activity of Rap1p through the putative BRCT domain (Callebaut

and Mornon, 1997). This region has been shown also to potentiate DNA bending *in vitro* (Muller *et al.*, 1994). The C terminus is the target for all of the protein-protein interactions involving Rap1p characterized to date, including interactions with the Sir proteins Sir3p and Sir4p and competing interactions with the Rif proteins Rif1p and Rif2p (Hardy *et al.*, 1992; Hecht *et al.*, 1996; Moretti *et al.*, 1994; Wotton and Shore, 1997). Rap1p binds to (C₁₋₃A)_n repeats at chromosome ends and regulates telomere length by recruiting the Rap1p interacting factors Rif1p and Rif2p whereas the interaction of Rap1p with Sir2p, Sir3p, and Sir4p represses telomeric transcription (Moretti *et al.*, 1994). The Rap-Sir complex also represses transcription at the silent mating type loci *HML* and *HMR*. (Aparicio *et al.*, 1991). Apart from its interaction at telomere and silent mating type loci Rap1p also acts as a transcriptional regulator of many essential *S.cerevisiae* genes, including genes encoding ribosomal proteins and glycolytic enzymes (Warner, 1999). The function of Rap1p in regulating the transcriptional program of *S.cerevisiae* is still unclear mainly because the mutations that abolish DNA Binding are lethal (Graham *et al.*, 1999) and overexpression of Rap1p is toxic (Freeman *et al.*, 1995).

RAP1 homologues have been identified in other yeasts like *Kluyveromyces lactis*, *Candida glabrata*, and *Saccharomyces castelli*. *RAP1* from *C.glabrata* and *S.castelli* but not from *K.lactis* are able to complement the temperature sensitivity of *S.cerevisiae rap1* mutants (Larson *et al.*, 1994; Haw *et al.*, 2001; Wahlin and Cohn, 2002). A human Rap1p homolog was shown to be localized to chromosome ends and to be involved in telomere length regulation, but its function in transcriptional regulation is not known (Li *et al.*, 2000). However the low overall sequence similarity of human Rap1p to the yeast proteins suggests that Rap1p could serve as a specific target to inhibit an essential function of fungal pathogens.

4.2.1.1. Identification of the *C.albicans RAP1* gene

A BLAST search identified an open reading frame in the genome sequence of *C.albicans* strain SC5314 with significant similarity to the *S.cerevisiae* Rap1 protein (ScRap1p). The corresponding gene has been annotated as *RAP1* at the Stanford Genome Technology Center (<http://www-sequence.stanford.edu/group/candida/>). The encoded protein (CaRap1p) is much shorter than ScRap1p and contains only 430 amino acids (Fig. 30 and Fig. 31). The overall identity of CaRap1p to ScRap1p is 24%. Significant similarity to ScRap1p was found only in the C-terminal part of CaRap1p, which corresponds to the DNA binding domain of ScRap1p. Two regions of high similarity are present in this region, from amino

acid positions 255 to 353 of CaRap1p (65% similarity, 44% identity), and from positions 375 to 417 (55% similarity, 41% identity). In contrast, the N-terminal region of CaRap1p did not exhibit similarity to ScRap1p, and the C-terminal region of ScRap1p was absent from the *C.albicans* protein. Polymerase chain reaction (PCR) amplification with different sets of primers (see section 3.2 and section 3.4) and sequencing of the corresponding region from *C.albicans* SC5314, confirmed the presence of a stop codon at position 1291-1293 of *CaRAP1*, and the downstream sequence also did not exhibit sequence similarity to the C-terminal part of ScRap1p, confirming that *RAP1* in *C.albicans* is truncated in comparison to its counterpart in *S.cerevisiae*.

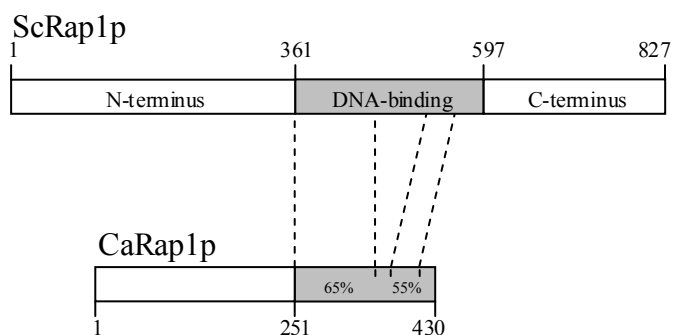


Fig. 30. Schematic comparison of Rap1p from *S.cerevisiae* (ScRap1p) and *C.albicans* (CaRap1p). The amino acid positions delineating the borders of the different regions in the proteins are indicated. The two blocks with the highest similarity in the region corresponding to the DNA binding domain of ScRap1p are bracketed by the stippled lines, and the percent similarity (65% and 55%) is given in the *C.albicans* protein.

ScRap1p	--MSSPDDFETAPAEYVDALDPSMVVDSGSAAVTAPSDSAAEVKANQNEENTGATAAET
CgRap1p	MSANDSEQFDTAPNEFVDALETNIHIDPPNQAQSKIDESSRKEKNNND-----
ScasRap1p	--MSSPQNFEFAQQYMDLSLSDSNNSHMENQQQQDASPNANGNGAVTTEETN--VDPSSIT
KlRap1p	--MSHADDFTALDSPSVQIKEDVG-----
CaRap1p	-MNYPYSSFEDDGQYQTDLSVEASRNADEEAAGHQQQQLQYHRRVQIEEATR-----
	..*:
ScRap1p	SEKVDQTEVEKKDDDDTTEVGVTTTTTSPSIADTAATANIASTSGASVTEPTTDDTADEKK
CgRap1p	-----LGVEMTSVDPALGTGDMNEAHTKETAAEQNG
ScasRap1p	NVKMEGTNNADADITIALPATQDVNNSNGTAAADKGNPNNETSTSTGENPQKQDNAT
KlRap1p	-----
CaRap1p	-----QRQQQQHHQQQTSPSSSDDFNFESQRI
ScRap1p	EQVSGPPLSNMKFYLNRDADAHDSLNDIDQLARLIRANGGEVLDKSKPRES---KENVFIV
CgRap1p	EKG---IFNGMVFYLNDRDSNAHDSIIIVEQLKNLILLNGGDI VNKLPNKDSAEAKHI IVV
ScasRap1p	PVAISTLFGQMNFFMNRNNDADHSAHDVDQLARLIMAHSGNVLASLPEDTT-DVSNVYVI
KlRap1p	-----VFDGVSFFIDP-----LINDMEALGNAVRNNGGAVLIEAPEKSSREWEAAYFV
CaRap1p	KPNRPKNSPPKPIFVDKDGKSMFLFYIPEDEPNRNKYRDLIIRYGGVIVEKG--FPTVILL
	:::: : : :
ScRap1p	SP-YNHTNLPTVTPTYIKACCQSNLLNMENY--LVPYDN--FREVDSRLQEESHNGV
CgRap1p	SP-YNNTLTKTVTSTFIRACVQSNKLLDMKNY--LVPYDS--FNALLDDAMSPPSRQEPT
ScasRap1p	SP-YNDTKLPVTVTPTYIKACVSNNTLLNINHY--LVPYDE--FRSVIDTQLQSETNND
KlRap1p	SKRYDEYRIFVHPSYILDCIDAGTLLNVHDY--LGKPESSGFVRFDSNSISDEYNIGSQ
CaRap1p	SN--NEDLYGFSKLKFIDDCIAKNQLLSVFDYGTGYTNNPEDAAFDTSIINELNDDLS
	* : . . . * . ** : * : . . . :
ScRap1p	DNSNSNSDNKDSIRPKTEIISTNTNGATEDSTSEKVMVDAEQARLQEQALLRQHVSS
CgRap1p	ISESSVNEGQPTASKPPQNIA-----
ScasRap1p	HVDHDEASKRNLFEADPEEATQLNSTEPQGTSTQLPQDNKTASNPTTISAQPENNQEAN
KlRap1p	LSDLPGSDVTRA AVKIATGINESIDSENTRG-----QREMSDSSSP
CaRap1p	SNISSFSSTIEGTSSMVEVPVAAPAAIPLPP-----


```

ScRap1p      ASITSGGHNDLVQIEQPQKDTSNNNNSNVNDEDNDLLTQDNNPQTAEDEGNASFQAQRSMI
CgRap1p      -----KRDIPTKKVSANTG-----
ScasRap1p    NAAQQQTTEEQLRLLQEHAEVNVQQAEPNSVSDVDVN-----YEERAYM
KlRap1p      EVKMSSKDDEIASHDQQQLTHTDVEDAN-----DLIL
CaRap1p      -----PHQQQRSIDAFPNPNIN-----
      .
      :

ScRap1p      SRGALPSHNSASFTDEEDEFILDVVRKNPTRRTHTLYDEISHYVNP--HTGNSIRHRFR
CgRap1p      -----VSKTSFTEEEDEFILDVVRKNPMRRTHTLYDEISHYVNP--HTGNSIRHRFR
ScasRap1p    MRAALPSHNSASFTEADEFILDVVRKNPTRRTHTLYDEISHYVNP--HTGNSIRHRFR
KlRap1p      HEQASSSHNSSTFKEEDEFILDVVRKNPTKRTHHTLYDEISHYVNP--HTGNSIRHRFR
CaRap1p      --NARRGSSGHRFTIEQDEFILHIRKPRFRQSQKFYAQLALLEPLRGHTGNSIRSRFR
      .   ** :*****: :*: * * : : : : : * * * * * * * *
      :

ScRap1p      VYLSKRLEYVYEVDFKGLVLRDDGNLIKT--KVLPPSIKRRKFADEYTLAIAVKKQFY
CgRap1p      VHLSKRLEDFVYQVDQYKGLVRDENGNIKT--KVLPPSIKRRKFADEYELAIKQQFY
ScasRap1p    VYLSKRLDYVYQVDSYKGLVRDENGNIKT--KTLPPSIKRRKFADEYILALAVKKQFY
KlRap1p      VYLSKRLEFVYQVDEGKLVLRDQGNLIKT--DILPGLKRRKFTSEEDYNLAVAVKKQFY
CaRap1p      KHLESRLNYIKTDDQQLIRDEAGNLIKIGLDEMPGTLKKNKFTPEDDYLLCCVALEYMA
      :*..**::*:*. .:***: ***** . : * :*.**:::*** * . . : :
      :

ScRap1p      RDLFQIDPDTGRSLITDEDTPTAIARRNMTMDPNHVPGEPNFAAYRTQSRRGPIAREFF
CgRap1p      KDIYQLDPVTGQSLISDNPPARVAKRQMMMDPNVQRGSEPPFSKYRVGTRRGPIAREFF
ScasRap1p    RDLYQIDPDTGTLNISNEDSPTAIARRNMTMDPNHVPGEPNFNDFRVNDRRGPFVAREFF
KlRap1p      RDAFQRDPDTGASLIAEDDEPNIVAKRQLVMNTEIDPSEVPSFEKYTVNDRRGPLSREFF
CaRap1p      SNNIDS-----IGLRYSEFF
      :   :
      :   :

ScRap1p      KHFAEEHAAHTENAWRDRFRKFLAYG-IDDYISYEAKAQNREPEPMKNLTNRPKRPG
CgRap1p      KQFTENHPHTESAWRDRFRKFLLEYG-VDKYIEYYETQKANNDEPEAMKNLTIRTKRDN
ScasRap1p    KSFADANVSHSENAWRDRFRKFLTFG-VDHYIEYFEQETNAGRKPEPMKNLTNRPRRKA
KlRap1p      KLFALEVPTHSENAWRDRFRKFILPYG-IDSYISYEEKMEEGIEPESIKNMTNRPKRE-
CaRap1p      DGMYRKYRNHTLQSWRDRFRKYIRDKSDLVDYKEYYENCEKVGMAPRCLTRIAP-----
      . : * :.*****: . : * .:* * . * . : : :
      :

ScRap1p      VTPPGNYNSAAKRARNYSSQRNVQPTANAASANAAAAAASN-----SYAIPEN
CgRap1p      FPTPGNYGNAAKRQKYEVSSE-----VENTLKSQ-----AGDIPDA
ScasRap1p    GITPGNYNSAIKRQRAYSISKAVHDQNSNISNAAVVAANAASGDNTDTHSTPSYPIPEN
KlRap1p      GSPSPGNYNTTLKKSRSSTEGG-----TQQSTDTSLN-----D
CaRap1p      -----
      :

ScRap1p      ELLDEDTMNFISSLKNDLSNISN-----SLPFEPHEIAERIRSDFSNE-DIYDNIDP
CgRap1p      ELLDEDTMKFISSLKNDLSKIDN-----NFGFDYTNEIAEAIRNDFSEEEAIYDNIDP
ScasRap1p    ELLDEDTMNFISNLKNDLSKLESNNNGNNNLPFEYSPEIAEAIRNDFDNEGKEFDNIDP
KlRap1p      FFLESDAFDLIDGIRDLHAAETQOE---EQARSLYADDVAERIRHQVALEHEEYDNYDF
CaRap1p      -----
      :

ScRap1p      DTISFPFKIATTD-LFLPLFFHFGSTRQFMDKLHEVISGDYEPSQAEKLVQDLCDGTGIR
CgRap1p      NTIPFPPIATID-LFLPQFFRMSSTQEFIEKIREIIQRDYEPSQAEKLVQDLNDEAGIR
ScasRap1p    DTIKFPPEIATID-LFLPIFFQFGSTRNFLEKVENVIKRDYEPSQAEKLVQDLNDEAGVR
KlRap1p      DSIPFPFKLADNDDFDHTFFNFRSTKEFIQKLEEIIITREYDESQADVLVHDLVVECGIR
CaRap1p      -----
      :

ScRap1p      KNFSTSILTCLSGDLMVFPFYFLNMFKDNVNPVPPVPGIWTHTHDDDESLSKNDQEIQIRKLV
CgRap1p      KTFTSSILGSLSGDLMVLPFYFLNMFKNQNPPIIDIPGIWTSGDDDLRRGDEAEVSKLV
ScasRap1p    RGFSTSILTALSGDLMIFFPFYFLNMFKNVNPVPLNVPGIWTHEDDAMLSSNDSSEDLRHL
KlRap1p      KKYATSVLTALTGDISLFPYILTSFKYGVHLPQNVPGIWTKEDDVILRSKNPDGMKMLE
CaRap1p      -----
      :

ScRap1p      KKHGTGRMEMRKRFFEKDLL
CgRap1p      KRQGAGRVEMRKKFLERNLI
ScasRap1p    KKHGAARIAIRRRFVERDLV
KlRap1p      KKHGIARMQMRIRFQENNLV
CaRap1p      -----
      :

```

Fig. 31. ClustalW (<http://www.ebi.ac.uk/clustalw/#>) analysis of CaRap1p with ScRap1p, Rap1 from *C. glabrata* (CgRap1p), *S. castelli* (ScasRap1p) and *K. lactis* (KlRap1p). Identical and similar amino acids are indicated by asterisks and colons, respectively. DNA binding domains of the proteins are indicated in red.

4.2.1.2. Expression of *CaRAP1* in temperature-sensitive *S.cerevisiae rap1* mutants

Certain temperature-sensitive alleles of *ScRAP1* render *S.cerevisiae* nonviable at 37°C (Kurtz and Shore, 1991). To test whether *CaRAP1* can complement the temperature-sensitive phenotype of *S.cerevisiae rap1* mutants, *CaRAP1* was cloned under its own promoter in the vector pRS426 (see section 3.2). The resulting plasmid was named pRS-RAP1. *S.cerevisiae* strains YDS 407 (*rap1-1*) and YDS 408 (*rap1-2*) were transformed with the plasmid pRS-RAP1 and the empty control vector pRS426. Uridine-prototrophic transformants were selected on SD agar plates without uracil at room temperature (permissive conditions). The transformants were then restreaked on SD agar plates and allowed to grow at both 25°C and 37°C. Neither of the transformants grew at 37°C, suggesting that *CaRAP1* does not complement a defect in *ScRAP1* (Fig. 32).



Fig. 32. Expression of *CaRAP1* in temperature-sensitive *rap1* mutants of *S.cerevisiae*. The strains were streaked on SD agar plates and incubated at room temperature or 37°C for 4 days.

4.2.1.3. Construction of *C.albicans rap1* deletion mutants

In order to find out whether *RAP1* is an essential gene also in *C.albicans*, an attempt was taken to knock-out both *CaRAP1* alleles of this diploid yeast by targeted gene deletion using the *URA3*-flipping strategy (see section 4.1.3). The *ura3*-negative strain CAI4 was transformed with a deletion cassette in which almost all of the *CaRAP1* coding sequence had been replaced by the *URA3* flipper (see section 3.2 and Fig. 33A).

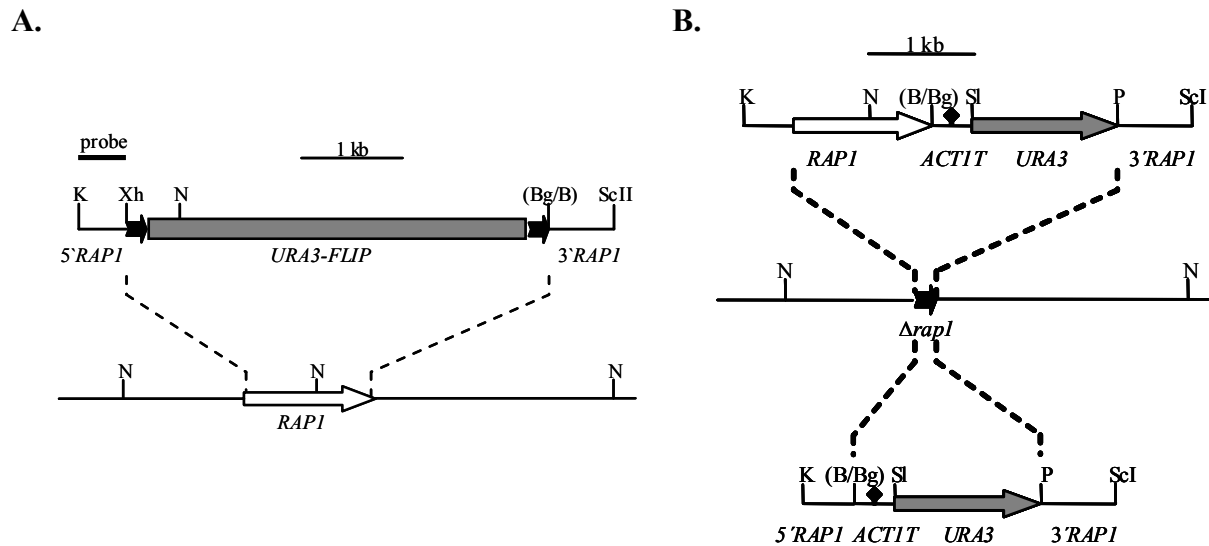


Fig. 33. (A) Structure of the deletion cassette from plasmid pRAP1M2 and genomic structure of the *CaRAP1* locus in the parent strain CAI4. The *CaRAP1* coding region is represented by the white arrow, and the upstream and downstream sequences by the solid line. The 34 bp *FRT* sites (black arrows) are not drawn to scale. (B) Structure of the DNA fragments from pRAP1K1 (upper part) and pRAP1M4 (lower part), which were used for reintegration of an intact *CaRAP1* copy (white arrow) or only the *URA3* marker (grey arrow), respectively, into one of the inactivated *rap1* alleles (middle). The *ACT1* transcription termination sequence (*ACT1T*) is indicated by the black diamond. Only relevant restriction sites are given. B, *Bam*HI; Bg, *Bgl*II; K, *Kpn*I; N, *Nsi*I; P, *Pst*I; ScI, *Sac*I; Sl, *Sal*I; Xh, *Xho*I. The *Bam*HI and *Bgl*II sites shown in parenthesis were destroyed by the cloning procedure. The probe used for Southern hybridization analysis of the mutants is indicated by the thick bar.

From two transformants in which the deletion cassette had been correctly inserted in one of the *CaRAP1* alleles (strains RAP1M1A and RAP1M1B, Fig. 34, lanes 2 and 3) the *URA3* flipper was excised again by FLP-mediated recombination, resulting in the ura-auxotrophic strains RAP1M2A and RAP1M2B (Fig. 34, lanes 4 and 5). When these strains were transformed again with the same deletion cassette, integration was successfully targeted to the remaining wild-type *CaRAP1* allele in several transformants of both parent strains, demonstrating that *CaRAP1* is not an essential gene in *C.albicans*. The *URA3* flipper was excised again from the two independent homozygous *rap1* mutants RAP1M3A and RAP1M3B (Fig. 34, lanes 6 and 7), generating the ura-auxotrophic derivatives RAP1M4A and RAP1M4B (Fig. 34, lanes 8 and 9). These strains served as hosts for reintroduction of a complete copy of the *CaRAP1* gene or the *URA3* selection marker alone into one of the inactivated $\Delta rap1$ alleles (see section 3.2 and Fig. 33B). This resulted in the generation of the two independent, prototrophic, homozygous *rap1* mutants RAP1M5A and RAP1M5B (Fig. 34, lanes 10 and 11) and the corresponding complemented strains RAP1MK1A and RAP1MK1B (Fig. 34, lanes 12 and 13).

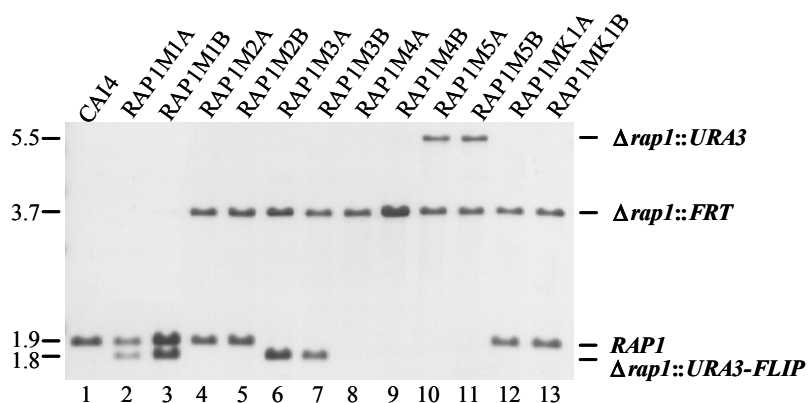


Fig. 34. Southern hybridization of *Nsi*I-digested genomic DNA of the parent strain CAI4 and mutant derivatives with a *CaRAP1*-specific probe shown in Fig. 33A. The sizes of the hybridizing fragments (in kb) are given on the left side of the blot and their identities are indicated on the right.

4.2.1.4. Growth analysis of the *rap1* deletion mutants

Since *CaRAP1* was not essential for viability of *C.albicans* it was tested whether its deletion conferred some growth defect upon the cells. However, the *rap1* deletion mutants RAP1M5A and RAP1M5B grew as well as wild-type strain SC5314 and the complemented strains RAP1MK1A and RAP1MK1B in rich medium (YPD) and also at defined medium (SD) at 30°C, 37°C and 42°C (Fig. 35 and data not shown). Similarly, the *ura3*-negative *rap1* mutants RAP1M4A and RAP1M4B grew equally well as the *ura3*-negative *CaRAP1* wild-type strain CAI4 in media supplemented with uridine (data not shown).

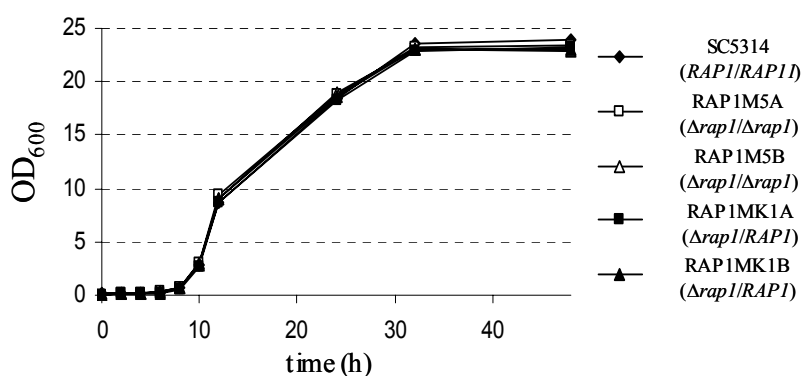


Fig. 35. Growth curves of *Δrap1* mutants and control strains in YPD liquid medium at 30°C. Cells from a YPD overnight culture were diluted in fresh medium and incubated at 30°C. Growth was followed by measuring the increase in optical density over time.

When grown on YPD or SD agar plates at 30°C, the *rap1* deletion mutants formed slightly smaller colonies with an irregular fringe, in contrast to the wild-type and complemented strains, which grew as round colonies under these conditions (Fig. 36A, upper

row). This phenotype was seen with both *URA3* and *ura3* strains when the mutants were compared with the respective control strains. Microscopic analysis of the cells from these colonies showed that colonies of *rap1* deletion mutants consisted of both yeast cells and short pseudohyphae, whereas the colonies of wild-type and complemented strains contained only yeast cells (Fig. 36A, lower row). Pseudohyphal growth of the $\Delta rap1$ mutants was also observed in YPD liquid medium, in which the wild-type and complemented strains grew almost exclusively as budding yeasts. In contrast, in cultures of $\Delta rap1$ mutants many cells with a pseudohyphal phenotype were observed in addition to yeast cells (Fig. 36B, and Table 5).

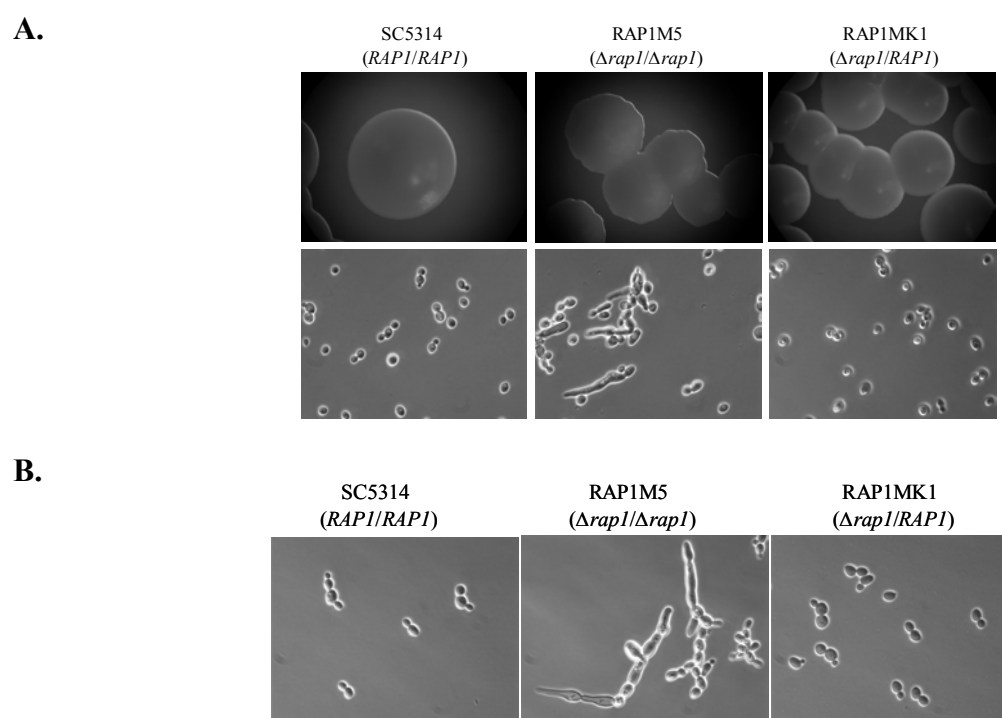


Fig. 36. Phenotype of wild-type strain SC5314, the homozygous $\Delta rap1$ mutants, and complemented strains on YPD agar and in YPD liquid medium. **(A)** Colony appearance on YPD agar plates of the wild-type strain SC5314, the homozygous $\Delta rap1$ mutants, and complemented strains (upper row). Photographs were taken after two days of growth at 30°C. The lower row shows the morphology of resuspended cells within the colonies, visualized by phase contrast microscopy using a 40x objective. The strain pairs RAP1M5A/B and RAP1MK1A/B looked identical and only one of them is shown. **(B)** Microscopic appearance of the wild-type strain SC5314, the homozygous $\Delta rap1$ mutants, and complemented strains after overnight growth in YPD liquid medium at 30°C. Shown are phase contrast micrographs of the cells taken with a 40x objective (upper row). The strain pairs RAP1M5A/B and RAP1MK1A/B looked identical and only one of them is shown.

Table 5.

Frequency of pseudohyphal cells in YPD cultures of *C.albicans* $\Delta rap1$ mutants and control strains.

Strain	Genotype	no. of cells counted	no. of yeast cells	no. of pseudohyphal cells	% pseudohyphal cells
<i>URA3</i>					
SC5314	<i>RAP1/RAP1</i>	8,757	8,754	3	0.03
RAP1M5A	$\Delta rap1/\Delta rap1$	3,275	3,096	179	5.47
RAP1M5B	$\Delta rap1/\Delta rap1$	2,403	2,275	128	5.33
RAP1MK1A	$\Delta rap1/\Delta rap1 + RAP1$	7,032	7,030	2	0.03
RAP1MK1B	$\Delta rap1/\Delta rap1 + RAP1$	6,643	6,641	2	0.03
<i>ura3</i>					
CAI4	<i>RAP1/RAP1</i>	7,438	7,433	5	0.07
RAP1M4A	$\Delta rap1/\Delta rap1$	948	896	52	5.49
RAP1M4B	$\Delta rap1/\Delta rap1$	976	923	53	5.43

When the cell suspensions were stained either with CFDA (5, [6]-carboxyfluorescein diacetate) which stains live cells, or with DiBAC (bis-[1,3-dibutylbarbituric acid] trimethine oxonol) which stains dead cells, it was found that the pseudohypha like cells are alive and this morphology was not due to death of the cells (Fig. 37A). The esterase activity of viable cells cleaves the acetate moieties from CFDA to produce free carboxyfluorescein, which is retained in cells whose membranes are intact. DiBAC is a member of the oxonol class of dyes that exhibit intense fluorescence upon binding to phospholipids. Normal membrane potential, which collapses with mortal injury upon cell death, prevents access of DiBAC to the inside of the cell (Bowmann *et al.*, 2002). Staining of cell wall chitin with calcofluor and nuclear staining with Hoechst dye demonstrated that the individual cellular compartments of the $\Delta rap1$ pseudohyphal cells usually were separated by chitin containing constrictions and contained one nucleus, as is typical for *C.albicans* pseudohyphae (Fig. 37B).

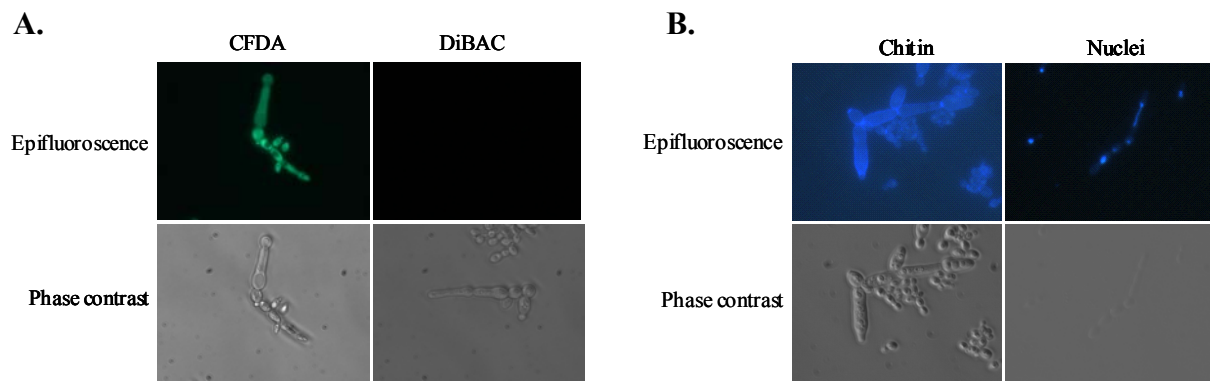


Fig. 37. (A) The homozygous $\Delta rap1$ mutants were grown in YPD at 30°C till mid log phase and stained either with CFDA to visualize live cells or with DiBAC to visualize dead cells. Shown are the corresponding fluorescence (top) and phase contrast (bottom) micrographs. (B) Fixed cells of $\Delta rap1$ mutants were stained with either calcofluor to visualize chitin in the septae (left), or with Hoechst dye 33258 to visualize nuclei (right). Shown are the corresponding fluorescence (top) and phase contrast micrographs (bottom). The strain pairs RAP1M5A/B behaved identically and only one of them is shown

4.2.1.5. Phenotypic analysis of $\Delta rap1$ mutants in hyphal growth induction medium

Since the $\Delta rap1$ mutants grew as a mixture of yeast and short pseudohyphae in hyphal non-inducing conditions, it was tested whether there was any change in the morphology of the $\Delta rap1$ mutants under conditions that induce hyphal growth in *C. albicans* (growth on SPIDER, Lee's and SLAD agar plates, growth in liquid SPIDER medium, Lee's medium, or RPMI + 10% serum). In all those conditions $\Delta rap1$ mutants formed germ tubes and hyphae as efficiently as the wild-type and complemented strains (Fig. 38 and data not shown). Occasional yeast and pseudohyphal cells were also seen when $\Delta rap1$ mutants were grown in RPMI medium +10% serum in which all cells of the control strains formed true hyphae.

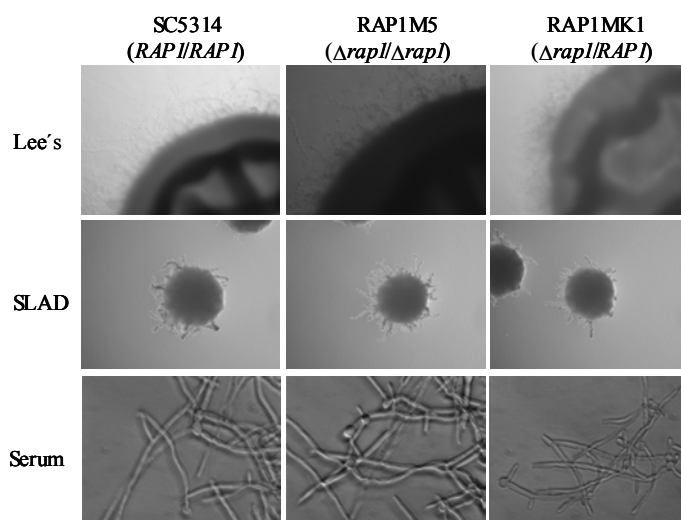


Fig. 38. Hyphal growth of the wild-type strain SC5314, the homozygous $\Delta rap1$ mutants, and complemented strains. The upper row shows colonies grown for 10 days on Lee's medium at 37°C. The middle row shows the colonies grown for 6 days on SLAD medium at 37°C. The lower row shows phase contrast micrographs of the cells after 4 hours of growth in RPMI 1640 with 10% serum at 37°C. The strain pairs RAP1M5A/B and RAP1MK1A/B looked identical and only one of them is shown.

4.2.2. Centromere Binding Factor 1

Centromeres are specific regions of eukaryotic chromosomes that provide attachment sites for the spindle microtubules that transport chromatids during anaphase. In contrast to the large regional centromeres of humans that span several kilobases of DNA, centromeric DNA sequences in budding yeasts such as *S.cerevisiae* are contained within 125-400 bp and are called 'point' centromeres (Clarke and Carbon, 1980). Regional centromeres often are associated with short nucleosome-length satellite repeats (such as the α satellite of humans) present within an untranscribed (AT)-rich region of DNA, whereas point centromeres have conserved DNA sequence elements and an (AT)-rich core (Choo, 1997). In the yeast *S.cerevisiae*, a centromere consists of three conserved regions, named as centromeric DNA elements (CDEI, CDEII, and CDEIII). Single base pair changes in CDEI and CDEIII result in chromosome loss and several proteins that bind to CDEI and CDEIII have been identified (Baker *et al.*, 1989; Bram and Kornberg, 1987; Cai and Davis, 1990). These proteins are named as centromere binding factors (Cbf) and assemble into a centromere complex.

Centromere binding factor 1 (Cbf1; also called Cpl and Cpf1) has been well studied in *S.cerevisiae* (Baker and Masison 1990; Cai and Davis, 1990; Mellor *et al.*, 1990) and is an abundant basic-helix-loop-helix leucine zipper protein which binds as a homodimer to the consensus sequence CACGTG (the CDEI region of the centromere) (Baker *et al.*, 1989; Bram and Kornberg, 1987; Jiang and Phillipsen, 1989). *S.cerevisiae* $\Delta cbf1$ mutants show an increased rate of chromosome and plasmid loss and have a slow growth phenotype. In addition to its centromere binding function, ScCbf1p is also a transcription factor that is necessary for the expression of genes involved in methionine biosynthesis, and deletion of *CBF1* renders *S.cerevisiae* methionine auxotrophic. The role of ScCbf1p in methionine prototrophy is due to its binding to a CDEI motif in the promoter region of the genes of the sulphate assimilation pathway, a part of the sulphur amino acids biosynthetic pathway, facilitating the transcriptional activation of these genes (Kuras and Thomas, 1995). Analysis of *CBF1* alleles with mutations revealed that its role as a centromere binding protein and as a transcription factor is separable. The N-terminal 209 amino acids of Cbf1p are required for optimal binding to centromeric DNA (Wieland *et al.*, 2001) and residues 210 to 351 are sufficient to relieve methionine auxotrophy of *cbf1* null mutants (Kuras *et al.*, 1997).

In contrast to *S.cerevisiae*, deletion of the *CBF1* gene is lethal in the related yeast *Kluyveromyces lactis*, and recently it was shown that *CBF1* also is an essential gene in the pathogenic yeast *Candida glabrata* (Mulder *et al.*, 1994; Stoyan *et al.*, 2001). These findings

suggested that Cbf1p might serve as a target for the inhibition of an essential cellular function in fungal pathogens.

The *CBF1* gene has recently been cloned from *Candida albicans* (Eck *et al.*, 2001). When expressed in *S.cerevisiae* *CaCBF1* complemented the slow growth, methionine auxotrophy, and plasmid instability phenotypes of $\Delta cbf1$ mutants. However, the role of *CaCBF1* for growth and viability of *C.albicans* itself has not been investigated so far. Therefore, this gene was functionally characterized by the construction and analysis of *C.albicans* $\Delta cbf1$ mutants.

4.2.2.1. Construction of *C.albicans cbf1* deletion mutants

For inactivation of the *CBF1* gene in the diploid *C.albicans* the *URA3*-flipping strategy was used (see section 4.1.3). The *ura3*-negative strain CAI4 was transformed with a deletion cassette in which the whole *CaCBF1* coding sequence had been replaced by the *URA3* flipper (see section 3.2 and Fig. 39A). From two transformants in which the deletion cassette had been correctly inserted in one of the *CaCBF1* alleles (strains CBF1M1A and CBF1M1B, Fig. 40, lanes 2 and 3) the *URA3* flipper was excised again by FLP-mediated recombination, resulting in the uridine-auxotrophic strains CBF1M2A and CBF1M2B (Fig. 40, lanes 4 and 5). When these strains were transformed again with the same deletion cassette, integration was successfully targeted to the remaining wild-type *CaCBF1* allele in several transformants of both parent strains, demonstrating that *CaCBF1* is not an essential gene in *C.albicans*. The *URA3* flipper was excised from the two independent homozygous *cbf1* mutants CBF1M3A and CBF1M3B (Fig. 40, lanes 6 and 7), generating the uridine-auxotrophic derivatives CBF1M4A and CBF1M4B (Fig. 40, lanes 8 and 9). These strains served as hosts for reintroduction of a complete copy of the *CaCBF1* gene or the *URA3* selection marker alone into one of the inactivated $\Delta cbf1$ alleles (see section 3.2 and Fig. 39B). This resulted in the generation of the two independent, prototrophic, homozygous $\Delta cbf1$ mutants CBF1M5A and CBF1M5B (Fig. 40, lanes 10 and 11) and the corresponding complemented strains CBF1MK1A and CBF1MK1B (Fig. 40, lanes 12 and 13).

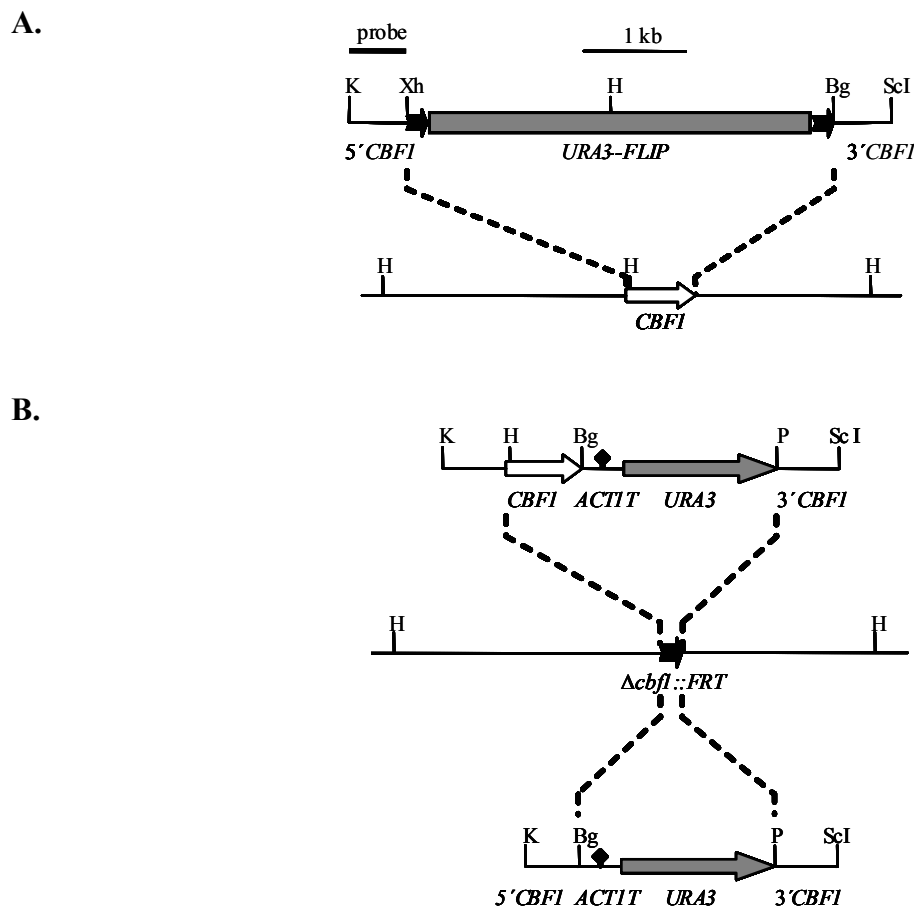


Fig. 39. (A) Structure of the deletion cassette from plasmid pCBF1M2 (top) and genomic structure of the *CaCBF1* locus in the parental strain CAI4 (bottom). The *CaCBF1* coding region is represented by the white arrow, and the upstream and downstream sequences by the solid lines. The 34 bp *FRT* sites (black arrows) are not drawn to scale. The probe used for Southern hybridization analysis of the mutants is indicated by the thick bar. (B) Structure of the DNA fragments from pCBF1K1 (top) and pCBF1M4 (bottom), which were used for reintegration of an intact *CaCBF1* copy (white arrow) or only the *URA3* marker (grey arrow), respectively, into one of the inactivated *CaCBF1* alleles (middle). The *ACT1* transcription termination sequence (*ACT1T*) is indicated by the black diamond. Only relevant restriction sites are given. Bg, *Bgl*III; H, *Hind*III; K, *Kpn*I; P, *Pst*I; ScI, *Sac*I; Xh, *Xho*I.

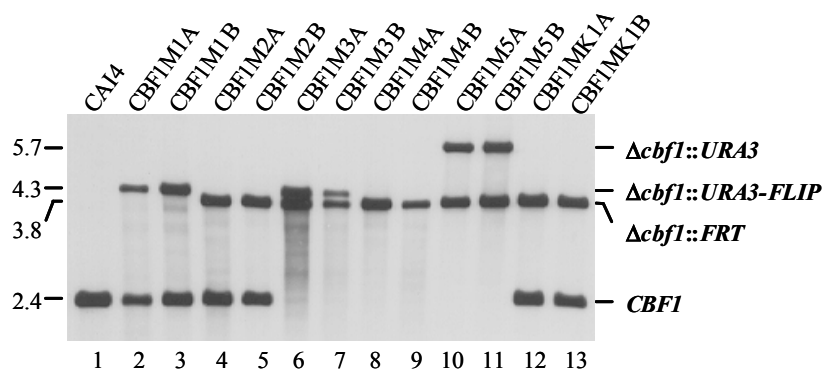


Fig. 40. Southern hybridization of *Hind*III-digested genomic DNA of the parental strain CAI4 and mutant derivatives with a *CaCBF1*-specific probe shown in Fig. 39A. The sizes of the hybridizing fragments (in kb) are given on the left side of the blot and their identities are indicated on the right.

4.2.2.2. Growth and phenotypic analysis of $\Delta cbf1$ mutants

Since *CaCBF1* was not essential for viability of *C.albicans*, it was tested whether its deletion conferred some growth defect upon the cells. When grown on rich medium YPD at 30°C or 37°C, the $\Delta cbf1$ mutants CBF1M5A and CBF1M5B grew very slowly, similar to what has been described for *S. cerevisiae* $\Delta cbf1$ mutants (Fig. 41). In addition, the *C.albicans* $\Delta cbf1$ mutants were temperature-sensitive, since no growth was observed at 42°C. The same phenotypes were seen for the *ura3*-negative $\Delta cbf1$ mutants CBF1M4A and CBF1M4B (data not shown). The slow growth phenotype was also observed in SD medium. Reintroduction of a functional *CaCBF1* copy in the complemented strains CBF1MK1A and CBF1MK1B restored normal growth (Fig. 41).

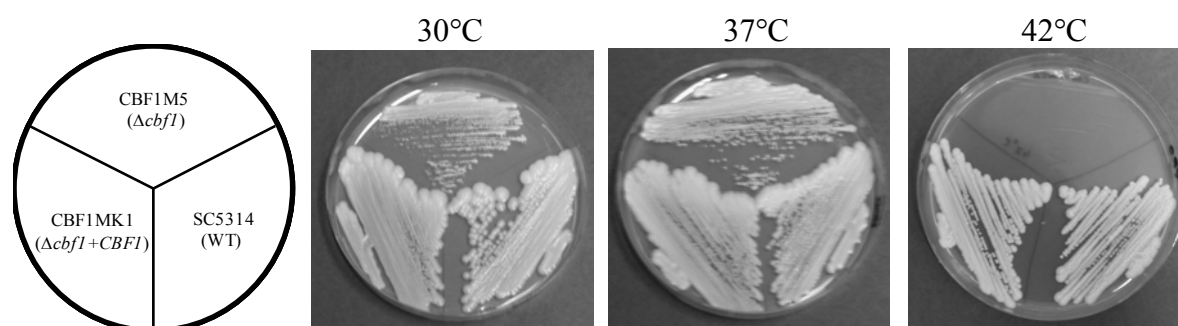


Fig. 41. *C.albicans* $\Delta cbf1$ mutants have a slow growth phenotype and are temperature-sensitive. Strains were streaked on YPD agar plates and grown for 3 days at 30°C or 37°C, or for 6 days at 42°C. The strain pairs CBF1M5A/B and CBF1MK1A/B behaved identically and only one of them is shown in each case.

Microscopic examination of cells grown in YPD medium demonstrated that a significant number of $\Delta cbf1$ mutant cells were abnormally large and the cells tended to aggregate, a phenotype that was reverted by reintroduction of a functional *CaCBF1* copy (Fig. 42, upper row). The $\Delta cbf1$ mutants were able to form hyphae upon induction by serum, although hyphae formation was delayed in comparison with the wild-type and complemented strains because of their slow growth phenotype. In addition, and in contrast to the control strains, not all cells of the $\Delta cbf1$ mutants formed hyphae under these conditions but some grew as unusually large yeast cells (Fig. 42, lower row).

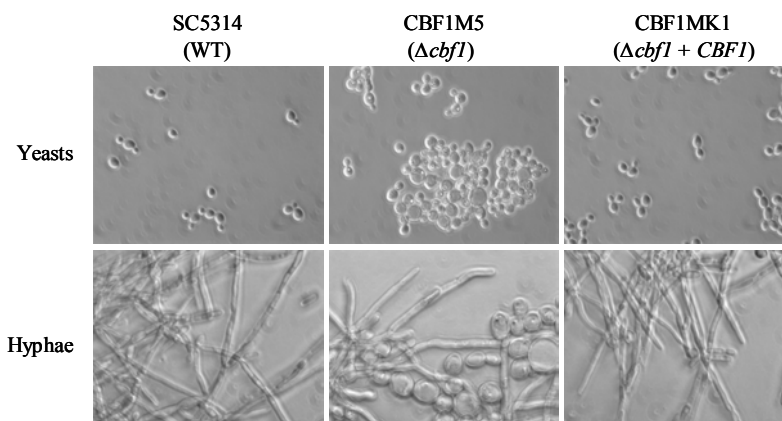


Fig. 42. Yeast and hyphal growth of *C. albicans* $\Delta cbf1$ mutants. Strains were grown at 30°C in YPD liquid medium to promote growth as budding yeast, or at 37°C in RPMI 1640 medium containing 10% serum to induce hyphal growth. The strain pairs CBF1M5A/B and CBF1MK1A/B behaved identically and only one of them is shown in each case.

4.2.2.3. *C. albicans* $\Delta cbf1$ mutants are methionine and cysteine auxotrophic

In contrast to the wild-type strain, the $\Delta cbf1$ mutants CBF1M5A and CBF1M5B were unable to grow on unsupplemented SD minimal medium. When methionine or cysteine were added to this unsupplemented minimal medium, the slow growth phenotype of the mutants was restored. The same phenotype was observed when *ura3* mutant strains CBF1M4A and CBF1M4B or *URA3* mutant strains CBF1M5A and CBF1M5B were checked. Reintroduction of a functional copy of *CaCBF1* into the mutant strains suppressed this auxotrophic phenotype (Fig. 43). These results suggest that *CaCBF1* is required for the biosynthesis of sulphur amino acids in *C. albicans*.

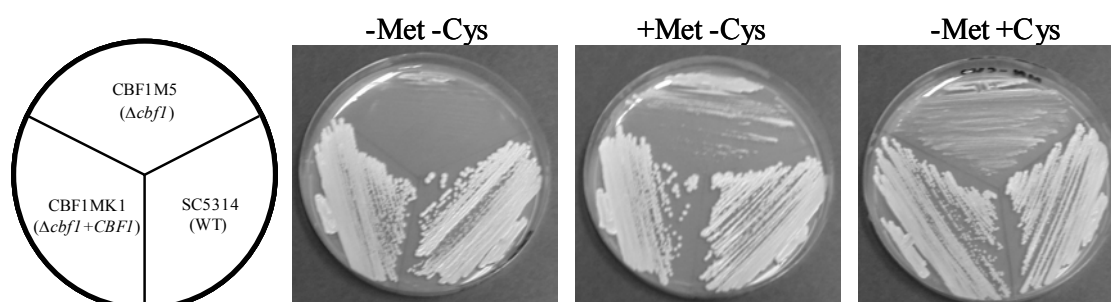


Fig. 43. *C. albicans* $\Delta cbf1$ mutants are auxotrophic for sulphur amino acids. Strains were grown for 3 days at 30°C on SD agar plates without CSM, supplemented (+) or not (-) with methionine (Met) or cysteine (Cys). The strain pairs CBF1M5A/B and CBF1MK1A/B behaved identically and only one of them is shown in each case.

4.2.2.4. Chromosome stability in *C.albicans* $\Delta cbf1$ mutants



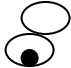
In *C.glabrata*, where *CBF1* is essential, depletion of Cbf1p results in the generation of enlarged cells with unseparated or undetectable nuclei (Stoyan *et al.*, 2001). Similarly, the formation of enlarged cells arrested in the large-budded stage was recently described for *C.albicans* mutants depleted for the essential centromere protein Cse4p (Sanyal and Carbon, 2002). The observation of the presence of the unusually large cells in the *C.albicans* $\Delta cbf1$ mutants, together with the known centromere function of Cbf1p in other yeasts, pointed to a possible role of *CaCBF1* in mitosis.

Nuclear staining showed that many of the unusually large cells of the *C.albicans* $\Delta cbf1$ mutants indeed contained anucleate large buds (between 7 and 9% of all cells, see Table 6). In addition, the $\Delta cbf1$ mutants also produced aberrantly large cells with anucleate small or nucleate large buds. This result suggested that deletion of *CaCBF1* may have caused a defect in chromosome segregation, which may be responsible for the production of morphologically aberrant cells. However, the aberrant cell morphology could also be due to some other functional defect of the $\Delta cbf1$ mutants. Therefore, additional experiments were carried out to address a possible role of *CaCBF1* in chromosome segregation in *C.albicans*.

Table 6.

Frequency of aberrant cells in *C.albicans* $\Delta cbf1$ mutants and control strains.

The symbols in columns 4-6 indicate unusually large cells with small buds, unusually large cells with a large bud after or during nuclear division, and unusually large cells with a large anucleate bud, respectively. The number of cells exhibiting these different aberrant morphologies is given for each strain along with the total number of counted cells.

Strain	Genotype	Total no. of cells counted			
<i>URA3</i>					
SC5314	<i>CBF1/CBF1</i>	277	0	0	0
CBF1M5A	$\Delta cbf1/\Delta cbf1$	315	1	39	23
CBF1M5B	$\Delta cbf1/\Delta cbf1$	243	5	32	19
CBF1MK1A	$\Delta cbf1/\Delta cbf1 + CBF1$	277	1	0	0
CBF1MK1B	$\Delta cbf1/\Delta cbf1 + CBF1$	292	0	3	1
<i>ura3</i>					
CAI4	<i>CBF1/CBF1</i>	287	0	0	0
CBF1M4A	$\Delta cbf1/\Delta cbf1$	221	1	32	18
CBF1M4B	$\Delta cbf1/\Delta cbf1$	214	5	36	19

ScCbf1p is involved in centromere function and hence *S.cerevisiae cbf1* null mutants are hypersensitive to microtubule disrupting drugs like thiabendazole (Cai and Davis, 1990). It was found that the deletion of *CaCBF1* did not cause hypersensitivity to thiabendazole in *C.albicans*. At thiabendazole concentrations that reduced growth of the wild-type strain, the $\Delta cbf1$ mutants were still able to grow, and the growth difference compared with the wild-type and complemented strains was similar to that observed on plates without the drug (Fig. 44). This phenotypic difference between *S.cerevisiae* and *C.albicans* $\Delta cbf1$ mutants indirectly argued against a role of CaCbf1p in centromere function in *C.albicans*. Therefore, it was tried to directly assess a possible role of *CaCBF1* in chromosome stability in *C.albicans*.

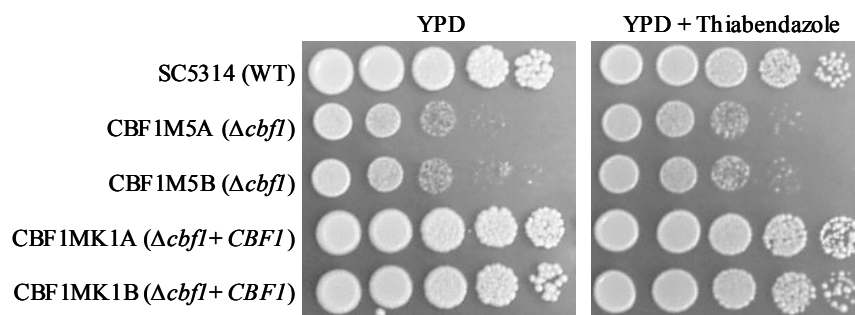


Fig. 44. Deletion of *CaCBF1* does not cause hypersusceptibility to thiabendazole in *C.albicans*. The indicated strains were grown to stationary phase in YPD medium, and serial 10-fold dilutions were spotted onto YPD plates or YPD plates containing 100 $\mu\text{g/ml}$ thiabendazole and grown for 2 days at 30°C.

S.cerevisiae $\Delta cbf1$ mutants also show an increased rate of centromeric plasmid loss, which facilitates detection of defects in chromosome stability. However, since there are no centromeric plasmids available for *C.albicans*, plasmid stability in the *C.albicans* $\Delta cbf1$ mutants could not be investigated as for *S.cerevisiae*. To assess an effect of *CaCBF1* deletion on chromosome stability, the genomic hybridization pattern of wild-type strains and $\Delta cbf1$ mutants with the *C.albicans*-specific repetitive DNA element *CARE-2* was analyzed. This DNA element is present on most, if not all *C.albicans* chromosomes (Lasker *et al.*, 1992). Loss of chromosomes should therefore result in the disappearance or a decrease in the relative signal strength of some hybridizing bands. Three individual colonies of each analyzed strain were picked from an SD agar plate and separately grown for 48 hours at 30°C in YPD liquid medium. The cultures were then diluted 10^{-2} in fresh YPD medium and again grown for 48 hours at 30°C. This procedure was repeated several times. After seven passages (about 50 generations) suitable dilutions of the cultures were spread onto YPD agar plates. One colony

from each culture was then used for isolation of genomic DNA and Southern hybridization with the *C.albicans*-specific repetitive DNA element *CARE-2* as described previously (Franz *et al.*, 1998). The *CARE-2* hybridization patterns of all strains were identical (Fig. 45), demonstrating that none of the clones had suffered a detectable chromosome loss.

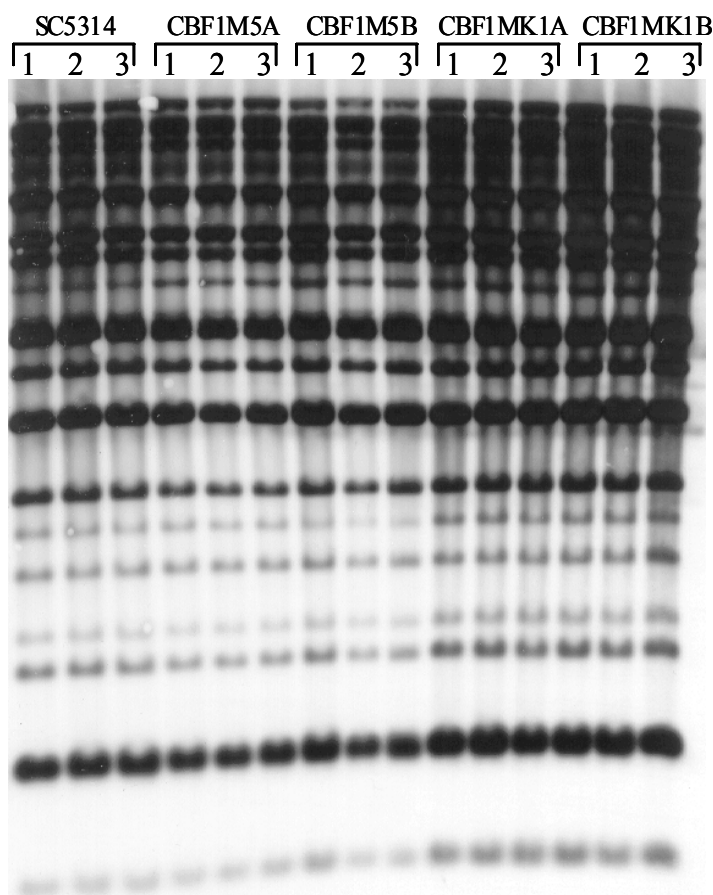
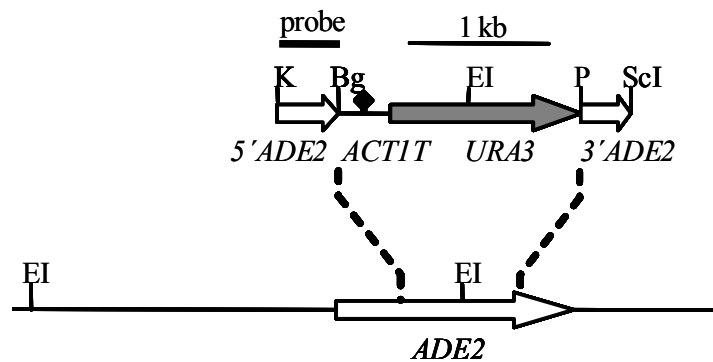


Fig. 45. *CARE-2* hybridization pattern of *C.albicans* $\Delta cbf1$ mutants and control strains. Three independent colonies of each strain were grown for approximately 50 generations in YPD liquid medium at 30°C. Genomic DNA of each clone was isolated, digested with *EcoRI*, and analyzed by Southern hybridization with the *CARE-2* probe. The banding pattern is identical for all clones. Differences in signal strength between individual lanes are due to slightly unequal loading.
SC5314, wild-type; CBF1M5A/B, $\Delta cbf1$; CBF1MK1A/B, $\Delta cbf1$ + *CaCBF1*.

Since chromosome loss might still be a relatively rare event even if it is enhanced in $\Delta cbf1$ mutants, an additional approach was used to detect a low frequency loss of a specific chromosome. For this purpose, one of the two alleles of *ADE2* gene, which is located on chromosome 3 (<http://alces.med.umn.edu/bin/genelist?genes>), was disrupted in the parental strain CAI4 and in the $\Delta cbf1$ mutants (Fig. 46A and B). Individual colonies of the strains in which the other *ADE2* allele was inactivated were taken from an SD agar plate and grown to stationary phase in YPD medium at 30°C. Appropriate dilutions were spread on SD agar plates and the frequency of red *ade2* colonies was monitored after 7 days of incubation at

30°C. Cells that have lost the chromosome 3 homolog containing the intact *ADE2* allele become auxotrophic for adenine and can be detected as red colonies on plates containing limited amounts of adenine (Barton and Gull, 1992). Red *ade2* colonies were detected at similar frequencies in all the strains (see Table 7). Such *ade2* mutants can be generated in different ways: inactivation of the intact *ADE2* allele due to point mutations, loss of the intact *ADE2* allele by mitotic recombination or gene conversion, or loss of the chromosome 3 homolog containing the intact *ADE2* allele, as outlined above. To differentiate between these possibilities, several red *ade2* clones from wild-type and $\Delta cbf1$ parent strains were analyzed by Southern hybridization (Fig. 47).

A.



B.

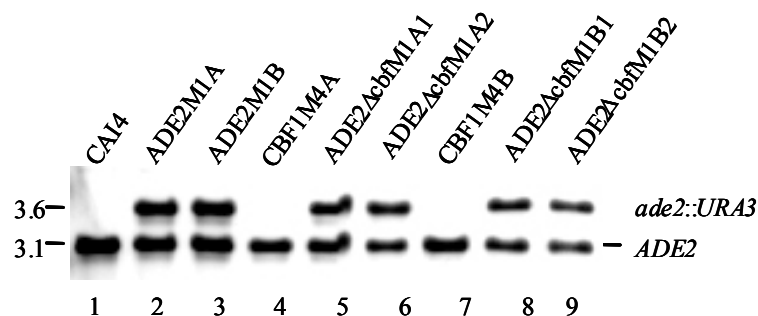


Fig. 46. Inactivation of one of the *ADE2* alleles in strain CAI4 and $\Delta cbf1$ mutants by insertion of the *URA3* marker. (A) Structure of the deletion cassette from plasmid pADE2M2 (top) and genomic structure of the *ADE2* locus in the parental strains (bottom). The *ADE2* coding region is represented by the white arrow, and the upstream and downstream sequences by the solid lines. The probe used for Southern hybridization analysis of the mutants is indicated by the thick bar. Only relevant restriction sites are given. Bg, *Bgl*II; EI, *Eco*RI; K, *Kpn*I; P, *Pst*I; ScI, *Sac*I. (B) Southern hybridization of *Eco*RI-digested genomic DNA of the parental strains CAI4 (wild-type, lane 1) and CBF1M4A/B ($\Delta cbf1$, lanes 4 and 7) and their *ADE2/ade2::URA3* derivatives (lanes 2, 3, 5, 6, 8, 9) with an *ADE2*-specific probe. The sizes of the hybridizing fragments (in kb) are given on the left side of the blot and their identities are indicated on the right.

Table 7.

Frequency of *ade2* cells in wild-type and $\Delta cbf1$ mutants.

Strain	Relevant Genotype	Exp. no. ^a	Total no. of colonies	No. of red <i>ade2</i> colonies ^b	Frequency of red <i>ade2</i> colonies
ADE2M1A	<i>CBF1/CBF1</i> <i>ADE2/ade2::URA3</i>	1	28,730	2 (1)	7.0×10^{-5}
		2	17,650	0	-
		3	82,400	2	2.4×10^{-5}
		4	93,800	3	3.2×10^{-5}
ADE2M1B	<i>CBF1/CBF1</i> <i>ADE2/ade2::URA3</i>	1	16,570	0	-
		2	16,210	0	-
		3	88,800	1 (1)	1.1×10^{-5}
		4	82,400	2	2.4×10^{-5}
ADE2 Δ cbfM1A1	$\Delta cbf1::FRT/\Delta cbf1::FRT$ <i>ADE2/ade2::URA3</i>	1	19,090	0	-
		2	28,910	1 (2)	3.4×10^{-5}
		3	95,200	4	4.2×10^{-5}
		4	74,400	3	4.0×10^{-5}
ADE2 Δ cbfM1A2	$\Delta cbf1::FRT/\Delta cbf1::FRT$ <i>ADE2/ade2::URA3</i>	1	28,730	3	1.0×10^{-4}
		2	15,310	0	-
		3	67,200	2	3.0×10^{-5}
		4	75,200	3	4.0×10^{-5}
ADE2 Δ cbfM1B1	$\Delta cbf1::FRT/\Delta cbf1::FRT$ <i>ADE2/ade2::URA3</i>	1	27,740	3	1.1×10^{-4}
		2	15,490	0	-
		3	88,000	2	2.3×10^{-5}
		4	69,600	3	4.3×10^{-5}
ADE2 Δ cbfM1B2	$\Delta cbf1::FRT/\Delta cbf1::FRT$ <i>ADE2/ade2::URA3</i>	1	19,810	1	5.0×10^{-5}
		2	17,650	0	-
		3	90,400	2 (1)	2.2×10^{-5}
		4	77,600	2	2.6×10^{-5}

^a Experiments no. 1 and 2 were performed on the same day, using two independent colonies of each strain. Experiments no. 3 and 4 were performed on a separate occasion and a higher no. of cells from each colony was plated.

^b The first no. indicates the no. of red colonies, i.e. the no. of cells that had lost the *ADE2* gene before plating. The no. in parenthesis gives the no. of sectored colonies, i.e. those cases in which the *ADE2* gene was lost during growth of the progeny colony.

Hybridization with an *ADE2* probe demonstrated that all analyzed clones had lost the fragment containing the intact *ADE2* allele and retained the fragment containing the disrupted copy, excluding the possibility that they were generated by a simple point mutation (Fig. 47A, lanes 4-16). The blot was then rehybridized with a fragment from the *YMR211* gene, which is also located on chromosome 3 but on a different contig (<http://www-sequence.stanford.edu/group/candida/>) and is therefore not closely linked to the *ADE2* gene (Fig. 47B), and with a fragment from the *ACT1* gene, which is located on chromosome 1 (<http://alces.med.umn.edu/bin/genelist?genes>) (Fig. 47C). The *YMR211* and *ACT1* probes produced signals of comparable strength in the parental strains (Fig. 47B and C, lanes 1-3). In contrast, in several of the red *ade2* clones the *YMR211* signal was clearly reduced in comparison to the *ACT1* signal (e.g. lanes 4 and 16), indicating that these clones had lost one of the chromosome 3 homologs. In other red *ade2* clones the *ACT1* and *YMR211* signals were comparable, as in their parents (e.g. lanes 5 and 15). These clones might have lost the intact *ADE2* copy by mitotic recombination, but there are also other possible explanations (see section 5.2.2). Altogether, these experiments provide evidence that deletion of the *CaCBF1* gene does not result in an increased chromosome 3 loss.

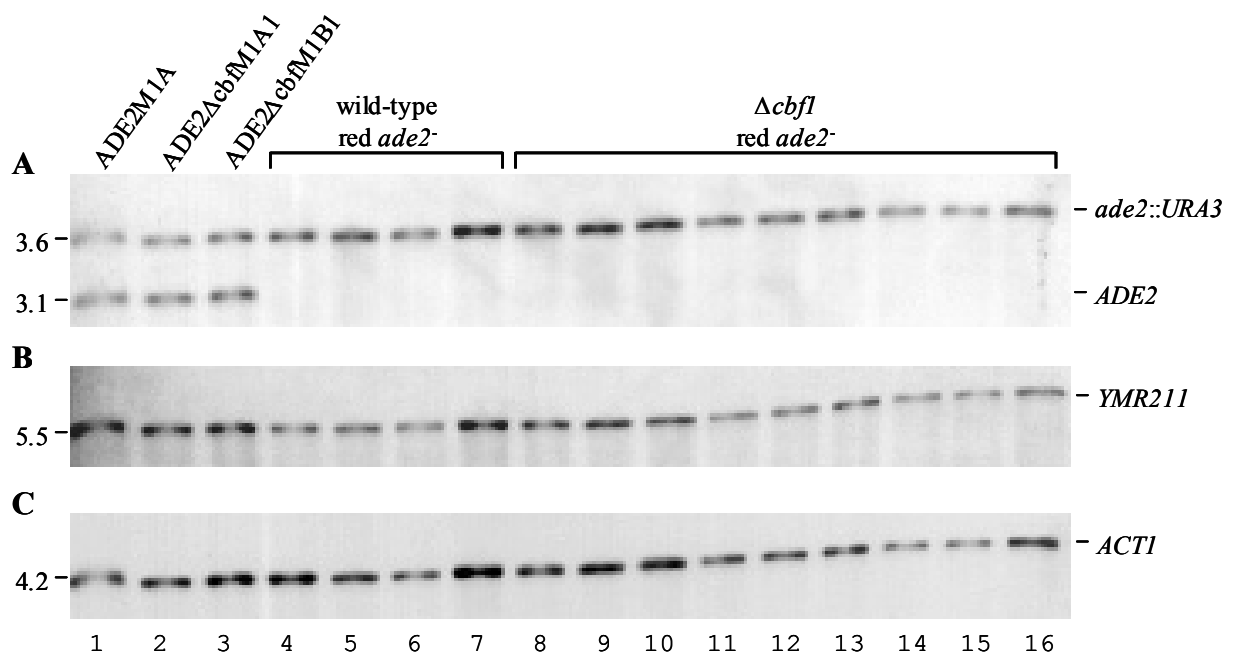


Fig.47. Analysis of red *ade2* colonies by Southern hybridization. *EcoRI* digested genomic DNA of the parental strains (lanes 1-3) and red *ade2* derivatives (lanes 4-16) was hybridized with probes specific for *ADE2* (A), *YMR211* (B), or *ACT1* (C). The sizes of the hybridizing fragments (in kb) are given on the left side of the blots and their identities are indicated on the right.




4.2.2.5. Phenotype of $\Delta cbf1$ mutants at the non-permissive temperature

The inability of the $\Delta cbf1$ mutants to grow at 42°C suggested that CaCbf1p might have a more important function at the higher as opposed to lower temperatures. Therefore, whether the morphological defect of the mutants was aggravated at the non-permissive temperature was examined. However, it was found that morphologically abnormal cells appeared with comparable frequencies at 30°C and 42°C (compare the data in Table 8 with those in Table 6), demonstrating that the temperature-sensitivity of the $\Delta cbf1$ mutants was not due to an increased number of cells with defects in morphology. A few very small, anucleate cells were observed when the strains were incubated at 42°C, but their frequency (0.5 to 2.5 %) was comparable in $\Delta cbf1$ mutants and control strains.

Table 8.

Frequency of aberrant cells in *C.albicans* $\Delta cbf1$ mutants and control strains at 42°C

The symbols in columns 4-6 indicate unusually large cells without or with small buds, unusually large cells with a large bud after or during nuclear division, and unusually large cells with a large anucleate bud, respectively. The number of cells exhibiting these different aberrant morphologies is given for each strain along with the total number of counted cells.

Strain	Genotype	Total no. of cells counted			
<i>URA3</i>					
SC5314	<i>CBF1/CBF1</i>	263	0	0	0
CBF1M5A	$\Delta cbf1/\Delta cbf1$	280	9	43	26
CBF1M5B	$\Delta cbf1/\Delta cbf1$	256	10	30	16
CBF1MK1A	$\Delta cbf1/\Delta cbf1 + CBF1$	276	1	4	0
CBF1MK1B	$\Delta cbf1/\Delta cbf1 + CBF1$	259	1	2	0
<i>ura3</i>					
CAI4	<i>CBF1/CBF1</i>	271	0	1	0
CBF1M4A	$\Delta cbf1/\Delta cbf1$	260	8	28	18
CBF1M4B	$\Delta cbf1/\Delta cbf1$	248	8	31	15

Whether $\Delta cbf1$ mutants might exhibit an increased rate of chromosome loss at 42°C, the strains were first grown to mid log phase at 30°C and then transferred to a 42°C water bath and incubated for 24 hours. Appropriate dilutions were spread on SD agar plates and the frequency of red *ade2* colonies was monitored after 7 days of incubation at 30°C. As shown

in Table 9, red *ade2* mutants arose with similar frequency in $\Delta cbf1$ mutants and control strains also at the elevated temperature, demonstrating that the temperature sensitivity of the $\Delta cbf1$ mutants was not caused by an increased chromosome loss at 42°C.

Table 9.**Frequency of *ade2* cells in wild-type and $\Delta cbf1$ mutants at 42°C**

Strain	Relevant Genotype	Exp. no. ^a	Total no. of colonies	No. of red <i>ade2</i> colonies ^b	Frequency of red <i>ade2</i> colonies
ADE2M1A	<i>CBF1/CBF1</i> <i>ADE2/ade2::URA3</i>	1	31,720	3 (4)	9.4 x 10 ⁻⁵
		2	28,090	2 (4)	7.1 x 10 ⁻⁵
ADE2M1B	<i>CBF1/CBF1</i> <i>ADE2/ade2::URA3</i>	1	20,670	1 (1)	4.8 x 10 ⁻⁵
		2	26,500	2 (1)	7.5 x 10 ⁻⁵
ADE2 $\Delta cbf1$ M1A1	$\Delta cbf1::FRT/\Delta cbf1::FRT$ <i>ADE2/ade2::URA3</i>	1	21,660	1	4.6 x 10 ⁻⁵
		2	17,290	1	5.8 x 10 ⁻⁵
ADE2 $\Delta cbf1$ M1A2	$\Delta cbf1::FRT/\Delta cbf1::FRT$ <i>ADE2/ade2::URA3</i>	1	25,760	2	7.8 x 10 ⁻⁵
		2	22,400	1	4.5 x 10 ⁻⁵
ADE2 $\Delta cbf1$ M1B1	$\Delta cbf1::FRT/\Delta cbf1::FRT$ <i>ADE2/ade2::URA3</i>	1	36,550	3 (3)	8.2 x 10 ⁻⁵
		2	22,110	2 (2)	9.0 x 10 ⁻⁵
ADE2 $\Delta cbf1$ M1B2	$\Delta cbf1::FRT/\Delta cbf1::FRT$ <i>ADE2/ade2::URA3</i>	1	27,160	2 (3)	7.4 x 10 ⁻⁵
		2	21,840	2	9.1 x 10 ⁻⁵

^a Experiments no. 1 and 2 were performed using two independent colonies of each strain.

^b The first no. indicates the no. of red colonies, i.e. the no. of cells that had lost the *ADE2* gene before plating. The no. in parenthesis gives the no. of sectored colonies, i.e. those cases in which the *ADE2* gene was lost during growth of the progeny colony.

Finally, it was examined whether the temperature sensitivity of the $\Delta cbf1$ mutants reflected an inability to grow or cell killing. Since CaCbf1p might function during active growth, cell survival was determined in one set experiments during incubation in rich medium YPD at 42°C (see section 3.7). As shown in Fig. 48A, a moderate killing of the $\Delta cbf1$ mutants was detected after 24 hours of incubation at 42°C, since the number of viable cells was reduced to about 15%. In contrast, the cell numbers of wild-type and control strains had slightly increased during that time. This difference could be explained if a proportion of the cell population of both mutants as well as wild-type and control strains is killed at 42°C, but in contrast to the former the latter strains can overcome the reduction in cell number by growing fast enough. To confirm this assumption, survival of the strains at 42°C was also

tested in PBS, which does not support growth, instead of YPD medium. As shown in Fig. 48B, in this case the number of viable cells decreased in all strains and was only 2 to 3 fold higher in wild-type and control strains than in the $\Delta cbf1$ mutants, presumably due to some residual growth in the former after transfer from rich medium to PBS. From these experiments it is obvious that the temperature sensitivity of the $\Delta cbf1$ mutants is caused by their slow growth rate, which does not allow them to overcome the rate of cell killing at 42°C, instead of a specific function of CaCbf1p at the elevated temperature.

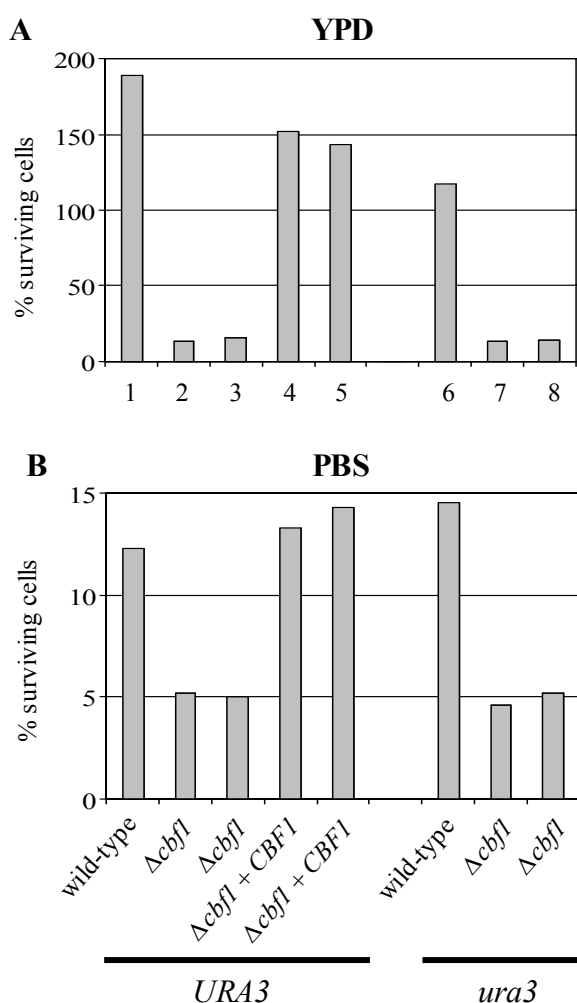


Fig. 48. Survival of *C. albicans* $\Delta cbf1$ mutants and control strains at 42°C. Strains were grown at 30°C in YPD medium to log phase and then incubated for 24 h at 42°C either in YPD medium (A) or in PBS (B). The bars indicate the percent survival of the cells at 42°C (see section 3.7). The following strains were used: 1, SC5314; 2, CBF1M5A; 3, CBF1M5B; 4, CBF1MK1A; 5, CBF1MK1B; 6, CAI4; 7, CBF1M4A; 8, CBF1M4B

4.2.3. *YIL19*

ORF *YIL19* encodes a protein of 328 amino acids of unknown function in *C.albicans*. The homolog of this ORF in *S.cerevisiae* has been very recently designated as *FAF1* in SGD (*Saccharomyces* Genome Database). Whole genome analysis of *S.cerevisiae* had shown before that this ORF is essential for cell viability. Recently Shirai *et al.* (2004) and Karkusiewicz *et al.* (2004) independently have shown that this gene in *S.cerevisiae* is involved in the processing of 18S rRNA, and depletion of *YIL019w* (*FAF1*) gene product affect 40S ribosomal subunit biogenesis, resulting from a decrease in the production of 18S rRNA.

Biogenesis of ribosomes is one of the major metabolic processes of the cell and appears to be conserved throughout eukaryotes. In *S.cerevisiae* this process is very well characterised and its genome contains 100-200 copies of rDNA. Each rDNA copy encodes two rRNA precursors, the 35S and 5S rRNA transcribed by RNA polymerases I and III, respectively. The 35S precursor contains the sequences for the mature 18S rRNA of the 40S subunit and 5.8S and 25S rRNAs of the 60S subunit. These 18S, 5.8S and 25S rRNAs in 35S pre-rRNA are separated by two internal transcribed spacer sequences, ITS1 and ITS2, and flanked by two external transcribed spacer sequences, 5'-ETS and 3'-ETS (Fig. 49).

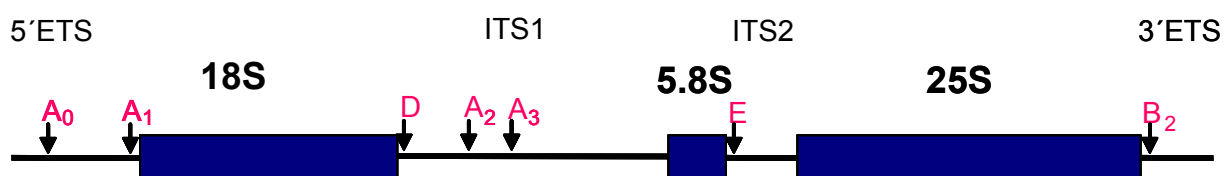


Fig. 49. Structure and processing sites of 35S pre-rRNA in *S.cerevisiae*. The processing sites are indicated by arrows.

The 35S pre-rRNA is first cleaved at site A_0 to generate the 33S pre-rRNA which is subsequently processed at sites A_1 and A_2 . The latter cleavage results in the separation of the pre-rRNAs destined for the small and large ribosomal subunits. Final cleavage at the site D of the 20S precursor leads to mature 18S rRNA. The all steps of rRNA processing and maturation from 35S precursor RNA, as well as modification of rRNAs through ribose methylation and isomerization of uridines, are well characterized in *S.cerevisiae* (Kressler *et al.*, 1999; Venema and Tollervey 1999). Concomitant with its synthesis and processing,

rRNA assembles with the ribosomal proteins and this assembly requires also transient association with a number of proteins which are not present in mature ribosomes. Many proteins are predicted to be associated with the pre-ribosomes, however the precise roles of these proteins remain undefined (Huh *et al.*, 2003).

4.2.3.1. *In silico* characterization of Yil19 protein

ORF 6.3009 has been annotated at the Stanford Genome Technology Center (<http://www-sequence.stanford.edu/group/candida/>) as *YIL19* based on its similarity to the previously uncharacterized ORF *YIL019* in *S.cerevisiae*. The encoded protein is 328 amino acids long. ClustalW (<http://www.ebi.ac.uk/clustalw/#>) analysis of the total Yil19p sequences of different ascomycetes like *S.cerevisiae*, *Schizosachharomyces pombe*, *Neurospora crassa* found that all these proteins share well conserved regions (Fig. 50A). Analysis by the PSORT program showed the presence of the classical type of nuclear localization signals (NLS), pat4 which is composed of 4 basic amino acids 'RKRR', starting at amino acid 325 and, pat7 which is a pattern starting with P and followed within 3 residues by a basic segment containing 3 K/R residues out of 4, starting at amino acid 191 (Fig. 50A), in *C.albicans*. On the other hand these nuclear localization signals are absent in *S.cerevisiae*, but there is a bipartite NLS, located at the C terminal part of the protein, starting at the 279th amino acid. This nuclear localization signal is important for the proper functioning of the protein in *S.cerevisiae* (Karkusiewicz *et al.*, 2004). Another interesting feature is that this gene is clustered with the *HIS6* gene in the genome of all these ascomycetes. Moreover in *C.albicans* and *S.cerevisiae* the gene for the subunit 3 of RNA polymerase II is preserved in this cluster (Fig. 50B) (Karkusiewicz *et al.*, 2004). It was found by microarray experiments in *S.cerevisiae* that the pair *YIL019-HIS6* is co-regulated in the cell-cycle, during diauxic shift and sporulation (Kruglyak and Tang, 2000). Although polycistronic transcription units are not evident in eukaryotes, clustering and co-expression of neighbouring genes are common (Fukuoka *et al.*, 2004; Overbeek *et al.*, 1999).

A.

<i>C. albicans</i>	-----MSEDDEY	7
<i>S. cerevisiae</i>	-----MTLDDDDY	8
<i>Sz. pombe</i>	-----MS	2
<i>N. crassa</i>	MPSATLLGKRKSIAAQPEAKKKRVAEDLEVKKKQKLAKKEEKPVKKANEEEEEQQDI	60
<i>C. albicans</i>	IKALEIQRNFEAQFGSIEDMGFEDKSKTQVELEDEDERSSQDSPDQS-----	55
<i>S. cerevisiae</i>	IKQMEIQRKAFESQFGSLESFEDKTKNIRTEVDTRDSSGDEIDNSD-----	56
<i>Sz. pombe</i>	ENALLALQRHFEDQFGHIEGLQPVSAKPSETAFNSDASEKEQSPTTSN-----	50
<i>N. crassa</i>	SDALSVFQRAFEARFKPIASAPATTTTTKAESKSTKNKTRKAQEDGDGVDNLEDEDQIL	120
	. : : * * :	
<i>C. albicans</i>	SGEDEEDSKFDEIDSDSNEEEMDFLGDDEEQDDIPK--PKVFKLNDSSNTPLPVVSKQDR	113
<i>S. cerevisiae</i>	HGSDFKDGTIESSNS-SDEDSGNETAEENNQDSKPKTQPKVIRFNGPSDVYVPPS-KKTQ	114
<i>Sz. pombe</i>	EEEDAISDMEDKEDVDFGSKILRVSHQEVKPTLSATVGRVSVFLKMPKLEDEEEE----	105
<i>N. crassa</i>	EDDDAVDSGSEDDSSGLEDEEDYSGSDSEEEKDDDEDAPKVMVVDYSKDPKVDTSKMSK	180
	. * . . : . . . : : : * . . .	
<i>C. albicans</i>	KLLKSGRA-PTLLEISKKEKLAQAQSKQSAKSAEEDENLANDLKLQRLKESHILAN	172
<i>S. cerevisiae</i>	KLLRSG---KTLTQINKKLESTEAKKEKED---ETLEAENLQNDLELQQFLRESHLISA	167
<i>Sz. pombe</i>	-----ILAKKREEQKLRKRSRQNDGSDDEVENLKNLQKLLRESHLHE	153
<i>N. crassa</i>	KELKAYLSSKPPNAILDNSQNGTKAKKDKDGEDESAAFLANDLALQRLIAESHLISA	240
 : : : . * * * * * : : : * * * * *	
<i>C. albicans</i>	T-----LEYSGADLTLQTIIDFDDP-----TGKARRALDSRIRELASTNSRTGG	216
<i>S. cerevisiae</i>	FNNGSGSTNSGVSLTLQSMGGNDDGIVYQDDQVIGKARSRTLEMRLNRLSRVNGHQDK	227
<i>Sz. pombe</i>	ATSR-----TGQVQLVAEGKIRHKVQVQHQHIAQLG	282
<i>N. crassa</i>	AGGNASHYLSAAAETDKN-----TRAFAGRIRKKTDMRMQALGAKG	284
	.	
<i>C. albicans</i>	LPKKLEKMPMAMRKGMIKKRDERIKKYEQDARDAGIVLSKVRKGEIQRDLQDAGRGSTSSSD	276
<i>S. cerevisiae</i>	IN-KLEKVPMHIRRGIMDKHVRIKKYEQEAAGGIVLSKVKKQFRKIESTYKKDIEERR	286
<i>Sz. pombe</i>	GKKETEKMPMAARRGMKKKQKHIEKVIENEARESGTVLAKKRK-----	325
<i>N. crassa</i>	SVLEQEKMPMNRKGIKKASETYEQKRREARENGIILEKASGKG-----	329
	: * * : * * * * : . : : * : * : * * *	
<i>C. albicans</i>	RLGTGKKIDKR---IRDRGLKINGIGRSTRNGLVISQGEIDRVNRGGKKG-----FKRKR	328
<i>S. cerevisiae</i>	IGGSIKARDKEKATKREGLKISSVGRSTRNGLIVSKRDIARISGGERSGKFKNGKKSR	346
<i>Sz. pombe</i>	-----ERKQFKKGFPRVTFAPGKLVGGTLLLPKSMIPK-----	359
<i>N. crassa</i>	-----KGTVKKRSGDRPVDMPGIGKMRGAQLTISSREIRSMENSGPVGRGGRMGGA	383
	. * : : . * : * : . . . *	
<i>C. albicans</i>	-----	
<i>S. cerevisiae</i>	-----	
<i>Sz. pombe</i>	-----	
<i>N. crassa</i>	KGGHRKRR	391

B.

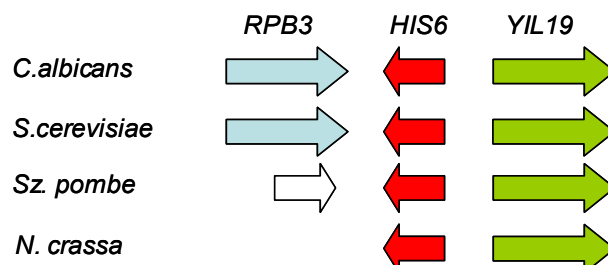


Fig. 50. Comparison of amino acid sequence and genomic organization of Yil19. **(A)** Clustal W (<http://www.ebi.ac.uk/clustalw/#>) analysis of Yil19 from *C. albicans*, *S. cerevisiae*, *Sz. pombe* and *N. crassa*. Identical and similar amino acids are indicated by asterisks and colons, respectively. Amino acids positions are indicated on the right. The NLS of the *C. albicans* protein is shown in red and that of *S. cerevisiae* in blue. **(B)** Gene clustering around the *YIL19* gene in four ascomycetes. The gene not coloured is not homologous to other Rpb3 proteins (adapted from Karkusiewicz *et al.*, 2004).

4.2.3.2. *YIL19* is an essential gene in *C.albicans*

For targeted gene deletion of the two *YIL19* wild-type alleles the *URA3*-flipping strategy was used (see section 4.1.3). The *ura3*-negative strain CAI4 was transformed with the plasmid pYIL19M2 in which almost all of the *YIL19* coding sequence had been replaced by the *URA3* flipper (see section 3.2 and Fig. 51). In strain CAI4, the two alleles of *YIL19* (arbitrarily designated as *YIL19-1* and *YIL19-2*) can be distinguished by a *SalI* restriction site polymorphism. From two transformants in which the deletion cassette has been integrated in either of the two possible *YIL19* alleles (strains YIL19M1A and YIL19M1B, Fig. 52, lanes 2 and 3), the *URA3* flipper was excised by FLP-mediated recombination, resulting in strains YIL19M2A and YIL19M2B (Fig. 52, lanes 4 and 5). When those two strains were again transformed with the same deletion cassette from plasmid pYIL19M2, all analysed transformants from both parent strains showed integration into the already inactivated *YIL19* allele (data not shown). The absence of allelic integration bias in the first allele transformation and the failure to delete the second allele in either of the two parent strains provided evidence that this gene might be an essential gene in *C.albicans*.

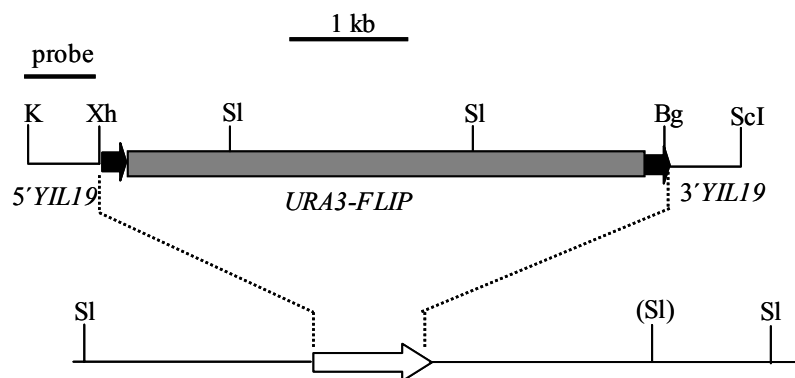


Fig. 51. Structure of the deletion cassette from plasmid pYIL19M2 (top) and genomic structure of the *YIL19* locus in the parental strain CAI4 (bottom). The *YIL19* coding region is represented by the white arrow, and the upstream and downstream sequences by the solid lines. The 34 bp *FRT* sites (black arrows) are not drawn to scale. The probe used for Southern hybridization analysis of the mutants is indicated by the thick bar. Only relevant restriction sites are given. Bg, *BglII*; K, *KpnI*; P, *PstI*; ScI, *SacI*; Xh, *XhoI*; Sl, *SalI*. The downstream *SalI* restriction site shown in parenthesis is present only in the *YIL19-2* allele.

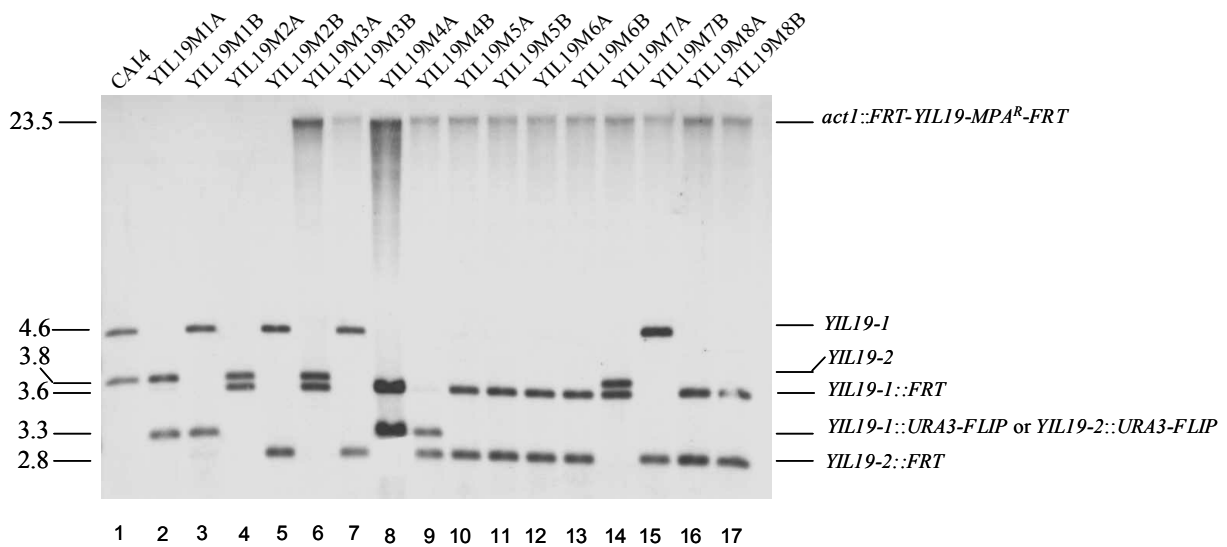


Fig. 52. Southern hybridization of *SalI*-digested genomic DNA of the parental strain CAI4 and mutant derivatives with a *YIL19*-specific probe shown in Fig. 51. The sizes of the hybridizing fragments (in kb) are given on the left side of the blot and their identities are indicated on the right.

4.2.3.3. Construction of conditional *yil19* deletion mutant

To construct the conditional *yil19* mutants the inducible gene deletion (Michel *et al.*, 2002), was used. A copy of the *YIL19* gene including its own regulatory sequences to ensure proper expression, and the dominant selection marker *MPA^R* were flanked by direct repeats of the *FRT* site (pYIL19D1) and integrated into *ACT1* locus of the heterozygous mutants YIL19M2A and YIL19M2B (Fig. 53). Excision of the *MPA^R* marker along with the cloned copy the gene by the expression of *FLP* gene allowed the screening for the loss of the extra copy of *YIL19* gene. The cassette was targeted to the *ACT1* locus as efficient excision of the *MPA^R* marker from this genomic site had been achieved in previous experiments, and disruption of one *ACT1* allele did not cause the alteration of growth of *C.albicans* (Staib *et al.*, 1999; 2000). Southern analysis showed the correct integration of *FRT-YIL19-MPA^R-FRT* cassette into one of the *ACT1* allele, resulting the strains YIL19M3A and YIL19M3B (Fig. 52 and Fig. 54, lanes 6 and 7).

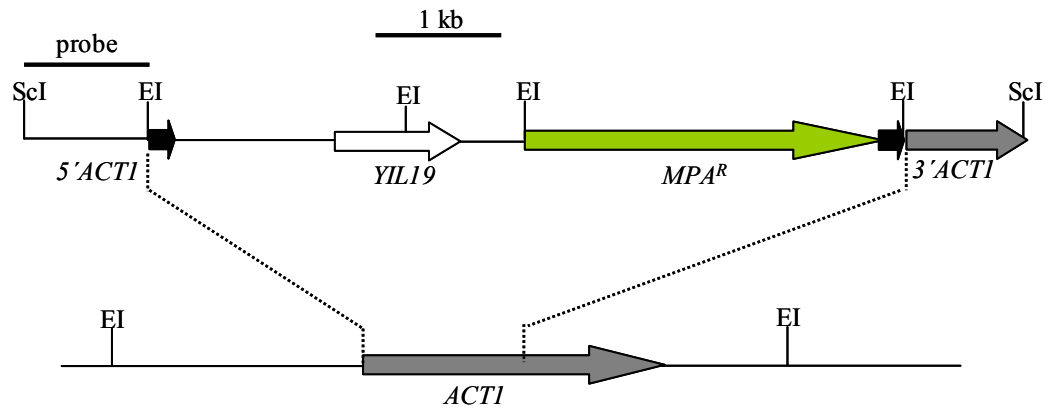


Fig. 53. Integration of the *FRT-YIL19-MPA^R-FRT* cassette from pYIL19D1 (top) into one of the genomic *ACT1* alleles (bottom). The *ACT1* coding region is indicated by grey arrow. The 34 bp *FRT* sites (black arrows) are not drawn to scale. The probe used for Southern hybridization analysis of the mutants is indicated by the thick bar. Only relevant restriction sites are given. EI, *EcoRI*; ScI, *SacI*.

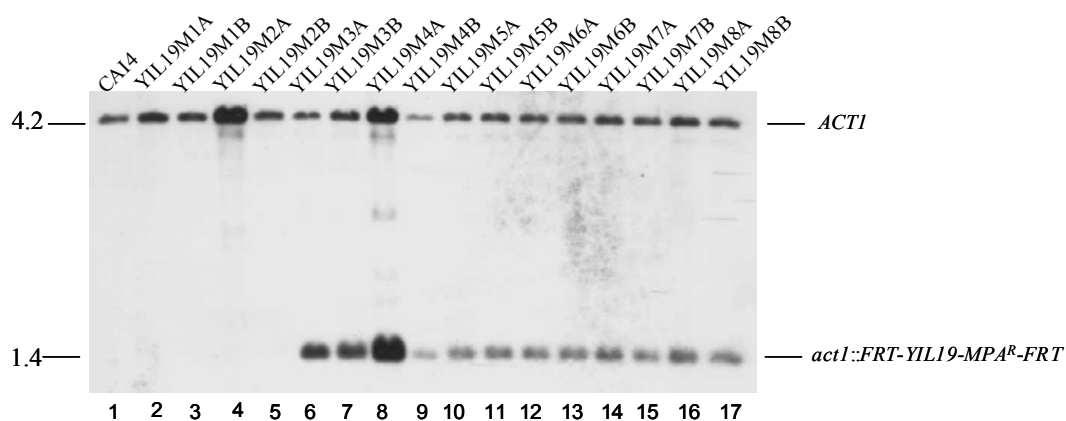


Fig. 54. Southern hybridization of *EcoRI*-digested genomic DNA of the parental strain CAI4 and mutant derivatives with *ACT1*-specific probe shown in Fig. 53. The sizes of the hybridizing fragments (in kb) are given on the left side of the blot and their identities are indicated on the right.

When strains YIL19M3A and YIL19M3B were transformed with the deletion cassette from pYIL19M2, integration was successfully targeted to the remaining wild-type *YIL19* allele, generating strains YIL19M4A and YIL19M4B (Fig. 52, lanes 8 and 9). The *URA3* flipper was then excised from these strains by FLP-mediated recombination, generating the strains YIL19M5A and YIL19M5B, both of which retained the deletable additional copy of the *YIL19* gene (Fig. 52, lanes 10 and 11).

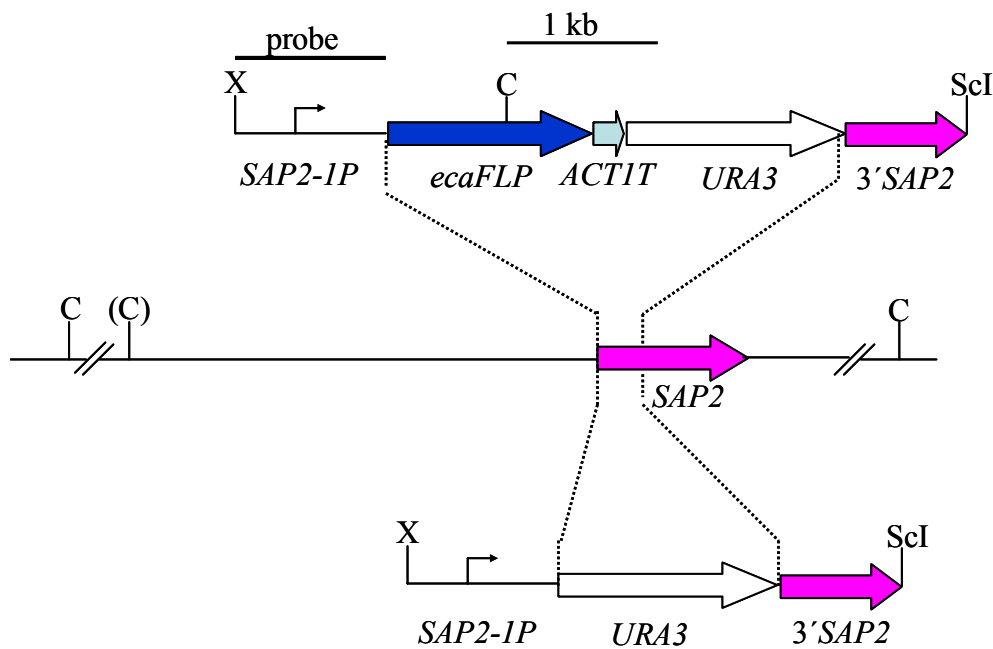


Fig. 55. Integration of the *SAP2-1P-ecaFLP* fusion (top) from pSFL213 or the *URA3* marker (bottom) from plasmid pSFL28 into the *SAP2* locus (middle). The *SAP2* coding region is indicated by the pink arrow. The upstream *Cla*I restriction site shown in parenthesis is present only in the *SAP2-1* allele into which the fragments were inserted. Only the relevant restriction sites are shown, C, *Cla*I; ScI, *Sac*I; X, *Xba*I.

The *SAP2-1P-ecaFLP* fusion from plasmid pSFL213 was integrated into the *SAP2-1* allele of strains YIL19M5A and YIL19M5B generating the strains YIL19M6A and YIL19M6B, respectively (Fig. 55, top and Fig. 56, lanes 12 and 13). In these strains induction of the *SAP2* promoter results in expression of the *ecaFLP* gene and allow efficient deletion of the *YIL19* copy integrated at *ACT1* locus. Two types of control strains were also constructed. Integration of the *SAP2-1P-ecaFLP* fusion into the *SAP2-1* allele in YIL19M3A and YIL19M3B generated the strains YIL19M7A and YIL19M7B, respectively (Fig. 56, lanes 14 and 15), which carried the additional *YIL19* copy in a heterozygous background, ensuring that one of the wild-type *YIL19* alleles remains after deletion of the *MPA^R-YIL19* cassette. The strains YIL19M8A and YIL19M8B (Fig. 56, lanes 16 and 17) were obtained by integrating only the *URA3* selection marker rather than the *SAP2-1P-ecaFLP* fusion (Fig. 55, bottom) into YIL19M5A and YIL19M5B. Those latter strains would be unable to delete the *ACT1*-integrated *YIL19* copy under *SAP2*-inducing conditions.

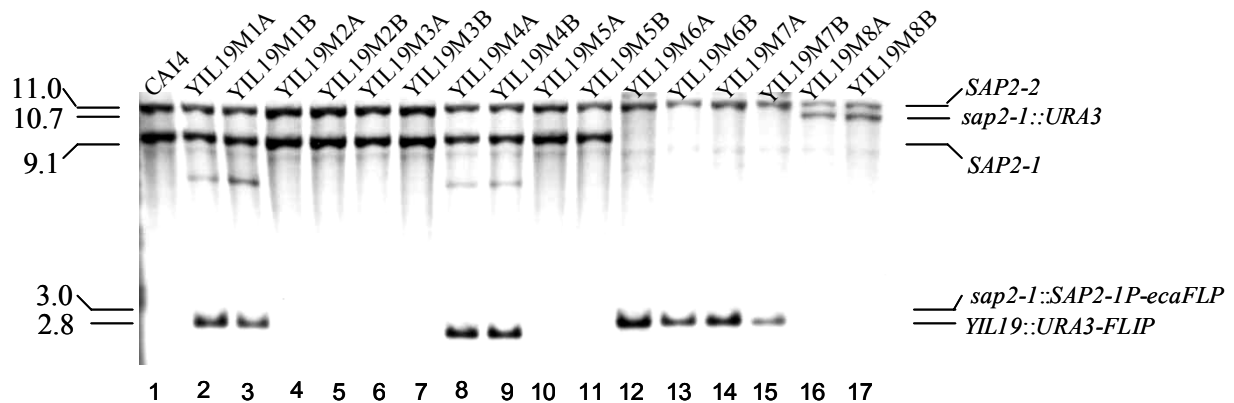


Fig. 56. Southern hybridization of *ClaI*-digested genomic DNA of the parental strain CAI4 and mutant derivatives with the *SAP2*-specific probe shown in Fig. 55. The sizes of the hybridizing fragments (in kb) are given on the left side of the blot and their identities are indicated on the right.

4.2.3.4. *YIL19* deletion is lethal in *C.albicans*

To determine the effect of *YIL19* deletion in *C.albicans* strains YIL19M6A and YIL19M6B, in which the original *YIL19* alleles were inactivated, were grown for 16 hours in YCB-BSA medium. The *SAP2* promoter is repressed in commonly used laboratory media, such as YPD, and can be induced in media containing a protein as the sole nitrogen source, such as YCB-BSA; this induction occurs after several hours of growth when low-molecular-weight nitrogen sources are exhausted (Staib *et al.*, 1999). Wild-type strain SC5314, the strains YIL19M7A and YIL19M7B which retained one of the wild-type *YIL19* allele in addition to the deletable copy, and strains YIL19M8A and YIL19M8B which contained only the deletable *YIL19* copy but not the *ecaFLP* gene were included as controls. All the strains had reached the same optical density (O.D₆₀₀ between 28 and 30) and by microscopic appearance, the cells of all strains looked like wild-type (Fig. 57).

To determine the colony forming units (cfu), the cultures from all these strains were diluted and plated on YPD as well as MPA indicator plates. The cultures of the control strains YIL19M7A/B or YIL19M8A/B were shown to contain $\sim 4 \times 10^8$ ml⁻¹ viable cells, which is comparable to the no of viable cells from the culture of the wild-type strain SC5314 ($\sim 6 \times 10^8$ ml⁻¹). The colonies from the wild-type and strains YIL19M7A/B were MPA sensitive whereas the colonies from YIL19M8A/B were MPA resistant, which indicates the efficient deletion of *YIL19-MPA^R* from YIL19M7A/B. In contrast, the cultures of strains YIL19M6A/B produced only $\sim 2 \times 10^5$ cfu ml⁻¹, and these were MPA resistant, indicating that <0.1% of the cells had escaped FLP-mediated excision of the *YIL19-MPA^R* cassette and that all other cells were

unable to generate viable colonies. These results demonstrate that *YIL19* is an essential gene in *C.albicans* and the FLP-mediated gene deletion effectively generated an almost pure population of *yil19* null mutants.

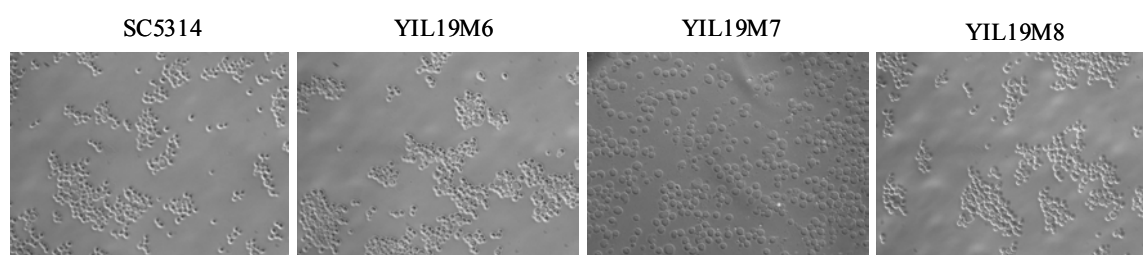


Fig. 57. Phase contrast micrographs of the cells. A single colony of each strain was inoculated into 10 ml of YCB-BSA medium and grown for 16 hours at 30°C. The strain pairs YIL19M6A/B, YIL19M7A/B and YIL19M8A/B looked identical, and only one of them is shown.

To assess the effect of *YIL19* deletion on vegetative growth and cell morphology, the cells were diluted in fresh YPD medium after 16 hours growth in YCB-BSA. Comparisons of the growth of the population of null mutants in liquid YPD medium at 30°C along with wild-type strain SC5314 and control strains YIL19M8A/B showed that the YIL19M6A/B strains were impaired in growth. The control strains, which contain a single copy of *YIL19* gene, grew slightly slower than the wild-type strain (Fig. 58). When the cells were observed by microscope, it was found that the cells of YIL19M6A/B were slightly bigger than those of the wild-type and control strains (Fig. 59). To determine whether *YIL19* deletion affected hyphae formation in *C.albicans*, the YCB-BSA cultures of the mutant and control strains were diluted 10^{-2} into fresh RPMI+10% serum and incubated for 8 hours at 37°C. It was found that both mutant and control strains were able to elongate the cells equally well and there was no effect of deletion of this gene on the development of hyphae (Fig. 60).

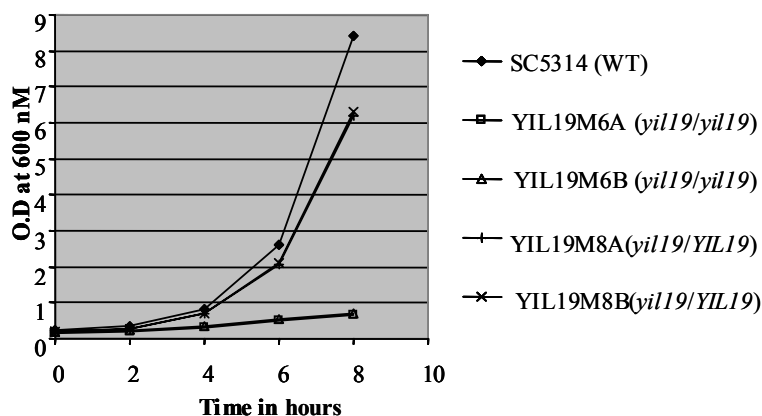


Fig. 58. Effect of *YIL19* deletion on vegetative growth of *C. albicans*. The YCB-BSA cultures shown in Fig. 57 were diluted 10^{-2} into fresh YPD medium and grown for 8 hours at 30°C . Growth was followed by measuring the increase in optical density over time.

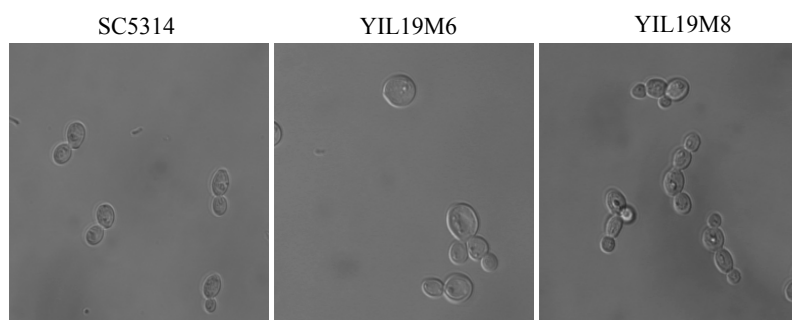


Fig. 59. Morphologies of *C. albicans* cells grown in YPD after deletion of *YIL19*. The YCB-BSA cultures shown in Fig. 57 were diluted 10^{-2} into fresh YPD and the cells were analysed by phase-contrast microscopy after 8 hours growth at 30°C . The strain pairs YIL19M6A/B and YIL19M8A/B looked identical, and only one of them is shown.

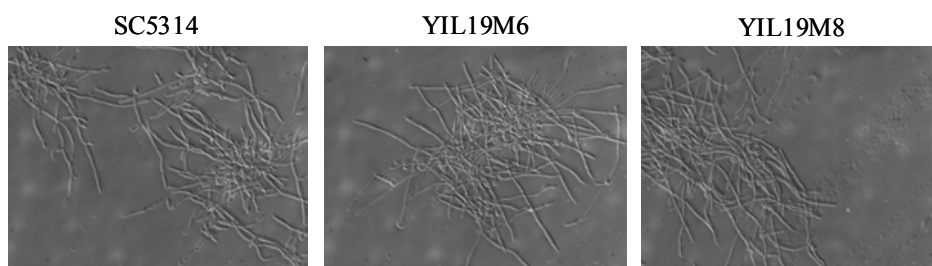


Fig. 60. The YCB-BSA cultures shown in Fig. 57 were diluted 10^{-2} into RPMI 1640 with 10% serum and the cells were analysed by phase-contrast microscopy after 8 hours growth at 37°C . The strain pairs YIL19M6A/B and YIL19M8A/B looked identical, and only one of them is shown.

4.2.3.5. *YIL19* depleted cells are impaired in the maturation of 18S rRNA

Yil19p (Faf1p) of *S. cerevisiae* has very recently been shown to be involved in 18S rRNA maturation and is also essential in this organism (Shirai *et al.*, 2004; Karkusiewicz *et al.*, 2004). The similarity of *YIL19* in *C. albicans* and *S. cerevisiae* and the essentiality in both

organisms, suggested that Yil19p might function in rRNA processing also in *C.albicans*. To test this hypothesis, the steady state level of rRNA was examined by Northern blotting. After 16 hours induction in YCB-BSA (see section 4.2.3.4), cells of the wild-type strain SC5314, the *yil19* null mutants YIL19M6A/B, and the control strains YIL19M8A/B, were grown in YPD medium at 30°C for 8 hours. Total RNA was prepared and equal amounts of RNA were electrophoresed and blotted on a nylon membrane. Visualization of RNA by methylene blue staining of the blot indicated that the level of 18S rRNA was reduced in the mutant cells, whereas the level of 25S rRNA was comparable to the wild-type and the control strains (Fig. 61). To determine whether the reduced level of 18S rRNA resulted from a defect in rRNA processing, the Northern blot was hybridised with probes specific to the ITS regions of the 35S pre-rRNA transcript. Northern hybridization with the probe specific for the ITS1 region (oligo ITS1.3) showed the accumulation of two bands in the mutants positioned between the 25S and 18S rRNAs (Fig. 62B, left). Moreover, there was a slight increase in the amount of 35S pre-rRNA in the mutant cells, confirming the inhibition of the processing of rRNA (Fig. 62B, left). The control strains YIL19M8A and YIL19M8B, which retain one *YIL19* copy, also showed the accumulation of one precursor rRNA band, which might be due to a gene dosage effect. Hybridization with the probe ITS 2.1, specific for the precursor containing 5.8S and 25S rRNA showed a similar level of the 7S intermediate in the wild-type, control and mutant cells, indicating that the processing steps leading to the 5.8S were not disturbed in the mutant cells (Fig. 62B, right). All these data together showed that *YIL19*, like its counterpart in *S.cerevisiae* also had a role in the processing of 18S rRNA in *C.albicans*.

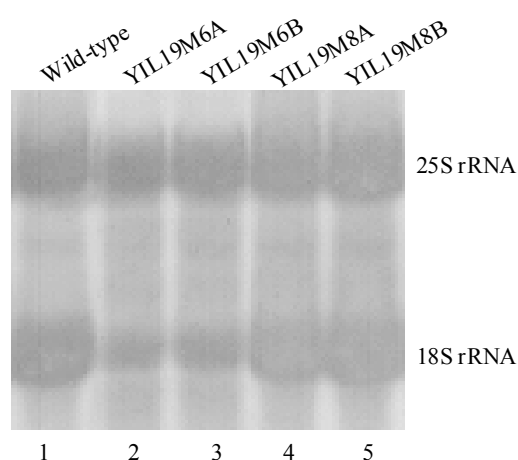


Fig. 61. Methylene blue stained blot of total RNA extracted from the wild-type strain (SC5314) and, the homozygous (YIL19M6A/B) and heterozygous (YIL19M8A/B) mutants of *YIL19*.

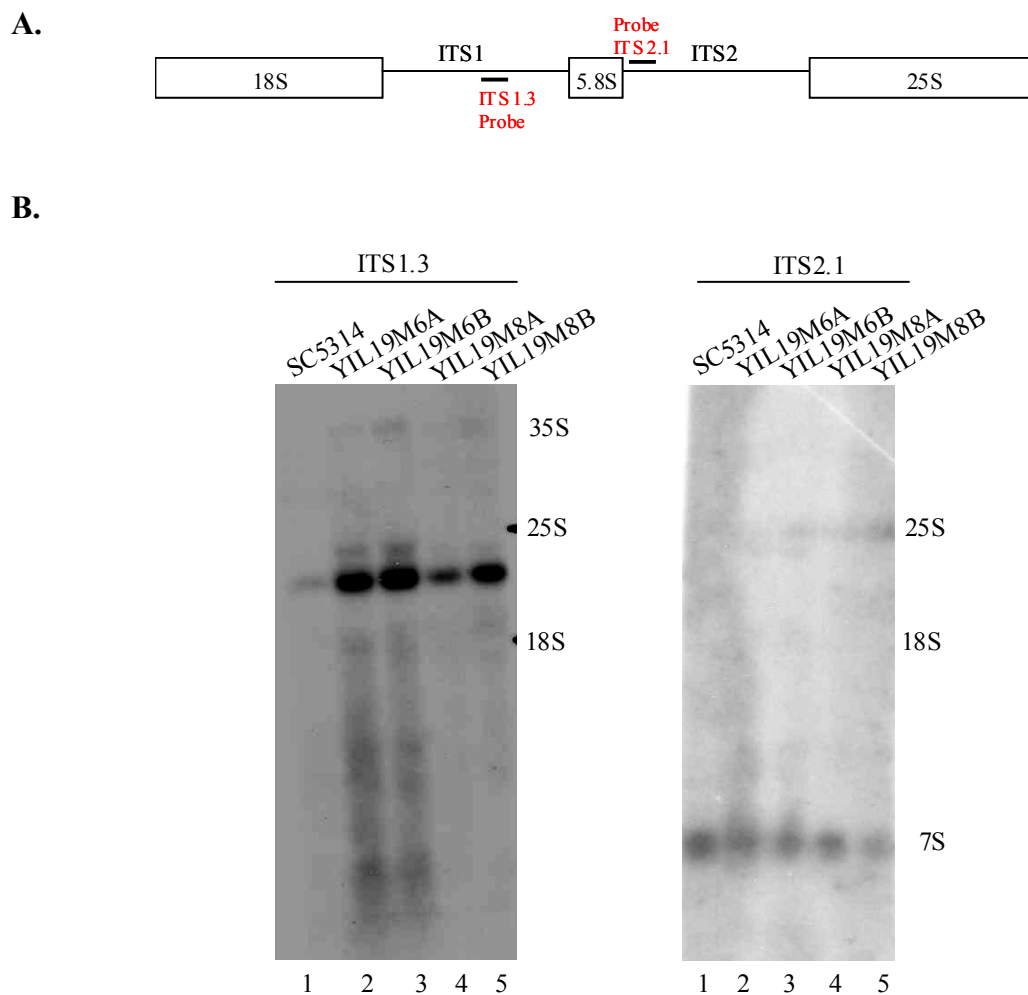


Fig. 62 (A) Structure of 35S pre-rRNA and positions of oligonucleotide probes. (B) Autoradiographs of the blot shown in Fig. 61 hybridized with oligonucleotide probes indicated on the top. Positions of different pre-rRNAs and mature rRNAs are indicated.

5. Discussion

5.1. Nitrogen starvation induced filamentous growth and ammonium transporters

In its natural habitat *C.albicans* encounters a wide variety of nitrogen sources. However, not all nitrogen sources support growth equally well. Good nitrogen sources result in a relatively higher growth rate than poor nitrogen sources. Moreover, nutrient limitation is a stress situation for the cells. When *C.albicans* cells are grown in the presence of limiting nutritional sources, their morphological behaviour changes and they start to grow in a filamentous form to seek nutrients in their surroundings. The present work showed that limiting concentrations of any nitrogen source induce filamentous growth in *C.albicans* and that nitrogen starvation induced filamentation was suppressed by sufficient amount of a preferred nitrogen source, like ammonium. Limjindaporn *et al.* (2003) reported that filamentation in *C.albicans* is not under nitrogen repression, but they used glutamine at high concentration rather than ammonium. In the present study it was observed that, when relatively high concentrations (10 mM) of glutamine were used as sole nitrogen source, filamentation was induced, although filaments started to emerge after 5 days of incubation and that filamentous growth was repressed only in presence of very high concentrations of ammonium (100 mM). Although glutamine is a preferred nitrogen source, high concentrations may have caused an imbalance in nitrogen metabolism, that resulted in filamentous growth. Repression of filamentation by ammonium was not extended to the other filament inducing conditions, like the presence of serum, which indicates that the repression of filamentation by ammonium occurs only when the response is due to nitrogen starvation and not in case of the other environmental conditions which also causes filamentation in this opportunistic pathogen. Moreover, nitrogen starvation induced filamentation was observed only in solid media and not in liquid media. When the colonies grow on a solid surface, they initially use up the locally available nitrogen and then for further growth they need to scavenge the nutrients from the other parts of the plate and need to elongate the cells, which is done through the formation of filaments. It is also important to keep in mind that initially on the plate smooth colonies are formed and after 3 days of incubation filaments start to come up from the borders of the colonies.

Ammonium, either taken up directly from the external medium or derived from amino acids, is often considered as a preferred source of nitrogen in microorganisms (ter Schure *et al.*, 2000). Ammonium uptake by *S.cerevisiae* involves at least three ammonium permeases,

Mep1p, Mep2p and Mep3p (Marini *et al.*, 1994; 1997), which belong to a multigene family, the so-called Mep/Amt family (Marini *et al.*, 1994; Ninnemann *et al.*, 1994). This study showed that *C.albicans* possesses two genes, *CaMEP1* and *CaMEP2*, encoding ammonium permeases that allow growth when low concentrations of ammonium are the sole nitrogen source. *CaMEP1* is more similar to *ScMEP1* than to *ScMEP3* in that it allowed normal growth and ammonium uptake when it was the only *MEP* gene present, as has been demonstrated for *ScMEP1*, whereas *S.cerevisiae* cells expressing only *MEP3* exhibit reduced ammonium uptake and reduced growth under limiting ammonium conditions (Lorenz and Heitman, 1998a; Marini *et al.*, 1997). The *C.albicans* genome sequence contains a third gene (ORF 6.7259) which shows homology to ammonium permeases. However, deletion of *CaMEP1* and *CaMEP2* rendered *C.albicans* incapable of growing at low ammonium concentration, and hence, the studies were focused on only these two genes. Although ORF 6.7259 may act as an ammonium permease, CaMep1p and CaMep2p seem to be the major ammonium transporters in *C.albicans*. It is possible that the encoded protein of the ORF 6.7259 is involved in ammonium uptake at higher ammonium concentration (76 mM), which would explain that the deletion of *CaMEP1* and *CaMEP2* did not affect growth at higher ammonium concentrations. But the entry of ammonium into the cell through simple diffusion at higher concentrations can not be ruled out. However, expression of either CaMep1p or CaMep2p alone resulted in specific ammonium transport activity, demonstrating these proteins are indeed ammonium transporters.

Although ammonium permeases from various other organisms can rescue the ammonium uptake defect of *S.cerevisiae* $\Delta mep1 \Delta mep2 \Delta mep3$ triple mutants, only some of them are able to restore pseudohyphal growth. Therefore, it is assumed that a certain subclass of ammonium permeases possesses structural features which are required for morphogenesis and which are absent from the other ammonium permeases that have only a transporter function (Smith *et al.*, 2003). CaMep2p was found to be required for filamentation in response to nitrogen starvation in *C.albicans*. Although the main physiological function of Mep proteins is to scavenge the ammonium from the medium for use as a nitrogen source, CaMep2p but not CaMep1p, is required for filamentation. The specific function of CaMep2p in nitrogen starvation induced filamentous growth of *C.albicans* is similar to the role of its counterpart ScMep2p in pseudohyphal growth of *S.cerevisiae* under limiting ammonium conditions (Lorenz and Heitman, 1998a), but an important difference between *CaMEP2* and *ScMEP2* is that the former is required for filamentous growth under nitrogen starvation conditions in general, whereas the latter plays a role only under limiting ammonium

conditions, but not when other limiting nitrogen sources induce pseudohyphal growth (Lorenz and Heitman, 1998a). Moreover, growth and ammonium import were found to be normal in *Δmep2* mutant, indicating that the filamentation defect of these mutants is not due to growth impairment. Interestingly, when arginine was used as a limiting source of nitrogen, filamentation was found not to be dependent on CaMep2p. At higher concentrations (10 mM) arginine was found to inhibit the growth of *C.albicans* (data not shown) and the induction of filamentous growth by arginine may therefore represent a different type of stress response. When other conditions, like serum, agar embedding, or any other liquid filament induction medium was used, filamentation was not dependent on CaMep2p. In these conditions the filamentation induction pathways seem to be activated in different ways.

One can envisage different models to explain the requirement for *CaMEP2* in filamentous growth of *C.albicans* when nitrogen sources other than ammonium are limiting. One possibility is that the role of CaMep2p in filamentous growth is not that of an ammonium sensor, which is in contrast to the suggested role of Mep2p in *S.cerevisiae*. Evidently, CaMep2p is not the primary sensor of nitrogen starvation, since expression of *CaMEP2* itself was induced under these conditions. It is likely that *C.albicans* senses limiting concentrations of nitrogen metabolites within the cell, for example with the help of Gln3p, a putative glutamine sensor, or Gat1p, a putative glutamate sensor (Magasanik and Kaiser, 2002). These GATA transcription factors may then induce expression of *CaMEP2* and *CaMEP1*, which contain GATA binding sites in their upstream regions. *CaMEP2* expression was induced irrespective of the nature of the limiting nitrogen source in the growth medium, indicating that *C.albicans* tries to obtain the preferred nitrogen source ammonium even when amino acids are available as nitrogen source and the simple presence of CaMep2p would then induce the yeast-hyphal switch also in the absence of ammonium. The second model implies that CaMep2p signals filamentous growth in the presence of limiting nitrogen sources other than ammonium because intracellular ammonium leaks out of the cells which is then transported back into the cell by CaMep2p. In this model signaling would depend on ammonium recognition/transport by CaMep2p, in concordance with a role of CaMep2p as an ammonium sensor. There is some evidence that ammonia secretion may facilitate intercolony communication in yeast (Palkova *et al.*, 1997).

What makes the CaMep2 permease specific for the regulation of filamentation? The results of the present study demonstrate that the specific role of CaMep2p in filamentous growth of *C.albicans* is due at least in part to its higher expression as compared with CaMep1p. Lowering the expression level of *CaMEP2* abolished its ability to induce

filamentous growth, and artificially increasing the expression level of *CaMEP1* conferred on it the ability to induce a weak filamentation. The elevated expression of *CaMEP2* seems to be caused both by increased promoter activity and by increased mRNA stability. Higher amounts of mRNA and a stronger fluorescence of the cells were observed when *CaMEP2*- or *CaMEP1-GFP* fusions were expressed from the *CaMEP2* promoter than from the *CaMEP1* promoter, indicating that the former is induced more strongly than the latter in response to nitrogen starvation. In addition, regardless of the promoter used, *CaMEP2-GFP* mRNA levels were always higher than *CaMEP1-GFP* mRNA levels expressed from the same promoter, indicating that the sequences within the *CaMEP1* and *CaMEP2* coding regions determine the stability of the respective mRNAs and result in increased *CaMEP2* transcript levels. Together these mechanisms ensure that much higher amounts of CaMep2p than of CaMep1p are present in the cytoplasmic membrane, as judged from the signals obtained with the GFP-tagged proteins. Since the same expression levels for CaMep1p as for CaMep2p were not achieved, even when expressing *CaMEP1* from the strong *ADHI* promoter, it is possible that the specific role of CaMep2p in filamentous growth of *C.albicans* relies solely on its higher expression as compared with CaMep1p. However, it is likely that CaMep2p has also evolved structural features that made it a more efficient signaling protein instead of an efficient ammonium transporter.

The results obtained with C-terminally truncated proteins clearly demonstrate that the C-terminal cytoplasmic tail of CaMep2p is dispensable for ammonium transport but essential for the induction of filamentous growth, and therefore, has a specific signaling function. At first sight, this result came as a surprise since it has been reported that the C-terminal cytoplasmic domain of ScMep2p is not required for its ability to induce pseudohyphal growth in response to ammonium starvation in *S.cerevisiae* (Lorenz and Heitman, 1998a). However, from the alignment of the sequences of the ammonium transporters from *C.albicans* and *S.cerevisiae* it became clear that the C-terminal deletion of ScMep2p described by Lorenz and Heitman did not completely remove the cytoplasmic tail and correspond almost exactly to the Δ C440 truncation in CaMep2p described in the present study, which retained its capacity to induce filamentous growth. Interesting observation made in this study was that the deletion of the distal half of the CaMep2p C-terminal domain in fact resulted in a hyperfilamentous growth under low ammonium conditions, without affecting the growth at low ammonium concentrations and ammonium uptake. This raises the possibility that the extreme C-terminal part of CaMep2p functions as an autoinhibitory domain that might interact with the signaling domain to prevent filamentous growth under certain conditions. But, the Northern data

suggested that the deletion of this region increases the transcript stability and possibly this deletion results in an increase of the amount of protein which might then cause hyperfilamentation. This provides another evidence that the expression level of *CaMEP2* plays a major role for its signaling function. In contrast, further deletions close to the last predicted trans-membrane domain resulted in a protein that allowed wild-type growth under low ammonium conditions and also ammonium uptake like the full length protein, demonstrating that it was functional as a permease, but it lost its capacity to induce filamentous growth, although the deletion of this region increased the stability of the transcript. This result provides evidence that the C-terminal cytoplasmic domain of CaMep2p (and possibly also of ScMep2p) has a role in signaling. Surprisingly, the region involved in signaling comprises the part of the C-terminal region in which CaMep2p has the highest similarity to CaMep1p and also other Mep proteins that do not induce morphogenesis. Furthermore, the substitution of the C-terminal cytoplasmic tail for the corresponding region in *CaMEP1* did not confer signaling activity to the latter protein, which suggests that there is some other region in CaMep2p which needs to interact with the cytoplasmic region to transmit the signal and that region is different in CaMep1p and CaMep2p. Additional experiments to identify the regions which interact with the C-terminal region were not successful because of the failure to make the functional hybrids of CaMep2p and CaMep1p when the fusion points were not in the C-terminal cytoplasmic region (data not shown).

When CaMep2p is involved in signaling for morphogenesis, then what are the downstream regulators? The pseudohyphal growth defect of *Scmep2* mutants could not be rescued by activation of the MAP kinase cascade with a dominant active *STE11* allele, but addition of exogenous cAMP or dominant active *GPA2* or *RAS1* alleles overcame the defect (Lorenz and Heitman, 1998a). Several components of the MAP kinase pathway and the cAMP-dependent signaling pathway have been shown to be required for filamentous growth of *C.albicans* under low ammonium conditions (Bahn and Sundstrom, 2001; Csank *et al.*, 1998; Rocha *et al.*, 2001; Sanchez-Martinez and Perez-Martin, 2002). It was therefore reasonable to assume that CaMep2p might induce filamentous growth by activating one of these pathways. The ability of an artificially activated component of a signaling pathway to bypass the requirement for another component is often taken as evidence that the artificially activated component is located downstream of the defective component in the same signaling pathway. It was observed in this study that the dominant active alleles of *GPA2* or *RAS1*, or the addition of exogenous cAMP rescued the filamentation defect of $\Delta mep2$ mutants, indicating that CaMep2p acts upstream of *GPA2* and *RAS1*. The Ras1p is known to act

upstream of the MAP kinase and the cAMP pathway to regulate filamentation, and the G α protein, Gpa2p is also involved in the regulation of filamentous growth upstream of cAMP pathway. However, since different signaling pathways can induce filamentous growth in response to environmental conditions in *C.albicans* it is also possible that artificial activation of one pathway bypasses the normal requirement of a parallel pathway, as has been suggested for *S.cerevisiae* (Gagiano et al., 1999; Lorenz and Heitman, 1998b). Therefore, another approach using the hyperactive *CaMep2 Δ C⁴⁴⁰* allele, was taken to gain information about how CaMep2p induces filamentous growth in *C.albicans*. Assuming that CaMep2p is a sensor that is localized at the head of a signaling pathway, the ability of the hyperactive *CaMep2 Δ C⁴⁴⁰* allele to bypass a defect in a downstream component of one of the pathways would indicate that CaMep2p is able to signal through another pathway. The hyperactive *CaMep2 Δ C⁴⁴⁰* allele induced filamentous growth in mutants deleted for transcription factors of either the MAP kinase or the cAMP pathway, but not in mutants defective for both pathways, suggesting that in wild-type cells CaMep2p activates both the MAP kinase pathway and the cAMP pathway to induce the switch from yeast to filamentous growth. Although other explanations are possible, the results are consistent with a model in which CaMep2p, directly or indirectly, activates Ras1p to induce filamentation, since the *CaMep2 Δ C⁴⁴⁰* allele could not rescue the filamentation defect of *ras1* mutant. Ras1p in turn may then activate both the MAP kinase pathway and the cAMP pathway. But it is also possible that Ras1p is required only for the activation of the cAMP pathway, and the resulting adenylyl cyclase activity then enables components of the MAP kinase pathway to become fully active (Rocha *et al.*, 2001). The latter hypothesis is supported from the observation that the hyperactive *CaMep2 Δ C⁴⁴⁰* allele was unable to induce filamentation in *cdc35* mutants whereas the addition of cAMP restored the filamentous growth of Δ *mep2* mutants. Gpa2p, which is also required for filamentous growth under these conditions, may be activated by additional signals through the putative sugar sensor Gpr1p (Miwa *et al.*, 2004) and then contribute to the activation of one or both signaling pathways.

Since nitrogen starvation is sensed before the expression of the ammonium permeases is induced, the question arises why *C.albicans* has integrated an ammonium transporter into the signaling pathways that regulate filamentous growth instead of directly inducing morphogenesis under these conditions. A possible explanation is that such a regulatory circuit allows *C.albicans* to fine-tune morphogenetic development in response to the availability of the preferred nitrogen source ammonium. Except at very high ammonium concentrations, ammonium permeases are required to take up sufficient ammonium to allow growth at an

optimal rate. Therefore, at intermediate extracellular ammonium concentrations the activity of the transporters creates intracellular conditions in which *C.albicans* prefers to grow as budding yeast and, consequently, signaling by CaMep2p must be blocked. An attractive hypothesis is that the signaling activity of CaMep2p depends on its transport activity. When no or low concentrations of ammonium are available, CaMep2p would not be involved in ammonium transport most of the time and be able to activate the signaling pathways, resulting in filamentous growth. At higher ammonium concentrations CaMep2p would increasingly become engaged in transport, and this status might block the signaling activity of the C-terminal cytoplasmic tail. The results of this study indicate that CaMep2p is a less efficient ammonium transporter than CaMep1p, and needs to be expressed at much higher levels to allow sufficient ammonium uptake and growth when ammonium concentrations are limiting. These features, a high number of CaMep2p molecules in the cell membrane and inefficient ammonium transport, may be requirements for CaMep2p to regulate morphogenesis in response to ammonium availability. It is noteworthy that this model contrasts with the one proposed for the function of ScMep2p as an ammonium sensor in *S.cerevisiae* in that the signaling activity of CaMep2p is inhibited by ammonium.

One must assume an additional level of regulation in the presence of moderate ammonium concentrations, conditions in which *CaMEP2* is still expressed but no filamentous growth occurs. Under these conditions CaMep2p signaling seems to be blocked by other regulatory mechanisms, for example the sensing of sufficient intracellular nitrogen sources. But, it can also not be ruled out that at moderate ammonium concentration *CaMEP2* expression is not as high as in low concentration as suggested by the fluorescence level of GFP fusion protein. Further support for the control of gene expression in *C.albicans* by sufficiently high intracellular concentrations of ammonium (or its assimilation products) also comes from the observation that the dominant active allele of *GPA2* or *RASI*, or the addition of exogenous cAMP did not induce filaments at moderate ammonium concentration (10 mM). This is in contrast to the regulation of morphogenesis in *S.cerevisiae* where such conditions have been reported not only to bypass the requirement for ScMep2p but also to induce pseudohyphal growth even at high ammonium concentrations (Lorenz and Heitman, 1998a). The mechanism how ammonium represses filamentation in *C.albicans* at this level and how this repression is overcome by other environmental signals, like serum, remains unknown. However, it is intriguing that *C.albicans* has installed a regulatory circuit in which an inhibitor of filamentous growth is taken up into the cell by the same transporter that is essential for the induction of morphogenesis in response to nitrogen starvation.

However, the main regulation of filamentation by CaMep2p is by the regulation of its expression. Studies of the regulation of expression will provide more insights into the filament formation pathways at low nitrogen conditions. The *S.cerevisiae* mutant strains deleted for *GLN3*, *URE2*, or *NPR1*, which control ScMep2p levels, also display a pseudohyphal growth defect even when other nitrogen sources like glutamine or proline are limiting, and it was suggested that these regulatory proteins have additional targets that are critical for the regulation of dimorphism (Lorenz and Heitman, 1998a). *ScMEP2* expression in *S.cerevisiae* requires at least the presence of a functional GATA factor, Gln3p or Gat1p (Marini *et al.*, 1997). Promoters of *CaMEP1* and *CaMEP2* contain several binding sites of GATA factors. *C.albicans* *GATI* has recently been characterized and *GATI* deletion did not affect the filamentation in low nitrogen medium (Limjindaporn *et al.*, 2003). Since CaMep2p is required for filamentation under these conditions, *gat1* mutants should have filamentation defect if *CaMEP2* expression is controlled by Gat1p. The presence of several GATA factors suggests that other factors than Gat1p are involved in the expression of this ammonium permease. It is possible that the expression of *CaMEP2* may only require Gln3p, like in the *S.cerevisiae* *ScMEP1* and *ScMEP3* expression, which require only Gln3p and not Gat1p (Marini *et al.*, 1997). This hypothesis can be addressed by the construction of *gln3* mutants in *C.albicans* and studying the expression of the ammonium permeases in those deletion strains. However, this study proposes how the difference in the expression of these two ammonium permeases controls filament formation, a virulence factor of *C.albicans*, and opens a new direction towards the understanding of the correlation of nitrogen regulation, filament formation and virulence in *C.albicans*.

5.2. Analysis of putative essential genes in *C.albicans*

With the significant increase of fungal infections it has become essential to understand the biology of virulence factors, as their inactivation is likely to block the progression of disease. Although some virulence factors might be good targets for antifungal drug development, most are not shared among all fungal pathogens, and thus drugs that target these factors are likely to have a rather narrow spectrum. To develop new therapies and treatments for fungal infections, identification and characterization of essential genes which are conserved among most fungal pathogens and show significant divergence in higher

eukaryotes, are favoured by most pharmaceutical companies. For the development of new antifungal agents, a detailed knowledge about the consequences of loss of gene function will help to design inhibitors as well as screening systems to test them. Therefore, in an attempt to identify potential antifungal targets, the knowledge obtained from functional genomic analyses was used and *C.albicans* homologs of three genes which show no or low homologies to higher eukaryotes and are essential in other fungi were selected in collaboration with an industrial partner. The selected genes were then characterized by analysing the deletion mutants of these genes in *C.albicans*.

5.2.1. Repressor/Activator Protein 1

CaRap1p is different from Rap1p of *S.cerevisiae* and other yeasts like *C.glabrata*, *K.lactis* or *S.castelli*. CaRap1p is truncated at its C-terminal region which is involved in transcriptional activation and silencing in ScRap1p. In contrast, all other published yeast Rap1 proteins contain all three regions described for ScRap1p, although similarity is highest in the essential DNA binding domain (Larson *et al.*, 1994; Haw *et al.*, 2001; Wahlin and Cohn 2002). Since CaRap1p shows similarity to the central DNA binding region of ScRap1p, it was interesting to check whether it could complement conditional *rap1* mutants of *S.cerevisiae*. The inability of CaRap1p to complement might not be surprising, because KIRap1p which was also cloned on the basis of its similarity to the DNA binding domain and is more similar to ScRap1p than CaRap1p was unable to complement the growth defect of a temperature-sensitive *rap1* mutant (Larson *et al.*, 1994). However the possibility remains that *CaRAPI* was not functionally expressed in the heterologous host, for example because of the non-standard codon usage of *C.albicans* or the inability of *CaRAPI* promoter to function in *S.cerevisiae*. Importantly, this study showed that *CaRAPI* is not an essential gene in *C.albicans* and that its deletion did not negatively affect the growth of the cells under most conditions. It is important to keep in mind the CaRap1p in *C.albicans* is much shorter than ScRap1p and this difference may explain the finding that *CaRAPI* is not essential in *C.albicans*. The essential functions of ScRap1p may reside in other proteins in *C.albicans* which were not identified by homology searches. Recently Uemura *et al.* (2004) have shown that CaRap1p is able to bind *in vitro* to the RPG-box present in the *S.cerevisiae* *ENO1* promoter and suggests a possible involvement of CaRap1p in the regulation of glycolytic genes in *C.albicans* (Uemura *et al.*, 2004). It seems that some functions of ScRap1p are

retained in CaRap1p but there is a loss of the major functions of this protein. Therefore, CaRap1p does not seem to be useful as a target for the development of drugs against the pathogenic yeast *C.albicans*.

The most obvious phenotype of *rap1* deletion mutants was the formation of pseudohyphae under conditions that normally promote yeast form growth. However, although the percentage of pseudohyphal cells was 100-fold enhanced in $\Delta rap1$ mutants as compared with the wild type strains, the majority of the cells still grew as budding yeasts. In contrast, mutation of the gene *FKH2* causes the majority of the cells to grow as pseudohyphal cells in yeast form promoting growth medium (Bensen *et al.*, 2002). Mutants with deletions of other morphogenesis regulators, like *TUP1*, *NRG1*, or *RFG1*, grow also predominantly or exclusively in a filamentous form (Braun and Johnson, 1997; Braun *et al.*, 2001; Kadosh and Johnson, 2001; Khalaf and Zitomer, 2001; Murad *et al.*, 2001). It seems possible that the DNA binding domain of *CaRAP1* does play some role in the efficient repression of pseudohyphal growth under yeast growth conditions, but does not play a major role in morphogenesis.

5.2.2. Centromere Binding Factor 1

A previous study has demonstrated that *CBF1* from *C.albicans* complements the known defects of an *S.cerevisiae* $\Delta cbf1$ mutant, i.e. slow growth, methionine auxotrophy, and plasmid instability (Eck *et al.*, 2001). Since the roles of Cbf1p as a centromere binding protein and as a transcription factor in *S.cerevisiae* are separable (Foreman and Davis, 1993; McKenzie *et al.*, 1993), these results suggested that CaCbf1p has retained both activities and has the same functions in *C.albicans* as its counterpart in *S.cerevisiae*.

Analyses of the $\Delta cbf1$ mutants in this study demonstrated that deletion of *CaCBF1* in *C.albicans* indeed results in a slow growth phenotype and auxotrophy for sulphur amino acids, as in *S.cerevisiae*. Interestingly, the sequence TCACGTG is present within 350 bp from the start codon of all the genes of the sulphate assimilation pathway in *C.albicans*, *MET3*, *MET10*, *MET14*, *MET16*, and *MET25* (*MET15*) (<http://www-sequence.stanford.edu/group/candida/>). Therefore, as in *S.cerevisiae*, by binding to this sequence CaCbf1p may allow transcriptional activation of these genes also in *C.albicans*, explaining the inability of the $\Delta cbf1$ mutants to assimilate sulphate from the medium.

A possible role of *CaCBF1* in the fidelity of chromosome segregation in *C.albicans* was also investigated in this study. The morphological abnormalities observed in the $\Delta cbf1$ mutants indicated such a possibility, since many cells were unusually large and frequently contained large buds without nuclei. Generation of enlarged cells with large, anucleate buds has recently been described for conditional *C.albicans* mutants depleted for the essential centromere protein Cse4p and may be a consequence of a block in nuclear division due to inefficient chromosome segregation (Sanyal and Carbon, 2002). However, the *C.albicans* $\Delta cbf1$ mutants did not exhibit increased susceptibility to the microtubule destabilizing agent thiabendazole, a phenotype described for *S.cerevisiae* $\Delta cbf1$ mutants, which argued against a role of CaCbf1p in centromere function in *C.albicans*, and the aberrantly large cells might be due to some other defect of the $\Delta cbf1$ mutants.

Increased chromosome instability in *C.albicans* spindle assembly checkpoint mutants has recently been detected by measuring the frequency of mutant cells that are able to grow on sorbose (Bai *et al.*, 2002). Such sorbose utilizing mutants arise after loss of one of the chromosome 5 homologs (Janbon *et al.*, 1998), so that a higher frequency of sorbose utilizing cells can be taken as indication for increased chromosome instability. Since sorbose utilizing mutants appear as visible colonies after six and more days of growth on sorbose plates, this approach was found unreliable for the analysis of the *C.albicans* $\Delta cbf1$ mutants because of their slow growth phenotype. To directly observe an effect of *CaCBF1* deletion on chromosome stability, the *CARE-2* hybridization pattern of individual clones of mutants and control strains which were isolated after growth in rich medium for many generations was analyzed. Because *CARE-2* is present on most or even all *C.albicans* chromosomes, there was a high probability that loss of one homolog of any chromosome would result in an alteration in the hybridization pattern. The failure to detect increased chromosome instability by this approach provided some evidence that *CaCBF1* does not have a major role in centromere function in *C.albicans*. However, it was possible that chromosome loss occurs with increased frequency in $\Delta cbf1$ mutants but still remains a relatively rare event, since deletion of *CBF1* in *S.cerevisiae* increases chromosome loss only about 10-fold (Baker and Masison, 1990; Cai and Davis, 1990). In addition, if cells that have lost one or more chromosomes exhibit reduced fitness they might be overgrown by other cells, such that the clones with an unaltered genome were selected for analysis. To detect a possible moderate increase in chromosome loss in $\Delta cbf1$ mutants the frequency of loss of the *ADE2* containing chromosome 3 in heterozygous *ADE2/ade2* mutants was determined. Adenine-auxotrophic clones were detected at comparable frequencies in both wild-type and $\Delta cbf1$ mutants, and Southern

hybridization with an *ADE2*-specific probe demonstrated that all red *ade2* clones had lost the DNA fragment containing the intact *ADE2* allele. Some of these clones also exhibited a reduced hybridization signal with another, unlinked, chromosome 3-specific probe, indicating that they had lost one of the chromosome 3 homologs. In other clones the intensity of signals with chromosome 3-specific probes and the chromosome 1-specific *ACT1* probe were comparable, and they might have lost the *ADE2* gene by mitotic recombination. However, it is likely that these clones also arose by loss of the *ADE2* containing chromosome 3 homolog and subsequent reduplication of the remaining chromosome 3 by a second missegregation event, as has been described previously by Barton and Gull (1992). These authors reported that aneuploid *ade2* mutants, which were obtained after chromosome loss in an *ADE2/ade2* heterozygous strain, were unstable and frequently regained a second copy of the chromosome. The aneuploid *ade2* mutants formed smaller colonies than their parental strains, but returned to normal colony size after chromosome reduplication, and it was suggested that it was the loss of the respective chromosome, and not the adenine auxotrophy, that caused the reduced growth. Interestingly, the red *ade2* clones derived from $\Delta cbf1$ mutant and control strains also formed smaller colonies than their *ADE2/ade2* heterozygous parents (data not shown). After restreaking they formed larger colonies with high frequency, although these large red colonies were still slightly smaller than those of the prototrophic parental strains, indicating that adenine auxotrophy reduces the growth rate even on supplemented medium in the strain background used in this study. Therefore, *C.albicans* does not seem to tolerate aneuploidy for chromosome 3 well and chromosome loss may not always be detectable after passage of the *ade2* clones. The fact that all red *ade2* clones derived from the $\Delta cbf1$ mutant and control strains initially formed smaller colonies than those of the prototrophic parental strains suggests that they resulted from chromosome 3 loss instead of mitotic recombination, the frequency of which has been reported to be one order of magnitude lower (10^{-5} to 10^{-6}) (Fonzi and Irwin, 1993) than the frequency of chromosome loss observed in the present study (10^{-4} to 10^{-5}), although the former depends on the relative location of a marker with respect to the centromere. In the $\Delta cbf1$ background no growth difference between *ade2* clones and their *ADE2* parents was observed, indicating that the slow growth phenotype caused by deletion of *CaCBF1* masks any growth defect resulting from the loss of one chromosome 3 homolog or from adenine auxotrophy. The failure to detect an increased frequency of red *ade2* mutants in the $\Delta cbf1$ mutants suggests that CaCbf1p is not required for maintenance of this chromosome. Together with the results from the other experiments in this study it can be concluded that CaCbf1p does not have a major role in chromosome segregation in *C.albicans*.

The temperature sensitivity of $\Delta cbf1$ mutants apparently was not caused by a specific requirement of CaCbf1p at 42°C as opposed to lower temperature. At 42°C there is a certain degree of killing of *C.albicans* cells. Wild-type cells are nevertheless able to grow at this temperature since the rate of growth exceeds the rate of cell killing, at least in rich medium. This is not the case in the slowly growing $\Delta cbf1$ mutants, resulting in their failure to grow at higher temperature. An augmentation of the morphological defect of the $\Delta cbf1$ mutants by the higher temperature was also not detected, since the frequency of morphologically abnormal cells was similar at 30°C and 42°C. In addition, there was no increased chromosome 3 loss in the $\Delta cbf1$ mutants at 42°C, demonstrating that CaCbf1p is not required for chromosome stability at the non-permissive temperature.

Recently Sanyal *et al.* (2004) have characterized *C.albicans* centromeres and found that they are completely different from those of *S.cerevisiae* point centromeres and also from the regional centromeres found in *Schizosaccharomyces pombe* and higher eukaryotes. Moreover, centromeres of each chromosome of *C.albicans* contain a different and unique centromeric DNA sequence, a centromeric property previously unobserved in other organisms. None of these centromeric DNA sequences in any chromosome contain the binding sites for CaCbf1p, suggesting that CaCbf1p acts only as a transcription factor and have no role in centromere binding in *C.albicans*. Nevertheless, the results of the analysis of CaCbf1p in *C.albicans* demonstrate that a functional CaCbf1p is important for efficient growth of this pathogen and may therefore represent an attractive target for the development of antifungal drugs.

5.2.3. *YIL19*: An essential gene in *Candida albicans*

The Yil19p is essential for cell viability and is required for the proper processing of 18S rRNA in *S.cerevisiae*. This gene product has been found in *S.cerevisiae* to interact with a multifunctional protein, Krr1p, which is associated with the 90S pre-ribosomes (Karkusiewicz *et al.*, 2004) and also with Ebp2p, the yeast homolog of human Epstein-Barr virus nuclear antigen 1-binding protein 2, essential for the biogenesis of the 60S ribosomal subunit (Shirai *et al.*, 2004). This gene was selected as a putative target for antifungal drug development. In an attempt to analyse the function of this gene, mutants were constructed. Inability to delete both wild-type alleles of this gene suggested that this gene has an essential function in *C.albicans*, too. Moreover, when an ectopic *YIL19* allele was deleted by FLP-mediated gene

excision, the cells became nonviable. Microscopic examination of the mutants after deletion of this gene showed that the cells became enlarged in comparison to the wild type and control strains. However, it is unlikely that *YIL19* is required for cell elongation, because the mutants were able to form filaments in the presence of hyphal inducer, serum. Northern blot analysis suggested that *YIL19* is required for 18S rRNA maturation. Lower levels of mature 18S rRNA in the mutant strains was accompanied by the accumulation of intermediate RNA products and also the pre-rRNA transcript. The exact processing site of rRNA is still not known in *C.albicans* although it is well characterized in *S.cerevisiae*. The mutants accumulated RNAs with a size between that of the 18S and 25S rRNAs, possibly representing 23S and 20S rRNA. The accumulation of the 23S rRNA product indicates that rRNA was cleaved at the A₃ site without being cleaved at A₀, A₁, and A₂ sites (Venema and Tollervey, 1999; Lee and Baserga, 1999). The slightly increased amount of 35S rRNA in the mutant cells also confirms the inhibition of cleavage at site A₀. An exact knowledge of rRNA maturation steps in *C.albicans* and further characterization of the Yil19p will provide detailed information about how this protein works in the processing of 18S rRNA. The involvement of this gene in rRNA maturation provides a possible explanation for the increased cell size of the mutants. Systematic determination of cell size distributions for the complete set of ~6000 *S.cerevisiae* gene deletion strains have identified a complex network that governs critical cell size, and ribosome biogenesis has been found to be intimately linked with cell size (Jorgensen *et al.*, 2002). Since, *YIL19* is essential for viability in *C.albicans* and the observation that the presence of Yil19p is limited to ascomycetes and not present in higher eukaryotes, it might be a good target for the development of antifungal drugs.

Appendix

A.1. Construction of plasmids

A.1.1. Plasmids used to study ammonium transporters

A.1.1.1. Plasmids used for *CaMEP1* and *CaMEP2* deletion

pMEP1M1 (8.6 kb): 3'-fragment of *CaMEP1* was amplified from the chromosomal DNA of CAI4 using the primers MEP13 (+ 1569 to + 1597 in the + strand) and MEP14 (+ 2137 to + 2112 in the – strand). The *Bgl*II and *Sac*I sites were introduced at position + 1577 in the primer MEP13 and at position + 2126 in the primer MEP14, respectively. The MEP13 primer also contains a *Pst*I site at position + 1584. The PCR product was then digested with *Bgl*II-*Sac*I and ligated into the *Bgl*II-*Sac*I digested plasmid pYMR211M2 (Bader T, unpublished data), to replace the 3'-fragment of *YMR211* by 3'-*CaMEP1*.

pMEP1M2 (8.2 kb): 5'-fragment of *CaMEP1* was amplified from the chromosomal DNA of CAI4 using the primers MEP11 (- 620 to - 594 in the + strand) and MEP12 (+ 13 to - 13 in the – strand). The *Kpn*I and *Xho*I sites were introduced at position - 608 in the primer MEP11 and at position - 3 in the primer MEP12, respectively. The PCR product was then digested with *Kpn*I-*Xho*I and ligated into the *Kpn*I-*Xho*I digested plasmid pMEP1M1. The resulting plasmid thus contains the *URA3* flipper flanked by the 5' and 3' of *CaMEP1*. The 5.3 kb *Kpn*I-*Sac*I digested fragment [5'*MEP1-FRT-SAP2P-caFLP-ACT1T-URA3-FRT-3'MEP1*] from this plasmid was used to generate the *CaMEP1* deletion strains.

pMEP1M3 (6.2 kb): 5'-fragment of *CaMEP1* was amplified from the chromosomal DNA of CAI4 using the primers MEP15 (- 647 to - 622 in the + strand) and MEP17 (+ 23 to - 4 in the – strand). The *Xho*I and *Bgl*II sites were introduced at position - 640 in the MEP15 and at position + 9 in the primer MEP17, respectively. The PCR product was then digested with *Xho*I-*Bgl*II and ligated into the *Xho*I-*Bgl*II digested plasmid pSAP2-1K (Staib *et al.*, 2002).

pMEP1M4 (5.8 kb): 3'-fragment of *CaMEP1* was amplified from the chromosomal DNA of CAI4 using the primers MEP13 (+ 1569 to + 1597 in the + strand) and MEP14 (+ 2137 to + 2112 in the – strand). The *Pst*I and *Sac*I sites were introduced at position + 1584 in the primer MEP13 and at position + 2126 in the primer MEP14, respectively. The MEP13 primer also contains a *Bgl*II site at position + 1577. The PCR product was then digested with *Pst*I-*Sac*I and ligated into the *Pst*I-*Sac*I digested plasmid pMEP1M3. The 2.9 kb *Kpn*I-*Sac*I digested fragment [5'*MEP1-ACT1T-URA3-3'MEP1*] from this plasmid was used to generate the uridine-prototrophic *CaMEP1* deletion strains.

pMEP2M1 (8.3 kb): 5'-fragment of *CaMEP2* was amplified from the chromosomal DNA of SC5314 using the primers MEP3 (- 619 to - 586 in the + strand) and MEP4 (+ 47 to + 19 in the – strand). The *Kpn*I and *Xho*I sites

were introduced at position - 608 in the primer MEP3 and at position + 32 in the primer MEP4, respectively. The PCR product was then digested with *KpnI-XhoI* and ligated into the *KpnI-XhoI* digested plasmid pCBF1M1.

pMEP2M2 (8.1 kb): 3'-fragment of *CaMEP2* was amplified from the chromosomal DNA of SC5314 using the primers MEP5 (+ 1345 to + 1372 in the + strand) and MEP6 (+ 1779 to + 1751 in the - strand). The *BglII* and *SacI* sites were introduced at position + 1354 in the primer MEP5 and at position + 1769 in the primer MEP6, respectively. The PCR product was then digested with *BglII-SacI* and ligated into the *BglII-SacI* digested plasmid pMEP2M1. The resulting plasmid thus contains the *URA3* flipper flanked by 5' and 3' of *CaMEP2*. The 5.2 kb *KpnI-SacI* digested fragment [5'*MEP2-FRT-SAP2P-caFLP-ACT1T-URA3-FRT-3'MEP2*] from this plasmid was used to generate the *CaMEP2* deletion strains.

pMEP2M3 (5.6 kb): 3'-fragment of *CaMEP2* was amplified from the chromosomal DNA of SC5314 using the primers MEP8 (+ 1345 to + 1372 in the + strand) and MEP6 (+ 1779 to + 1751 in the - strand). The *PstI* and *SacI* sites were introduced at position + 1362 in the primer MEP8 and at position + 1769 in the primer MEP6, respectively. The PCR product was then digested with *PstI-SacI* and ligated into the *PstI-SacI* digested plasmid pCBF1M4.

pMEP2M4 (5.7 kb): 5'-fragment of *CaMEP2* was amplified from the chromosomal DNA of SC5314 using the primers MEP3 (- 619 to - 586 in the + strand) and MEP7 (+ 47 to + 19 in the - strand). The *KpnI* and *BglII* sites were introduced at position - 608 in the MEP3 and at position + 28 in the primer MEP7, respectively. The PCR product was then digested with *KpnI-BglII* and ligated into the *KpnI-BglII* digested plasmid pMEP2M3. The 2.8 kb *KpnI-SacI* digested fragment [5'*MEP2-ACT1T-URA3-3'MEP2*] from this plasmid was used to generate the uridine-prototrophic *CaMEP2* deletion strains.

A.1.1.2. Plasmids containing *lacZ* reporter gene fusions

pLACZ2 (6.0 kb): A fragment containing the N-terminal region of the *Streptococcus thermophilus lacZ* ORF was amplified from the plasmid pAU36 (Uhl and Johnson, 2001) with the primers LACZ1 (+ 1 to + 22 in the + strand) and LACZ2 (+ 1230 to + 1209 in the - strand). A *XhoI* site was introduced in the LACZ1 primer. The PCR product was then digested at *XhoI* and at internal *ClaI* sites (position + 1196) and ligated together with a 2.1 kb *ClaI-BamHI* fragment from the plasmid pAU36 containing the remainder of the *lacZ* ORF into the *XhoI-BamHI* digested plasmid pBluescript (Stratagene, Heidelberg, Germany).

pLACZ3 (6.4 kb): A fragment containing the *ACT1* terminator region (*ACT1T*) was amplified using the primers ACT16 (+ 1784 to + 1811 in the + strand) and ACT19 (+ 2180 to + 2156 in the - strand) from the plasmid pSAP2-7 (Staib *et al.*, 2000). The *BglII* and *SacII* sites were introduced into the ACT16 and ACT19, respectively. The PCR product was then digested with *BglII-SacII* and ligated into the *BamHI-SacII* digested plasmid pLACZ2.

pLACZ4 (7.4 kb): A 1.1 kb *ACT1* promoter fragment was PCR amplified using the primers UNI (5'-GTAAAACGACGGCCAGT-3') and ACT20 (- 10 to - 35 in the - strand) from the plasmid pGFP31 (Morschhäuser *et al.*, 1998). The ACT20 primer contains a *SaI* site. The *Bam*HI-*SaI* digested PCR product was ligated together with a 3.5 kb *Xho*I-*Sac*II fragment from the plasmid pLACZ3 containing *lacZ*-*ACT1T*, into the *Bam*HI-*Sac*II digested plasmid pGFP31 (Morschhäuser *et al.*, 1998). The 4.5 kb *Bam*HI-*Sac*II fragment [*ACT1P-lacZ-ACT1T*] from this plasmid was used to generate the strain CALACZ1.

pMEP1LACZ2 (8.9 kb): The 2.9 kb *Kpn*I-*Bam*HI fragment containing *MEP2P-lacZ* from the plasmid pMEP2LACZ1 was ligated into the *Kpn*I-*Bgl*II digested plasmid pMEP1M4.

pMEP1LACZ3 (8.9 kb): The *Kpn*I-*Xho*I fragment containing the *CaMEP1* promoter from the plasmid pMEP1M2 was ligated into the *Kpn*I-*Xho*I digested plasmid pMEP1LACZ2 and generated a plasmid in which the *lacZ* gene is under the control of *CaMEP1* promoter. A 6.0 kb *Kpn*I-*Sac*I fragment [*MEP1P-lacZ-ACT1T-URA3-3'MEP1*] from this plasmid was used to generate the strains CLACZ1A and CLACZ1B.

pMEP2LACZ1 (6.6 kb): A fragment containing the *CaMEP2* promoter was amplified with the primers MEP3 (- 619 to - 586 in the + strand) and MEP24 (+ 8 to - 22 in the - strand) from the plasmid pMEP2K1. The *Kpn*I and *Xho*I sites were introduced at position - 608 in the primer MEP3 and at position - 5 in the primer MEP24. The PCR product was then digested with *Kpn*I-*Xho*I and ligated into the *Kpn*I-*Xho*I digested plasmid pLACZ2.

pMEP2LACZ2 (8.8 kb): The 3.7 kb *Kpn*I-*Bam*HI fragment containing *MEP2P-lacZ* from the plasmid pMEP2LACZ1 was ligated into the *Kpn*I-*Bgl*II digested plasmid pMEP2M4 generating a plasmid in which the *lacZ* gene is under the control of *CaMEP2* promoter. A 5.9 kb *Kpn*I-*Sac*I fragment [*MEP2P-lacZ-ACT1T-URA3-3'MEP2*] from this plasmid was used to generate the strains CLACZ2A and CLACZ2B.

A.1.1.3. Plasmids containing *CaMEP1* and *CaMEP2* under different promoters

pMEP1K1 (7.5 kb): A fragment containing the *CaMEP1* promoter and coding region was amplified from the chromosomal DNA of CA14 using the primers MEP16 (+ 1629 to + 1604 in the - strand) and MEP18 (- 618 to - 592 in the + strand). The *Bgl*II and *Xho*I sites were introduced at position + 1616 in the primer MEP16 and at position - 608 in the primer MEP18, respectively. The PCR product was then digested with *Xho*I-*Bgl*II and ligated into the *Xho*I-*Bgl*II digested plasmid pMEP1M4. The resulting plasmid contains the full length *CaMEP1* gene. A 4.6 kb *Xho*I-*Sac*I fragment [*MEP1P-MEP1-ACT1T-URA3-3'MEP1*] from this plasmid was used to reintroduce *CaMEP1* into the Δ *mep1* mutants and Δ *mep1* Δ *mep2* double mutants to generate the strains MEP1MK1A, MEP1MK1B, MEP12MK1A, and MEP12MK1B.

pMEP1K2 (7.3 kb): A fragment containing the *CaMEP1* coding region was amplified from the plasmid pMEP1K1 using the primers MEP16 (+ 1629 to + 1604 in the - strand) and MEP27 (- 14 to + 16 in the + strand). The *Bgl*II and *Xho*I sites were introduced at position + 1616 in the primer MEP16 and at position - 7 in the primer MEP27, respectively. The PCR product was then digested with *Xho*I and *Apa*I (located at position + 519)

and ligated together with the 2.5 kb *ApaI-NdeI* fragment [3'*MEP1-ACT1T-5'URA3*] from plasmid pMEP1K1 into the *XhoI-NdeI* digested plasmid pMEP2LACZ2. The resulting plasmid thus contains the full length *CaMEP1* gene under the control of *CaMEP2* promoter. A 4.4 kb *SacI*-partial *KpnI* fragment [*MEP2P-MEP1-ACT1T-URA3-3'MEP2*] from this plasmid was used to generate the strains MEP12MK3A, and MEP12MK3B.

pMEP1E2 (7.8 kb): The 2.7 kb *XhoI-EcoRI* fragment [*MEP1-ACT1T-5'URA3*] from the plasmid pMEP1K2 was ligated into the *SalI-EcoRI* digested plasmid pADH1G2 (Kusch *et al.*, 2004). The resulting plasmid contains the full length *CaMEP1* gene under the control of *ADH1* promoter. A 4.9 kb *XhoI-SacI* fragment [*ADH1P-MEP1-ACT1T-URA3-3'ADH1*] from this plasmid was used to generate the strains MEP12ME1A, and MEP12ME1B.

pMEP2K1 (7.15 kb): A fragment containing the *CaMEP2* promoter and coding region was amplified from the chromosomal DNA of SC5314 using the primers MEP3 (- 619 to - 586 in the + strand) and MEP9 (+ 1522 to + 1494 in the - strand). The *BglII* and *KpnI* sites were introduced at position + 1507 in the primer MEP9 and at position - 608 in the primer MEP3, respectively. The PCR product was then digested with *KpnI-BglII* and ligated into the *KpnI-BglII* digested plasmid pMEP2M3. The resulting plasmid contains the full length *CaMEP2* gene. A 4.25 kb *KpnI-SacI* fragment [*MEP2P-MEP2-ACT1T-URA3-3'MEP2*] from this plasmid was used to reintroduce *CaMEP2* into the $\Delta mep2$ mutants and $\Delta mep1 \Delta mep2$ double mutants to generate the strains MEP2MK1A, MEP2MK1B, MEP12MK2A, and MEP12MK2B. This 4.25 kb *KpnI-SacI* fragment was also transformed into CAI4 and different signaling mutants to generate the control strains (see section 3.3).

pMEP2K2 (7.3 kb): A fragment containing the *CaMEP2* coding region was amplified from the plasmid pMEP2K1 using the primers MEP21 (- 13 to + 20 in the + strand) and MEP9 (+ 1522 to + 1494 in the - strand). The *BglII* and *XhoI* sites were introduced at position + 1507 in the primer MEP9 and at position - 7 in the primer MEP21, respectively. The 0.4 kb *XhoI-EcoRV* fragment containing the N-terminus of CaMep2p from the PCR product was ligated together with 2.25 kb *EcoRV-EcoRI* fragment [3'*MEP2-ACT1T-5'URA3*] from the plasmid pMEP2K1 into the *XhoI-EcoRI* digested pMEP1LACZ3. The resulting plasmid thus contains the full length *CaMEP2* gene under the control of *CaMEP1* promoter. A 4.4 kb *KpnI-SacI* fragment [*MEP1P-MEP2-ACT1T-URA3-3'MEP1*] from this plasmid was used to generate the strains MEP12MK4A, and MEP12MK4B.

pMEP2E2 (7.7 kb): A fragment containing the *CaMEP2* coding region was amplified from the plasmid pMEP2K1 using the primers MEP21 (- 13 to + 20 in the + strand) and MEP9 (+ 1522 to + 1494 in the - strand). The *BglII* and *XhoI* sites were introduced at position + 1507 in MEP9 and at position - 7 in primer MEP21, respectively. The PCR product was then digested with *XhoI-BglII* and ligated together with the 1.0 kb *BamHI-EcoRI* fragment [*ACT1T-5'URA3*] from the plasmid pYPR127E2 (Kusch *et al.*, 2004) into the *SalI-EcoRI* digested pADH1G2 (Kusch *et al.*, 2004). The resulting plasmid contains the full length *CaMEP2* gene under the control of *ADH1* promoter. A 4.8 kb *KpnI-SacI* fragment [*ADH1P-MEP2-ACT1T-URA3-3'ADH1*] from this plasmid was used to generate the strains MEP12ME2A, and MEP12ME2B.

A.1.1.4. Plasmids containing the GFP-tagged *CaMEP1* and *CaMEP2* genes

pMEP1G1 (8.2 kb): A fragment containing the *CaMEP1* coding region was amplified from the plasmid pMEP1K1 using the primers MEP37 (+ 1615 to + 1587 in the - strand) and MEP27 (- 14 to + 16 in the + strand). The *Bam*HI site was introduced in the primer MEP37 at position + 1603 replacing the *CaMEP1* stop codon and *Xho*I site at position - 7 in the primer MEP27. The PCR product was then digested with *Bam*HI and *Sal*I (located at position + 957) and ligated together with the 1.7 kb *Bam*HI-*Eco*RI fragment [*GFP-ACT1T-5'URA3*] from the plasmid pMEP2G2 into the *Sal*I-*Eco*RI digested plasmid pMEP1K1. The resulting plasmid contains the full length *CaMEP1-GFP* fusion under the control of *CaMEP1* promoter. This fusion results into a CaMep1-GFP fusion protein with two amino acids (Gly-Ser) in between the two proteins. A 5.3 kb *Xho*I-*Sac*I fragment [*MEP1P-MEP1-GFP-ACT1T-URA3-3'MEP1*] from this plasmid was used to generate the strains CMEP1GA, CMEP1GB, MEP12MG1A, and MEP12MG1B.

pMEP1G2 (8.0 kb): The 2.8 kb *Apa*I-*Eco*RI fragment [*3'MEP1-GFP-ACT1T-5'URA3*] from the plasmid pMEP1G1 was ligated into the *Apa*I-*Eco*RI digested plasmid pMEP1K2. The resulting plasmid thus contains the *CaMEP1-GFP* fusion under the control of the *CaMEP2* promoter. A 5.1 kb *Sac*I-partial *Kpn*I fragment [*MEP2P-MEP1-GFP-ACT1T-URA3-3'MEP2*] from this plasmid was used to generate the strains CMEP1G2A, CMEP1G2B, MEP12MG3A, and MEP12MG3B.

pMEP1G3 (8.5 kb): The 2.8 kb *Clal*-*Eco*RI fragment [*3'MEP1-GFP-ACT1T-5'URA3*] from the plasmid pMEP1G1 was ligated into the *Clal*-*Eco*RI digested plasmid pMEP1E2. The resulting plasmid thus contains the *CaMEP1-GFP* fusion under the control of *ADH1* promoter. A 5.5 kb *Xba*I-*Sac*I fragment [*ADH1P-MEP1-GFP-ACT1T-URA3-3'ADH1*] from this plasmid was used to generate the strains CMEP1EGA, CMEP1EGB, MEP12MEG1A, and MEP12MEG1B.

pMEP2G1 (7.8 kb): A fragment containing the *CaMEP2* coding region was amplified from the plasmid pMEP2K1 using the primers MEP21 (- 13 to + 20 in the + strand) and MEP32 (+ 1454 to + 1426 in the - strand). The *Bam*HI site was introduced in the primer MEP32 at position + 1441 replacing the *CaMEP2* stop codon and *Xho*I site at position - 7 in the primer MEP21. The PCR product was then digested at an internal *Sal*I site and at the *Bam*HI site introduced in the MEP32 primer and ligated together with 1.5 kb *Kpn*I-*Sal*I fragment from the plasmid pMEP2K1 into the *Kpn*I-*Bam*HI digested pOP4G1 (Park Yang-Nim, unpublished data). The resulting plasmid thus contains the full length *CaMEP2-GFP* fusion. This fusion results into a CaMep2-GFP fusion protein with two amino acids (Gly-Ser) in between the two proteins.

pMEP2G2 (7.8 kb): The 1.3 kb *Eco*RI-*Sac*I fragment containing *3'URA3-3'MEP2* from the plasmid pMEP2K1 was ligated into the *Eco*RI-*Sac*I digested plasmid pMEP2G1. A 4.9 kb *Kpn*I-*Sac*I fragment [*MEP2P-MEP2-GFP-ACT1T-URA3-3'MEP2*] from this plasmid was used to generate the strains CMEP2GA, CMEP2GB, MEP12MG2A, and MEP12MG2B.

pMEP2G4 (8.4 kb): The 1.3 kb *Bam*HI-*Pst*I fragment containing *ADH1P-5'MEP2* from the plasmid pMEP2E2 was ligated along with the 2.1 kb *Pst*I-*Eco*RI fragment containing *3'MEP2-GFP-ACT1T-5'URA3* from the

plasmid pMEP2G1 into the *Bam*HI-*Eco*RI digested plasmid pMEP2E2. The resulting plasmid thus contains the *CaMEP2-GFP* fusion under the control of *ADHI* promoter. A 5.5 kb *Xba*I-*Sac*I fragment [*ADHIP-MEP2-GFP-ACTIT-URA3-3'ADHI*] from this plasmid was used to generate the strains CMEP2EGA, CMEP2EGB, MEP12MEG2A, and MEP12MEG2B.

pMEP2G5 (8.0 kb): The 2.9 kb *Eco*RV-*Eco*RI fragment containing 3'*MEP2-GFP-ACTIT-URA3* from the plasmid pMEP2G4 was ligated into the *Eco*RV-*Eco*RI digested plasmid pMEP2K2. The resulting plasmid thus contains the *CaMEP2-GFP* fusion under the control of *CaMEP1* promoter. A 5.1 kb *Kpn*I-*Sac*I fragment [*MEP1P-MEP2-GFP-ACTIT-URA3-3'MEP1*] from this plasmid was used to generate the strains CMEP2G1A, CMEP2G1B, MEP12MG5A, and MEP12MG5B.

A.1.1.5. Plasmids containing the truncation of *CaMEP1* and *CaMEP2* genes

pMEP1ΔC1 (6.8 kb): A fragment containing the *CaMEP1* promoter and coding region was amplified from the plasmid pMEP1K1 using the primers MEP20 (+ 1224 to + 1193 in the - strand) which introduces stop codon (+ 1212 to + 1215) behind Ile404 and MEP18 (- 618 to - 592 in the + strand). The *Bgl*II and *Xho*I sites were introduced at position + 1219 in the primer MEP20 and at position - 608 in the primer MEP18, respectively. The PCR product was then digested with *Xho*I-*Bgl*II and ligated into the *Xho*I-*Bgl*II digested plasmid pMEP1K1. The resulting plasmid contains the C-terminally truncated *CaMEP1ΔC⁴⁰⁴* gene. A 3.9 kb *Kpn*I-*Sac*I fragment [*MEP1P-MEP1ΔC⁴⁰⁴-ACTIT-URA3-3'MEP1*] from this plasmid was used to generate the strains MEP12MK1AΔC1, and MEP12MK1BAC1.

pMEP1ΔC2 (6.9 kb): A fragment containing the *CaMEP1* promoter and coding region was amplified from the plasmid pMEP1K1 using the primers MEP23 (+ 1327 to + 1294 in the - strand) which introduces stop codon (+ 1315 to + 1317) behind Val438 and MEP18 (- 618 to - 592 in the + strand). The *Bgl*II and *Xho*I sites were introduced at position + 1320 in the primer MEP23 and at position - 608 in the primer MEP18, respectively. The PCR product was then digested with *Xho*I-*Bgl*II and ligated into the *Xho*I-*Bgl*II digested plasmid pMEP1K1. The resulting plasmid contains the C-terminally truncated *CaMEP1ΔC⁴³⁸* gene. A 4.0 kb *Kpn*I-*Sac*I fragment [*MEP1P-MEP1ΔC⁴³⁸-ACTIT-URA3-3'MEP1*] from this plasmid was used to generate the strains MEP12MK1AΔC2, and MEP12MK1BAC2.

pMEP2ΔC1 (6.8 kb): A fragment containing the *CaMEP2* promoter and coding region was amplified from the plasmid pMEP2K1 using the primers MEP19 (+ 1232 to + 1199 in the - strand) which introduces stop codon (+ 1219 to + 1221) behind Met406 and MEP3 (- 619 to - 586 in the + strand). The *Bgl*II and *Kpn*I sites were introduced at position + 1226 in the primer MEP19 and at position - 608 in the primer MEP3, respectively. The PCR product was then digested with *Kpn*I-*Bgl*II and ligated into the *Kpn*I-*Bgl*II digested plasmid pMEP2K1. The resulting plasmid contains the C-terminally truncated *CaMEP2ΔC⁴⁰⁶* gene. A 3.9 kb *Kpn*I-*Sac*I fragment [*MEP2P-MEP2ΔC⁴⁰⁶-ACTIT-URA3-3'MEP2*] from this plasmid was used to generate the strains MEP12MK2AΔC1, and MEP12MK2BAC1.

pMEP2ΔC2 (6.8 kb): A fragment containing the *CaMEP2* promoter and coding region was amplified from the plasmid pMEP2K1 using the primers MEP22 (+ 1335 to + 1301 in the - strand) which introduces stop codon (+ 1321 to + 1323) behind Asp440 and MEP3 (- 619 to - 586 in the + strand). The *Bgl*III and *Kpn*I sites were introduced at position + 1327 in the primer MEP22 and at position - 608 in the primer MEP3, respectively. The PCR product was then digested with *Kpn*I-*Bgl*III and ligated into the *Kpn*I-*Bgl*III digested plasmid pMEP2K1. The resulting plasmid contains the C-terminally truncated *CaMEP2ΔC⁴⁴⁰* gene. A 4.0 kb *Kpn*I-*Sac*I fragment [*MEP2P-MEP2ΔC⁴⁴⁰-ACTIT-URA3-3'MEP2*] from this plasmid was used to generate the strains MEP12MK2AΔC2, and MEP12MK2BAC2. This 4.0 kb *Kpn*I-*Sac*I fragment was also transformed into CAI4 and different signalling mutants to replace one of the wild type *CAMEP2* allele by the truncated allele (see section 3.3).

pMEP2ΔC3 (6.9 kb): A fragment containing the *CaMEP2* promoter and coding region was amplified from the plasmid pMEP2K1 using the primers MEP25 (+ 1287 to + 1257 in the - strand) which introduces stop codon (+ 1270 to + 1272) behind Leu423 and MEP3 (- 619 to - 586 in the + strand). The *Bgl*III and *Kpn*I sites were introduced at position + 1280 in the primer MEP25 and at position - 608 in the primer MEP3, respectively. The PCR product was then digested with *Kpn*I-*Bgl*III and ligated into the *Kpn*I-*Bgl*III digested plasmid pMEP2K1. The resulting plasmid contains the C-terminally truncated *CaMEP2ΔC⁴²³* gene. A 4.0 kb *Kpn*I-*Sac*I fragment [*MEP2P-MEP2ΔC⁴²³-ACTIT-URA3-3'MEP2*] from this plasmid was used to generate the strains MEP12MK2AΔC3, and MEP12MK2BAC3.

pMEP2ΔC4 (6.8 kb): A fragment containing the *CaMEP2* promoter and coding region was amplified from the plasmid pMEP2K1 using the primers MEP26 (+ 1253 to + 1227 in the - strand) which introduces stop codon (+ 1240 to + 1242) behind Arg413 and MEP3 (- 619 to - 586 in the + strand). The *Bgl*III and *Kpn*I sites were introduced at position + 1247 in the primer MEP26 and at position - 608 in the primer MEP3, respectively. The PCR product was then digested with *Kpn*I-*Bgl*III and ligated into the *Kpn*I-*Bgl*III digested plasmid pMEP2K1. The resulting plasmid contains the C-terminally truncated *CaMEP2ΔC⁴¹³* gene. A 3.9 kb *Kpn*I-*Sac*I fragment [*MEP2P-MEP2ΔC⁴¹³-ACTIT-URA3-3'MEP2*] from this plasmid was used to generate the strains MEP12MK2AΔC4, and MEP12MK2BAC4.

A.1.1.6. Plasmids containing the *MEP* hybrids

pMEP12H2 (7.4 kb): The C-terminal part of *CaMEP2* was amplified using the primers MEP35 and MEP9 (+ 1522 to + 1494 in the - strand, with an introduced *Bgl*III site at position + 1507). Primer MEP35 consists of *CaMEP1* sequences from positions + 1233 to + 1248 including the *Cla*I site at position + 1241 followed by the *CaMEP2* sequences from positions + 1255 to + 1276. The PCR product was digested with *Cla*I-*Bgl*III and ligated into the *Cla*I-*Bgl*III digested plasmid pMEP1K1. This results into a plasmid containing the *CaMEP1-CaMEP2* hybrid gene expressed from the *CaMEP1* promoter and encodes a protein in which the first 416 amino acids of CaMep1p are fused to the last 62 amino acids of CaMep2p (amino acids 419-480). A 4.5 kb *Kpn*I-*Sac*I fragment [*MEP1P-MEP1¹⁻⁴¹⁶-MEP2⁴¹⁹⁻⁴⁸⁰-ACTIT-URA3-3'MEP1*] from this plasmid was used to generate the strains MEP12MK12AH2A, and MEP12MK12H2B.

pMEP12H3 (7.1 kb): The 1.6 kb *XbaI*-*BglII* fragment containing the *CaMEP1*-*CaMEP2* hybrid gene from the plasmid pMEP12H2 was ligated into the *XbaI*-*BglII* digested plasmid pMEP1K2. This results into a plasmid containing the *CaMEP1*-*CaMEP2* hybrid gene expressed from the *CaMEP2* promoter and encodes a protein in which the first 416 amino acids of CaMep1p are fused to the last 62 amino acids of CaMep2p (amino acids 419-480). A 4.2 kb *KpnI*-*SacI* fragment [*MEP2P-MEP1*¹⁻⁴¹⁶-*MEP2*⁴¹⁹⁻⁴⁸⁰-*ACT1T-URA3-3'MEP2*] from this plasmid was used to generate the strains MEP12MK12H3A, and MEP12MK12H3B.

pMEP12H4 (7.0 kb): A fragment containing the *CaMEP1*-*CaMEP2* hybrid gene was amplified using the primers MEP27 (- 14 to + 16 in the + strand of *CaMEP1* sequence) and MEP22 (+ 1335 to + 1301 in the - strand of *CaMEP2* sequence) which introduces stop codon (+ 1321 to + 1323) behind Asp440. A *BglII* site was introduced at position + 1327 in MEP22. The PCR product was then digested with *SalI* (located at position + 957 in *CaMEP1* sequence) and *BglII* and ligated together with the 2.3 kb *BglII*-*SacI* fragment containing [*ACT1T-URA3-3'MEP2*] into the *SalI*-*SacI* digested plasmid pMEP12H3. This resulted into a plasmid containing the *CaMEP1*-*CaMEP2* hybrid gene expressed from the *CaMEP2* promoter and encodes a protein in which the first 416 amino acids of CaMep1p are fused to the amino acids 419-440 of CaMep2p. A 4.1 kb *KpnI*-*SacI* fragment [*MEP2P-MEP1*¹⁻⁴¹⁶-*MEP2*⁴¹⁹⁻⁴⁴⁰-*ACT1T-URA3-3'MEP2*] from this plasmid was used to generate the strains MEP12MK12H4A, and MEP12MK12H4B.

pMEP21H2 (7.2 kb): A fragment containing the *CaMEP2* promoter and a portion of the coding region from the N-terminal part of *CaMEP2* was amplified from the plasmid pMEP2K1 using the primers MEP3 (- 619 to - 586 in the + strand) and MEP33p (+ 1254 to + 1234 in the - strand). The *KpnI* site was introduced at position - 608 in the primer MEP3. A C-terminal part of *CaMEP1* was also amplified using the primers MEP34p (+ 1249 to + 1270 in the + strand) and MEP16 (+ 1629 to + 1604 in the - strand). The *BglII* site was introduced at position + 1616 behind the stop codon in the primer MEP16. The MEP33p and MEP34p primers are phosphorylated at their 5' ends. The *CaMEP2* and *CaMEP1* fragments were then digested at the *KpnI* and *BglII* sites, respectively, fused at their blunt ends and ligated into the *KpnI*-*BglII* digested plasmid pMEP1K2. The resulting plasmid contains the *CaMEP2*-*CaMEP1* hybrid gene expressed from the *CaMEP2* promoter and encodes a protein in which the first 418 amino acids of CaMep2p are fused to the last 118 amino acids of CaMep1p (amino acids 417 to 534). A 4.3 kb *SacI*-partial *KpnI* digested fragment [*MEP2P-MEP2*¹⁻⁴¹⁸-*MEP1*⁴¹⁷⁻⁵³⁴-*ACT1T-URA3-3'MEP2*] from this plasmid was used to generate the strains MEP12MK21H2A and MEP12MK12H2B.

A.1.1.7. Plasmids containing the dominant active *RAS1*^{G13V} and *GPA2*^{Q354L} alleles

pRAS1E1 (6.9 kb): A fragment containing the *ACT1* promoter was amplified from the genomic DNA of SC5314 using the primers ACT31 (- 501 to - 475 in the + strand) and ACT20 (- 10 to - 35 in the - strand). The ACT31 and ACT20 primers contain *XbaI* and *SalI* sites, respectively. The *RAS1* ORF was then amplified from the genomic DNA of SC5314 with the primers RAS1 (- 12 to + 47 in the + strand) and RAS2 (+ 886 to + 856 in the - strand). The RAS1 primer contains a *SalI* site at position - 7 (in front of the start codon) and substitutes a valine specific GTT codon for the original glycine specific GGT codon at positions + 37 to + 39, whereas the RAS2 primer introduces a *BglII* site at position + 876, behind the stop codon. The *ACT1* upstream fragment and

the *RAS1*^{G13V} fragments were digested with *XbaI-SalI* and *SalI-BglII*, respectively, and were ligated together into the *XbaI-BglII* digested plasmid pSAP2-1K (Staib *et al.*, 2002). The resulting plasmid thus contains the dominant active *RAS1*^{G13V} under the control of *ACT1* promoter. A 4.0 kb fragment [*ACT1P-RAS1*^{G13V}-*ACT1T-URA3-3'ACT1*] from this plasmid was used to generate the strains RAS1E1A, RAS1E1B, MEP2MRAS1E1A and MEP2MRAS1E1B.

pGPA2 (6.9 kb): A fragment containing the N-terminal part of *GPA2* ORF was amplified using the primer GPA1 (- 12 to + 18 in the + strand) which introduces *SalI* site in front of the start codon (at position - 7) and the 5'-phosphorylated primer GPA2 (+ 1056 to + 1027 in the - strand), from the genomic DNA of CAI4. The remainder of *GPA2* ORF was amplified with the 5'-phosphorylated primer GPA3 (+ 1057 to + 1086 in the + strand) which substitutes the leucine specific TTA codon for the original glutamine specific CAA codon at positions + 1060 to + 1062, and primer GPA4 (+ 1518 to + 1584 in the - strand) which introduces a *BglII* site at position + 1508, from the genomic DNA of CAI4. The PCR products were digested with *SalI* and *BglII*, respectively, fused at their blunt ends and ligated into the *SalI-BglII* digested pCBF1M4.

pGPA2E1 (7.5 kb): The 1.5 kb *SalI-BglII* fragment from pGPA2 and the 1.0 kb *BglII-EcoRI* digested fragment containing *ACT1T-5'URA3* from the plasmid pRAS1E1 were ligated together into the *SalI-EcoRI* digested pRAS1E1. The resulting plasmid thus contains the dominant active *GPA2*^{Q354L} under the control of *ACT1* promoter. A 4.6 kb fragment [*ACT1P-GPA2*^{Q354L}-*ACT1T-URA3-3'ACT1*] from this plasmid was used to generate the strains GPA2E1A, GPA2E1B, MEP2MGPA2E1A and MEP2MGPA2E1B.

A.1.2. Plasmids used to study *C.albicans* Repressor/activator protein 1 (CaRap1p)

pRAP1M1 (8.7 kb): 3'-fragment of *CaRAP1* was amplified from the chromosomal DNA of SC5314 using the primers RAP3 (+ 1251 to + 1277 in the + strand) and RAP7 (+ 1890 to + 1861 in the - strand). The *BamHI* and *SacII* sites were introduced at position + 1260 in the primer RAP3 and at position + 1883 in the primer RAP7, respectively. The PCR product was then digested with *BamHI-SacII* and ligated into the *BglII-SacII* digested plasmid pYMR211M2 (Bader T, unpublished data), to replace the 3'-fragment of *YMR211* by 3'-*CaRAP1*.

pRAP1M2 (8.2 kb): 5'-fragment of *CaRAP1* was amplified from the chromosomal DNA of SC5314 using the primers RAP5 (- 463 to - 436 in the + strand) and RAP6 (+ 37 to + 10 in the - strand). The *KpnI* and *XhoI* sites were introduced at position - 448 in the primer RAP5 and at position + 20 in the primer RAP6, respectively. The PCR product was then digested with *KpnI-XhoI* and ligated into *KpnI-XhoI* digested pRAP1M1. The resulting plasmid thus contains the *URA3* flipper flanked by 5' and 3' of *CaRAP1*. The 5.3 kb *KpnI-SacI* digested fragment [*5'RAP1-FRT-SAP2P-caFLP-ACT1T-URA3-FRT-3'RAP1*] from this plasmid was used to generate the *CaRAP1* deletion strains.

pRAP1M3 (5.9 kb): 3'-fragment of *CaRAP1* was amplified from the chromosomal DNA of SC5314 using the primers RAP9 (+ 1156 to + 1188 in the + strand) and RAP10 (+ 1897 to + 1869 in the - strand). The *PstI* and

SacI sites were introduced at position + 1172 in the primer RAP9 and at position + 1885 in the primer RAP10, respectively. The PCR product was then digested with *PstI-SacI* and ligated into the *PstI-SacI* digested pCBF1M4.

pRAP1M4 (5.8 kb): 5'-fragment of *CaRAP1* was amplified from the chromosomal DNA of SC5314 using the primers RAP5 (- 463 to - 436 in the + strand) and RAP8 (+ 20 to - 10 in the - strand). The *KpnI* and *BamHI* sites were introduced at position - 448 in the primer RAP5 and at position + 6 in the primer RAP8, respectively. The PCR product was then digested with *KpnI-BamHI* and ligated into *KpnI-BglII* digested plasmid pRAP1M3. The 2.9 kb *KpnI-SacI* digested fragment [5'*RAP1-ACT1T-URA3-3'RAP1*] from this plasmid was used to generate the uridine-prototrophic *CaRAP1* deletion strains.

pRAP1K1 (7.1 kb): A fragment containing the *CaRAP1* promoter and coding region was amplified from the chromosomal DNA of SC5314 using the primers RAP5 (- 463 to - 436 in the + strand) and RAP11 (+ 1369 to + 1343 in the - strand). The *KpnI* and *BamHI* sites were introduced at position - 448 in the primer RAP5 and at position + 1354 in the primer RAP11, respectively. The PCR product was then digested with *KpnI-BamHI* and ligated into the *KpnI-BamHI* digested plasmid pRAP1M3. The resulting plasmid contains full length *CaRAP1* gene. A 4.2 kb *KpnI-SacI* fragment [*RAP1P-RAP1-ACT1T-URA3-3'RAP1*] from this plasmid was used to reintroduce *CaRAP1* into *rap1* null mutants.

pRSRAP1 (7.8 kb): A 2.3 kb *KpnI-SalI* fragment containing the *RAP1* promoter, coding region and *ACT1* terminator sequence from the plasmid pRAP1K1 was ligated into the *KpnI-SalI* digested yeast 2 μ plasmid pRS426.

A.1.3. Plasmids used to study *C.albicans* Centromere binding protein 1 (CaCbf1p)

pCBF1M1 (8.6 kb): 3'-fragment of *CaCBF1* was amplified from the chromosomal DNA of SC5314 using the primers CBF3 (+ 657 to + 682 in the + strand) and CBF4 (+ 1249 to + 1218 in the - strand). The *BglII* and *SacI* sites were introduced at position + 665 in the primer CBF3 and at position + 1236 in the primer CBF4, respectively. The PCR product was then digested with *BglII-SacI* and ligated into the *BglII-SacI* digested plasmid pYMR211M2 (Bader T, unpublished data), to replace the 3'-fragment of *YMR211* by 3'-*CaCBF1*.

pCBF1M2 (8.2 kb): 5'-fragment of *CaCBF1* was amplified from the chromosomal DNA of SC5314 using the primers CBF1 (- 588 to - 563 in the + strand) and CBF2 (+ 4 to - 24 in the - strand). The *KpnI* and *XhoI* sites were introduced at position - 577 in the primer CBF1 and at position - 11 in the primer CBF2, respectively. The PCR product was then digested with *KpnI-XhoI* and ligated into the *KpnI-XhoI* digested plasmid pCBF1M1. The resulting plasmid thus contains the *URA3* flipper flanked by the 5' and 3' of *CaCBF1*. The 5.3 kb *KpnI-SacI* digested fragment [5'*CBF1-FRT-SAP2P-caFLP-ACT1T-URA3-FRT-3'CBF1*] from this plasmid was used to generate the *CaCBF1* deletion strains.

pCBF1M3 (6.1 kb): 5'-fragment of *CaCBF1* was amplified from the chromosomal DNA of SC5314 using the primers CBF1 (- 588 to - 563 in the + strand) and CBF6 (+ 4 to - 24 in the - strand). The *KpnI* and *BglII* sites were introduced at position - 577 in the primer CBF1 and at position - 15 in the primer CBF6, respectively. The PCR product was then digested with *KpnI-BglII* and ligated into the *KpnI-BglII* digested plasmid pSAP2-1K (Staib *et al.*, 2002).

pCBF1M4 (5.8 kb): 3'-fragment of *CaCBF1* was amplified from the chromosomal DNA of SC5314 using the primers CBF5 (+ 657 to + 682 in the + strand) and CBF4 (+ 1249 to + 1218 in the - strand). The *PstI* and *SacI* sites were introduced at position + 672 in the primer CBF5 and at position + 1236 in the primer CBF4, respectively. The PCR product was then digested with *PstI-SacI* and ligated into the *PstI-SacI* digested plasmid pCBF1M3. The 2.9 kb *KpnI-SacI* digested fragment [5'*CBF1-ACTIT-URA3-3'CBF1*] from this plasmid was used to generate the uridine-prototrophic *CaCBF1* deletion strains.

pCBF1K1 (6.5 kb): A fragment containing the *CaCBF1* promoter and coding region was amplified from the chromosomal DNA of SC5314 using the primers CBF1 (- 588 to - 563 in the + strand) and CBF7 (+ 689 to + 661 in the - strand). The *KpnI* and *BglII* sites were introduced at position - 577 in the primer CBF1 and at position + 672 in the primer CBF7, respectively. The PCR product was then digested with *KpnI-BglII* and ligated into the *KpnI-BglII* digested plasmid pCBF1M4. The resulting plasmid thus contains the full length *CaCBF1* gene. A 3.6 kb *KpnI-SacI* fragment [*CBF1P-CBF1-ACTIT-URA3-3'CBF1*] from this plasmid was used to reintroduce *CaCBF1* into *cbf1* null mutants.

pADE2M1 (5.67 kb): 5'-fragment of *ADE2* was amplified from the chromosomal DNA of CAI4 using the primers ADE3 (+ 13 to + 37 in the + strand) and ADE4 (+ 484 to + 456 in the - strand). The *KpnI* and *BglII* sites were introduced at position + 23 in the primer ADE3 and at position + 469 in the primer ADE4, respectively. The PCR product was then digested with *KpnI-BglII* and ligated into the *KpnI-BglII* digested plasmid pCBF1M4.

pADE2M2 (5.36 kb): 3'-fragment of *ADE2* was amplified from the chromosomal DNA of CAI4 using the primers ADE5 (+ 1314 to + 1340 in the + strand) and ADE6 (+ 1690 to + 1669 in the - strand). *PstI* and *SacI* sites were introduced at position + 1326 in the primer ADE5 and at position + 1679 in the primer ADE6, respectively. The PCR product was then digested with *PstI-SacI* and ligated into the *PstI-SacI* digested plasmid pADE2M1. The 2.46 kb *KpnI-SacI* digested fragment [5'*ADE2-ACTIT-URA3-3'ADE2*] from this plasmid was used to generate the *ADE2/ade2* heterozygous mutant strains.

A.1.4. Plasmids used to study *C.albicans YIL19*

pYIL19M1 (8.0 kb): 5'-fragment of *YIL19* was amplified from the chromosomal DNA of CAI4 using the primers YIL1 (- 532 to - 509 in the + strand) and YIL2 (+ 13 to - 10 in the - strand). The *KpnI* and *XhoI* sites

were introduced at position - 519 in the primer YIL1 and at position - 1 in the primer YIL2, respectively. The PCR product was then digested with *KpnI-XhoI* and ligated into the *KpnI-XhoI* digested plasmid pMEP1M1.

pYIL19M2 (8.0 kb): 3'-fragment of *YIL19* was amplified from the chromosomal DNA of CAI4 using the primers YIL3 (+ 977 to + 999 in the + strand) and YIL4 (+ 1384 to + 1359 in the - strand). The *BglII* and *SacI* sites were introduced at position + 982 in the primer YIL3 and at position + 1373 in the primer YIL4, respectively. The PCR product was then digested with *BglII-SacI* and ligated into the *BglII-SacI* digested plasmid pYIL19M1. The resulting plasmid thus contains the *URA3* flipper flanked by the 5' and 3' of *YIL19*.

pYIL19 (5.6 kb): The *YIL19* gene was PCR amplified from the chromosomal DNA of CAI4 using the primers YIL5 (- 1180 to - 1153 in the + strand) and YIL 6 (+ 1495 to + 1469 in the - strand). The *XhoI* and *HindIII* sites were introduced at position - 1171 in the primer YIL5 and at position + 1484 in the YIL6, respectively. The PCR product was then digested with *XhoI-HindIII* and ligated into the *XhoI-HindIII* digested plasmid pBluescript KS II (Stratagene, Heidelberg, Germany).

pYIL19D1 (10.1 kb): The 1.2 kb *BamHI-SalI* fragment containing *ACT1P-FRT* fragment from pAFI3 (Staib *et al.*, 1999), the 2.8 kb *XhoI-HindIII YIL19*-fragment from pYIL19, and the 2.9 kb *HindIII-PstI MPA^R*-fragment from pAFI3 (Staib *et al.*, 1999) were ligated together into the 3.8 kb *BamHI-PstI* digested vector pAFI3 (Staib *et al.*, 1999).

A.2. Lee's medium

For 1000 ml of medium followings were mixed in distilled water:

Dextrose:	12.5 g
NaCl :	5.0 g
Ammonium sulphate:	5.0 g
K ₂ HPO ₄ :	2.5 g
L-Leucine:	1.3 g
L-Lysine:	1.0 g
L-Alanine:	0.5 g
L-Phenylalanine:	0.5 g
L-Proline:	0.5 g
L-Threonine:	0.5 g
L-Methionine:	0.1 g
L-Ornithine:	0.07 g
L-Arginine:	0.07 g
pH adjusted to 6.7-6.8	
d-Biotin:	1.0 mg

After autoclaving, it was cooled to < 65°C and the followings were added:

100 µM Zinc-Sulphate:	1.0 ml
MgSO ₄ ·7H ₂ O (20 g/L):	10.0 ml

To make the agar plates of Lee's medium 2% agar was used.

A.3. Abbreviations

A:	Absorbance
bp:	base pair
<i>caFLP</i> :	<i>C.albicans</i> adapted <i>FLP</i> (recombinase) gene
cfu:	colony forming units
Ci:	Courie
cm:	centimeter
CSM:	Complete Supplement Medium
DEPC:	Diethyl pyrocarbonate
DNA:	Deoxyribonucleic acid
dNTPs:	deoxy nucleoside phosphates
DTT:	Dithiothreitol
<i>ecaFLP</i> :	'enhanced' <i>C.albicans</i> adapted <i>FLP</i> (recombinase) gene
EDTA:	Ethylediaminetetraacetate
<i>FRT</i> :	<i>FLP</i> recognition site
g:	gram
<i>GFP</i> :	Green fluorescent protein
h:	hour
IAA:	Isopropyl alcohol
kb:	kilobasepair
kD:	kilo Dalton
Kv:	Kilovolt
<i>lacZ</i> :	β -galactosidase gene
LB:	Luria-Bertani
M:	Molar
ml:	milliliter
mM:	millimolar
mRNA:	messenger Ribonucleic acid
ng:	nanogram
nm:	nanometer
<i>MPA^R</i> :	Mycophenolic acid resistance gene
OD:	Optical density
P, 5' and 3':	Promoter, 5' and 3' regions of any gene, respectively
PBS:	Phosphate-buffered saline
PNK:	Polynucleotide kinase
RNA:	Ribonucleic acid
RNase A:	Ribonuclease A
rpm:	rotation per minute
RT:	Room temperature

rRNA:	ribosomal Ribonucleic acid
SD:	Synthetic Dextrose
SDS:	Sodium dodecyl sulphate
u:	unit
<i>URA3</i> :	Uridine-5' phosphate decarboxylase
v:	volume
w:	weight
WT:	Wild-type
YCB:	Yeast Carbon Base
YNB:	Yeast Nitrogen Base
μ:	micro.

References

- Aparicio, O.M., Billington, B.L., Gottschling, D.E. (1991) Modifiers of position effect are shared between telomeric and silent mating-type loci in *Saccharomyces cerevisiae*. *Cell*, **66**, 1279-1287.
- Ausubel, F., Brent, R., Kingston, R., Moore, D., Seidman, J., Smith, J., Struhl, K. (1989) Current protocols in molecular biology. In. Wiley, New York.
- Backen, A.C., Broadbent, I.D., Fetherston, R.W., Rosamond, J.D., Schnell, N.F., Stark, M.J. (2000) Evaluation of the *CaMAL2* promoter for regulated expression of genes in *Candida albicans*. *Yeast*, **16**, 1121-1129.
- Bahn, Y.S., Sundstrom, P. (2001) *CAP1*, an adenylate cyclase-associated protein gene, regulates bud-hypha transitions, filamentous growth, and cyclic AMP levels and is required for virulence of *Candida albicans*. *J. Bacteriol.*, **183**, 3211-3223.
- Bai, C., Ramanan, N., Wang, Y.M., Wang, Y. (2002) Spindle assembly checkpoint component CaMad2p is indispensable for *Candida albicans* survival and virulence in mice. *Mol. Microbiol.*, **45**, 31-44.
- Baker, R.E., Fitzgerald-Hayes, M., O'Brien, T.C. (1989) Purification of the yeast centromeric binding protein CP1 and a mutational analysis of its binding site. *J. Biol. Chem.*, **264**, 10843-10850.
- Baker, R.E., Masison, D.C. (1990) Isolation of the gene encoding the *Saccharomyces cerevisiae* centromere-binding protein CP1. *Mol. Cell. Biol.*, **10**, 2458-2467.
- Banerjee, A., Ganesan, K., Datta, A. (1991) Induction of secretory acid proteinase in *Candida albicans*. *J. Gen. Microbiol.*, **137**, 2455-2461.
- Barton, R.C., Gull, K. (1992) Isolation, characterization, and genetic analysis of monosomic, aneuploid mutants of *Candida albicans*. *Mol. Microbiol.*, **6**, 171-177.
- Basrai, M.A., Zhang, H.L., Miller, D., Naider, F., Becker, J.M. (1992) Toxicity of oxalysine and oxalysine-containing peptides against *Candida albicans*: regulation of peptide transport by amino acids. *J. Gen. Microbiol.*, **138**, 2353-2362.
- Bensen, E.S., Filler, S.G., Berman, J. (2002) A forkhead transcription factor is important for true hyphal as well as yeast morphogenesis in *Candida albicans*. *Eukaryot. Cell*, **1**, 787-798.
- Black, T., Hare, R. (2000) Will genomics revolutionize antimicrobial drug discovery? *Curr. Opin. Microbiol.*, **3**, 522-527.
- Bockmühl, D.P., Ernst, J.F. (2001) A potential phosphorylation site for an A-type kinase in the Efg1 regulator protein contributes to hyphal morphogenesis of *Candida albicans*. *Genetics*, **157**, 1523-1530.
- Bockmühl, D.P., Krishnamurthy, S., Gerads, M., Sonneborn, A., Ernst, J.F. (2001) Distinct and redundant roles of the two protein kinase A isoforms Tpk1p and Tpk2p in morphogenesis and growth of *Candida albicans*. *Mol. Microbiol.*, **42**, 1243-1257.
- Bowman, J.C., Hicks, P.S., Kurtz, M.B., Rosen, H., Schmatz, D.M., Liberator, P.A., Douglas, C.M. (2002) The antifungal Echinocandin caspofungin acetate kills growing cells of *Aspergillus fumigatus* *in vitro*. *Antimicrob. Agents. Chemother.*, **46**, 3001-3012.

- Bram, R.J., Kornberg, R.D. (1987) Isolation of a *Saccharomyces cerevisiae* centromeric DNA-binding protein, its human homolog, and its possible role as a transcription factor. *Mol. Cell. Biol.*, **7**, 403-409.
- Braun, B.R., Johnson, A.D. (1997) Control of filament formation in *Candida albicans* by the transcriptional repressor TUP1. *Science*, **277**, 105-109.
- Braun, B.R., Kadosh, D., Johnson, A.D. (2001) NRG1, a repressor of filamentous growth in *Candida albicans*, is down-regulated during filament induction. *EMBO J.*, **20**, 4753-4761.
- Brown, D.H.J., Giusani, A.D., Chen, X., Kumamoto, C.A. (1999) Filamentous growth of *Candida albicans* in response to physical environmental cues and its regulation by the unique *CZF1* gene. *Mol. Microbiol.*, **34**, 651-662.
- Cai, M., Davis, R. (1990) Yeast centromere binding protein Cbf1, of the helix-loop-helix protein family, is required for chromosome stability and methionine prototrophy. *Cell*, **61**, 437-446.
- Calderone, R.A., Fonzi, W.A. (2001) Virulence factors of *Candida albicans*. *Trends Microbiol.*, **9**, 327-335.
- Callebaut, I., Mornon, J.P. (1997) From BRCA1 to RAP1: a widespread BRCT module closely associated with DNA repair. *FEBS Lett.*, **400**, 25-30.
- Care, R.S., Trevethick, J., Binley, K.M., Sudbery, P.E. (1999) The *MET3* promoter: a new tool for *Candida albicans* molecular genetics. *Mol. Microbiol.*, **34**, 792-798.
- Cheng, S., Clancy, C.J., Checkley, M.A., Handfield, M., Hillman, J.D., Progulske-Fox, A., Lewin, A.S., Fidel, P.L., Nguyen, M.H. (2003) Identification of *Candida albicans* genes induced during thrush offers insight into pathogenesis. *Mol. Microbiol.*, **48**, 1275-1288.
- Choo, K.H.A. (1997) The centromere. In: Oxford University Press, Oxford, United Kingdom.
- Clark, K.L., Feldmann, P.J., Dignard, D., Larocque, R., Brown, A.J., Lee, M.G., Thomas, D.Y., Whitway, M. (1995) Constitutive activation of the *Saccharomyces cerevisiae* mating response pathway by a MAP kinase kinase from *Candida albicans*. *Mol. Gen. Genet.*, **249**, 609-621.
- Clarke, L., Carbon, J. (1980) Isolation of a yeast centromere and construction of functional small circular chromosomes. *Nature*, **287**, 504-509.
- Cloutier, M., Castilla, R., Bolduc, N., Zelada, A., Martineau, P., Bouillon, M., Magee, B.B., Passeron, S., Giasson, L., Cantore, M.L. (2003) The two isoforms of the cAMP-dependent protein kinase catalytic subunit are involved in the control of dimorphism in the human fungal pathogen *Candida albicans*. *Fungal Genet. Biol.*, **38**, 133-141.
- Coffman, J.A., Rai, R., Loprete, D.M., Cunningham, T., Svetlov, V., Cooper, T.G. (1997) Cross regulation of four GATA factors that control nitrogen catabolite gene expression in *Saccharomyces cerevisiae*. *J. Bacteriol.*, **179**, 3416-3429.
- Conrad, M.N., Wright, J. H., Wolf, A. J., Zakian, V. A. (1990) RAP1 protein interacts with yeast telomeres in vivo: overproduction alters telomere structure and decreases chromosome stability. *Cell*, **63**, 739-750.
- Cormack, B.P., Bertram, G., Egerton, M., Gow, N.A., Falkow, S., Brown, A.J. (1997) Yeast-enhanced green fluorescent protein (yEGFP) a reporter of gene expression in *Candida albicans*. *Microbiology*, **143**, 303-311.

- Corner, B.E., Magee, P.T. (1997) *Candida* pathogenesis: unraveling the threads of infection. *Curr. Biol.*, **7**, 691-694.
- Cowen, L.E., Sanglard, D., Calabrese, D., Sirjusingh, C., Anderson, J.B., Kohn, L.M. (2000) Evolution of drug resistance in experimental populations of *Candida albicans*. *J. Bacteriol.*, **182**, 1515-1522.
- Csank, C., Makris, C., Meloche, S., Schröppel, K., Röllinghoff, M., Dignard, D., Thomas, D.Y., Whiteway, M. (1997) Derepressed hyphal growth and reduced virulence in a VH1 family-related protein phosphatase mutant of the human pathogen *Candida albicans*. *Mol. Biol. Cell*, **8**, 2539-2551.
- Csank, C., Schröppel, K., Leberer, E., Harcus, D., Mohamed, O., Meloche, S., Thomas, D.Y., Whiteway, M. (1998) Roles of the *Candida albicans* mitogen-activated protein kinase homolog, Cek1p, in hyphal development and systemic candidiasis. *Infect. Immun.*, **66**, 2713-2721.
- Davis, D., Edwards, J.E. Jr., Mitchell, A.P., Ibrahim, A.S. (2000) *Candida albicans* RIM101 pH response pathway is required for host-pathogen interactions. *Infect. Immun.*, **68**, 5953-5959.
- De Backer, M.D., Nelissen, B., Logghe, M., Viaene, J., Loonen, I., Vandoninck, S., de Hoogt, R., Dewaele, S., Simons, F.A., Verhasselt, P., Vanhoof, G., Contreras, R., Luyten, W.H. (2001) An antisense-based functional genomics approach for identification of genes critical for growth of *Candida albicans*. *Nat. Biotechnol.*, **19**, 212-213.
- Delbruck, S., Ernst, J.F. (1993) Morphogenesis-independent regulation of actin transcript levels in the pathogenic yeast *Candida albicans*. *Mol. Microbiol.*, **10**, 859-866.
- Eck, R., Stoyan, T., Künkel, W. (2001) The centromere-binding factor Cbf1p from *Candida albicans* complements the methionine auxotrophic phenotype of *Saccharomyces cerevisiae*. *Yeast*, **18**, 1047-1052.
- El Barkani, A., Kurzai, O., Fonzi, W.A., Ramon, A., Porta, A., Frosch, M., Muhlschlegel, F.A. (2000) Dominant active alleles of *RIM101* (*PRR2*) bypass the pH restriction on filamentation of *Candida albicans*. *Mol. Cell. Biol.*, **20**, 4635-4647.
- Feng, Q., Summers, E., Guo, B., Fink, G. (1999) Ras signaling is required for serum-induced hyphal differentiation in *Candida albicans*. *J. Bacteriol.*, **181**, 6339-6346.
- Fonzi, W.A., Irwin, M.Y. (1993) Isogenic strain construction and gene mapping in *Candida albicans*. *Genetics*, **134**, 717-728.
- Foreman, P.K., Davis, R.W. (1993) Point mutations that separate the role of *Saccharomyces cerevisiae* centromere binding factor 1 in chromosome segregation from its role in transcriptional activation. *Genetics*, **135**, 287-296.
- Fradin, C., Kretschmar, M., Nichterlein, T., Gaillardin, C., d'Enfert, C., Hube, B. (2003) Stage-specific gene expression of *Candida albicans* in human blood. *Mol. Microbiol.*, **47**, 1523-1543.
- Franz, R., Kelly, S.L., Lamb, D.C., Kelly, D.E., Ruhnke, M., Morschhäuser, J. (1998) Multiple molecular mechanisms contribute to a stepwise development of fluconazole resistance in clinical *Candida albicans* strains. *Antimicrob. Agents. Chemother.*, **42**, 3065-3072.
- Freeman, K., Gwadz, M., Shore, D. (1995) Molecular and genetic analysis of the toxic effect of *RAP1* overexpression in yeast. *Genetics*, **141**, 1253-1262.
- Fukuoka, Y., Inaoka, H., Kohane, I.S. (2004) Inter-species differences of co-expression of neighbouring genes in eucaryotic genomes. *BMC Genomics*, **5**, 4.

- Gagiano, M., van Dyk, D., Bauer, F.F., Lambrechts, M.G., and Pretorius, I.S. (1999) Msn1p/Mss10p, Mss11p and Muc1p/Flo11p are part of signal transduction pathway downstream of Mep2p regulating invasive growth and pseudohyphal differentiation in *Saccharomyces cerevisiae*. *Mol. Microbiol.*, **31**, 103-116.
- Gerami-Nejad, M., Berman, J., Gale, C.A. (2001) Cassettes for PCR-mediated construction of green, yellow, and cyan fluorescent protein fusions in *Candida albicans*. *Yeast*, **18**, 859-864.
- Ghannoum, M.A., Abu-Elteen, K.H. (1990) Pathogenicity determinants of *Candida*. *Mycoses*, **33**, 265-282.
- Gillum, A.M., Tsay, E.Y. and Kirsch, D.R. (1984) Isolation of the *Candida albicans* gene for orotidine-5'-phosphate decarboxylase by complementation of *S. cerevisiae ura3* and *E. coli pyrF* mutations. *Mol. Gen. Genet.*, **198**, 179-182.
- Gimeno, C.J., Ljungdahl, P.O., Styles, C.A., Fink, G.R. (1992) Unipolar cell divisions in the yeast *Saccharomyces cerevisiae* lead to filamentous growth: regulation by starvation and RAS. *Cell*, **68**, 1077-1090.
- Giusani, A.D., Vinces, M., Kumamoto, C.A. (2002) Invasive filamentous growth of *Candida albicans* is promoted by Czflp-dependent relief of Efg1p-mediated repression. *Genetics*, **160**, 1749-1753.
- Graham, I.R., Haw, R.A., Spink, K.G., Halden, K.A., Chambers, A. (1999) In vivo analysis of functional regions within yeast Rap1p. *Mol. Cell. Biol.*, **19**, 7481-7490.
- Guhad, F.A., Csank, C., Jensen, H.E., Thomas, D.Y., Whiteway, M., Hau, J. (1998a) Reduced pathogenicity of a *Candida albicans* MAP kinase phosphatase (*CPP1*) mutant in the murine mastitis model. *APMIS*, **106**, 1049-1055.
- Hackette, S.L., Skye, G.E., Burton, C., Segel, I.H. (1970) Characterization of an ammonium transporter system in filamentous fungi with methylammonium-¹⁴C as the substrate. *J. Biol. Chem.*, **245**, 4241-4250.
- Hardy, C.F.J., Balderes, D., Shore, D. (1992) Dissection of a carboxy-terminal region of the yeast regulatory protein RAP1 with effects on both transcriptional activation and silencing. *Mol. Cell. Biol.*, **12**, 1209-1217.
- Hardy, C.F.J., Sussel, L., Shore, D. (1992) A RAP1-interacting protein involved in transcriptional silencing and telomere length regulation. *Genes Dev.*, **6**, 801-814.
- Haw, R., Yarragudi, A.D., Uemura, H. (2001) Isolation of a *Candida glabrata* homologue of *RAP1*, a regulator of transcription and telomere function in *Saccharomyces cerevisiae*. *Yeast*, **18**, 1277-1284.
- Hecht, A., Strahl-Bolsinger, S., Grunstein, M. (1996) Spreading of transcriptional repressor SIR3 from telomeric heterochromatin. *Nature*, **383**, 92-95.
- Hensel, M., Arst, H.N., Jr, Aufauvre-Brown, A., Holden, D.W. (1998) The role of the *Aspergillus fumigatus areA* gene in invasive pulmonary aspergillosis. *Mol. Gen. Genet.*, **258**, 553-557.
- Holmes, A.R., Shepherd, M.G. (1987) Proline induced germ-tube formation in *Candida albicans*: role of proline uptake and nitrogen metabolism. *J. Gen. Microbiol.*, **133**, 3219-3228.
- Hube, B., Monod, M., Schofield, D.A., Brown, A.J., Gow, N.A. (1994) Expression of seven members of the gene family encoding secretory aspartyl proteinase in *Candida albicans*. *Mol. Microbiol.*, **14**, 87-99.

- Hube, B., Sanglard, D., Odds, F.C., Hess, D., Monod, M., Schafer, W., Brown, A.J., Gow, N.A.R. (1997) Disruption of each of the secreted aspartyl proteinase genes *SAP1*, *SAP2*, and *SAP3* of *Candida albicans* attenuates virulence. *Infect. Immun.*, **65**, 3529-3538.
- Huh, W.K., Falvo, J.V., Gerke, L.C., Carroll, A.S., Howson, R.W., Weissman, J.S., O'shea, E.K. (2003) Global analysis of protein localization in budding yeast. *Nature*, **425**, 686-691.
- Janbon, G., Sherman, F., Rustchenko, E. (1998) Monosomy of a specific chromosome determines L-sorbose utilization: a novel regulatory mechanism in *Candida albicans*. *Proc. Natl. Acad. Sci. USA*, **95**, 5150-5155.
- Javelle, A., Morel, M., Rodriguez-Pastrana, B.R., Botton, B., Andre, B., Marini, A.M., Brun, A., Chalot, M. (2003a) Molecular characterization, function and regulation of ammonium transporters (Amt) and ammonium-metabolizing enzymes (GS, NADP-GDH) in the ectomycorrhizal fungus *Hebeloma cylindrosporum*. *Mol. Microbiol.*, **47**, 411-430.
- Javelle, A., Andre, B., Marini, A.M., Chalot, M. (2003b) High-affinity ammonium transporters and nitrogen sensing in mycorrhizas. *Trends Microbiol.*, **11**, 53-55.
- Jiang, W., Phillipsen, P. (1989) Purification of a protein binding to the CDE1 subregion of *Saccharomyces cerevisiae* centromere DNA. *Mol. Cell. Biol.*, **9**, 5585-5593.
- Jorgensen, P., Nishikawa, J.L., Breikreutz, B-J., Tyers, M. (2002) Systematic identification of pathways that couple cell growth and division in yeast. *Science*, **297**, 395-400.
- Kadosh, D., Johnson, A.D. (2001) Rfg1, a protein related to the *Saccharomyces cerevisiae* hypoxic regulator Rox1, controls filamentous growth and virulence in *Candida albicans*. *Mol. Cell. Biol.*, **21**, 2496-2505.
- Takeya, H., Miyazaki, Y., Miyazaki, H., Nyswaner, K., Grimberg, B., Bennett, J.E. (2000) Genetic analysis of azole resistance in the Darlington strain of *Candida albicans*. *Antimicrob. Agents. Chemother.*, **44**, 2985-2990.
- Karkusiewicz, I., Rempola, B., Gromadka, R., Grynberg, M., Rytka, J. (2004) Functional and physical interactions of Faf1p, a *Saccharomyces cerevisiae* nucleolar protein. *Biochem. Biophys. Res. Comm.*, **319**, 349-357.
- Khalaf, R.A., Zitomer, R.S. (2001) The DNA binding protein Rfg1 is a repressor of filamentation in *Candida albicans*. *Genetics*, **157**, 1503-1512.
- Köhler, J.R., Fink, G.R. (1996) *Candida albicans* strains heterozygous and homozygous for mutations in mitogen-activated protein kinase signalling components have defects in hyphal development. *Proc. Natl. Acad. Sci. USA*, **93**, 13223-13228.
- Köhler, G.A., White, T.C. and Agabian, N. (1997) Overexpression of a cloned IMP dehydrogenase gene of *Candida albicans* confers resistance to the specific inhibitor mycophenolic acid. *J. Bacteriol.*, **179**, 2331-2338.
- Kressler, D., Linder, P., and de la Cruz, J. (1999) Protein *trans*-acting factors involved in ribosome biogenesis in *Saccharomyces cerevisiae*. *Mol. Cell. Biol.*, **19**, 7897-7912.
- Kruglyak, S., Tang, H. (2000) Regulation of adjacent yeast genes. *Trends Genet.*, **16**, 109-111.
- Kuras, L., Barbey, R., Thomas, D. (1997) Assembly of a bZIP-bHLH transcription activation complex: formation of the yeast Cbf1-Met4-Met28 complex is regulated through Met28 stimulation of Cbf1 DNA binding. *EMBO J.*, **16**, 2441-2451.

- Kuras, L., and Thomas, D. (1995) Identification of the yeast methionine biosynthetic genes that require the centromere binding factor 1 for their transcriptional activation. *FEBS Lett.*, **367**, 15-18.
- Kurtz, S., Shore, D. (1991) RAP1 protein activates and silences transcription of mating-type genes in yeast. *Genes Dev.*, **5**, 616-628.
- Kusch, H., Biswas, K., Schwanfelder, S., Engelmann, S., Rogers, P.D., Hecker, M., Morschhäuser, J. (2004) A proteomic approach to understanding the development of multidrug-resistant *Candida albicans* strains. *Mol. Gen. Genet.*, **271**, 554-565.
- Land, G.A., McDonald, W.C., Stjernholm, R.L., Friedman, T.L. (1975) Factors affecting filamentation in *Candida albicans*: relationship of the uptake and distribution of proline to morphogenesis. *Infect. Immun.*, **11**, 1014-1023.
- Lane, S., Birse, C., Zhou, S., Matson, R., Liu, H. (2001a) DNA array studies demonstrate convergent regulation of virulence factors by Cph1, Cph2, and Efg1 in *Candida albicans*. *J. Biol. Chem.*, **276**, 48988-48996.
- Lane, S., Zhou, S., Pan, T., Dai, Q., Liu, H. (2001b) The basic helix-loop-helix transcription factor Cph2 regulates hyphal development in *Candida albicans* partly via *TEC1*. *Mol. Cell. Biol.*, **21**, 6418-6428.
- Larson, G.P., Castanotto, D., Rossi, J.J., Malafa, M.P. (1994) Isolation and functional analysis of a *Kluyveromyces lactis* *RAP1* homologue. *Gene*, **150**, 35-41.
- Lasker, B.A., Page, L.S., Lott, T.J., Kobayashi, G.S. (1992) Isolation, characterization, and sequencing of *Candida albicans* repetitive element 2. *Gene*, **116**, 51-57.
- Leberer, E., Harcus, D., Broadbent, I.D., Clark, K.L., Dignard, D., Ziegelbauer, K., Schmidt, A., Gow, N.A., Brown, A.J., Thomas, D.Y. (1996) Signal transduction through homologs of the Ste20p and Ste7p protein kinases can trigger hyphal formation in the pathogenic fungus *Candida albicans*. *Proc. Natl. Acad. Sci. USA.*, **93**, 13217-13222.
- Leberer, E., Harcus, D., Dignard, D., Johnson, L., Ushinsky, S., Thomas, D.Y., Schröppel, K. (2001) Ras links cellular morphogenesis to virulence by regulation of the MAP kinase and cAMP signaling pathways in the pathogenic fungus *Candida albicans*. *Mol. Microbiol.*, **42**, 673-687.
- Lee, S.J., Baserga, S.J. (1999) Imp3p and Imp4p, two specific components of the U3 small nucleolar ribonucleoprotein that are essential for pre-18S rRNA processing. *Mol. Cell. Biol.*, **19**, 5441-5452.
- Li, B., Oestreich, S., de Lange, T. (2000) Identification of human Rap1: implication for telomere evolution. *Cell*, **101**, 471-483.
- Limjindaporn, T., Khalaf, R.A., Fonzi, W.A. (2003) Nitrogen metabolism and virulence of *Candida albicans* require GATA type transcriptional activator encoded by *GAT1*. *Mol. Microbiol.*, **50**, 993-1004.
- Liu, H., Köhler, J., Fink, G.R. (1994) Suppression of hyphal formation in *Candida albicans* by mutation of a *STE12* homolog. *Science*, **266**, 1723-1726.
- Liu, H. (2001) Transcriptional control of dimorphism in *Candida albicans*. *Curr. Opin. Microbiol.*, **4**, 728-735.
- Liu, H. (2002) Co-regulation of pathogenesis with dimorphism and phenotypic switching in *Candida albicans*, a commensal and a pathogen. *Int. J. Med. Microbiol.*, **292**, 299-311.

- Lo, H.J., Köhler, J.R., DiDomenico, B., Loebenberg, D., Cacciapuoti, A., Fink, G.R. (1997) Nonfilamentous *C. albicans* mutants are avirulent. *Cell*, **90**, 939-949.
- Lorenz, M.C., Heitman, J. (1997) Yeast pseudohyphal growth is regulated by *GPA2*, a G protein [alpha] homolog. *EMBO J.*, **16**, 7008-7018.
- Lorenz, M.C., and Heitman, J. (1998a) The MEP2 ammonium permease regulates pseudohyphal differentiation in *Saccharomyces cerevisiae*. *EMBO J.*, **17**, 1236-1247.
- Lorenz, M.C., and Heitman, J. (1998b) Regulators of pseudohyphal differentiation in *Saccharomyces cerevisiae* identified through multicopy suppressor analysis in ammonium permease mutant strains. *Genetics*, **150**, 1443-1457.
- Lustig, A.J., Kurtz, S., Shore, D. (1990) Involvement of the silencer and UAS binding protein RAP1 in regulation of telomere length. *Science*, **250**, 549-553.
- Magasanik, B. (1992) Regulation of nitrogen utilization. In: Strathern, J.N., Jones, E.W., and Broach, J.R. (ed.). The molecular and cellular biology of the Yeast *Saccharomyces cerevisiae*: Metabolism and Gene Expression. Cold Spring Harbor Laboratory Press, Cold Spring Harbor, NY, pp. 283-317.
- Magasanik, B., and Kaiser, C.A. (2002) Nitrogen regulation in *Saccharomyces cerevisiae*. *Gene*, **290**, 1-18.
- Marini, A.M., Soussi-Boudekou, S., Vissers, S., Andre, B. (1994) Cloning and expression of the MEP1 gene encoding an ammonium transporter in *Saccharomyces cerevisiae*. *EMBO J.*, **13**, 3456-3463.
- Marini, A.M., Soussi-Boudekou, S., Vissers, S. and Andre, B. (1997) A family of ammonium transporters in *Saccharomyces cerevisiae*. *Mol. Cell. Biol.*, **17**, 4282-4293.
- Marini, A.M., and Andre, B. (2000) In vivo N-glycosylation of the Mep2 high-affinity ammonium transporter of *Saccharomyces cerevisiae* reveals an extracytosolic N-terminus. *Mol. Microbiol.*, **38**, 552-564.
- Marini, A.M., Matassi, G., Raynal, V., Andre, B., Carton, J.P., Cheffir-Zahar, B. (2000a) The human rhesus-associated RhAG protein and a kidney homologue promote ammonium transport in yeast. *Nat. Genet.*, **26**, 341-344.
- Marini, A.M., Springael, J.Y., Frommer, W.B. and Andre, B. (2000b) Cross-talk between ammonium transporters in yeast and interference by the soybean SAT1 protein. *Mol. Microbiol.*, **35**, 378-385.
- Martinez, P., Ljungdahl, P.O. (2003) An ER packaging chaperone determines the amino acid uptake capacity and virulence of *Candida albicans*. *Mol. Microbiol.*, **51**, 371-384.
- Marzluf, G.A. (1997) Genetic regulation of nitrogen metabolism in the fungi. *Microbiol. Molec. Biol. Rev.*, **61**, 17-32.
- Mayser, P., Laabs, S., Heuer, K.U., Grunder, K. (1996) Detection of extracellular phospholipase activity in *Candida albicans* and *Rhodotorula rubra*. *Mycopathologia*, **135**, 149-155.
- McKenzie, E.A., Kent, N.A., Dowell, S.J., Moreno, F., Bird, L.E., Mellor, J. (1993) The centromere and promoter factor, 1, CPF1, of *Saccharomyces cerevisiae* modulates gene activity through a family of factors including SPT21, RPD1 (SIN3), RPD3 and CCR4. *Mol. Gen. Genet.*, **240**, 374-386.
- Mellor, J., Jiang, W., Funk, M., Rathjen, J., Barnes, C.A., Hinz, T., Hegemann, J.H., Philippsen, P. (1990) CPF1, a yeast protein which functions in centromeres and promoters. *EMBO J.*, **9**, 4017-4026.

- Michel, S., Ushinsky, S., Klebl, B., Leberer, E., Thomas, D., Whiteway, M., Morschhäuser, J. (2002) Generation of conditional lethal *Candida albicans* mutants by inducible deletion of essential genes. *Mol. Microbiol.*, **46**, 269-280.
- Miwa, T., Takagi, Y., Shinozaki, M., Yun, C.W., Scell, W.A., Perfect, J. R., Kumagai, H., Tamaki, H. (2004) Gpr1, a putative G-protein-coupled receptor, regulates morphogenesis and hypha formation in the pathogenic fungus *Candida albicans*. *Eucaryot. Cell*, **3**, 919-931.
- Monahan, B.J., Fraser, J.A., Hynes, M.J., Davis, M.A. (2002a) Isolation and characterization of two ammonium permease genes, *meaA* and *mepA*, from *Aspergillus nidulans*. *Eucaryot. Cell*, **1**, 85-94.
- Monahan, B.J., Unkles, S.E.I.T.T., Kinghorn, J.R., Hynes, M.J., Davis, M.A. (2002b) Mutation and functional analysis of the *Aspergillus nidulans* ammonium permease MeaA and evidence for interaction with itself and MepA. *Fungal Genet. Biol.*, **36**, 35-46.
- Montanini, B., Moretto, N., Soragni, E., Percudani, R., Ottonello, S. (2002) A high-affinity ammonium transporter from the mycorrhizal ascomycete *Tuber borchii*. *Fungal Genet. Biol.*, **36**, 22-34.
- Moretti, P., Freeman, K., Coodly, L., Shore, D. (1994) Evidence that a complex of SIR proteins interacts with the silencer and telomere-binding protein RAP1. *Genes Dev.*, **8**, 2257-2269.
- Morschhäuser, J., Michel, S., Hacker, J. (1998) Expression of a chromosomally integrated, single-copy GFP gene in *Candida albicans*, and its use as a reporter of gene regulation. *Mol. Gen. Genet.*, **257**, 412-420.
- Morschhäuser, J., Michel, S., Staib, P. (1999) Sequential gene disruption in *Candida albicans* by FLP-mediated site-specific recombination. *Mol. Microbiol.*, **32**, 547-556.
- Mulder, W., Winkler, A.A., Scholten, I.H., Zonneveld, B.J., de Winde, J.H., Yde Steensma, H., Grivell, L.A. (1994) Centromere promoter factors (CPF1) of the yeasts *Saccharomyces cerevisiae* and *Kluyveromyces lactis* are functionally exchangeable, despite low overall homology. *Curr. Genet.*, **26**, 198-207.
- Muller, T., Gilson, E., Schmidt, R., Giraldo, R., Sogo, J., Gross, H., Gasser, S.M. (1994) Imaging the asymmetrical DNA bend induced by repressor activator protein 1 with scanning tunneling microscopy. *J. Struct. Biol.*, **113**, 1-12.
- Murad, A.M., d'Enfert, C., Gaillardin, C., Tournu, H., Tekaia, F., Talibi, D., Marechal, D., Marchais, V., Cottin, J., Brown, A.J. (2001a) Transcript profiling in *Candida albicans* reveals new cellular functions for the transcriptional repressors CaTup1, CaMig1 and CaNrg1. *Mol. Microbiol.*, **42**, 981-993.
- Murad, A.M., Leng, P., Straffon, M., Wishart, J., Macaskill, S., MacCallum, D., Schnell, N., Talibi, D., Marechal, D., Tekaia, F., d'Enfert, C., Gaillardin, C., Odds, F.C., Brown, A.J. (2001b) NRG1 represses yeast-hypha morphogenesis and hypha-specific gene expression in *Candida albicans*. *EMBO J.*, **20**, 4742-4752.
- Nakayama, H., Mio, T., Nagahashi, S., Kokado, M., Arisawa, M., Aoki, Y. (2000) Tetracycline-regulatable system to tightly control gene expression in the pathogenic fungus *Candida albicans*. *Infect. Immun.*, **68**, 6712-6719.
- Ninnemann, O., Jauniaux, J.C., Frommer, W.B. (1994) Identification of a high affinity NH₄⁺ transporter from plants. *EMBO J.*, **13**, 3464-3471.
- Odds, F.C. (1988) *Candida and candidosis*. 2nd ed, London, U.K.

- Overbeek, R., Fonstein, M., D'Souza, M., Pusch, G.D., Maltsev, N. (1999) The use of gene clusters to infer functional coupling. *Proc. Natl. Acad. Sci. USA*, **96**, 2896-2901.
- Palkova, Z., Janderova, B., Gabriel, J., Zikanova, B., Pospisek, M., Forstova, J. (1997) Ammonia mediates communication between yeast colonies. *Nature*, **390**, 532-536.
- Payne, J.W., Barrett-Bee, K.J., Shallow, D.A. (1991) Peptide substrate rapidly modulate expression of dipeptide and oligopeptide permeases in *Candida albicans*. *FEMS Microbiol. Lett.*, **63**, 15-20.
- Porta, A., Wang, Z., Ramon, A., Muhlschlegel, F.A., and Fonzi, W.A. (2001) Spontaneous second-site suppressors of the filamentation defect of *prf1* delta mutants define a critical domain of Rim101p in *Candida albicans*. *Mol. Gen. Genet.*, **266**, 624-631.
- Ramage, G., VandeWalle, K., Lopez-Ribot, J.L., Wickes, B.L. (2002) The filamentation pathway controlled by the Efg1 regulator protein is required for normal biofilm formation and development in *Candida albicans*. *FEMS Microbiol. Lett.*, **214**, 95-100.
- Ramon, A.M., Porta, A., Fonzi, W.A. (1999) Effect of environmental pH on morphological development of *Candida albicans* is mediated via the PacC-related transcription factor encoded by *PRR2*. *J. Bacteriol.*, **181**, 7524-7530.
- Rex, J.H., Rinaldi, M.G., Pfaller, M.A. (1995) Resistance of *Candida* species to fluconazole. *Antimicrob. Agents. Chemother.*, **39**, 1-8.
- Rocha, C.R., Schröppel, K., Harcus, D., Marcil, A., Dignard, D., Taylor, B.N., Thomas, D.Y., Whiteway, M., Leberer, E. (2001) Signaling through adenylyl cyclase is essential for hyphal growth and virulence in the pathogenic fungus *Candida albicans*. *Mol. Biol. Cell.*, **12**, 3631-3643.
- Ross, I.K., De Bernardis, F., Emerson, G.W., Cassone, A., Sullivan, P.A. (1990) The secreted aspartate proteinase of *Candida albicans*: physiology of secretion and virulence of a proteinase-deficient mutant. *J. Gen. Microbiol.*, **136**, 687-694.
- Sabie, F.T., Gadd, G.M. (1992) Effect of nucleosides and nucleotides and the relationship between cellular adenosine 3',5'-cyclic monophosphate (cyclic AMP) and germ tube formation in *Candida albicans*. *Mycopathologia*, **119**, 147-156.
- Sambrook, J., Fritsch, E.F., Maniatis, T. (1989) Molecular cloning: a laboratory manual, 2nd ed. In. Cold Spring Harbor Laboratory Press, Cold Spring Harbor, NY.
- Sanchez-Martinez, C., Perez-Martin, J. (2002) Gpa2, a G-protein alpha subunit required for hyphal development in *Candida albicans*. *Eukaryot. Cell.*, **1**, 865-874.
- Sanger, F., Nicklen, S., Coulson, A.R. (1977) DNA sequencing with chain-terminating inhibitors. *Proc. Natl. Acad. Sci. USA*, **74**, 5463-5467.
- Sanglard, D., Hube, B., Monod, M., Odds, F.C., Gow, N.A.R. (1997) A triple deletion of the secreted aspartyl proteinase genes, *SAP4*, *SAP5*, and *SAP6* of *Candida albicans* causes attenuated virulence. *Infect. Immun.*, **65**, 3539-3546.
- Santos, M.A., Perreau, V.M., Tuite, M.F. (1996) Transfer RNA structural change is a key element in the reassignment of the CUG codon in *Candida albicans*. *EMBO J.*, **15**, 5060-5068.
- Sanyal, K., Carbon, J. (2002) The CENP-A homolog CaCse4p in the pathogenic yeast *Candida albicans* is a centromere protein essential for chromosome transmission. *Proc. Natl. Acad. Sci. USA*, **99**, 12969-12974.

- Sanyal, K., Baum, M., Carbon, J. (2004) Centromeric DNA sequences in the pathogenic yeast *Candida albicans* are all different and unique. *Proc. Natl. Acad. Sci. USA*, **101**, 11374-11379.
- Saville, S.P., Lazzell, A.L., Monteagudo, C., and Lopez-Ribot, J.L. (2003) Engineered control of cell morphology *in vivo* reveals distinct roles for yeast and filamentous forms of *Candida albicans* during infection. *Eucaryot. Cell*, **2**, 1053-1060.
- Scherer, S., Magee, P.T. (1990) Genetics of *Candida albicans*. *Microbiol. Rev.*, **54**, 226-241.
- Schweizer, A., Rupp, S., Taylor, B.N., Rollinghoff, M., Schröppel, K. (2000) The TEA/ATTS transcription factor CaTec1p regulates hyphal development and virulence in *Candida albicans*. *Mol. Microbiol.*, **38**, 435-445.
- Shirai, C., Takai, T., Nariai, M., Horigome, C., Mizuta, K. (2004) Ebp2p, the yeast homolog of Epstein-Barr virus nuclear antigen 1-binding protein 2, interacts with factors of both the 60S and the 40S ribosomal subunit assembly. *J. Biol. Chem.*, **279**, 25353-25358.
- Shore, D. (1994) RAP1: a protein regulator in yeast. *Trends Genet.*, **10**, 408-412.
- Shore, D., Nasmyth, K. (1987) Purification and cloning of a DNA binding protein from yeast that binds to both silencer and activator elements. *Cell*, **51**, 721-732.
- Singh, P., Ghosh, S., Datta, A. (1997) A novel MAP-kinase kinase from *Candida albicans*. *Gene*, **190**, 99-104.
- Smith, D.J., Garcia-Pedrajas, M.D., Gold, S.E., Perlin, M. H. (2003) Isolation and characterization from pathogenic fungi of genes encoding ammonium permeases and their roles in dimorphism. *Mol. Microbiol.*, **50**, 259-275.
- Sohn, K., Urban, C., Brunner, H., Rupp, S. (2003) *EFG1* is a major regulator of cell wall dynamics in *Candida albicans* as revealed by DNA microarrays. *Mol. Microbiol.*, **47**, 89-102.
- Soll, D.R. (1992) High-frequency switching in *Candida albicans*. *Clin. Microbiol. Rev.*, **5**, 183-203.
- Sonneborn, A., Bockmühl, D.P., Gerads, M., Kurpanek, K., Sanglard, D., Ernst, J.F. (2000) Protein kinase A encoded by *TPK2* regulates dimorphism of *Candida albicans*. *Mol. Microbiol.*, **35**, 386-396.
- Soupene, E., Ramirez, R.M. and Kustu, S. (2001) Evidence that fungal MEP proteins mediate diffusion of the uncharged species NH₃ across the cytoplasmic membrane. *Mol. Cell. Biol.*, **21**, 5733-5741.
- Southern, E.M. (1975) Detection of specific sequences among DNA fragments separated by gel electrophoresis. *J. Mol. Biol.*, **98**, 503-517.
- Srikantha, T., Klapach, A., Lorenz, W.W., Tsai, L.K., Laughlin, L.A., Gorman, J.A., Soll, D.R. (1996) The sea pansy *Renilla reniformis* luciferase serves as a sensitive bioluminescent reporter for differential gene expression in *Candida albicans*. *J. Bacteriol.*, **178**, 121-129.
- Staib, P., Kretschmar, M., Nichterlein, T., Köhler, G., Michel, S., Hof, H., Morschhäuser, J. (1999) Host-induced, stage-specific virulence gene activation in *Candida albicans* during infection. *Mol. Microbiol.*, **32**, 533-546.
- Staib, P., Kretschmar, M., Nichterlein, T., Hof, H., Morschhäuser, J. (2000) Differential activation of a *Candida albicans* virulence gene family during infection. *Proc. Natl. Acad. Sci. USA*, **97**, 6102-6107.
- Sternberg, S. (1994) The emerging fungal threat. *Science*, **266**, 1632-1634.

- Stoldt, V.R., Sonneborn, A., Leuker, C.E., Ernst, J.F. (1997) Efg1p, an essential regulator of morphogenesis of the human pathogen *Candida albicans*, is a member of a conserved class of bHLH proteins regulating morphogenetic processes in fungi. *EMBO J.*, **16**, 1982-1991.
- Stoyan, T., Gloeckner, G., Diekmann, S., Carbon, J. (2001) Multifunctional centromere binding factor 1 is essential for chromosome segregation in the human pathogenic yeast *Candida glabrata*. *Mol. Cell. Biol.*, **21**, 4875-4888.
- Sundstrom, P. (2002) Adhesion in *Candida* spp. *Cell. Microbiol.*, **4**, 461-469.
- Talbot, N.J., McCafferty, H.R.K., Ma, M., Moore, K., Hamer, J.E. (1997) Nitrogen starvation of the rice blast fungus *Magnaporthe grisea* may act as an environmental cue for disease symptom expression. *Physiol. Mol. Plant Pathol.*, **50**, 179-195.
- Teakle, G.R., Gilmartin, P.M. (1998) Two forms of type IV zinc-finger motif and their kingdom-specific distribution between the flora, fauna and fungi. *Trends Biochem. Sci.*, **23**, 100-102.
- ter Schure, E.G., van Riel, N.A., Verrips, C.T. (2000) The role of ammonia metabolism in nitrogen catabolite repression in *Saccharomyces cerevisiae*. *FEMS Microbiol. Rev.*, **24**, 67-83.
- Theiss, S., Kohler, G.A., Kretschmar, M., Nichterlein, T., Hacker, J. (2002) New molecular methods to study gene functions in *Candida* infections. *Mycoses*, **45**, 345-350.
- Thomas, G.H., Mullins, J.G.L., Merrick, M. (2000) Membrane topology of the Mep/Amt family of ammonium transporters. *Mol. Microbiol.*, **37**, 331-344.
- Tripathi, G., Wiltshire, C., Macaskill, S., Tournu, H., Budge, S. and Brown, A.J. (2002) Gcn4 coordinates morphogenetic and metabolic responses to amino acid starvation in *Candida albicans*. *EMBO J.*, **21**, 5448-5456.
- Uemura, H., Watanabe-Yoshida, M., Ishii, N., Shinzato, T., Haw, R., Aoki, Y. (2004) Isolation and characterization of *Candida albicans* homologue of *RAP1*, a repressor and activator protein gene in *Saccharomyces cerevisiae*. *Yeast*, **21**, 1-10.
- Uhl, M.A., Johnson, A.D. (2001) Development of *Streptococcus thermophilus lacZ* as a reporter gene for *Candida albicans*. *Microbiology*, **147**, 1189-1195.
- Vanden Bossche, H. (1997) Mechanism of antifungal resistance. *REV. Iberoam. Micol.*, **14**, 44-49.
- Venema, J., and Tollervey, D. (1999) Ribosome biosynthesis in *Saccharomyces cerevisiae*. *Annu. Rev. Genet.*, **33**, 261-331.
- Wahlin, J., Cohn, M. (2002) Analysis of the *RAP1* protein binding to the homogenous telomeric repeats in *Saccharomyces castellii*. *Yeast*, **19**, 241-256.
- Walther, A., Wendland, J. (2003) An improved transformation protocol for the human fungal pathogen *Candida albicans*. *Curr. Genet.*, **42**, 339-343.
- Warner, J.R. (1999) The economics of ribosome biosynthesis in yeast. *Trends Biochem. Sci.*, **24**, 437-440.
- White, T.C., Agabian, N. (1995) *Candida albicans* secreted aspartyl proteinases: Isoenzyme pattern is determined by cell type, and levels are determined by environmental factors. *J. Bacteriol.*, **177**, 5215-5221.

- White, T.C., Marr, K.A., Bowden, R.A. (1998) Clinical, cellular, and molecular factors that contribute to antifungal drug resistance. *Clin. Microbiol. Rev.*, **11**, 382-402.
- Whiteway, M., Dignard, D., Thomas, D.Y. (1992) Dominant negative selection of heterologous genes: isolation of *Candida albicans* genes that interfere with *Saccharomyces cerevisiae* mating factor-induced cell cycle arrest. *Proc. Natl. Acad. Sci. USA*, **89**, 9410-9414.
- Wickes, B.L., Mayorga, M.E., Edman, U., Edman, J.C. (1996) Dimorphism and haploid fruiting in *Cryptococcus neoformans*: Association with the alpha-mating type. *Proc. Natl. Acad. Sci. USA*, **93**, 7327-7331.
- Wieland, G., Hemmerich, P., Koch, M., Stoyan, T., Hegemann, J., Diekmann, S. (2001) Determination of the binding constants of the centromere protein Cbf1 to all 16 centromere DNAs of *Saccharomyces cerevisiae*. *Nucleic Acids Res.*, **29**, 1054-1060.
- Wilson, R.B., Davis, D., Mitchell, A.P. (1999) Rapid hypothesis testing with *Candida albicans* through gene disruption with short homology regions. *J. Bacteriol.*, **181**, 1868-1874.
- Wotton, D., Shore, D. (1997) A novel Rap1p-interacting factor, Rif2p, cooperates with Rif1p to regulate telomere length in *Saccharomyces cerevisiae*. *Genes Dev.*, **11**, 748-760.
- Zheng, X., Wang Y., Wang Y. (2004) Hgc1, a novel hypha-specific G1 cyclin-related protein regulates *Candida albicans* hyphal morphogenesis. *EMBO J.*, **23**, 1845-1856.

Curriculum Vitae

Name: Kajal Biswas

Date of Birth: 08th April, 1975

Place of Birth: Nadia, India

Nationality: Indian

Academic Qualifications:

1991-1995: **Bachelor of Science** (Agriculture)
Bidhan Chandra Krishi Viswavidyalaya, Mohonpur, India

1996-1998: **Master of Science** (Biotechnology)
Madurai Kamaraj University, Madurai, India

Title of M.Sc. Dissertation:

Characterization of a *Streptomyces peucetius* mutant (SPRHO), defective in daunorubicin biosynthetic pathway and partial purification of the accumulated product.

Research Experiences:

August 1998- June 2001: Research Fellow at School of Life Science, Jawaharlal Nehru University, New Delhi, India

July 2001- 2004: Ph.D thesis work in the workgroup of Prof. Dr. J. Morschhaeuser, at Institute for Molecular Infectionsbiology, Wuerzburg University, Wuerzburg, Germany

Academic Achievements:

1991-1995: Recipient of National Scholarship from Government of India

1995: Qualified in Junior Fellowship program in the subject of Biochemistry, conducted by Indian Council of Agricultural Research

1996-1998: Recipient of Fellowship of Department of Biotechnology, Government of India

1998: Qualified in National Eligibility Test (NET) conducted jointly by Council for Scientific and Industrial Research, and University Grants Commission, India

Lebenslauf

Name: Kajal Biswas

Geburtsdatum: 08.04.1975

Geburtsort: Nadia, Indien

Nationalität: Inder

Akademische Qualifikationen:

1991-1995: **Bachelor of Science** (Landwirtschaft)
Bidhan Chandra Krishi Viswavidyalaya, Mohonpur,
Indien

1996-1998: **Master of Science** (Biotechnologie)
Madurai Kamaraj University, Madurai, India

Titel der M.Sc. Arbeit:

„Characterization of a *Streptomyces peucetius* mutant (SPRHO), defective in daunorubicin biosynthetic pathway and partial purification of the accumulated product.“

Forschungserfahrung:

August 1998 - Juni 2001: Wissenschaftlicher Mitarbeiter an der School of Life Science, Jawaharlal Nehru Universität, Neu Delhi, Indien

Juli 2001 - 2004: Doktorarbeit in der Arbeitsgruppe von Prof. Dr. J. Morschhäuser am Institut für Molekulare Infektionsbiologie an der Universität Würzburg, Deutschland

Akademische Leistungen:

1991-1995: Empfänger des Nationalen Stipendiums der Regierung von Indien

1995: Qualifikation für das „Junior Fellowship program“ für Biochemie, Indian Council of Agricultural Research

1996-1998: Empfänger des Stipendiums des Department of Biotechnology, Regierung von Indien

1998: Qualifikation für den "National Eligibility Test", Council for Scientific and Industrial Research und University Grants Commission, Indien

Publications

- 1) **Biswas, K.**; Rieger, K.-J.; Morschhäuser, J. (2003) Functional analysis of *CaRAPI*, encoding the repressor/activator protein 1 of *Candida albicans*. **Gene** 307: 151-158.
- 2) **Biswas, K.**; Rieger, K.-J.; Morschhäuser, J. (2003) Functional characterization of *CaCBF1*, the *Candida albicans* homolog of centromere binding factor 1. **Gene** 323: 43-55.
- 3) Kusch, H.; **Biswas, K.**; Schwanfelder, S.; Engelmann, S.; Rogers, P.D.; Hecker, M.; Morschhäuser, J. (2004) A proteomic approach to understanding the development of multidrug-resistant *Candida albicans* strains. **Mol Genet Genomics** 271: 554-65.
- 4) **Biswas, K.**, Morschhäuser, J. Mep2 ammonium permease controls nitrogen starvation induced hyphal growth in *Candida albicans* (under revision to **Mol Microbiol**).